DI Johanna Wiesbauer

# From protein-protein interactions and accelerated stress conditions towards more stable therapeutic proteins

DISSERTATION

zur Erlangung des akademischen Grades einer
Doktorin der technischen Wissenschaften

eingereicht an der

Technischen Universität Graz

betreut durch:
Univ.-Prof. DI Dr. Bernd Nidetzky
Institut für Biotechnologie und Bioprozesstechnik
Technische Universität Graz

2012

## EIDESSTATTLICHE ERKLÄRUNG

Ich erkläre an Eides statt, dass ich die vorliegende Arbeit selbstständig verfasst, andere als die angegebenen Quellen/Hilfsmittel nicht benutzt, und die den benutzten Quellen wörtlich und inhaltlich entnommene Stellen als solche kenntlich gemacht habe.

Graz, am ……  ……..

(Unterschrift)

## STATUTORY DECLARATION

I declare that I have authored this thesis independently, that I have not used other than the declared sources/resources, and that I have explicitly marked all material which has been quoted either literally or by content from the used sources.

……  ……..

date  (signature)

# Acknowledgements

I would like to thank my supervisor Prof. Bernd Nidetzky for providing the topic, laboratory resources and the scientific environment for this work. Further I would like the RCPE GmbH and Dr. Stefan Leitgeb for funding and use of equipment. I was very fortunate to be given the freedom to investigate topics beyond the initial project description. I would also like to thank our project team A2.21b for numerous discussions and my master students Alexandra and Ulrich.

Further I would like to thank my thesis committee Prof. Matthäus Siebenhofer, Prof. Michael Murkovic and Dr. Monika Oberer. The most interesting part of this thesis was always to get input from different views. Especially without the inputs from an engineering point of view, I would not have asked the necessary questions and would not have found many of the presented answersI would also like to thank all my collaborators for their help.

I would also like to thank Prof. Christopher J. Roberts for accepting me for my research stay. We might not have had the best start due to clogging proteins, but his motivating and encouraging optimism and knowledge were inspiring. Additionally the time in the US was also a great personal experience.

Alone we are often lost, so I would like to thank the whole team of the Institute of Biotechnology and Biochemical Engineering (IBB) for their help and support. Without Margaretha Schiller, Karin Longus and Monika Kaube most things would have been more difficult. And I would like to thank my colleagues and friends for chatting and having fun and especially my last office mates Kathi and Sarah for enduring my writing.

And of course I want to thank my friends for being there, listening to all the problems and also successes. See you for a drink after this task is accomplished ;o)

Without my parents this work might not have been possible. Although they never entered university they always encouraged and supported me. Furthermore they taught me to work hard and keep my feet on the ground.

Definitely this thesis would not exist without Christian. I am so lucky to have you on my side. I thank you for your humour, patience and your love.

## Abstract

Protein pharmaceuticals and proteins in general are subject to chemical and physical instabilities leading to undesired modification, denaturation, aggregation and even precipitation.
Beside chemical modifications protein aggregation represents probably the most common and troubling manifestation of protein instability, affecting the shelf life and bioactivity of the product as well as an increased activation of an immune response
As increased amounts of aggregates do not meet pharmaceutical and regulatory requirements, the level of aggregation has to be controlled and minimized. This is normally achieved by choosing stabilizing excipients for the protein formulation. Stability itself has to be tested by ICH Guidelines in long-term studies and has to meet the desired regulative levels. As these stability studies might take months, accelerated stress conditions like vortexing, stirring, shaking, rotation and shearing by concentric cylinder-based shear systems are used especially for the early stage of formulation development during screening. In order to be reproducible, quick, down-scalable and appropriate for high-throughput-testing a better understanding of these accelerated conditions is needed. Over the years it was found that small globular proteins might not be sensitive to the shear itself in these devices but rather on the present interfaces (air-liquid). Nevertheless, e.g. shaking and stirring are numerously reported to lead to different aggregation results. Therefore the main aim of this thesis was to compare three different accelerated stress conditions in order to analyze differences and common features. From our studies we found that shaking, stirring and bubble aeration of human growth hormone (hGH) shows differences regarding aggregation rates, particle size and shape but they all result in noncovalent binding aggregates with affinity towards hydrophobic dyes and show reversible refolding upon addition of chaotropic salts and are stabilized in the presence of surfactants. Therefore we conclude that in all three methods the air-liquid interface is the dominating factor influencing aggregation.
Apart from hGH also the human granulocyte-colony stimulating factor (hG-CSF), a structurally similar cytokine, was tested using stirring and bubble aeration. We see similarities regarding hGH, whereas here a free cysteine is present and involved in covalent aggregation.

## Zusammenfassung

Generell gesehen sind pharmazeutische Proteine chemischen und physikalischen Instabilitäten ausgesetzt, welche zu ungewünschten Modifikationen, Denaturierung und Aggregation bis hin zur Präzipitation führen können. Neben chemischen Modifikationen ist die Aggregation die bedeutendste Beeinträchtigung der Proteinstabilität. Sie kann zu reduzierter Haltbarkeit, Wirksamkeit und auch zu erhöhter Immunantwort führen. Aus diesem Grunde ist der Gehalt an Aggregaten in Pharmazeutika beschränkt, weswegen deren Kontrolle und Vermeidung von großer Wichtigkeit sind. Eine Stabilisierung wird oft durch die Zugabe von Hilfsstoffen (= Formulierung) erreicht. Stabilitätstests werden normalerweise über Monate gemäß ICH Richtlinien durchgeführt. Da dies gerade im anfänglichen Stadium der Entwicklung zu lange dauert, werden hier oft für Screeningzwecke beschleunigte Stressbedingungen wie vortexen, rühren, schütteln, rotieren oder Scherexperimente in konzentrischen Viskosimetern durchgeführt. Da diese Methoden schnell, reproduzierbar und miniaturisierbar sein sollen, ist ein gutes Verständnis der Vorgänge während der Experimente nötig.

Für kleine globuläre Proteine wird immer wieder berichtet, dass sie nicht empfindlich sind gegenüber Scherstress, sehr wohl aber auf Grenzflächen (gas-flüssig). Interessanterweise werden jedoch für Schüttel- und Rührexperimente immer wieder sehr unterschiedliche Aggregationsabläufe und Ergebnisse veröffentlicht. Daher war es Ziel dieser Arbeit drei verschiedene Stressbedingungen miteinander zu vergleichen und herauszufinden warum es zu Unterschieden kommt, und wo Gemeinsamkeiten liegen. In meiner Arbeit habe ich herausgefunden, dass Schütteln, Rühren und Belüftung (Gasblasen) von humanem Wachstumshormon (hGH) große Unterschiede zeigen, was die Aggregationsraten, Partikelgröße und Form betrifft. Jedoch lässt sich auch zeigen, dass alle Aggregate nicht kovalent verbunden sind, hohe Affinität zu einem hydrophoben Fluoreszenzfarbstoff zeigen und nach Zugabe von chaotropen Salzen reversibel rückfaltbar sind. Weiters führt die Zugabe von Surfactants zur Stabilisierung von hGH bei allen drei Stressmethoden.

Daraus schließen wir, dass die gas-flüssig Grenzfläche der dominierende Faktor ist, welcher zur Aggregation führt.

Neben hGH wurde auch der humane Granulozyten stimulierende Faktor (hG-CSF), welcher strukturell dem hGH sehr ähnlich ist, in Rühr- und Belüftungsexperimenten getestet. Wir sehen durchaus Ähnlichkeiten zu den Ergebnissen von hGH, obwohl hier eine neue Komponente zu berücksichtigen ist: G-CSF besitzt ein freies Cystein, welche zu kovalenten Aggregaten führt.

## Table of contents

# 1 Introduction

## 1.1 Stability of Protein Pharmaceuticals

The improved availability of proteins and the possibilities to produce them in large amounts by recombinant DNA technology increased the importance of biopharmaceuticals in the last decades (Manning et al., 1989). Dealing with proteins as active pharmaceutical ingredient (API) one has to investigate all kinds of protein instabilities. In general they are classified into chemical and physical instabilities.

Chemical instabilities cover numerous chemical reactions known to influence protein stability. Well known is deamidation of the side chain amide of Asn and Gln at higher pH values or elevated temperature (Cleland et al., 1993). Further oxidation of the amino acids His, Met, Cys, Trp and Tyr is reported as a product of light induced photooxidation or in connection with the presence of metal ions as metal catalyzed oxidations (MCO) (Hovorka et al., 2001; Manning et al., 2010). Proteolysis, hydrolysis, beta-elimination, racemization and disulfide exchange are also listed as chemical instabilities (Cleland et al., 1993; Manning et al., 2010; Manning et al., 1989).

Apart from the reported chemical instabilities also physical instabilities like the independent structural changes of the protein can lead to denaturation, aggregation, precipitation and adsorption (Manning et al., 2010; Manning et al., 1989). Denaturation goes along with the loss of the three-dimensional structure of the proteins or even the secondary structure. The chemical composition of the protein remains unchanged. So far thermal, cold, chemical, pressure-induced denaturation as well as denaturation in the solid state (freeze-thawing) or intrinsically denatured proteins (IDPs) are observed (Manning et al., 2010; Manning et al., 1989). Aggregation is precisely spoken a microscopic phenomenon with precipitation as its macroscopic equivalent. In the following thesis we focused on protein aggregation and on adsorption at interfaces occurring during the application of accelerated stress conditions.

Facing all these instabilities the challenge is to formulate an active pharmaceutical ingredient (API, protein) in a fashion that a shelf life of 12-24 months with minimal level of aggregation and high bioavailability is achieved (Cleland et al., 1993).

### 1.1.1 Protein Aggregation

During the last decade, protein aggregation has increasingly gathered attention because of its role in the pathology of numerous neurodegenerative diseases (Bellotti et al., 1999; C M Dobson, 1999; Huff et al., 2003; Pastore & Temussi, 2012). These are connected with the presence of aggregates which consist of fibers containing misfolded proteins with a highly structured β-sheet conformation (amyloid) (Ross & Poirier, 2004). Amyloids are responsible for numerous neurodegenerative diseases, such as Alzheimer's, Parkinson's and Hungtington's diseases and mechanisms are elucidated to enable treatment and prophylaxis (Dobson, 1999; Dobson, 2003; Stefani & Dobson, 2003). Recently the role of the fibrils and plaques as toxic species is re-thought, since low molecular weight oligomers of amyloidogenic peptides (Aβ oligomers) are more toxic in cell culture (Huff et al., 2003). Additionally, it was shown that all amino acid sequences might potentially be able to misfold and form fibrils *in vitro*, however only a few proteins expose these structures *in vivo* (Dobson, 1999; Huff et al., 2003). These findings suggest that aggregation can be seen as a general property of polypeptide chains rather than being restricted to a small number of specific protein sequences. Nevertheless, aggregation is not automatically dangerous in a physiological sense as shown by the formation of amyloid-like structures for cellular protein interactions or storage (Capstick et al., 2011; Dobson, 1999; Huff et al., 2003; Maji et al., 2009; Wang et al., 2008).

Apart from medical implication aggregation occurs during the production (Fink, 1998; Jungbauer & Kaar, 2007; Kopito, 2000; Mitraki & King, 1989) and processing of proteins (e.g. purification, formulation, freeze-thawing, freeze-drying, ultrafiltration, vial and syringe filling, pumping, transportation and storage) and influences the shelf life of biopharmaceuticals (API) and is therefore of interest for biotechnology and pharmaceutical industry (Chi et al., 2003; Cleland et al., 1993; Cromwell et al., 1998; Mahler et al., 2008; Mitraki & King, 1989; Rathore & Rajan, 2008; Schein, 1990; Simon et al., 2011; Wang, 1999; Wang et al., 2010). Further the administration of protein aggregates may lead to increased immune reactions occasionally leading to patient morbidity and even death (Cleland et al., 1993; Rosenberg, 2006).

While we can conceptually understand why intrinsically unfolded proteins tend to aggregate (Babu et al., 2011) it is more difficult to understand why globular proteins aggregate. In fact, literature mainly reports aggregation in combination with environmental perturbations and external effects like temperature, ionic strength, pH or stress conditions (Chi et al., 2003;

Y. F. Maa & Hsu, 1996, 1997; Mahler et al., 2008; Pastore & Temussi, 2012; Thomas & Geer, 2011; Virkar et al., 1981; Walstra, 2001; Wang, 1999).

Prior to discussing aggregation and its major causes a clear definition of several terms might be necessary. Protein association is often described as a reversible process, where two or more native protein molecules associate and often lead to reversible precipitation (Cleland et al., 1993). Aggregation is considered to be often irreversible if no drastic changes in the solvent environment occur. The interacting proteins can be partially unfolded or even denatured (Cleland et al., 1993; Philo & Arakawa, 2009). The definitions are summarized in Figure 1.

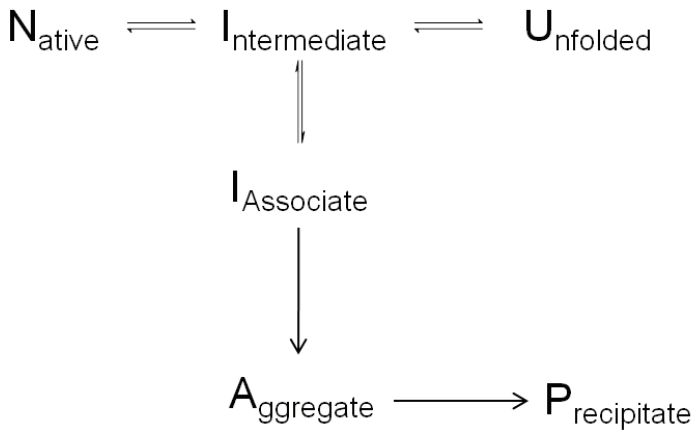


**Figure 1: Schematic description of association, aggregation and precipitation.** While all steps until the association can be reversible, aggregation and precipitation are considered irreversible if no drastic changes of the solvent conditions are made.

Protein aggregation is very complex and diverse, including different types of molecular assemblies. Recently a classification terminology was published in order to describe aggregates using size (e.g. subvisible, µm), reversibility/dissociation, conformation, chemical modifications and morphology (e.g. shape, optical properties) (Narhi et al., 2012). Regarding their conformation protein aggregates can be categorized into native and nonnative, where nonnative is referred to aggregates of initially native folded proteins exposing now a nonnative protein structure (Chi et al., 2003). Further aggregates can be amorphous (e.g. inclusion bodies) or highly structured (amyloid fibrils) (Fink, 1998). Chemical modifications involve covalent aggregates formed by disulfide bonds; noncovalent interactions include hydrogen bonds, hydrophobic and electrostatic interactions originating from different pathways (Fradkin et al., 2009; Mahler et al., 2008; Manning et al., 2010; Philo & Arakawa, 2009; Weiss et al., 2009). In literature so far five to seven different pathways of aggregation are described (Philo & Arakawa, 2009) and shown in Figure 2:

1. *Association* of native monomers
2. *Association/aggregation* of conformationally altered monomers – (partially) unfolded
3. *Unfolding and association/aggregation* of the conformationally altered monomers
4. *Amyloidosis* of intrinsically denatured proteins (IDPs)
5. *Surface induced aggregation*
6. Aggregation of *chemically modified monomers* (according to 2 or 3 and 7)
7. *Nucleation controlled* aggregation after formation of a critical nucleus or seed (not shown)

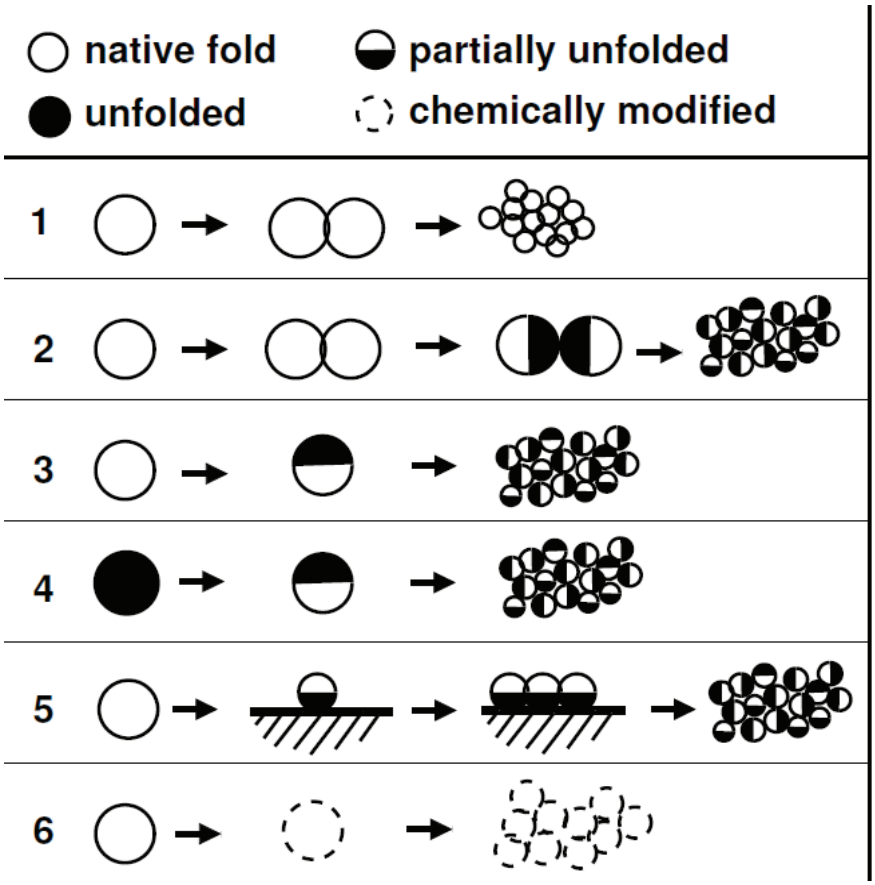


**Figure 2: General mechanisms of protein aggregation.** Adapted and extended from (Philo & Arakawa, 2009) by Dr. Michael Brunsteiner.

### 1.1.2 Surface Adsorption

Proteins are amphiphilic biomolecules and so they can absorb to different types of interfaces like air-liquid, ice-water, biomolecular and solid interfaces (containers, steel, glass, stirrers) (Andrade et al., 1992; Colombie et al., 2001; Felsovalyi et al., 2011; Manning et al., 2010; Maste et al., 1996; Norde, 1986; Sadana, 1992; Su et al., 1998; Zoungrana et al., 1997).

By molecular view mainly the tertiary structure and conformation are changed upon adsorption. In contact with hydrophobic air-liquid interfaces often at least partial unfolding and (reversible) denaturation occurs due to interactions between the surface and the (buried) hydrophobic protein core (Donaldson et al., 1980; Manning et al., 2010; Manning et al., 1989). Whereas adsorption is often irreversible, two models are described in literature for reversible adsorption (Felsovalyi et al., 2011): (1) the classical 4 state reversible model including adsorption, structural rearrangement (unfolding) and desorption into the bulk and reversible refolding (Figure 3, A) and (2) a two state model where only two species exist – the native protein and the unfolded adsorbed protein (lysozyme and fumed silica substrate) (Figure 3, B). Desorption of structurally perturbed proteins from the surface leads to nucleation and growth of particles (aggregation) in the bulk (Mahler et al., 2005; Manning et al., 2010).

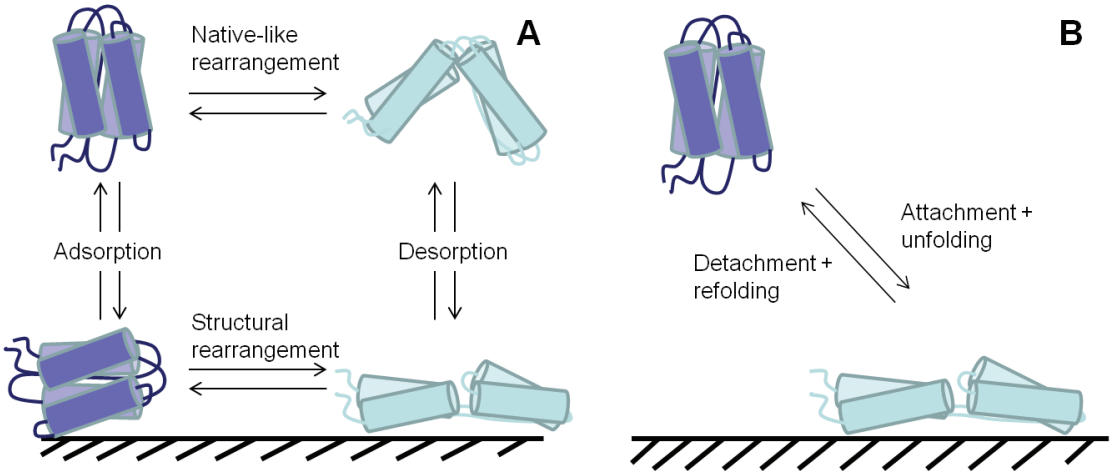


**Figure 3: Reversible adsorption mechanisms (Felsovalyi et al., 2011).** (A) Classical four state model. (B) Two state model (observed for lysozyme and fumed silica substrate).

Additionally, interfacial denaturation or unfolding is also dependent on several properties of the surface and protein: decrease in surface free energy, forces at the interface (surface tension), available surface area for adsorption, hydrophobicity and surface properties of the protein (hydrophobicity,charge patterns), number of disulfide bonds as well as the surface pressure against the molecule has to expand in order to unfold and the intrinsic protein stability (Andrade et al., 1992; Donaldson et al., 1980; Maa & Hsu, 1997; Manning et al., 2010; Thomas & Geer, 2011; Townsend & Nakai, 1983; Walstra, 2001; Wilde, 2000; Yampolskaya & Platikanov, 2006).

## 1.2 Human growth hormone (hGH)

### 1.2.1 Structure and function

Human growth hormone (hGH, Somatropin) is produced from a precursor protein including a signal sequence which is further processed (Uniprot: P01241). The mature monomeric single-chain protein consisting of 191 amino acids (22,125 Da) has a p*I* of 5.3 (Cleland et al., 1993; Pearlman & Wang, 1993). Further the protein shows a 4-helical cytokine fold and a up-up-down-down architecture (Figure 4) with two disulfide bridges Cys53-Cys165 and Cys182-Cys189 and is non-glycosylated (Chantalat et al., 1995; de Vos et al., 1992). With this fold it shares the structural features (4-helical cytokine fold) of a pharmaceutically relevant group of long chain cytokines (Hill et al., 1993). Interestingly, hGH has the tendency to form noncovalent dimers in the presence of metal ions e.g. zinc or other cations (Cunningham et al., 1991; Dienys et al., 2000). The zinc is bound by the solvent exposed residues His18, His21 (Helix 1) and Glu174 (Helix 4) (Cunningham et al., 1991). Further hGH is a bivalent ligand for its receptors and forms a 1:2 stoichiometry as shown in Figure 5 (Fuh et al., 1992; Horan et al., 1996).

hGH is involved in the regulation of many metabolic and physiological processes including the stimulation of cell growth and reproduction. In the human body it is secreted from the anterior pituitary gland under hypothalamic control and it is used for therapeutic treatment of growth disorders and dwarfism (Cholewinski et al., 1996; Cleland et al., 1997; Pearlman & Wang, 1993). Prior to the advent of recombinant production possibility of hGH (rhGH), the only source was a preparation (including a 20 kDa variant, deamidated, oxidized and aggregated) from human cadaver tissue until this pituitary hGH was connected to the Creutzfeld-Jakob syndrome (Cholewinski et al., 1996; Lewis et al., 1977; Pearlman & Wang, 1993). As the protein is non-glycosylated, *E.coli* can be used as a host organism (Crisman & Randolph, 2010; Patra et al., 2000; Singh et al., 2005). Therefore, two variants of hGH are available: Methionyl hGH (Met-hGH, Somatrem) and the methionyl-free variant hGH (Somatropin) (Pearlman & Wang, 1993).

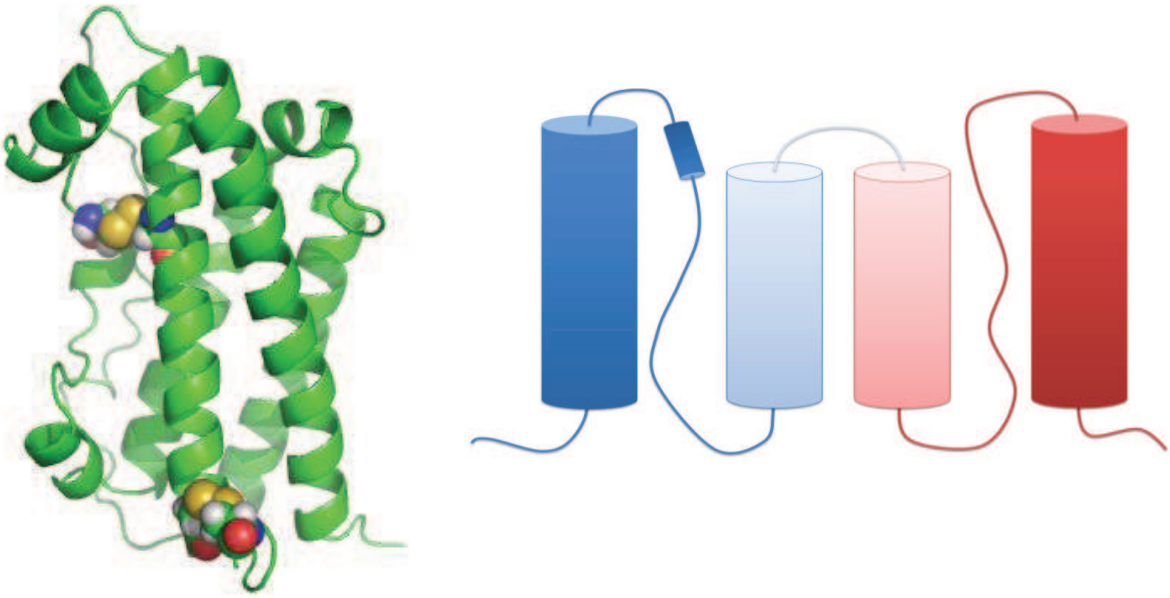

**Figure 4: Structure of hGH.** (left) Structure of hGH derived from PDB 3HHR (de Vos et al., 1992) which shows higher similarity to the solution conformation of the non-bound protein (Kasimova et al., 2002) than 1HGU (Chantalat et al., 1995). The disulfide bridges are highlighted as spheres. (right) up-up-down-down architecture.

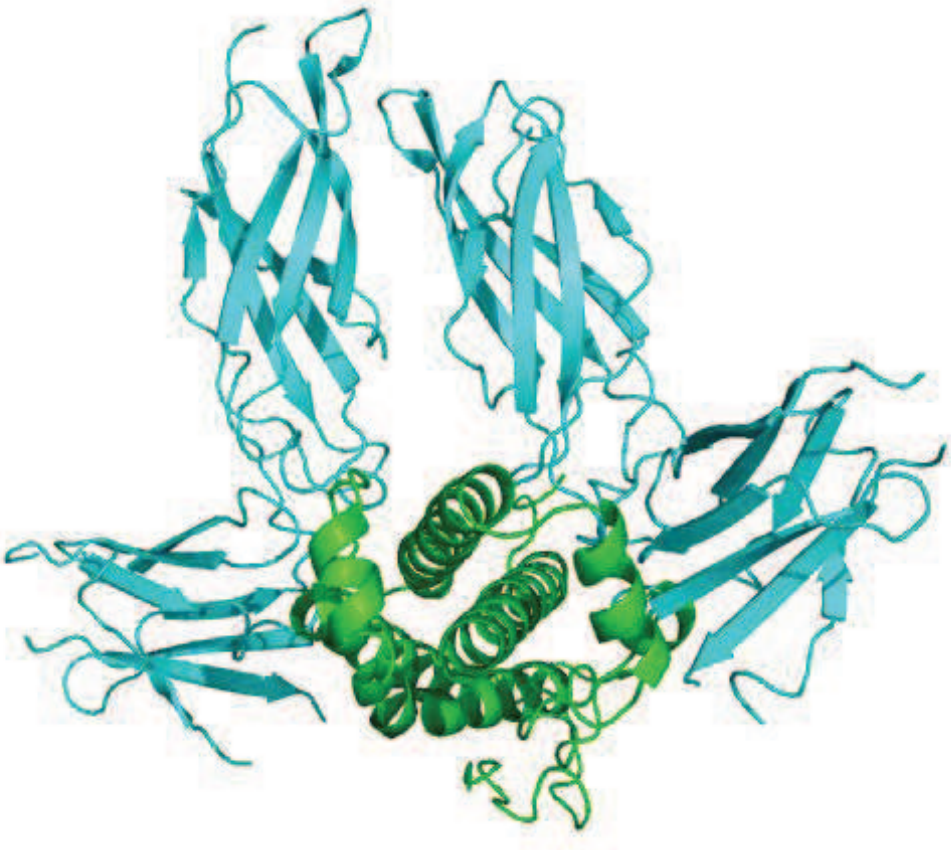

**Figure 5: Structure of the 1:2 hGH-receptor complex (3HHR).** .

### 1.2.2 Degradation pathways

Aggregation, deamidation, oxidation and amino-terminal degradation have been identified as major degradation routes for hGH in solution so far (Jones et al., 1997).

**Table 1**: **Most common degradation pathways for hGH in solution (Cholewinski et al., 1996; Pearlman & Wang, 1993).**

| **Degradation** | **Major factors** | **Reactive sites** |
|---|---|---|
| *Deamidation* | Neutral, basic pH, elevated T | Asn149 rather than Asn 152 |
| *Oxidation* | $H_2O_2$-incubation, UV light | Met14, Met125 (not at Met170) |
| *Aggregation* | Process and production conditions, air-liquid interfaces, freezing | Whole molecule |

In previous studies deamidation of hGH with its 9 asparagines (Asn) and 13 glutamine (Gln) residues has been examined. Gln residues generally deamidate much slower than Asn residues and so an Asn site, in detail $Asn^{149}$, was identified as the major site of modification (Ablinger et al., 2012; Becker et al., 1988; Cholewinski et al., 1996; Jenkins et al., 2008). However, an important point regarding deamidation of hGH has not been discussed yet, and this concerns the relationship between protein chemical modification and nonnative aggregation (Manning et al., 2010; Manning et al., 1989). Furthermore, deamidation is generally undesired because of the process-related impurities, degradation products and structural heterogeneity that it introduces to a given protein preparation (Doyle et al., 2007; Manning et al., 1989; Manning et al., 2010). Furthermore the formation of the non canonical amino acid iso-Asp can present a potential immunogenic risk (Catak et al., 2009; Jenkins et al., 2008). However, it has to be noted that the biological activity of deamidated hGH is known to be equal to that of the native protein (Becker et al., 1988; Riggin & Farid, 1990).

Numerous studies covering the aggregation of hGH were published so far (Bam et al., 1998; Fradkin et al., 2009; Katakam & Banga, 1997; Maa & Hsu, 1996, 1997; Maa & Hsu, 1996; Otzen et al., 2002). Based on SDS PAGE analysis it was shown that during agitation or vortexing only noncovalent aggregates are formed (Fradkin et al., 2009). If surfactants are supplemented aggregation can be prevented (Bam et al., 1998; Bam et al., 1996; Katakam et al., 1995; Katakam & Banga, 1997). From our results and other published studies (Maa & Hsu, 1997) we conclude that hGH is highly sensitive to air-liquid interfaces.

Based on refolding and equilibrium unfolding studies DeFelippis and coworkers have stated a folding intermediate (Defelippis et al. 1993; Defelippis et al., 1995). This Intermediate is a monomeric structurally altered protein species which tends to self associate ($I_{Associate}$). Therefore (partial) unfolding and aggregation might use a similar pathway as shown in Figure 6.

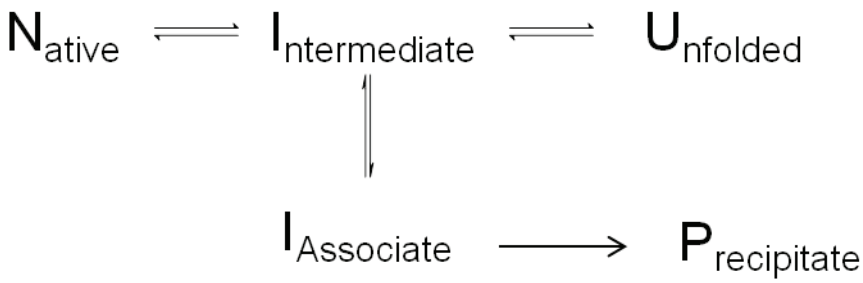


**Figure 6: Folding and refolding Mechanism of hGH.**

## 1.3 G-CSF

### 1.3.1 Structure and function

The mature human granulocyte colony-stimulating factor (hG-CSF) is derived after splicing of a signal sequence (Uniprot: P09919). Similar to hGH hG-CSF is a monomeric singlechain protein of 174 amino acids (19,600 Da) and has a p*I* of about 6.1 (Hill et al., 1993; Zink et al., 1994). hG-CSF shares with hGH the 4-helical cytokine fold and the up-up-down-down architecture (Figure 7), which is rather common among cytokines. Naturally occurring hG-CSF exists in a long and short variant due to different splicing patterns (Herman et al., 1996). In general two disulfide bridges (Cys36-Cys42 and Cys64-Cys74) are present and in contrast to hGH an O-linked glycosylation takes place in a loop region at Tyr133 (Hill et al., 1993). This glycosylation is reported to increase the stability of the protein due to reduced loop mobility around the glycosylation site (Hasegawa, 1993; Gervais et al., 1997; Oh-eda et al., 1990). Further a free cysteine C17 is present which is not essential for activity (Lu et al., 1992).

In contrast to hGH, hG-CSF is a monovalent ligand but interestingly the receptor-protein interaction occurs in a 2:2 stoichiometry. The dimerization was stated to origin from receptor-receptor interactions upon binding of hG-CSF (Horan et al., 1996). Receptor activation occurs probably via binding of the protein to the receptor followed by receptor dimerization like shown in Figure 8 (Gervais et al., 1997; Aritomi et al., 1999).

hG-CSF belongs to the group of hematopoietins which regulate the growth and differentiation of various blood cell lines from progenitor stem cells. It is mainly produced in endothelial cells, monocytes, macrophages and fibroblasts and shows high sequence similarity to members of the Interleukin-6 superfamily (Gervais et al., 1997). Further it induces the proliferation of neutrophil colonies and differentiation of precursor cells to neutrophils, and it stimulates the activity of mature neutrophils (Hill et al., 1993). hG-CSF is also used in oncology (chemotherapy, bone marrow transplants or treatment of acute myeloid leukemia) in order to increase production of white blood cells and reduce infection risks during chemotherapy (Bishop et al., 2001; Raso et al., 2005).

In our study we used Filgrastim, a non-glycosylated rhMet-G-CSF Cys37-Cys43, Cys65-Cys75 and C18 variant lacking three residues at position 37-39 and derived from *E. coli* expression (Herman et al., 1996). Another glycosylated form prepared in CHO cells (lenograstim) is also available on the market (Gervais et al., 1997).

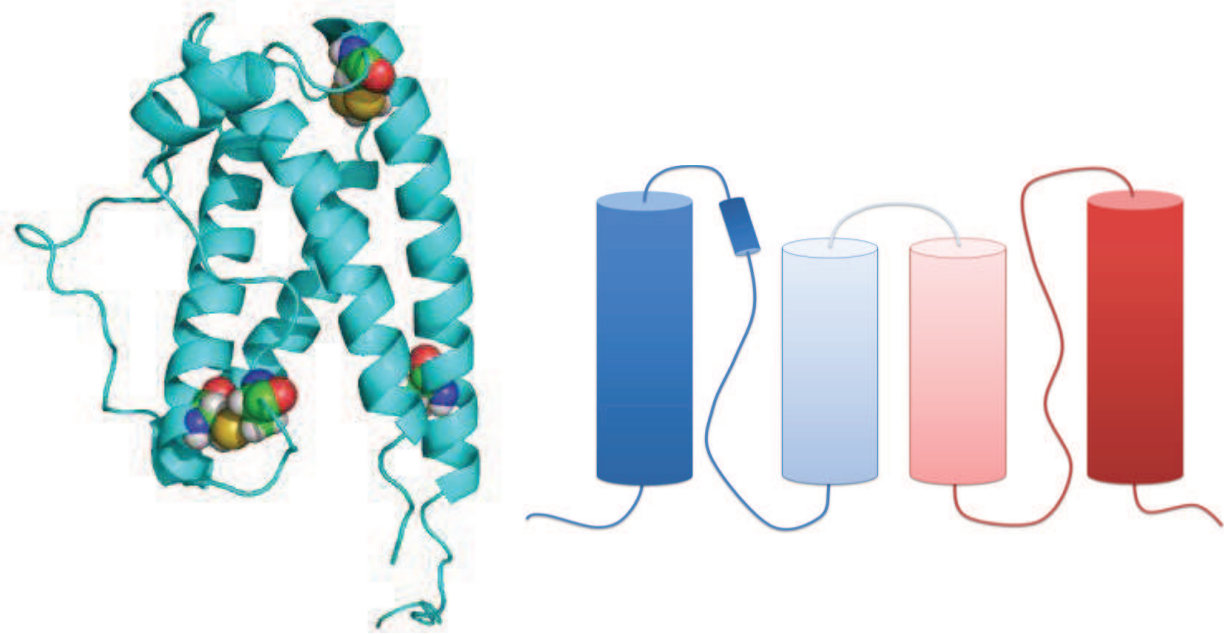

**Figure 7: Structure of G-CSF.** (left) Structure of G-CSF derived from PDB 1GNC (Zink et al., 1994). The disulfide bridges (bottom left, top right) and the free cysteine (bottom right) are highlighted as spheres. (right) up-up-down-down architecture.

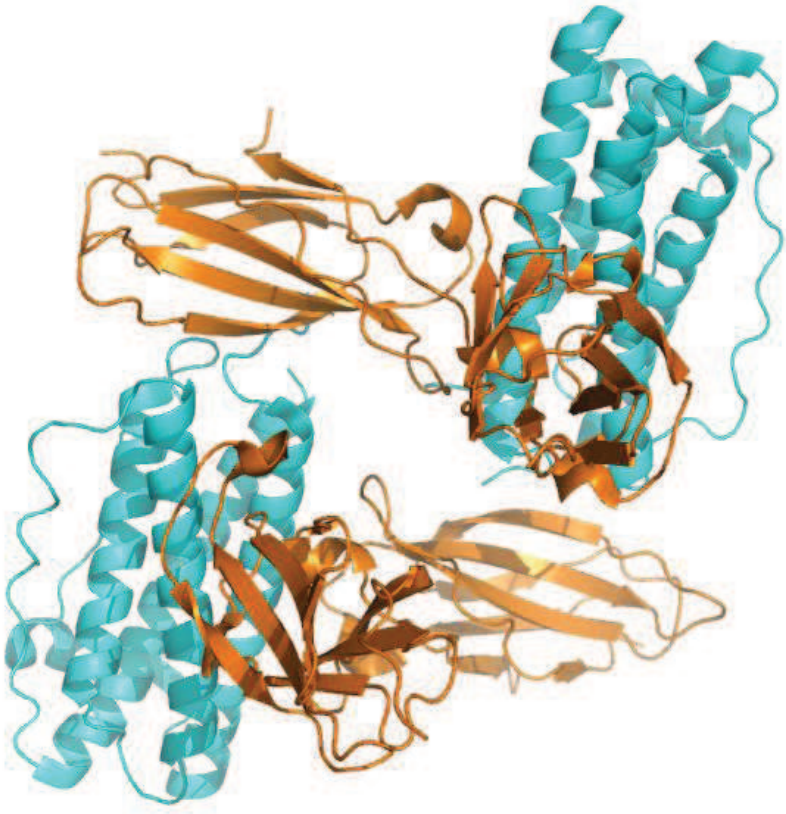

**Figure 8: Structure of the 2:2 G-CSF-receptor complex 1CD9 (Aritomi et al., 1999).**

### 1.3.2 Degradation pathways

Most reports about degradation of rhG-CSF involve storage at elevated temperature. For bovine G-CSF (bG-CSF, p*I* = 6.8) aggregation studies were performed from pH 2.9 to 6.2 at 50°C (Bartkowski et al., 2002) and pH 4.5 and 7.5 (Roberts et al., 2003). Whereas at low pH soluble noncovalent high molecular weight (HMW) aggregates are found, at higher pH values precipitation was dominant. Studies examining the re-dissolution of aggregates formed at pH 4.3 and 6.2 showed that the precipitates consist of covalent and noncovalent aggregates. SDS PAGE analysis confirmed that covalent aggregates are formed by disulfide bridges. As only one free cysteine is available, disulfide scrambling has to take place (Bartkowski et al., 2002). The pH dependency was explained by the fact that the free cysteine is partially solvent exposed and so the necessary ionization (pKa) is highly dependent on the actual microenvironment of the residue.

Another possible explanation for the pH dependency can be derived from different mechanism for disulfide formation at neutral (alkaline) and acidic pH as shown in Scheme 1 and 2 (Manning et al., 1989):

$$R'S^- + R''S\text{-}SR'' \leftrightarrow R'S\text{-}SR'' + R''S^-$$
$$R''S^- + R'S\text{-}SR' \leftrightarrow R''S\text{-}SR' + R'S^-$$

**Scheme 1: Disulfide exchange at neutral or alkaline pH.** The reaction is catalyzed by thiolate ions, which perform a nuelceophilic attack on a sulfur atom of the disulfide bridge (Manning et al., 1989).

$$R'S\text{-}SR' + H^+ \leftrightarrow [R'HS\text{-}SR']^+ \leftrightarrow R'SH + R'S^+$$

$$R'S^+ + R''S\text{-}SR'' \leftrightarrow R'S\text{-}SR'' + R''S^+$$
$$R''S^+ + R'S\text{-}SR' \leftrightarrow R''S\text{-}SR' + R'S^+$$

**Scheme 2: Proposed disulfide exchange at acidic pH**. Here the exchange should take place through an attack of a sulfenium cation.

Whatever the exact mechanism of disulfide rearrangement might be, it was found that mutagenesis of the free cysteine C17A led to noncovalent aggregates only and slowed down the kinetics, but could not prevent aggregation (Raso et al., 2005). Thus, also conformational stability ($\Delta G_{unf}$) seems to be involved in the aggregation mechanism. It was found that G-CSF is conformationally most stable at pH 4.5 to 3.3 (Narhi et al., 1991). Spectroscopic studies indicate that pH dependent conformations exist between pH 5.0 and 7.0 (Narhi et al., 1991).
Chi and coworkers have investigated aggregation of hG-CSF and proposed a general reaction mechanism for rhG-CSF (Chi et al., 2003; Krishnan et al., 2002). It suggests that aggregation occurred via a structurally expanded transition state species of the monomer, which forms due to increase of free energy. Irreversible dimerization was only possible upon the collision of two of the activated monomer species (Krishnan et al., 2002). At pH 7.0 aggregation seems to be controlled by the conformational stability of hG-CSF and the formation of the structurally expanded monomeric species. Interestingly a reversible dimer formation is observed, which is not involved in the aggregation mechanism (Krishnan et al., 2002). However, conformational stability at pH 3.5 is similar and therefore reduced aggregation cannot be explained. Here the role of colloidal stability of the protein was introduced using the second osmotic virial coefficient $B_{22}$ as a parameter for attractive or repulsive protein-protein interactions. This coefficient is a measure of nonideal solution behavior originating from two-body interactions, and is derived from statistical mechanics (Chi et al., 2003). As hG-CSF is positively charged at pH 3.5 repulsion seems to be dominant and the formation of a dimer of tho structurally perturbed monomers is rate limiting (Chi et al., 2003).

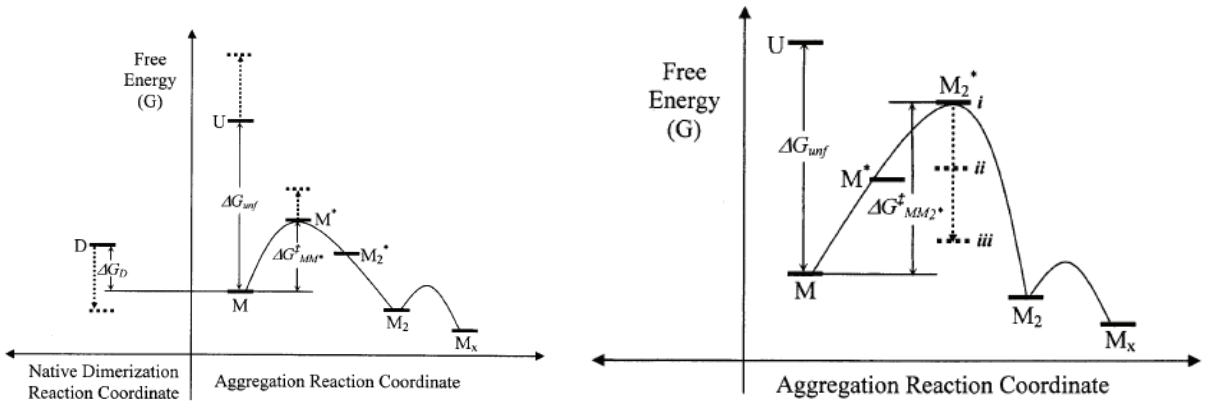


**Scheme 3: Aggregation mechanism of hG-CSF at pH 7.0 and 3.5. (left)** Aggregation mechanism of hG-CSF at pH 7.0. The conformational alteration into an expanded transition state of the monomer is rate limiting (conformational stability dependent). (right) Aggregation mechanism at pH 3.5. The formation of the irreversible dimer in the presence of strong repulsive protein-protein-interactions (charge) is rate limiting (colloidal stability dependent).

Based on this evidence the authors suggest to use this for stable formulation design (Chi et al., 2003). In solutions where the conformational stability dominates, increasing $\Delta G_{unf}$ decreases aggregation. Otherwise, if colloidal stability is dominant, solution conditions which reduce attractive interactions should be chosen (e.g. low pH and low ionic strength)

This might explain why the stable commercially available formulation of hG-CSF is used at pH 4.0, where the protein is stable for over 2 years at 2-8°C (Herman et al., 1996).

## References


Ablinger E, Wegscheider S, Keller W, Prassl R, Zimmer A. Effect of protamine on the solubility and deamidation of human growth hormone. Int J Pharm 2012;427:209-216.

Ali V, Prakash K, Kulkarni S, Ahmad A, Bhakuni V. 8-Anilino-1-naphthalene sulfonic acid (ANS) induces folding of acid unfolded cytochrome c to molten globule state as a result of electrostatic interactions. Biochemistry 1998;38:13635-13642.

Andrade JD, Hlady V, Wei AP. Adsorption of complex proteins at interfaces. Pure Appl Chem 1992;64:1777-1781.

Aritomi M, Kunishima N, Okamoto T, Kuroki R, Ota Y, Morikawa K. Atomic structure of the GCSF-receptor complex showing a new cytokine-receptor recognition scheme. Nature 1999;401:713-717.

Babu MM, van der Lee R, de Groot NS, Gsponer J. Intrinsically disordered proteins: regulation and disease. Curr Opin Struct Biol 2011;21:432-440.

Bam NB, Cleland JL, Yang J, Manning MC, Carpenter JF, Kelley RF, Randolph TW. Tween protects recombinant human growth hormone against agitation induced damage via hydrophobic interactions. J Pharm Sci 1998;87:1554-1559.

Bam NB, Cleland JL, Randolph TW. Molten globule intermediate of recombinant human growth hormone: stabilization with surfactants. Biotechnol Prog 1996;12:801-809.

Bartkowski R, Kitchel R, Peckham N, Margulis L. Aggregation of recombinant bovine granulocyte colony stimulating factor in solution. J Protein Chem 2002;21:137-143.

Becker GW, Tackitt PM, Bromer WW, Lefeber DS, Riggin RM. Isolation and characterization of a sulfoxide and a desamido derivative of biosynthetic human growth hormone. Biotechnol Appl Biochem 1988;10:326-337.

Bellotti V, Mangione P, Stoppini M. Biological activity and pathological implications of misfolded proteins. Cell Mol Life Sci 1999;55:977-991.

Bishop B, Koay DC, Sartorelli AC, Regan L. Reengineering granulocyte colony-stimulating factor for enhanced stability. J Biol Chem 2001;276:33465-33470.

Capstick DS, Jomaa A, Hanke C, Ortega J, Elliot MA. Dual amyloid domains promote differential functioning of the chapling proteins during Streptomyces aerial morphogenesis. Prot Natl Acad Sci U S A 2011;108:9821-9826.

Catak S, Monard G, Aviyente V, Ruiz-Lopez MF. Deamidation of asparagines residues: direct hydrolysis versus succinimide-mediated deamidation mechanisms. J Phys Chem A 2009;113:1111-1120.

Chantalat L, Jones ND, Korber F, Navaza J, Pavlovsky AG. The crystal structure of wild-type growth hormone at 2.5 Å resolution. Protein Peptide Lett 1995;2:333-340.

Chi EY, Krishnan S, Kendrick BS, Chang BS, Carpenter JF, Randolph TW. Roles of conformational stability and colloidal stability in the aggregation of recombinant human granulocyte colony stimulating factor. Protein Sci 2003;12:903-913.

Chi EY, Krishnan S, Randolph TW, Carpenter JF. Physical stability of proteins in aqueous solution: mechanism and driving forces in nonnative protein aggregation. Pharm Res 2003;20:1325-1336.

Cholewinski M, Lückel B, Horn H. Degradation pathways, analytical characterization and formulation strategies of a peptide and a protein. Calcitonine and human growth hormone in comparision. Pharm Acta Helv 1996;71:405-419.

Cleland JL, Mac A, Boyd B, Yang J, Duenas ET, Yeung D, Brooks D, Hsu C, Chu H, Mukku V, Jones AJ. The stability of recombinant human growth hormone in poly(lactic-co-glycolic acid) (PLGA) microspheres. Pharm Res 1997;14:420-425.

Cleland JL, Powell MF, Shire SJ. The development of stable protein formulations: a close look at protein aggregation, deamidation and oxidation. Crit Rev Ther Drug Carrier Syst 1993;10:307-377.

Colombie S, Gaunand A, Lindet B. Lysozyme inactivation under mechanical stirring effect of physical and molecular interfaces. Enzyme Microb Technol 2001;28:820-826.

Crisman RL, Randolph TW. Crystallization of recombinant human growth hormone at elevated pressures: pressure effects on PEG-induced volume exclusion interactions. Biotechnol Bioeng 2010;107:663-672.

Cromwell MEM, Hilario E, Jacobson F. Protein aggregation and bioprocessing. AAPS J 2006;8:E572-E579.

Cunningham BC, Mulkerrin MG, Wells J. Dimerization of human growth hormone by zinc. Science 1991;253:545-548.

Defelippis MR, Alter LA, Pekar AH, Havel HA, Brems DN. Evidence for a self-associating equilibrium intermediate during folding of human growth hormone. Biochemistry 1993;32:1555-1562.

Defelippis MR, Kilcomons MA, Lents MP, Youngman KM, Havel HA. Acid stabilization of hGH equilibrium folding intermediates. Biochim Biophys Acta 1995;1247:35-45.

Dienys G, Sereikaite J, Luksa V, Jarutiene O, Mistiniene E, Bumelis V-A. Dimerization of human growth hormone in the presence of metal ions. Bioconjug Chem 2000;11:646-651.

Dobson CM. Protein misfolding, evolution and disease. Trends Biochem Sci 1999;24:329-332.

Dobson CM. Protein folding and misfolding. Nature 2003;426:884-890.

Donaldson TL, Boonstra EF, Hammond JM. Kinetics of protein denaturation at gas-liquid interfaces. J Colloid Interface Sci 1989;74:441-450.

Doyle HA, Gee RJ, Mamula MF. Altered immunogenicity of isoaspartate containing proteins. Autoimmunity 2007;40:131-137.

Felsovalyi F, Mangiagalli P, Bureau C, Kumar SK, Banta S. Reversibility of the adsorption of lysozyme on silica. Langmuir 2011;27:11873-11882.

Fink AL. Protein aggregation: folding aggregates, inclusion bodies and amyloid. Fold Des 1998;3:R9-R23.

Fradkin AH, Carpenter JF, Randolph TW. Immunogenicity of aggregates of recombinant human growth hormone in mouse models. J Pharm Sci 2009;98:3247-3264.

Fuh G, Cunningham BC, Fukunaga R, Nagata S, Goeddel DV, Wells JA. Rational design of potent antagonists to the human growth hormone receptor. Science 1992;256:1677-1680.

Hasegawa M. A thermodynamic model for denaturation of granulocyte colony-stimulating factor. O-linked sugar chain suppresses not the triggering deprotonation but the succeeding denaturation. Biochim Biophys Acta 1993;1203:295-297.

Hawe A, Sutter M, Jiskoot W. Extrinsic fluorescent dyes as tools for protein characterization. Pharm Res 2008;25:1487-1499.

Herman AC, Boone TC, Lu HS. Characterization, formulation and stability of Neupogen® (Filgrastim), a recombinant human granulocyte-colony stimulating factor. Pharm Biotechnol 1996;9:303-328.

Hill CP, Osslund TC, Eisenberg D. The structure of granulocyte-colony-stimulating factor and its relationship to other growth factors. Prot Natl Acad Sci U S A 1993;90:5167-5171.

Horan T, Wen J, Narhi L, Parker V, Garcia A, Arakawa T, Philo J. Dimerization of the extracellular domain of granulocyte-colony stimulating factor receptor by ligand binding: a monovalent ligand induces 2:2 complexes. Biochemistry 1996;35:4886-4896.

Hovorka SW, Hong J, Cleland JL, Schöneich C. Metal-catalyzed oxidation of human growth hormone: modulation by solvent-induced changes of protein conformation. J Pharm Sci 2001;90:58-69.

Huff ME, Balch WE, Kelly JW. Pathological and functional amyloid formation orchestrated by the secretory pathway. Curr Opin Struct Biol 2003;13:674-682.

Gervais V, Zerial A, Oschkinat H. NMR investigations of the role of the sugar moiety in glycosylated recombinant human granulocyte-colony-stimulating factor. Eur J Biochem 1997;247:386-395.

Jenkins N, Murphy L, Tyther R. Post-translational modification of recombinant proteins: significance for biopharmaceuticals. Mol Biotechnol 2008;39:113-118.

Cleland JL, Johnson OL, Jones AJS. Recombinant human growth hormone poly(lactic-co-glycolic acid) microsphere formulation development. Adv Drug Deliv Rev 1997;28:71-84.

Jungbauer A, Kaar W. Current status of technical protein refolding. J Biotechnol 2007;128:587-596.

Kasimova MR, Kristensen SM, Howe PWA, Christensen T, Matthiesen F, Petersen J, Sørensen HH, Led JJ. NMR studies of the backbone flexibility and structure of human growth hormone: a comparison of high and low pH conformations. J Mol Biol 2002;318:679-695.

Katakam M, Bell LN, Banga AK. Effect of surfactants on the physical stability of recombinant human growth hormone. J Pharm Sci 1995;84:713-716.

Katakam M, Banga AK. Use of polymers to stabilize recombinant human growth hormone against various processing stresses. Pharm Dev Technol 1997;2:143-149.

Kopito RR. Aggresomes, inclusion bodies and protein aggregation. Trends Cell Biol 2000;10:524-530.

Krishnan S, Chi EY, Webb JN, Chang BS, Shan D, Goldenberg M, Manning MC, Randolph TW, Carpenter JF. Aggregation of granulocyte colony stimulating factor under physiological conditions: characterization and thermodynamic inhibition. Biochemistry 2002;41:6422-6431.

Lewis UJ, Peterson SM, Bonewald LF, Seavey BK, VanderLaan WP. An interchain disulfide dimer of human growth hormone. J Biol Chem 1977;252:3697-3702.

Lu HS, Clogston CL, Narhi LO, Merewether LA, Pearl WR, Boone TC. Folding and oxidation of recombinant human granulocyte colony stimulating factor produced in Escherichia coli. Characterization of the disulfide-reduced intermediates and cysteine-serine analogs. J Biol Chem 1992;267:8770-8777.

Maa YF, Hsu CC. Effect of high shear on proteins. Biotechnol Bioeng 1996;51:458-465.

Maa YF, Hsu CC. Protein denaturation by combined effect of shear and air-liquid interface. Biotechnol Bioeng 1997;54:503-512.

Maa YF, Hsu CC. Aggregation of recombinant human growth hormone induced by phenolic compounds. Int J Pharm 1996;140:155-168.

Mahler H-C, Friess W, Grauschopf U, Kiese S. Protein aggregation: pathways, induction factors and analysis. J Pharm Sci 2009;98:2909-2934.

Mahler H-C, Mueller R, Friess W. Delille A, Matheus S. Induction and analysis of aggregates in a liquid IgG1-antibody formulation. Eur J Pharm Biopharm 2005;59:407-417.

Maji SK, Perrin MH, Sawaya MR, Jessberger S, Vadodaria K, Rissman RA, Singru PS, Nilsson KPR, Simon R, Schubert D, Eisenberg D, Rivier J, Sawchenko P, Vale W, Riek R. Functional amyloids as natural storage of peptide hormones in pituitary secretory granules. Science 2009;325:328-332.

Manning MC, Chou DK, Murphy BM, Payne RW, Katayama DS. Stability of protein pharmaceuticals: an update. Pharm Res 2010;27:544-575.

Manning MC, Patel K, Borchardt RT. Stability of protein pharmaceuticals. Pharm Res 1989;6:903-918.

Maste MCL, Pap EHW, van Hoek AV, Norde W, Visser AJWG. Spectroscopic investigation of the structure of a protein adsorbed on a hydrophobic latex. J Colloid Interface Sci 1996;180:632-633.

Mitraki A, King J. Protein folding intermediates and inclusion body formation. Nat Biotechnol 1989;7:690-697.

Narhi LO, Kenney WC, Arakawa T. Conformational changes of recombinant human granulocyte-colony stimulating factor induced by pH and guanidine hydrochloride. J Protein Chem 1991;10:359-367.

Narhi LO, Schmit J, Bechtold-Peters K, Sharma D. Classification of protein aggregates. J Pharm Sci 2012;101:493-498.

Norde W. Adsorption of proteins from solution at the solid-liquid interface. Adv Colloid Interface Sci 1986;25:267-340.

Oh-eda M, Hasegawa M, Hattori K, Kuboniwa H, Kojima T, Orita T, Tomonou K, Yamazaki T, Ochi N. O-linked sugar chain of human granulocyte colony-stimulating factor protects it against polymerization and denaturation allowing it to retain its biological activity. J Biol Chem 1990;265:11432-11435.

Otzen DE, Knudsen BR, Aachmann F, Larsen KIML, Wimmer R. Structural basis for cyclodestrins‘ suppression of human growth hormone aggregation. Protein Sci 2002;11:1779-1787.

Pastore A, Temussi P. Protein aggregation and misfolding: good or evil? J Phys Condens Matter 2012;24:244101-244109.

Patra AK, Mukhopadhyay R, Mukhija R, Krishnan A, Garg LC, Panda AK. Optimization of inclusion body solubilization and renaturation of recombinant human growth hormone from Escherichia coli. Protein Expr Purif 2000;18:182-192.

Pearlman R, Wang JY. Stability and characterization of human growth hormone. In Pearlman R, Wang JY, editors. Stability and Characterization of Protein and Peptide Drugs: Case Histories. New York: Plenum Press; 1993. p 1-58.

Philo JS, Arakawa T. Mechanisms of protein aggregation. Curr Pharm Biotechnol 2009;10:348-351.

Raso SW, Abel J, Barnes JM, Maloney KM, Pipes G, Treuheit MJ, King J, Brems DN. Aggregation of granulocyte-colony stimulating factor in vitro involves a conformationally altered monomeric state. Protein Sci 2005;14:2246-2257.

Rathore N, Rajan RS. Current perspectives on stability of protein drug products during formulation, fill and finish operations. Biotechnol Prog 2008;24:504-514.

Riggin RM, Farid NA. Analytical chemistry of therapeutic proteins. In Horvath C, Nikelly JG, Analytical Biotechnology: Capillary Electrophoresis and Chromatography. Washington DC: American Chemical Society; 1990. p 113-126.

Roberts CJ. Kinetics of irreversible protein aggregation: analysis of extended Lumry-Eyring models and implications for predicting protein shelf life. J Phys Chem B 2003;107:1194-1207.

Rosenberg AS. Effects of protein aggregates: an immunologic perspective. AAPS J 2006;8:E501-E507.

Ross CA, Poirier MA. Protein aggregation and neurodegenerative disease. Nat Med 2004;10:S10-S17.

Sadana A. Protein adsorption and inactivation on surfaces. Influence of heterogeneities. Chem Rev 1992;92:1799-1818.

Schein CH. Solubility as a function of protein structure and solvent components. Nat Biotechnol 1990;8:308-317.

Simon S, Krause HJ, Weber C, Peukert W. Physical degradation of proteins in well-defined fluid flows studied within a four-roll apparatus. Biotechnol Bioeng 2011;108:2914-2922.

Singh SM, Eshwari ANS, Garg LC, Panda AK. Isolation, solubilization, refolding, and chromatographic purification of human growth hormone from inclusion bodies of Escherichia coli cells: a case study. Methods Mol Biol 2005;308:163-176.

Stefani M, Dobson CM. Protein aggregation and aggregate toxicity: new insights into protein folding, misfolding diseases and biological evolution. J Mol Med 2003;81:678-699.

Su TJ, Lu JR, Thomas RK, Cui ZF, Penfold J. The adsorption of lysozyme at the silica-water interface: a neutron reflection study. J Colloid Interface Sci 1998;203:419-429.

Thomas CR, Geer D. Effects of shear on proteins in solution. Biotechnol Lett 2011;33:443-456.

Townsend AA, Nakai S. Relationships between hydrophobicity and foaming characteristics of food proteins. J Food Sci 1983;48:588-594.

Virkar PD, Narendranathan TJ, Hoare M, Dunnill P. Studies of the effect of shear on globular proteins: extension to high shear fields and to pumps. Biotechnol Bioeng 1981;23:425-429.

de Vos AM, Ultsch M, Kossiakoff AA. Human growth hormone and extracellular domain of its receptor: crystal structure of the complex. Science 1992;255:306-312.

Walstra P. Effect of agitation on proteins. In: Dickinson E, Miller R, editors. Food colloids: fundamentals of formulation. Cambridge: Royal Society of Chemistry; 2001. p 245–254.

Wang W. Instability, stabilization, and formulation of liquid protein pharmaceuticals. Int J Pharm 1999;185:129-188.

Wang W, Nema S, Teagarden D. Protein aggregation – pathways and influencing factors. Int J Pharm 2010;390:89-99.

Wang X, Hammer ND, Chapman MR. The molecular basis of functional bacterial amyloid polymerization and nucleation. J Biol Chem 2008;283:21530-21539.

Weiss WF, Young TM, Roberts CJ. Principles, approaches, and challenges for predicting protein aggregation rates and shelf life. J Pharm Sci 2009;98:1246-1277.

Wilde PJ. Interfaces: their role in foam and emulsion behavior. Curr Opin Colloid Interface Sci 2000;5:176-181.

Yampolskaya G, Platikanov D. Proteins at fluid interfaces: adsorption layers and thin liquid films. Adv Colloid Interface Sci 2006;128-130:159-183.

Zink T, Ross A, Lüers K, Cieslar C, Rudolph R, Holak TA. Structure and dynamics of the human granulocyte colony-stimulating factor determined by NMR spectroscopy. Loop mobility in a four-helix-bundle protein. Biochemistry 1994;33:8453-8463.

Zoungrana T, Findenegg GH, Norde W. Structure, stability and activity of adsorbed enzymes. J Colloid Interface Sci 1997;190:437-448.

## 2 Shaking and stirring: comparison of accelerated stress conditions applied to the human growth hormone

Submitted to Process Biochemistry

# Shaking and stirring: comparison of accelerated stress conditions applied to the human growth hormone

Johanna Wiesbauer[1,2], Massimiliano Cardinale[3] and Bernd Nidetzky[1,2] *

[1]*Research Center Pharmaceutical Engineering, Graz, Austria*

[2]*Institute of Biotechnology and Biochemical Engineering, University of Technology Graz, Austria; telephone: +43 316 873 8400; fax: +43 316 873 8434,*

*e-mail: bernd.nidetzky@tugraz.at*

[3]*Institute of Environmental Biotechnology, University of Technology Graz, Austria*

* *Corresponding author*: Nidetzky, B. (bernd.nidetzky@tugraz.at).

**ABSTRACT**

Shaking or stirring in a miniaturized device is often applied in the development of protein pharmaceuticals, serving as a test of stability under conditions that mimic the physical stresses of the real process. The overall purpose of these "stress tests" is to accelerate protein aggregation that would otherwise take place at a much slower rate, thereby enhancing experimental throughput to speed up the determination of critical process parameters of stability. Results are often used to determine critical parameters for formulation development. However, shaking differs from stirring in the forces applied on proteins in solution and therefore, there is concern that characteristics of protein stability interrogated with each method may not be the same. We have performed a detailed, time-resolved analysis of nonnative aggregation of the human growth hormone (hGH), exposed to stirring and shaking in a well-defined and comparable mini-reactor set-up. We show that aggregation of hGH is not the result of protein deamidation that occurs as accompaniment of the incubation conditions used. We also show that both under stirring and shaking, the protein undergoes phase transitions from solution into mainly circular particles, whereas only minor amounts of soluble aggregates are detected. The precipitate contains partly unfolded protein that has a substantial amount of hydrophobic surface exposed. An air-liquid interface, constantly renewed by stirring or shaking, was identified to be mainly responsible for aggregation of hGH under each of the stress conditions applied.

**Keywords:** protein aggregation; stability; mechanical stress; stirring; shaking; air-liquid interface; accelerated stress test

## 1. Introduction

The shelf life of protein drugs is often critically impaired by chemical and physical instabilities [1-3] of the active pharmaceutical ingredient (API). Formation of protein aggregates (native or nonnative) is a common manifestation of these instabilities [3-7]. Nonnative aggregation is described by the assembly of initially native proteins into aggregates exposing nonnative protein structures [4]. In terms of definitions we can also distinguish protein association and aggregation. Protein association is often described as a reversible process, where two or more native protein molecules associate and often lead to reversible precipitation [7]. Aggregation is considered to be mainly irreversible if no drastic changes in the solvent environment are performed. The interacting proteins can be partially unfolded or even denatured [7,8]. Even though nonnative aggregation has been emphasized particularly in association with protein formulation and storage, it constitutes a problem of drug manufacture in general. Aggregation potentially occurs in each phase of the production chain [1,9,10], including protein biosynthesis and purification as well as formulation [4,11,12]. Drugs containing nonnative protein aggregates may display reduced pharmacological activity or worse, their administration results in immune reactions [13]. Therefore, the amount of aggregates in the final product has to be monitored, reduced and controlled.

Antagonizing and controlling API aggregation at all stages of production would seem to be a compelling solution. However, rational design of API production and drug formulation for suppressed protein aggregation is difficult due to the molecular [8] and kinetic [12,14-16] complexities of the denaturation pathways involved in the aggregation. Experimental determination of critical parameters regarding stability and composition of formulations is laborious and therefore constitutes a potential bottleneck of the overall development. Therefore stressing times of 24-48 h would be preferred in the initial formulation development stage [17] in comparison to the ICH thermal stability testing guidelines of several months [18]. A

critical requirement is the availability of advanced methodology, allowing for fast (high-throughput) measurement of protein aggregation at miniature scale, under conditions that reproduce relevant features of the real process. A defining characteristic of the so-called "stress tests" is that they try to augment the denaturing conditions of different process steps (e.g. fill-and-finish operations [10,19], mixing in general, transport, storage) [3,17,20-24] to accelerate the aggregation that would otherwise take place at rate by far too slow to enable data collection in a reasonable time. The external stresses used to enhance protein aggregation can be divided according to the possible involvement of interfacial effects in the denaturation. Factors such as temperature, pH, and additives are effective in the liquid bulk whereas stirring, shaking, and other types of agitation usually implicate interaction of the protein with different interfaces (gas, solid, liquid) [1,4-6,14,24,25].

In this study, we focus on stirring and shaking as the two most commonly used "accelerated stress" methods for examining the role of agitation on API stability [3,11,16,23]. Even though the actual forces applied on the protein are generally not well defined during stirring and shaking [20], there is consensus that the information on protein stability provided by both methods could be highly useful in the development of strategies for API stabilization [17,20,23,26]. However, recent studies of IgG1 antibody stability [17,23] revealed that insoluble protein aggregates produced by stirring and shaking differed not only in size but also in regard to the relative amount of non-covalent associates formed. Therefore, the pathways leading to aggregation under shaking and stirring may not be the same, and this raises the concern that the properties of stability interrogated by the two methods might be fundamentally different. Therefore a critical evaluation and characterization of stirring and shaking might be needed regarding screening of stability and robustness of pharmaceutical proteins and formulations. .Unlike shearing, which *per se* is thought to have minor effects on protein stability, shaking and stirring are usually performed in the presence of a gas-liquid interface as well as a solid/liquid interface [20,27], implying that various additional factors of protein denatura-

tion come into play. Shaking is described to constantly renew the gas-liquid interface in the system. Protein may become adsorbed to this interface and undergo partial unfolding there. Aggregation may be part of the denaturation occurring at the interface, or it could also take place while or after the (partly) denatured protein has been transported back into solution [23,28-32]. Several studies have examined the role of the liquid fill level during shaking, considering that incomplete filling increases the gas-liquid interface [21,23,33].

For stirring, the applied stress is usually thought to result from the combined effects of shear, protein-deforming forces at gas-liquid and liquid-solid interfaces, cavitation, and local temperature gradients [34]. A number of studies have attempted to disentangle the individual components of the overall stress of stirring [19,21,22,24,33,35,36]. A common conclusion is that shear does not constitute a dominant force [37-39]. It was shown that small globular proteins are not sensitive to shear alone [21,22,36,40,41], and this view has recently been extended to antibodies [20]. Force calculations revealed that very high shear rates would be necessary to deform most proteins, whereas air-liquid interfaces possess high deformation energies [24,42]. Recent studies showed that elongation flows in regions of shear gradients, e.g. during filling processes, can lead to aggregation even at moderate shear conditions [19,43].

In summary, therefore, a number of important issues concerning the application of shaking and stirring as “accelerated stress” and screening tests for the analysis of protein stability require clarification. For practical use, it is perhaps most relevant to determine if the two methods, compared under suitable conditions, show equivalent denaturation. Considering that in the majority of the reported set-ups for stirring or shaking, hydrodynamic and interfacial forces were combined to a largely unknown extent [24], it is also vital to identify the dominating parameter of aggregation in these systems. This would also facilitate extrapolation of the results of “accelerated stress” tests between the different methods used as well as to the conditions of the real process [14,15,44]. A critical requirement is, therefore, that shaking and stir-

ring are analyzed in a comparable experimental design. We have performed this work, using the human growth hormone (hGH) as a model protein [45-47]. hGH was chosen because characteristics of its stability in solution have been very well characterized [48-50]. Denaturation of hGH under conditions of vortex mixing [51,52], shearing [22] and shaking [26,53,54] has been examined, providing important information for the design of our experimental set-up and for selection of relevant analytical tools. Further these studies suggest that nonnative aggregates are found due to the formation of beta-sheet enriched structures (nonnative aggregates) [26,53,55]. Moreover, aside from being an important API itself, hGH also serves to represent the group of long-chain cytokines [56-58] that are collectively of substantial pharmaceutical interest.

A detailed time-resolved analysis of destabilizing steps involved in nonnative aggregation of hGH under stirred and shaken incubation conditions was carried out. One general aspect not addressed closely in previous studies concerns the possibility that physical denaturation/unfolding is accompanied by chemical modification, and that these processes take place in a mutual dependence one of another. We show that in hGH, aggregation occurs uncoupled from deamidation, which is the major chemical modification of this protein in solution [47,59,60]. Even though biological activity of deamidated hGH is known to be equal to that of the native protein [60,61], deamidation is generally undesired because of the structural heterogeneity that it introduces to a given protein preparation [1,2,62]. We further show that for hGH, during controlled shaking and stirring, the gas-liquid interface which is constantly renewed is mainly responsible for the aggregation under each of the stress conditions applied.

## 2. Materials and Methods

### 2.1. Materials

A recombinant preparation of hGH produced in *E. coli*, termed rhGH, was kindly supplied by Sandoz GmbH (Kundl, Austria). The protein was provided in 10 mM sodium phosphate buffer, pH 7.0. The pI of hGH is at approximately 5.3 [7,46]. The protein concentration of the stock solution was 10.0 ± 0.4 mg/mL. Prior to use, the bulk solution was filtered using 0.22 µm PVDF filters from Millipore (Carrigtwohill, Ireland). Unless noted otherwise, all chemicals were bought from Carl Roth (Karlsruhe, Germany). Fluorescein 5(6)-isothiocyanate (FITC) was from Sigma Aldrich (Vienna, Austria), and 8-anilino-1-naphthalenesulfonic acid ammonium salt (ANSA) was from Merck KGaA (Darmstadt, Germany). Molecular mass marker proteins were from GE Healthcare (Vienna, Austria). SlowFade® Gold Antifade Reagent was from Molecular Probes (Eugene, OR, USA). Erlenmeyer flasks (25 mL, NS 14/23) were from Carl Roth.

### 2.2. Accelerated stress methods

#### 2.2.1. Denaturation at elevated temperature

Experiments were performed in miniature Erlenmeyer flasks (Supporting Figure S1). rhGH stock solution was diluted to a concentration of 3.4 ± 0.3 mg/mL using 10 mM sodium phosphate buffer, pH 7.0 (25 °C). Incubations were carried out at 45 ± 2 °C using static incubation conditions or stirring at 250 rpm on a Thermo Scientific Telesystem 60 magnetic stirring plate (Vienna, Austria). Note: the melting point of hGH was determined as 80 °C [54], implying that temperature stress of 45 °C should not promote complete unfolding of the rhGH used. The used magnetic stirrer bars were coated with polytetrafluoroethylene (PTFE) and had dimensions of 6 × 25 mm. An alternative set-up used stirring at 300 rpm on an IKA RCT magnetic stirrer (Staufen, Germany). Unstirred incubation at 25 °C was used as reference for all

experiments. Each experiment was performed at least in duplicate. Table 1 summarizes key physical parameters for the set-ups used: gas-liquid interfacial area, Reynolds number, and shear rate.

To monitor the course of protein aggregation, samples (600 µL) were taken at certain times and analyzed with different techniques that are described below. Typically, UV absorbance (280 nm) and turbidity (400 nm) measurements were performed. Size exclusion and reversed phase HPLC (SEC-HPLC; RP-HPLC) as well as anionic non-denaturing PAGE (native PAGE) were used.

*2.2.2. Shaking and stirring*

A jacketed miniature reactor fabricated from borosilicate glass 3.3 was used. The reactor had cylindrical geometry with a diameter of 32 mm with a filling level of 1.4 cm, corresponding to a liquid volume of 12 mL (Supporting Figure S1). The reactor was closed with a PP capping and a Teflon fitting during all experiments, but the sample solution was never in contact with the capping material. Under static conditions, therefore, the gas-liquid interface was calculated as 804 mm² (Table 1). Experiments were performed at constant temperature (25 °C) that was controlled with a Julabo F25 Refrigerated/Heating Circulator (Seelbach, Germany). Stirring was done with a PTFE-coated magnetic stirrer bar (6 × 30 mm), using control from an IKA RCT basic stirrer. Shaking was carried out by fixing the glass reactor in a Sartorius Shaker Certomat BS-1 that was operated at an agitation rate of 300 rpm (shaking diameter: 5 cm) with temperature controlled at 25 °C.

For experiments with reduced air-liquid interface (190 mm²) an overall volume of 55 ml (Supporting Figure S2 and Table 1) was used. Note: we took care that the volume change resulting from the number of samples taken did not cause large changes in the available gas-

liquid surface area and therefore only 300 µL samples were taken over time (Figure S1, liquid level always within the three nozzles).

The hGH concentration used was 3.4 ± 0.3 mg/mL. Incubations were performed over a representative time-span that varied between a few hours to several days, depending on the aggregation rate. Samples (600 µL) were taken at suitable times, centrifuged at 13,200 rpm for 10 min to remove precipitated protein, and the supernatant was used for further analyses. To test for reversibility of the observed aggregation [2], we used an aliquot of the sample to prepare a series of dilutions in buffer (undiluted, 1:2, 1:5, 1:10) and incubated these at 4 °C for a week.

*2.3. Analytical methods*

*2.3.1. Protein concentration determination*

Protein concentration was determined using UV absorbance at 280 nm. In order to detect artifacts due to turbidity all measurements were carried out as wavelength scans. Furthermore turbid samples were centrifuged at 13,200 rpm for 10 min. A molar extinction coefficient of 17,670 $cm^{-1}M^{-1}$ was calculated using the ProtParam tool at the ExPASy webserver [63,64]. A molecular mass of 22,125 Da was assumed.

*2.3.2. Turbidimetric analysis*

For turbidity measurements wavelength scans were carried out using a Beckmann DU 800 spectrophotometer and the spectra were analyzed at 400 nm [52,65,66]. The instrument was calibrated against formazin reference suspensions [67]. All measurements were performed in triplicate at 25 °C.

*2.3.3. Size exclusion (SEC)-HPLC and reversed phase (RP)-HPLC analysis*

A Zorbax GF-250 column (Silica, 4 µm, 250 × 9.4 mm) and a Zorbax 300 Extend C18 column (3.5 µm, 100 × 4.6 mm) were obtained from Agilent (Waghaeusel-Wiesental, Germany). Analyses were carried out using a Merck-Hitachi LaChrome LC system equipped with a L-7250 autosampler and a L-7400 UV detector. All samples were centrifuged prior to analysis at 13,200 rpm for 10 min.

SEC-HPLC was used to detect soluble protein aggregates. It was done with the GF-250 column at 30 °C, applying a constant flow rate of 1 mL/min. The mobile phase was 50 mM $NH_4HCO_3$ in the pH range 7.8 - 8.2. Each sample was analyzed for 15 min. Absorbance detection at 214 nm was used.

RP-HPLC was used to detect hGH variants that have undergone chemical modification, in particular deamidation [60,61]. The C18 column was operated at 50 °C. A gradient of buffers A (10 % $CH_3CN$, 10.5 mM $NH_4HCO_3$, 0.105 mM EDTA) and B (70 % $CH_3CN$, 6.0 mM $NH_4HCO_3$, 0.060 mM EDTA) was used for elution. A linear ramp from 60 % to 95 % buffer B within 23 min was used. Then, after a 2-min equilibration with 95 % buffer B, a linear decrease to 60 % buffer B was applied in 1 min, and the analysis was continued under these conditions for 6 min. The flow rate was 1.0 mL/min, and absorbance was recorded at 210 nm. Before the analysis, all samples were diluted to a final protein concentration of 1 mg/mL, using glycine solution (20 mg/mL) of pH 7.0. Figure S2 shows an absorbance trace for a representative hGH sample that was analyzed. It is known from previous studies that oxidized and deamidated forms of hGH partially overlap in RP-HPLC analysis under the conditions used. Therefore, we focused on the main deamidated protein form, resulting from conversion of $Asn^{149}$ into Asp that is resolved well with the method applied. Further note that the exact identification of each deamidated or oxidized species was beyond the scope of this study. With the reasonable assumption that deamidation at $Asn^{149}$ does not change the UV absorbance of

hGH, native protein was used for peak area calibration and for calculation of molar deamidation rates.

*2.3.4. Analysis by PAGE*

We performed non-denaturing anionic PAGE and non-reducing SDS PAGE, using 12.5 % acrylamide in each case. The protein loading was between 5 to 15 µg. Gels were stained using Coomassie Brilliant Blue.

*2.3.5. Fluorescence measurements*

Measurements were done on a software-driven Hitachi F-4500 fluorescence spectrophotometer (Tokyo, Japan). Intrinsic tryptophan fluorescence was recorded at 25 °C, using an excitation wavelength of 295 nm. Emission spectra were obtained in the range 300 – 500 nm. Slit widths of 5 nm were used. The centrifuged samples were diluted to a concentration of 0.5 mg/mL. The native protein shows maximum emission at 333 to 335 nm, while for unfolded hGH, this value is at around 350 nm [46,68].

Measurement of solvent-accessible hydrophobic protein surface was done with the fluorescent dye 8-anilino-1-naphthalenesulfonic acid ammonium salt (ANSA) as reported for hGH (Ali, Prakash, Kulkarni, Ahmad, & Bhakuni, 1999; Narendra B Bam et al., 1996; Hawe, Sutter, & Jiskoot, 2008). The dye was mixed with protein in a molar ratio of 10:1 [72]. Therefore, 60 µL of ANSA solution (1.0 mM) were added to 600 µL of a solution of 0.25 mg/mL hGH (0.01 mM) at 25 °C. Excitation was at 388 nm, and emission was recorded between 400 and 650 nm. The emission is shifted from about 490 nm in aqueous environment to smaller wavelengths in unpolar environment. Note: In order to avoid scattering artifacts due to turbid samples ANSA-binding measurements were carried out only using samples in which protein precipitate had been carefully removed by centrifugation.

*2.3.6. Confocal laser scanning microscopy (CLSM)*

To visualize precipitated hGH by CLSM, labeling by FITC or ANSA was used. FITC was dissolved in DMSO and further diluted 1:5 with 10 mM sodium phosphate buffer, pH 7.0. Ten µL of this solution were incubated with 100 µL suspension of protein aggregate over night. Then, dialysis against buffer was performed. Labeling with ANSA was done in the presence of 10 mM dye. In order to prevent diffusion during the z-axis scan, all samples were dried and covered with Slow Fade Gold Antifade reagent.

CLSM images were acquired with a Leica TCS SPE confocal system (Leica Microsystems, Mannheim, Germany) equipped with solid state and UV lasers. The Images were generated by maximum projection of the individual confocal layers. ANSA measurements were carried out with laser excitation at 405 nm and detection of emitted light from 440 to 500 nm. For FITC measurements, a 488 nm laser and an emission bandwidth of 500 – 554 nm was used. All images were acquired with 400-fold magnification and with a picture size of 1024 × 1024 pixel. Three-dimensional confocal models were created with the software IMARIS 7.0 (Bitplane, Zurich, Switzerland). Data processing of the maximum projections was performed using ImageJ [73]. We chose circularity as shape descriptor of the insoluble protein particles. According to the software, this parameter is defined by $C = 4\pi \times [\text{area}] / [\text{perimeter}]^2$, and a C value of 1.0 indicates a perfect circle.

## 3. Results and Discussion

*3.1. Involvement of chemical protein modification in aggregation of hGH*

Partial deamidation of asparagine and glutamine residues is a well-known chemical modification of proteins that can occur at various stages of biopharmaceutical production as well as during transport and storage [1-3,7,74,75].

**Table 1: Accelerated stress conditions used to examine aggregation of hGH.**

| Stress type | Volume ($\times 10^{-6}$ m³) | Air-liquid interface ($\times 10^{-6}$ m²) | *Re* number | Shear rate ($s^{-1}$) | hGH aggregation |
|---|---|---|---|---|---|
| Control | 11.4 | 800 | 0 | 0 | None |
| Temperature | 11.4 | 1,200 | 0 | 0 | None, deamidation |
| Temperature, Stirring [a] | 11.4 | 1,200 [c] | 3,400 | 35-85 | Precipitation,turbidity formation, deamidation |
| Stirring [b] | 11.4 | 1,090 [c] | 4,800 | 40-100 [d] | Precipitation,turbidity formation |
| Stirring [b] | 54.7 | 190 | 4,800 | 40-100 [d] | None |
| Shaking | 11.4 | n.d. (» 1,090) [c] | 5,500 | 90 [d] | Precipitation,turbidity formation |
| Shaking | 54.7 | 190 | 5,500 | 20 [d] | None |

[a], [b] Stirring bar dimensions were 6 × 25 mm [a] or 6 × 30 mm [b].

[c] The surface area was calculated assuming a paraboloid of revolution; see the Supporting Information under Table S1. For shaking, the surface area could not be determined (n.d.). Entrainment of air bubbles under conditions of shaking and stirring is shown in Figure S7, indicating that surface area produced by shaking is probably larger than that produced by stirring.

[d] The Supporting Information shows determination of *Re* numbers and shear rates for the different conditions used [85-87]

For deamidation of hGH, $Asn^{149}$ was identified as the major site of modification [47,60]. However, an important characteristic of deamidation of hGH has not been established, and this concerns the relationship between protein chemical modification and aggregation. From studies of proteins other than hGH, it is not possible to infer a clear trend regarding the effect of deamidation on the aggregation propensity (increased or reduced effects) [1,7]. We therefore analyzed the deamidation of hGH at room temperature and under conditions of temperature stress (45 °C), applying static incubation or stirring at 300 rpm. Deamidation rates calculated from HPLC data were compared to the corresponding aggregation rates that were also measured (Table 2).

**Table 2: $Asn^{149}$ deamidation rates in hGH exposed to stresses of elevated temperature and stirring.**

| Conditions [a] | Deamidation rate (μM/h) |
|---|---|
| Non-agitated control (25 °C) | 0.015 ± 0.002 |
| Shaking at 25 °C | 0.028 ± 0.004 |
| Stirring at 25 °C | 0.037 ± 0.004 |
| Non-agitated incubation at 45 °C | 0.16 ± 0.01 |
| Stirring at 45 °C | 0.16 ± 0.01 [b] |

[a] Incubations were performed in Erlenmeyer flasks (Figure S1)

[b] *t*-test analysis showed that deamidation rates at 45 °C under stirred and non-agitated conditions are identical at *P*-level of 0.05.

We first applied non-denaturing PAGE to samples taken from the different incubations, considering that deamidation of hGH should be detectable overall by a corresponding decrease in protein mass-to-charge ratio, resulting in a greater mobility of the modified protein species in the gel [60,76]. Figure 1 shows that while hGH appears to have been completely stable at 25 °C, incubation at the elevated temperature went along with gradual transformation of the native protein into another, faster migrating form, as expected (lane 1-8). Further it is shown that aggregation could be only detected if the samples were stirred (Figure 1, lanes 5, 7 and 8). Addition of stirring as a second stress factor did not significantly change the pattern of protein denaturation at 45 °C, as observable by PAGE.

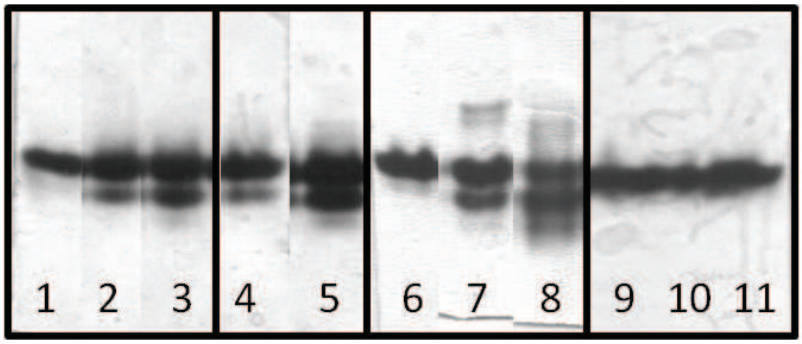


**Figure 1: Chemical modification and aggregation of hGH monitored by non-denaturing anionic PAGE.** Lanes 1-3: 45°C, no stirring; 0 h, 32.5 h, and 69.5 h. Lanes 4 and 5: 45 °C, stirring at 300 rpm; 32.5 h and 69.5 h. Lanes 6-8: 45°C, MSP stirring ; 0 h, 14 h, and 70 h. Lanes 9-11: 25 °C, no stirring: 26 h, 55 h, and 69 h.

We therefore examined aggregation of hGH at the elevated temperature and show results of turbidity measurements in Figure 2. Interestingly, solutions of hGH incubated under static conditions remained clear, irrespective of the applied temperature (25 or 45 °C). By contrast, protein solutions subjected to stirring became turbid within about a day, and the rate of formation of turbidity appeared to have been independent of the temperature used. Results at 400 and 350 nm show similar trends and therefore we exclude possible artifacts like

chromophores [65]. Note that the observed aggregation of hGH was not detectably reversible upon cooling or dilution of the sample in the absence of agitation over 10 days [2]. Therefore we consider the observed aggregation to be irreversible, as long as we do not change the solvent conditions or add cosolutes like SDS or chaotropic reagents [2,7]. We then applied analysis by RP-HPLC to clarify the suggestion from Figure 1 that incubation at 45 °C was responsible for deamidation of hGH. Samples taken from non-agitated and stirred incubations were shown to have undergone deamidation at $Asn^{149}$ to a substantial extent, up to 40 % ($Asp^{149}$) after incubation for about 3 days. The HPLC data revealed a roughly linear dependence of conversion of $Asn^{149}$ on the incubation time in the early phase of deamidation (Figure S3). We therefore calculated an apparent $Asn^{149}$ deamidation rate for each of the different incubations carried out. The results are summarized in Table 2, showing that deamidation was accelerated (about fivefold) by the temperature increase 25 $\rightarrow$ 45 °C whereas the effect of stirring on the deamidation rate at constant temperature was hardly significant. The evidence presented in Table 2 is interpreted to rule out deamidation of $Asn^{149}$ as a relevant molecular factor on aggregation of hGH under the conditions used. Mechanical agitation by stirring clearly drives the aggregation of hGH, and the step or steps controlling the aggregation rate under these conditions are not strongly dependent on temperature in the range 25 – 45 °C.

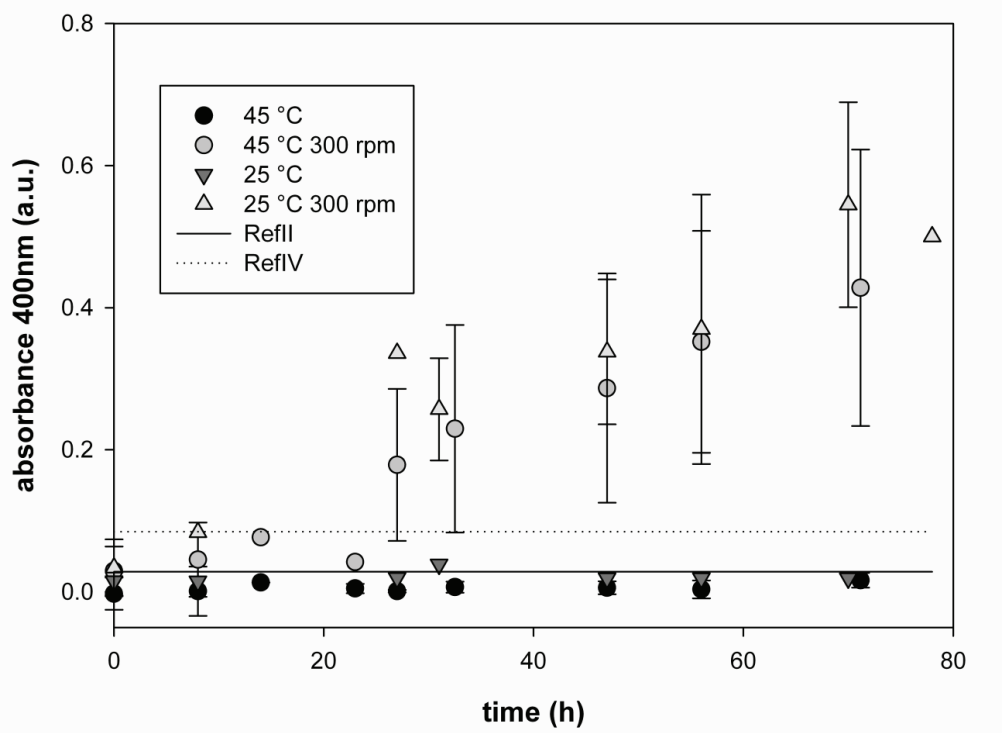


**Figure 2: Turbidity formation during exposure of hGH to stresses of at elevated temperature and stirring**

Turbidity is measured as absorbance at 400 nm. Results are mean values and standard deviation of triplicate experiments. Ref II and Ref IV are formazine reference measurements, shown as solid and broken line, respectively.

We applied SEC-HPLC for the analysis of samples from stirring experiments that showed aggregation to a varying degree (Figure S4), examining the formation of soluble protein associates during aggregation. Figure S4 depicts a representative UV absorbance trace obtained with the method used. Even though we were able to detect *the presence* of oligomeric forms of hGH, we could also show that these soluble aggregates had accumulated in extremely tiny amounts. Now, one can always argue that the composition of the sample may have been altered during the (off-line) analysis, because of dissociation of the reversibly aggregated proteins in solution, for example. Even though this possibility remains in principle, it is not very likely considering that an alternative method of direct detection of soluble oligomers (non-denaturing PAGE) also failed to reveal soluble hGH associates. Moreover, we could also demonstrate that the result of the SEC-HPLC analysis was not affected by variation

in the protocol of sample preparation (e.g. use of variable centrifugal force for removal of precipitated protein). We therefore think that the formation of aggregation-prone protein species during incubation of hGH under stirring is immediately followed by association into high molecular mass assemblies, which precipitate. The aggregation of hGH under agitated conditions was therefore examined in detail, comparing shaking and stirring.

*3.2. Effects of shaking and stirring on soluble-to-insoluble phase transition for hGH*

All experiments were carried out using the miniature reactor described under Materials and Methods. Using UV absorbance of the supernatant removal of precipitated protein by centrifugation, we first determined the change in soluble protein concentration in dependence of the incubation time. Figure 3 shows the results.

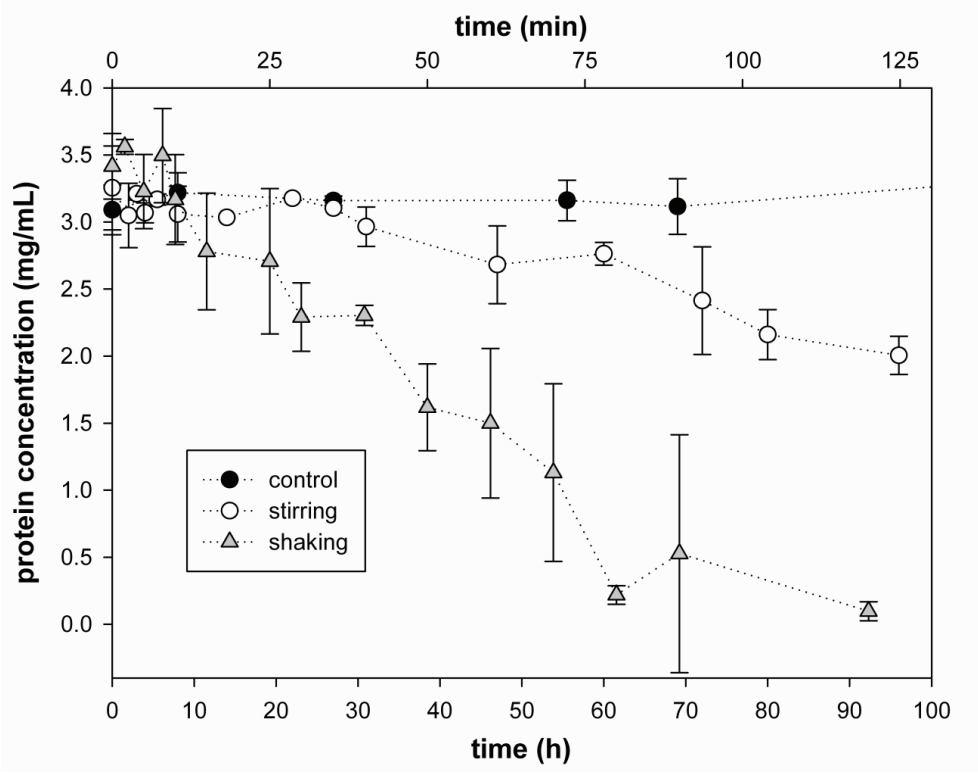


**Figure 3: Precipitation of hGH under stress of stirring and shaking at 25 °C**

The time axis for the non-agitated control and the stirring experiment is in h. The time axis for the shaking experiment is in min.

Shaking of the hGH solution went along with massive phase transition from soluble protein to an insoluble precipitate. Stirring also caused precipitation of hGH, however, less dramatic so than shaking. The non-agitated control carried out under otherwise identical conditions was stable (no precipitation). The time course of precipitation of hGH under stirring stress (Figure 3) displayed a distinct lag phase over 35 h in which the concentration of the protein in solution appeared to have been stable. When shaking was used, the lag phase was also present, but it was much shorter and less distinct than in the shaking experiment. We determined that the rate of precipitation of hGH was much (200-fold) higher during shaking as compared to stirring.

Table 1 shows that differences in bulk fluid dynamics for the stirred and shaken systems used are unlikely to have caused the large differences in precipitation rate. *Re* number and shear rate were in a well comparable range for the stirred and shaken reactors. We will discuss later that dynamic characteristics of the air-liquid interface might be the relevant factor causing the observed differences.

*3.3. Characterization of hGH aggregates formed under stress of stirring and shaking*

We applied different techniques in the analysis of the stressed hGH samples, trying to get deeper insight into the observed protein aggregation. Firstly, the possible involvement of covalent bonding during insoluble hGH aggregate formation was addressed using non-enaturing PAGE [26]. We show in Figure 4 that overall sample (i.e. supernatant *plus* precipitate) taken from the shaking and stirring experiments contained also protein species having a molecular mass higher than that of native protein. Lane 1 is the control sample at 0 h and should therefore be the same for all PAGE examples. The supernatant obtained after centrifugation of sample consisted mainly of protein having the expected mass of the native hGH monomer. In Figure 4b lanes 5 to 7 document the loss of soluble protein due to shaking (also see Figure 3 for comparison). Therefore, this indicates that protein oligomers present in the overall sample

are from the precipitate. Treatment of the sample with SDS in the absence of reducing agent resulted in complete dissolution of these oligomers, suggesting that they had been built exclusively from non-covalent interactions between constituent hGH monomers.

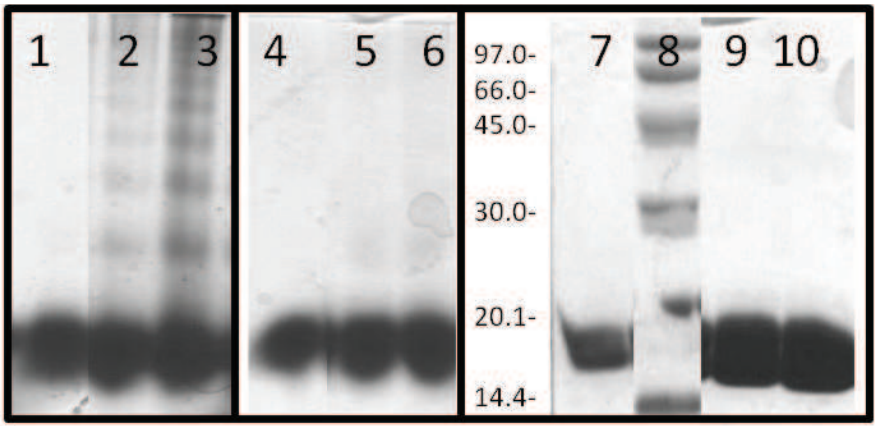


**Figure 4: Aggregation of hGH under stress of stirring and shaking, analyzed by non-denaturing and SDS PAGE**

*panel A: Non-denaturing (lanes 1 to 6) and SDS PAGE (lanes 7 to 10) of stirred samples*

(1-3) hGH total sample: 0 h, 30 h, and 72.5 h; (4-6) supernatant after centrifugation: 0 h, 54 h, 72.5 h; (7, 9, 10): 0 h, 54 h, and 72.5 h (total sample); (8) molecular mass standard.

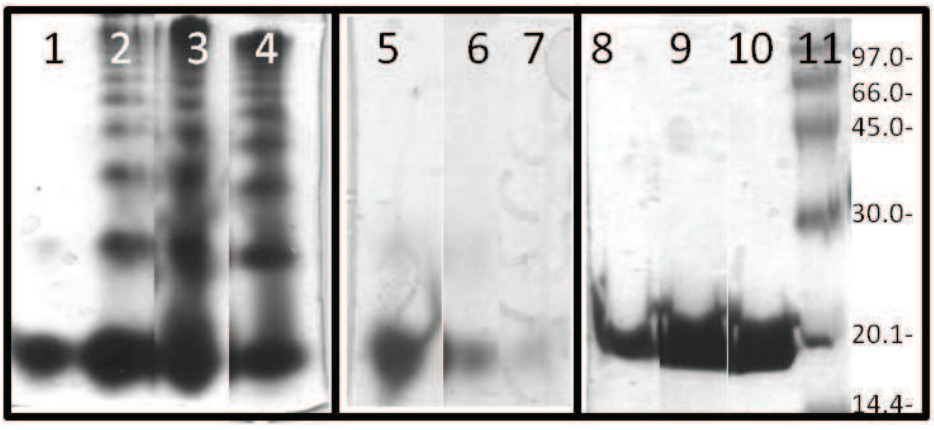


*panel B: Non-denaturing (lanes 1 to 7) and SDS PAGE (lanes 8 to 11) of samples from shaking*

(1-4) hGH total sample: 0 h, 10 min, 1 h, and 2 h; (5-7) supernatant after centrifugation: 0 min, 1 h, and 2 h; (8-10) (total sample) 0 h, 1 h, and 2 h; (11) molecular mass standard.

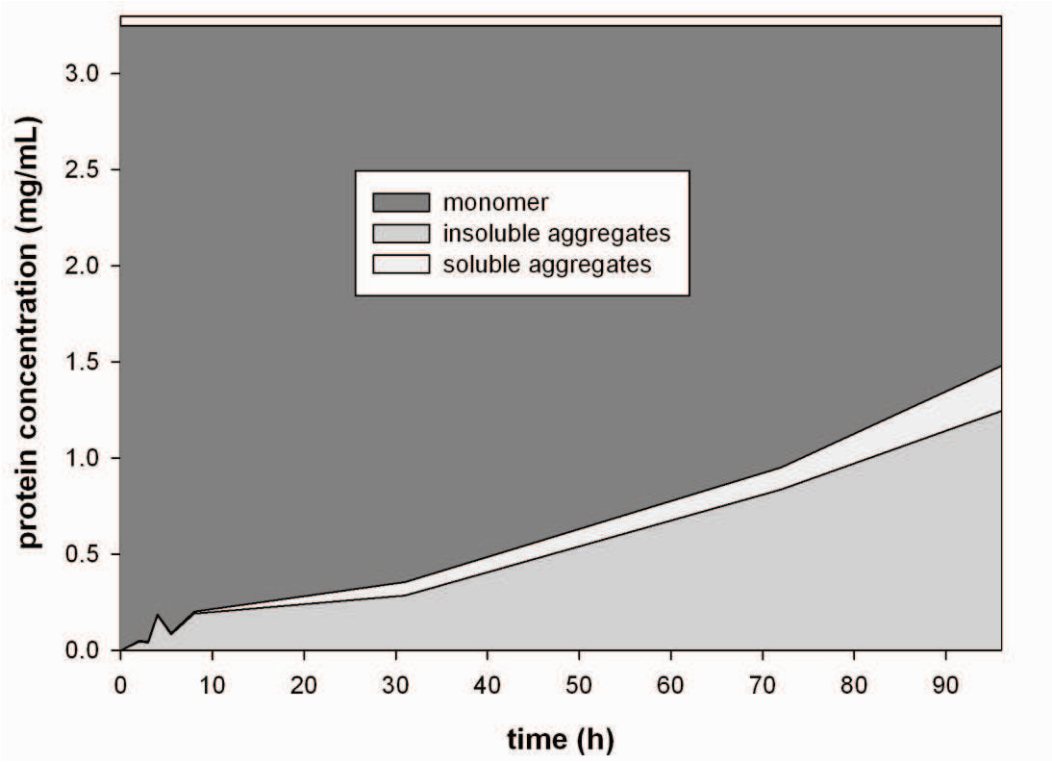


**Figure 5: Quantitative distribution of monomer, soluble aggregates and insoluble aggregates for stirring.**

The amount of insoluble precipitate and soluble protein was determined using UV measurements. The soluble protein fraction was further analyzed using SEC-HPLC analysis into monomer and associates.

Further, the finding of PAGE analysis that oligomeric protein was lacking in the soluble fraction of the stressed samples was confirmed using SEC-HPLC where only negligible amounts of oligomers were found (Figure 5 and S5). Precipitation of hGH was irreversible upon dilution or temperature change. The precipitate was however dissolved completely upon addition of SDS. In conclusion, therefore, precipitation of hGH does not involve intermolecular covalent bond formation.

A second approach was to apply spectroscopic probes of protein conformation in solution (intrinsic Trp fluorescence; binding of ANSA) to centrifuged samples taken from the stress experiments. ANSA fluorescence intensities normalized on protein concentration were unchanged over the time span of the experiment. Emission spectra for intrinsic Trp

fluoresence were hardly changed with respect to both emission wavelength and intensity in stressed hGH as compared to native protein. We conclude, therefore, that what remains in solution after the exposure of hGH to shaking or stirring is essentially the native protein monomer.

*3.4. Comparison of time dependences of turbidity and precipitate formation*

It is interesting to compare the time course of "protein aggregation" measured as increase in turbidity with the time course of protein precipitation from supernatant (Figure 6). Turbidity increased during the lag phase of the protein precipitation time course, and the amount of turbidity formed was slightly higher during stirring as compared to shaking (Figure 6). Note that in each experiment, the solution did not get turbid under conditions in which a high liquid level had minimized the air-liquid interface.

Generally, turbidity measurements cannot give information about size, shape and number of the scattering particles [65]. However, turbid hGH solutions were clear after centrifugation so that we can exclude artifacts of the measurement (e.g. Rayleigh scattering) [65,77]. Effective removal of turbidity by centrifugal force furthermore gives good evidence supporting the formation of high molecular weight hGH particles. Detailed size characterization of the particles was beyond the scope of this study. However, the available evidence points to a hypothetical scenario of hGH aggregation in which protein is partly unfolded through denaturing effects of the air-liquid interface; and aggregation prone hGH species coalesce rapidly into larger particles, generating the observed turbidity. The protein particles formed could also serve as nuclei for massive precipitation at later times during the incubation (see Colombie et al. (2001) for a similar denaturation pathway in lysozyme).

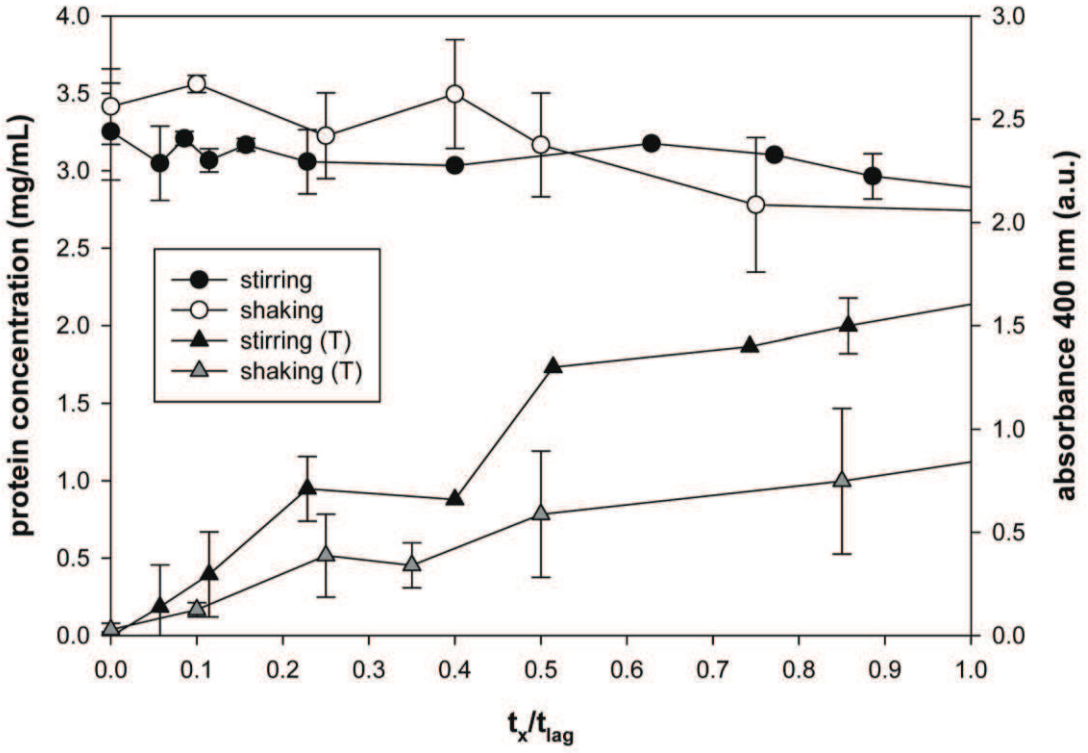


**Figure 6: Comparison of time dependence of turbidity formation and protein precipitation under the stress of stirring and shaking**

See Table 1 for the conditions used. The liquid fill level was 11.4 mL.

*3.5. Role of the air-liquid interface in promoting hGH aggregation*

In order to examine the proposed involvement of air-liquid interface in hGH denaturation, we increased the liquid level to decrease the interface (Table 1) and repeated the experiments for stirring and shaking. hGH did not precipitate under these modified conditions and appeared to be nearly as stable as in the non-agitated control, judging by data from PAGE analysis and turbidity measurements. These results support the idea that dynamic interactions between hGH and the air-liquid interface are mainly responsible for the observed aggregation and that the influence of the solid-liquid interface (reactor walls, magnetic stirrer) is only of minor importance (see also Table 1). Shaking and stirring with a reduced liquid level promote the renewal of the available interface and facilitate exchange of protein between liquid bulk and the interface. When no interface is present (high liquid level) or interfacial dynamics is lack-

ing (no agitation), the basis for protein denaturation is removed and hGH is therefore stable. Observation that hGH did not aggregate under stirred conditions when the liquid level was high further serves to indicate that denaturing effects of the stirrer bar on hGH can be ruled out rigorously. It was shown in studies of other proteins that stirrer bar abrasion could be a relevant factor, and protein adsorption to the stirrer bar has also been reported [78-81].

Observation that hGH aggregation (Figure 3: precipitation; Figure 6: turbidity formation and precipitation) was by two orders of magnitude faster during shaking as compared to stirring when parameters of bulk fluid dynamics (*Re*, shear rate) were similar for both conditions (Table 1; Table S1 in Supporting Information) can most probably be ascribed to differences in the available air-liquid surface area. We show in Figure S7 that entrainment of air bubbles into the liquid appears to have been substantially higher during shaking as compared to stirring, providing one possible explanation for the different aggregation rates under the two stress conditions.

*3.6. Characterization of the hGH precipitate using CLSM*

To obtain insights into the nature (size, shape, hydrophobicity) of the formed protein particles during hGH precipitation, we examined the turbid solutions using CLSM. Labeling of protein with FITC or ANSA was used, and each sample from stirring and shaking was analyzed for both labeling conditions. Several pictures were acquired for ImageJ particle analysis in an area of 275 × 275 μm, using different dilutions of the labeled protein suspension. Note, however, that the analysis done is restricted to a two-dimensional space and was performed on dried samples. It is not possible, therefore, to compare particle size measurements from CLSM to a hydrodynamic diameter determined by DLS. Use of FITC and ANSA labeled samples gave consistent results, and we therefore report the mean values of both procedures.

We found that the particles formed were essentially round shaped, reflected by ≥ 60 % of the particles showing a circularity value of 1. Moreover, ≥ 74 ± 10 % and ≥ 75 ± 9 % of the particles obtained by stirring and shaking, respectively, show a circularity of ≥ 0.8 (Figure 7). Concerning the area of the particles, we observed that 85 ± 10 % and 88 ± 10 % of the particles in the sample from stirring and shaking, respectively, displayed a size between 0.1 and 1 µm² (Figure S9). A plausible explanation for the round shape and small area of the particles formed could be the particular shape of the air-liquid interface (dissolved air bubbles) that is present during stirring and shaking (Figure S7). The dynamics at the air liquid interface [82,83], the mechanism of aggregation, and even the mechanical forces applied could also influence the shape and size of the aggregates [84].

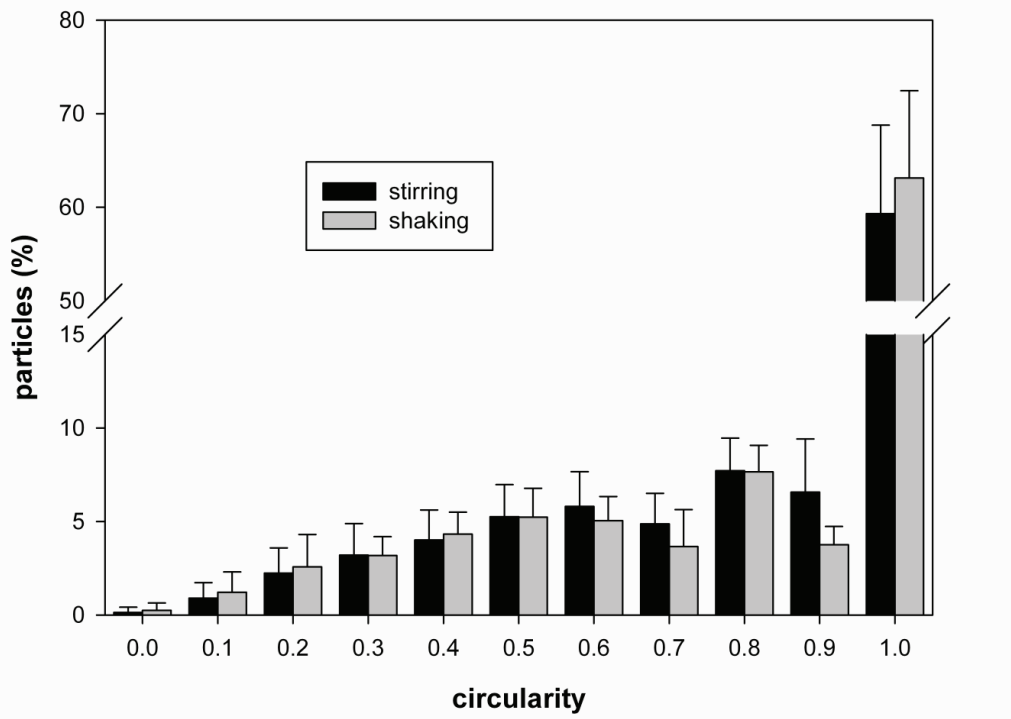


**Figure 8: Particle shape distribution for aggregates formed during shaking and stirring** Comparison of the circularity of hGH precipitate formed during stirring (after 96 h) and shaking (2 h), as determined by ImageJ analysis [73].

Three-dimensional models of the protein particles labeled with FITC (Figure 8) and ANSA (Figure S8) were highly similar one to another. In other words, detection of total protein (FITC) gave essentially the same result as measurement of exposed hydrophobic surface (ANSA). Therefore, this implies that hGH aggregates consisted mainly of unfolded (hydrophobic) protein. Properties of the aggregates did not change significantly depending on the stress method applied, consistent with the idea that protein unfolding at the hydrophobic air-liquid interface presents the main factor leading to aggregation under stirring and shaking.

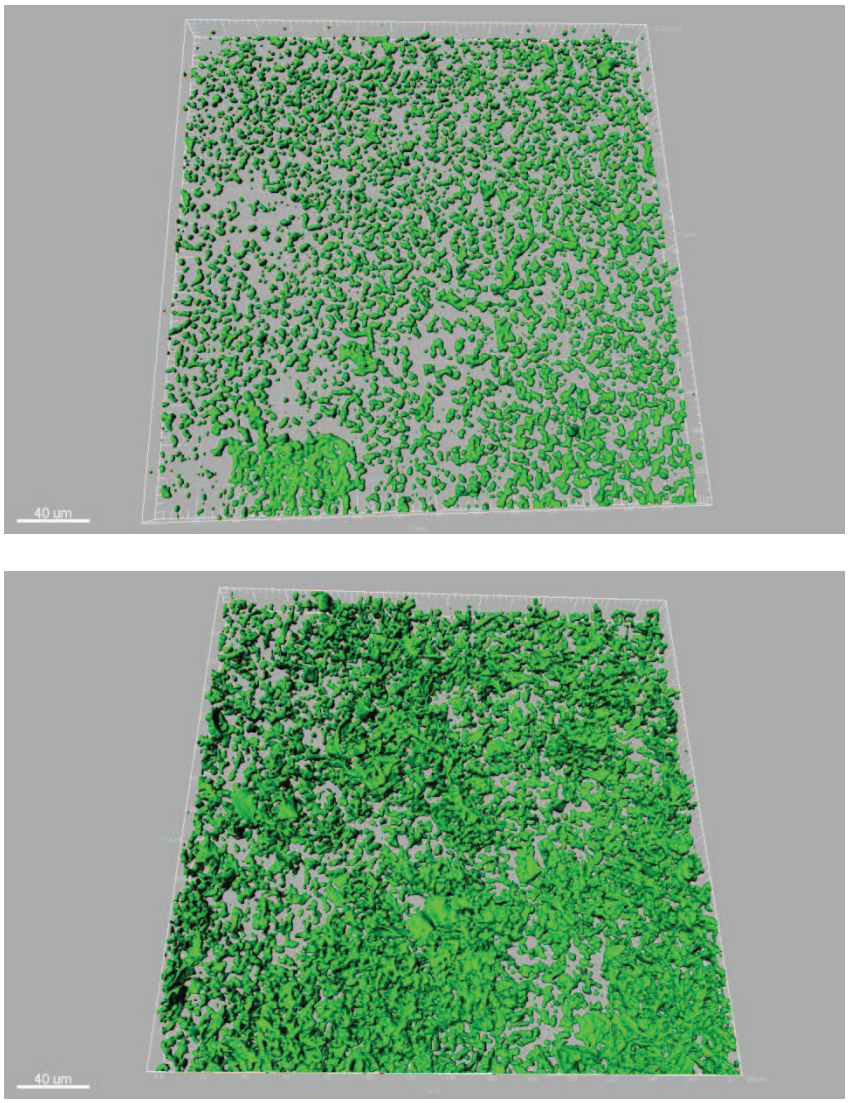


**Figure 8: Three-dimensional confocal models of hGH aggregates**

3D Imaris picture of covalently FITC-labeled aggregates formed by stirring (96 h, top) and shaking (2 h, bottom) at 300 rpm and 25 °C.

## 4. Conclusions

Detailed comparison of the accelerated stress conditions “stirring” and “shaking” in a miniaturized test system revealed that the presence of a dynamically renewed air-liquid interface is the major critical parameter of the hGH aggregation rate. When no interface is present (high liquid level) or interfacial dynamics is lacking (no agitation), the basis for protein perturbation is removed and hGH is therefore stable. A decrease in the interfacial dynamics resulting from the use of a size-reduced stirring bar leads to decreased aggregation under stirring stress. Furthermore, deamidation does not accelerate or prevent aggregation of hGH in the analyzed time span of several days. Analysis of precipitated protein by CLSM reveals essentially round particles that contain partly unfolded hGH exposing a substantial amount of hydrophobic surface, consistent with the notion of (partial) protein unfolding at the air-liquid interface preceding the phase transition. We could also show that there is hardly any accumulation of soluble protein aggregates and that larger particles are formed rapidly from the unfolded precursors. Controlled shaking and stirring therefore give fully consistent results concerning the overall stability of hGH and the main critical parameter leading to aggregation.

## Acknowledgements

This project was supported by FFG, Land Steiermark and SFG. Thanks go to Sandoz GmbH, Austria for kindly supplying the protein used in this study. Prof. Matthäus Siebenhofer, Prof. Günter Brenn, Prof. Michael Murkovic, Dr. Helmar Wiltsche, Dr. Marco Marchl and DI Bernhard Thonhauser are thanked for helpful discussion.

## References


[1] Manning MC, Chou DK, Murphy BM, Payne RW, Katayama DS. Stability of protein pharmaceuticals: an update. Pharm Res 2010;27:544-575.

[2] Manning MC, Patel K, Borchardt RT. Stability of protein pharmaceuticals. Pharm Res 1989;6:903-918.

[3] Wang W. Instability, stabilization, and formulation of liquid protein pharmaceuticals. Int J Pharm 1999;185:129–188.

[4] Chi EY, Krishnan S, Randolph TW, Carpenter JF. Physical stability of proteins in aqueous solution: Mechanism and driving forces in nonnative protein aggregation. Pharm Res 2003;20:1325–1336.

[5] Wang W, Nema S, Teagarden D. Protein aggregation--pathways and influencing factors. Int J Pharm 2010;390:89-99.

[6] Mahler H-C, Friess W, Grauschopf U, Kiese S. Protein aggregation: Pathways, induction factors and analysis. J Pharm Sci 2008;98:2909-2934.

[7] Cleland JL, Powell MF, Shire SJ. The development of stable protein formulations: A close look at protein aggregation, deamidation, and oxidation. Crit Rev Ther Drug Carrier Syst 1993;10:307–377.

[8] Philo JS, Arakawa T. Mechanisms of protein aggregation. Curr Pharm Biotechnol 2009;10:348-351.

[9] Cromwell MEM, Hilario E, Jacobson F. Protein aggregation and bioprocessing. AAPS Journal 2006;8:E572-E579

[10] Rathore N, Rajan RS. Current perspectives on stability of protein drug products during formulation, fill and finish operations. Biotechnol Prog 2008;24:504–514.

[11] Wang W. Protein aggregation and its inhibition in biopharmaceutics. Int J Pharm 2005;289:1–30.

[12] Roberts CJ. Nonnative protein aggregation kinetics. Biotechnol Bioeng 2007;98:927–938.

[13] Rosenberg A. Effects of protein aggregates: An immunologic perspective. AAPS J 2006;8:E501–E508.

[14] Roberts CJ, Das TK, Sahin E. Predicting solution aggregation rates for therapeutic proteins: Approaches and challenges. Int J Pharm 2011;418:1-16.

[15] Weiss WFI, Young TM, Roberts CJ. Principles, approaches, and challenges for predicting protein aggregation rates and shelf life. J Pharm Sci 2009;98:1246–1277.

[16] Wang W, Singh S, Zeng DL, King K, Nema S. Antibody structure, instability and formulation. J Pharm Sci 2007;96:1–26.

[17] Mahler H-C, Muller R, Friess W, Delille A, Matheus S. Induction and analysis of aggregates in a liquid IgG1-antibody formulation. Eur J Pharm Biopharm 2005;59:407–417.

[18] Q1A(R2): Stability testing of new drug substances and products. International conference on harmonization. 2003, 1-15.

[19] Simon S, Krause HJ, Weber C, Peukert W. Physical degradation of proteins in well-defined fluid flows studied within a four-roll apparatus. Biotechnol Bioeng 2011;108:2914-2922.

[20] Bee JS, Stevenson JL, Mehta B, Svitel J, Pollastrini J, Platz R, Freund E, Carpenter JF, Randolph TW. Response of a concentrated monoclonal antibody formulation to high shear. Biotechnol and Bioeng 2009;103:936-943.

[21] Maa Y-F, Hsu CC. Protein denaturation by combined effect of shear and air-liquid interface. Biotechnol Bioeng 1997;54:503–512.

[22] Maa Y-F, Hsu CC. Effect of high shear on proteins. Biotechnol Bioeng 1996;51:458–465.

[23] Kiese S, Papppenberger A, Friess W, Mahler HC. Shaken, not stirred: Mechanical stress testing of an IgG1 antibody. J Pharm Sci 2008;97:4347–4366.
[24] Thomas CR, Geer D. Effects of shear on proteins in solution. Biotechnol Lett 2011;33:443-456.
[25] Bee JS, Chiu D, Sawicki S, Stevenson JL, Chatterjee K, Freund E, Carpenter JF, Randolph TW. Monoclonal antibody interactions with micro- and nanoparticles: adsorption, aggregation, and accelerated stress studies. J Pharm Sci 2009;98:3218-3238.
[26] Fradkin AH, Carpenter JF, Randolph TW. Immunogenicity of aggregates of recombinant human growth hormone in mouse models. J Pharm Sci 2009;98:3247-3264.
[27] Biddlecombe JG, Smith G, Uddin S, Mulot S, Spencer D, Gee C, Fish BC, Bracewell DG. Factors influencing antibody stability at solid-liquid interfaces in a high shear environment. Biotechnol Prog 2009;25:1499-1507.
[28] Baszkin A, Boissonnade MM, Kamyshny A, Magdassi S. Native and hydrophobically modified human immunoglobulin G at the air/water interface. J Colloid Interface Sci 2001;239:1-9.
[29] Haas J, Voehringer-Martinez E, Boegehold A, Matthes Dirk, Hensen U, Pelah A, Abel B, Grubmueller H. Primary steps of pH-dependent insulin aggregation kinetics are governed by conformational flexibility. ChemBioChem 2009;10:1816-1822.
[30] Henson AF, Mitchell JR, Musselwhite PR. The surface coagulation of proteins during shaking. J Colloid Interface Sci 1970;32:162-165.
[31] Mahler H-C, Senner F, Maeder K, Mueller R. Surface activity of a monoclonal antibody. J Pharm Sci 2009;98:4525-4533.
[32] Thomas CR, Nienow AW, Dunnill P. Action of shear on enzymes: Studies with alcohol dehydrogenase. Biotechnol Bioeng 1979;21:2263–2278.
[33] Harrison JS, Gill A, Hoare M. Stability of a single-chain Fv antibody fragment when exposed to a high shear environment combined with air-liquid interfaces. Biotechnol Bioeng 1998;59:517-519.
[34] Colombie S, Gaunand A, Lindet B. Lysozyme inactivation under mechanical stirring: Effect of physical and molecular interfaces. Enzyme Microb Technol 2001;28:820–826.
[35] Donaldson TL, Boonstra EF, Hammond JM. Kinetics of protein denaturation at gas–liquid interfaces. J Colloid Interface Sci 1980;74:441–450.
[36] Jaspe J, Hagen SJ. Do protein molecules unfold in a simple shear flow? Biophys J 2006;91:3415-3424.
[37] Di Stasio E, De Cristofaro R. The effect of shear stress on protein conformation: Physical forces operating on biochemical systems: The case of von Willebrand factor. Biophys Chem 2010;153:1-8.
[38] Charm SE, Wong BL. Shear effects on enzymes. Enzyme Microb Technol 1981;3:111–118.
[39] Lee YK, Choo CL. The kinetics and mechanism of shear inactivation of lipase from Candida cylindracea. Biotechnol Bioeng 1989;33:183-190.
[40] Virkar PD, Narendranathan TJ, Hoare M, Dunnill P. Studies of the effect of shear on globular proteins: Extension to high shear fields and to pumps. Biotechnol Bioeng 1981;23:425–429.
[41] Kim MH, Lee SB, Ryu DDY, Reese ET. Surface deactivation of cellulase and its prevention. Enzyme Microb Technol 1982;4:99-103.
[42] Walstra P. Effect of agitation on proteins. In: Dickinson E, Miller R, editors. Food colloids: fundamentals of formulation. Cambridge: Royal Society of Chemistry; 2001. p 245–254.
[43] Sing CE, Alexander-Katz A. Elongational flow induces the unfolding of von Willebrand factor at physiological flow rates. Biophys J 2010;98:L35-L37.

[44] King AC, Woods M, Liu W, Lu Z, Gill D, Krebs MRH. High-throughput measurement, correlation analysis, and machine-learning predictions for pH and thermal stabilities of Pfizer-generated antibodies. Protein Sci 2011;20:1546-1557.
[45] Cleland JL, Mac A, Boyd B, Yang J, Duenas ET, Yeung D, Brooks D, Hsu C, Chu H, Mukku V, Jones AJ. The stability of recombinant human growth hormone in poly(lactic-co-glycolic acid) (PLGA) microspheres. Pharm Res 1997;14: 420-425.
[46] Pearlman R, Wang JY. Stability and characterization of human growth hormone. In Pearlman R, Wang JY, editors. Stability and Characterization of Protein and Peptide Drugs: Case Histories. New York: Plenum Press; 1993. p 1-58.
[47] Cholewinski M, Lückel B, Horn H. Degradation pathways, analytical characterization and formulation strategies of a peptide and a protein. Calcitonine and human growth hormone in comparison. Pharm Acta Helv 1996;71: 405-419.
[48] Lewis UJ, Peterson SM, Bonewald LF, Seavey BK, VanderLaan WP. An interchain disulfide dimer of human growth hormone. J Biol Chem 1977;252:3697-3702.
[49] Cunningham BC, Mulkerrin MG, Wells J. Dimerization of human growth hormone by zinc. Science 1991;253: 545-548.
[50] Dienys G, Sereikaite J, Luksa V, Jarutiene O, Mistiniene E, Bumelis VA. Dimerization of human growth hormone in the presence of metal ions. Bioconjug Chem 2000;11:646-651.
[51] Katakam M, Bell LN, Banga AK. Effect of surfactants on the physical stability of recombinant human growth hormone. J Pharm Sci 1995;84:713–716.
[52] Katakam M, Banga AK. Use of poloxamer polymers to stabilize recombinant human growth hormone against various processing stresses. Pharm Dev Technol 1997;2:143-149.
[53] John RJS, Carpenter JF, Balny C, Randolph TW. High pressure refolding of recombinant human growth hormone from insoluble aggregates. Structural transformations, kinetic barriers, and energetic. J Biol Chem 2001;276:46856-46863.
[54] Bam NB, Cleland JL, Yang J, Manning MC, Carpenter JF, Kelley RF, Randolph TW. Tween protects recombinant human growth hormone against agitation-induced damage via hydrophobic interactions. J Pharm Sci 1998;87:1554–1559.
[55] John RJS, Carpenter JF, Randolph TW. High pressure fosters protein refolding from aggregates at high concentrations. Proc Natl Acad Sci U S A 1999;96:13029-13033.
[56] Chantalat L, Jones ND, Korber F, Navaza J, Pavlovsky AG. The crystal structure of wild-type growth hormone at 2.5 Å resolution. Protein Pept Lett 1995,2:333-340.
[57] Hill CP, Osslund TD, Eisenberg D. The structure of granulocyte-colony-stimulating factor and its relationship to other growth factors. Proc Natl Acad Sci U S A 1993;90:5167-5171.
[58] de Vos AM, Ultsch M, Kossiakoff AA. Human growth hormone and extracellular domain of its receptor: crystal structure of the complex. Science 1992;255:306-312.
[59] Jones AJ, Putney S, Johnson OL, Cleland JL. Recombinant human growth hormone poly(lactic-co-glycolic acid) microsphere formulation development. Adv Drug Deliv Rev 1997;28:71-84.
[60] Becker GW, Tackitt PM, Bromer WW, Lefeber DS, Riggin RM. Isolation and characterization of a sulfoxide and a desamido derivative of biosynthetic human growth hormone. Biotechnol Appl Biochem 1988;10:326-337.
[61] Riggin RM, Farid NA. Analytical chemistry of therapeutic proteins. In Horvath C, Nikelly JG, Analytical Biotechnology: Capillary Electrophoresis and Chromatography. Washington DC: American Chemical Society; 1990. p 113-126.
[62] Doyle HA, Gee RJ, Mamula MJ. Altered immunogenicity of isoaspartate containing proteins. Autoimmunity 2007;40: 131-137.

[63] Wilkins MR, Gasteiger E, Bairoch A, Sanchez JC, Williams KL, Appel RD, Hochstrasser DF. Protein identification and analysis tools in the ExPASy server. Methods Mol Biol 1999;112:531-552.
[64] Gasteiger E, Hoogland C, Gattiker A, Duvaud S, Wilkins MR, Appel RD, Bairoch A. Protein Identification and Analysis Tools on the ExPASy Server. In: Walker JM, editor. The Proteomics Protocols Handbook. New York: Humana Press Inc; 2005. p 571-607.
[65] Eckhardt BM, Oeswein JQ, Yeung DA, Milby TD, Bewley TA. A turbidimetric method to determine visual appearance of protein solutions. J Pharm Sci Technol 1994;48:64–70.
[66] Ablinger E, Wegscheider S, Keller W, Prassl R, Zimmer A.Effect of protamine on the solubility and deamidation of human growth hormone. Int J Pharm 2012;427:209-216.
[67] Ph. Eur. 2.2.1. Clarity and degree of opalescense of liquids, 6th edition. European Directorate for the Quality of Medicine (EDQM) 2008.
[68] Vivian JT, Callis PR. Mechanisms of tryptophan fluorescence shifts in proteins. Biophys J 2001;80:2093-2109.
[69] Ali V, Prakash K, Kulkarni S, Ahmad A, Bhakuni V. 8-Anilino-1-naphthalene sulfonic acid (ANS) induces folding of acid unfolded cytochrome c to molten globule state as a result of electrostatic interactions. Biochemistry 1999;38:13635-13642.
[70] Bam NB, Cleland JL, Randolph TW. Molten globule intermediate of recombinant human growth hormone: stabilization with surfactants. Biotechnol Prog 1996;12:801-809.
[71] Hawe A, Sutter M, Jiskoot W. Extrinsic fluorescent dyes as tools for protein characterization. Pharm Res 2008;25:1487–1499.
[72] Dib I, Slavica A, Riethorst W, Nidetzky B. Thermal inactivation of D-amino acid oxidase from *Trigonopsis variabilis* occurs via three parallel paths of irreversible denaturation. Biotechnol Bioeng 2006;94:645–654.
[73] Abramoff MD, Magelhaes PJ, Ram SJ. Image processing with ImageJ. Biophotonics Int 2004;11:36-42.
[74] Jenkins N, Murphy L, Tyther R. Post-translational modifications of recombinant proteins: significance for biopharmaceuticals. Mol Biotechnol 2008;39:113-118.
[75] Stratton LP, Kelly RM, Rowe J, Shively JE, Smith DD, Carpenter JF, Manning MC. Controlling deamidation rates in a model peptide: effects of temperature, peptide concentration, and additives. J Pharm Sci 2001;90:2141-2148.
[76] Lewis UJ, Cheever EV, Hopkins WC. Kinetic study of the deamidation of growth hormone and prolactin. Biochim Biophys Acta 1970;214:498-508.
[77] Sukumar M, Doyle BL, Combs JL, Pekar AH. Opalescent appearance of an IgG1 antibody at high concentrations and its relationship to noncovalent association. Pharm Res 2004;21:1087–1093
[78] Felsovalyi F, Mangiagalli P, Bureau C, Kumar SK, Banta S. Reversibility of the adsorption of lysozyme on silica. Langmuir 2011;27:11873-11882.
[79] Su TJ, Lu JR, Thomas RK, Cui ZF, Penfold J. The adsorption of lysozyme at the silica-water interface: A neutron reflection study. J Colloid Interface Sci 1998;203:419-429.
[80] Maste MCL, Pap EHW, Hoek AV, Norde W, Visser AJWG. Spectroscopic Investigation of the Structure of a Protein Adsorbed on a Hydrophobic Latex. J Colloid Interface Sci 1996;180:632-633.
[81] Zoungrana T, Findenegg GH, Norde W. Structure, stability and activity of adsorbed enzymes. J Colloid Inferface Sci 1997;190:437-448.
[82] Tissot S, Farhat M, Hacker DL, Anderlei T, Kuehner M, Comninellis C, Wurm FM. 2010. Determination of a scale-up factor from mixing time studies in orbitally shaken bioreactors. Biochem Eng J 52:181-186.
[83] Tissot S, Oberbek A, Reclari M, Dreyer M, Hacker DL, Baldi L, Farhat M, Wurm FM. 2011. Efficient and reproducible mammalian cell bioprocesses without probes and controllers? N Biotechnol 28:382-390.

[84] Soos M, Moussa AS, Ehrl L, Sefcik J, Wu H, Morbidelli M. Effect of shear rate on aggregate size and morphology investigated under turbulent conditions in stirred tank. J Colloid Interface Sci 2008;319:577-589.
[85] Perez JAS, Porcel EMR, Lopez JLC, Sevilla JMF, Chisti Y. Shear rate in stirred tank and bubble column bioreactors. Chem Eng J 2006;124:1-5.
[86] Doran PM. Bioprocess Engineering Principles. London: Academic Press Limited; 2000. p 130-163.
[87] Buechs J, Maier U, Milbradt C, Zoels B. Power consumption in shaking flasks on rotary shaking machines: I. Power consumption measurement in unbaffled flasks at low liquid viscosity. Biotechnol Bioeng 2000;68:589-593.

## 2.1 Supporting Information

# Supporting Information

# Shaking and stirring: comparison of accelerated stress conditions applied to the human growth hormone

Johanna Wiesbauer[1,2], Massimiliano Cardinale[3] and Bernd Nidetzky[2*]

[1]*Research Center Pharmaceutical Engineering, Graz, Austria*

[2]*Institute of Biotechnology and Biochemical Engineering, University of Technology Graz, Austria; telephone: +43 316 873 8400; fax: +43 316 873 8434,*

*e-mail: bernd.nidetzky@tugraz.at*

[3]*Institute of Environmental Biotechnology, University of Technology Graz, Austria*

**Table S1: Reynolds number *Re* and shear rate for the different conditions used**

| Method | *Re*[1] | Shear rate ($s^{-1}$)[2] |
|---|---|---|
| Temperature stress (45 °C), no agitation | 0 | 0 |
| Temperature stress (45 °C), stirring ($N$ = 5 $s^{-1}$, $d_i$ = 0.025 m) | 3,400 | 35-85 |
| Control (room temperature, no agitation) | 0 | 0 |
| Stirring ($N$ = 5 $s^{-1}$, $d_i$ = 0.030 m) | 4,800 | 40-100 |
| Shaking ($N$ = 5 $s^{-1}$, $H$ = 0.014 m, $R_{shaking}$ = 0.025 m, $R_{flask}$ = 0.016 m) | 5,500 | 90[3] |
| Shaking at reduced gas-liquid interface ($N$ = 5 $s^{-1}$, $H$ = 0.068 m, $R_{shaking}$ = 0.025 m, $R_{flask}$ = 0.016 m) | 5,500 | 20[3] |
| Stirring at reduced gas-liquid interface ($N$ = 5 $s^{-1}$, $d_i$ = 0.030 m) | 4,800 | 40-100 |

[1] Reynolds number for stirring was calculated according to literature [1] using equation (1).

$$Re = \rho N d_i^2/\mu \quad (1)$$

where ρ is density in kg/m³, $N$ is the stirring rate (300 rpm) in $s^{-1}$, $d_i$ is stirrer bar diameter in m, and μ is the viscosity in Pa s. Density of hGH solution was measured on a DSA 5000 M density meter (Anton Paar, Graz Austria). An MCR 300 rotational viscosimeter (Anton Paar) equipped with a double-gap cylinder (DG26.7) was used to measure dynamic viscosity. Density of the hGH solution was 0.996 g/mL, dynamic viscosity was 0.927 mPa s. Analyses were performed at 25 °C.

Reynolds number for shaking was calculated according to [2] using equation (1), whereby $d$ is the inner diameter of the shaken flask used, and $N$ is the agitation rate (300 rpm) in $s^{-1}$.

[2] Shear rate (γ) in turbulent regime under stirred conditions was calculated using equation (2), where $N_p$ is dimensionless power number. To the best of our knowledge, $N_p$ for stirrer bars are

not available in literature. We approximated $N_p$ for the magnetically stirred system used by assuming the true $N_p$ to lie between a value of 2 (paddle impeller) and 0.35 (marine propeller) [1,3].

$$\gamma = (4\, N_p\, \rho\, d_i^2/(\pi\, 3^3\, \mu))^{1/2}\, N^{3/2} \qquad (2)$$

For shaking, we estimated $\gamma$ from its general definition in Couette flow, where $\gamma$ equals the ratio of fluid velocity and height, as shown in equation (3), with height being the difference between to plates. Velocity was calculated assuming an orbital movement of the shaker with a radius ($R_{shaking}$) of 2.5 cm. The flask radius ($R_{flask}$) was 1.6 cm. The liquid height ($H$) was 1.4 cm. Using reduced gas-liquid interface, $H$ had a value of 6.8 cm. The angular velocity was calculated according to $\omega = 2\, \pi\, N$, where $N$ is the agitation rate in $s^{-1}$.

$$\gamma = \omega\, (R_{shaking} + R_{flask})/H \qquad (3)$$

[3] Shear rates are smaller for systems having larger $H$, which is the case in our reduced gas-liquid interface set-up. However, differences in $\gamma$ are extremely unlikely to be responsible for the massive change in protein aggregation resulting from decrease in $H$ from 6.8 cm to 1.4 cm (see Figure 3 and text in the main part of the paper).


**Figure S1: Geometry of the Erlenmeyer flask and the double-walled glass reactors.** From left to right: 25 ml Erlenmeyer flask with maximum diameter 4.2 cm and height of 7.0 cm (area 12.0 $cm^2$), double-walled glass miniature bioreactor with a diameter of 3.2 cm (area 8.04 $cm^2$), and comparison with the reactor used for reduced air/liquid interfaces completely filled (area 1.90 $cm^2$, three nozzles).

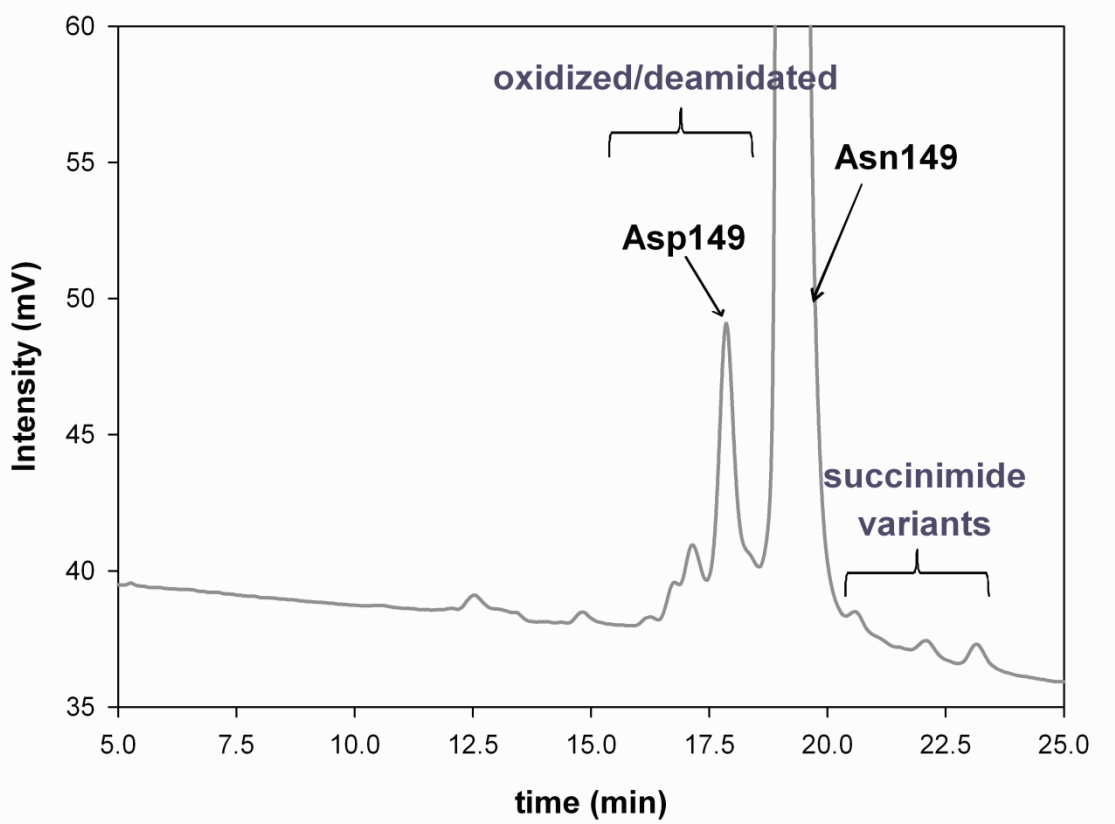


**Figure S2: RP-HPLC trace for partially deamidated sample of hGH**. Oxidized and deamidated variants elute before the native hGH containing $Asn^{149}$ elutes. Succinimide forms of the protein [4,5] (on the route to L-aspartyl-peptide or L-isoaspartyl-peptide) are also detected. The $Asp^{149}$ peak was further used to calculate protein deamidation rate in Area%/h and μM/h.

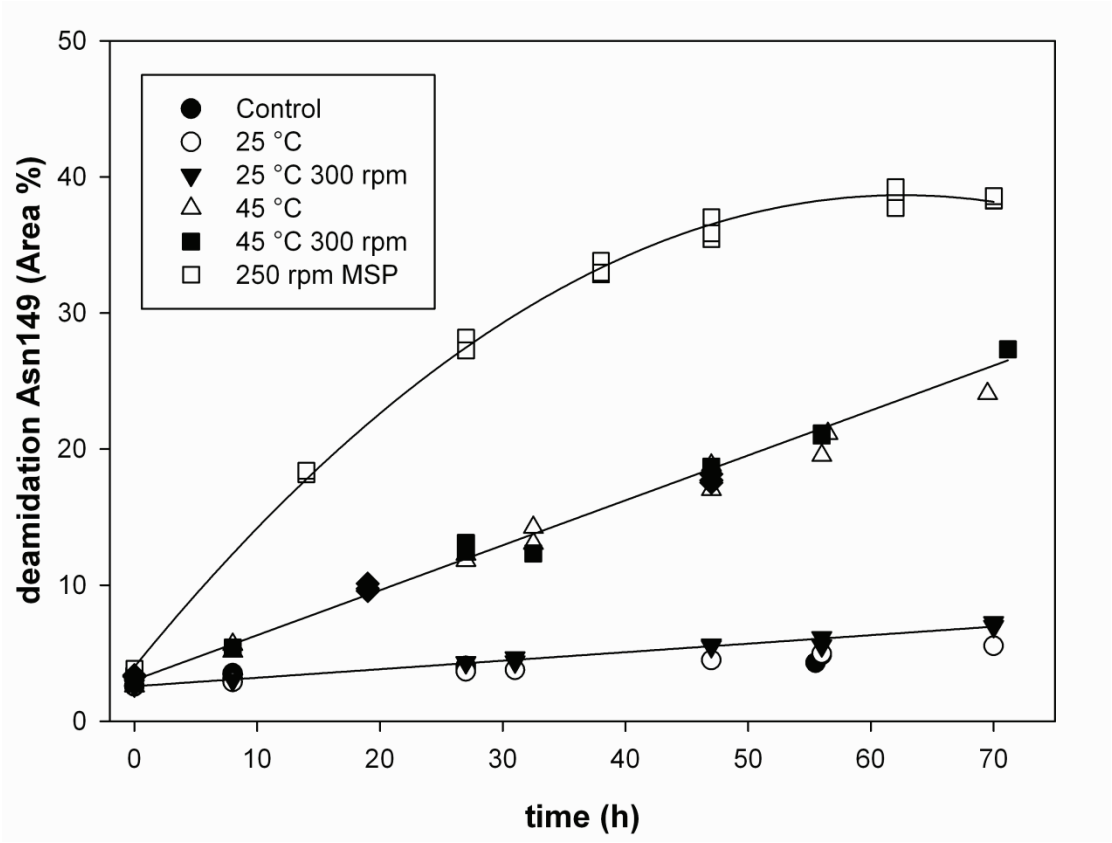


**Figure S3: Course of chemical modification of hGH, measured as deamidation of Asn$^{149}$ during incubation at 45 °C and 25 °C.** Time courses for deamidation of Asn$^{149}$ to Asp$^{149}$. The turbulent stirring on the sequential magnetic stirring plate (MSP) resulted in very high deamidation rates. Controlled stirring on a IKA RCT magnetic stirrer led to lower deamidation rates.

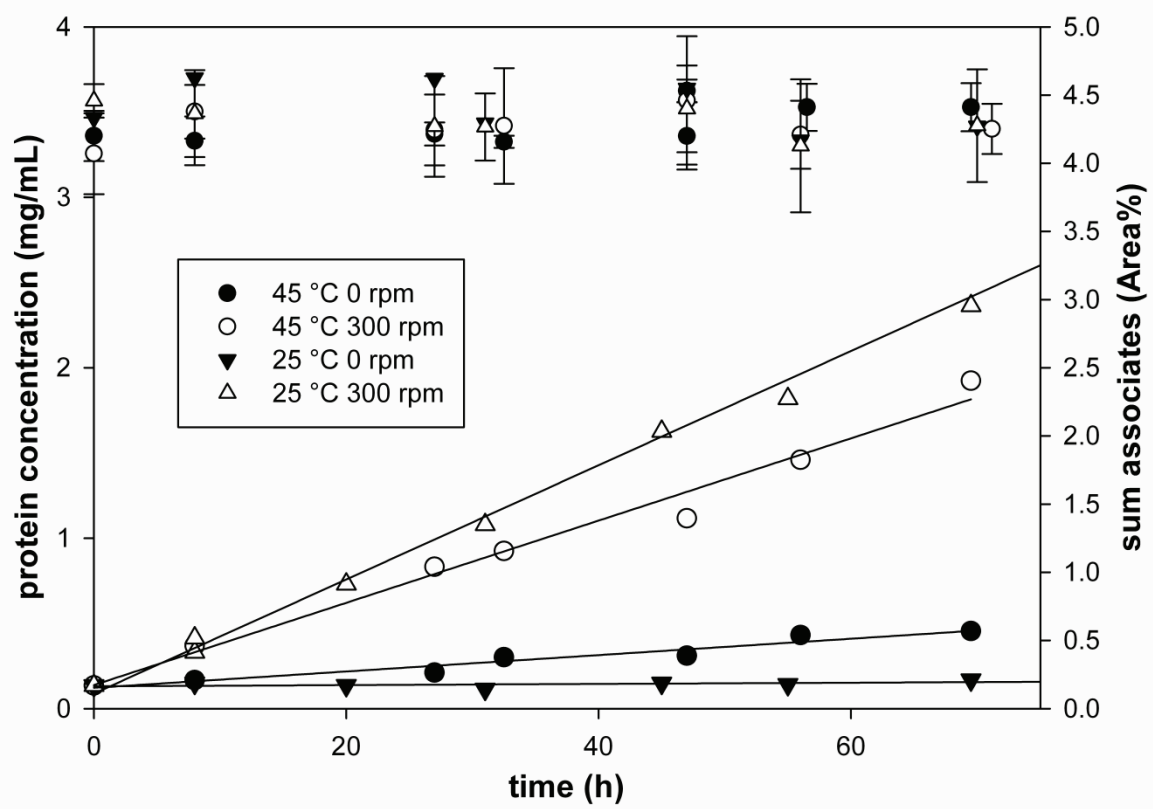


**Figure S4: Formation of soluble protein associates during nonnative aggregation of hGH under stirred conditions.** Total soluble protein was measured by UV absorbance, and soluble aggregates were measured by size exclusion (SEC) HPLC. The SEC-HPLC data reveal gradual increase in soluble protein aggregates due to stirring stress. Up to 3% of total protein was found in these aggregates. By comparison, the total protein concentration was unchanged over 70 h, indicating that only little (within SD of UV measurements) insoluble protein was formed. Data presented in main manuscript show that turbidity (visible particles) increased over time of incubation.

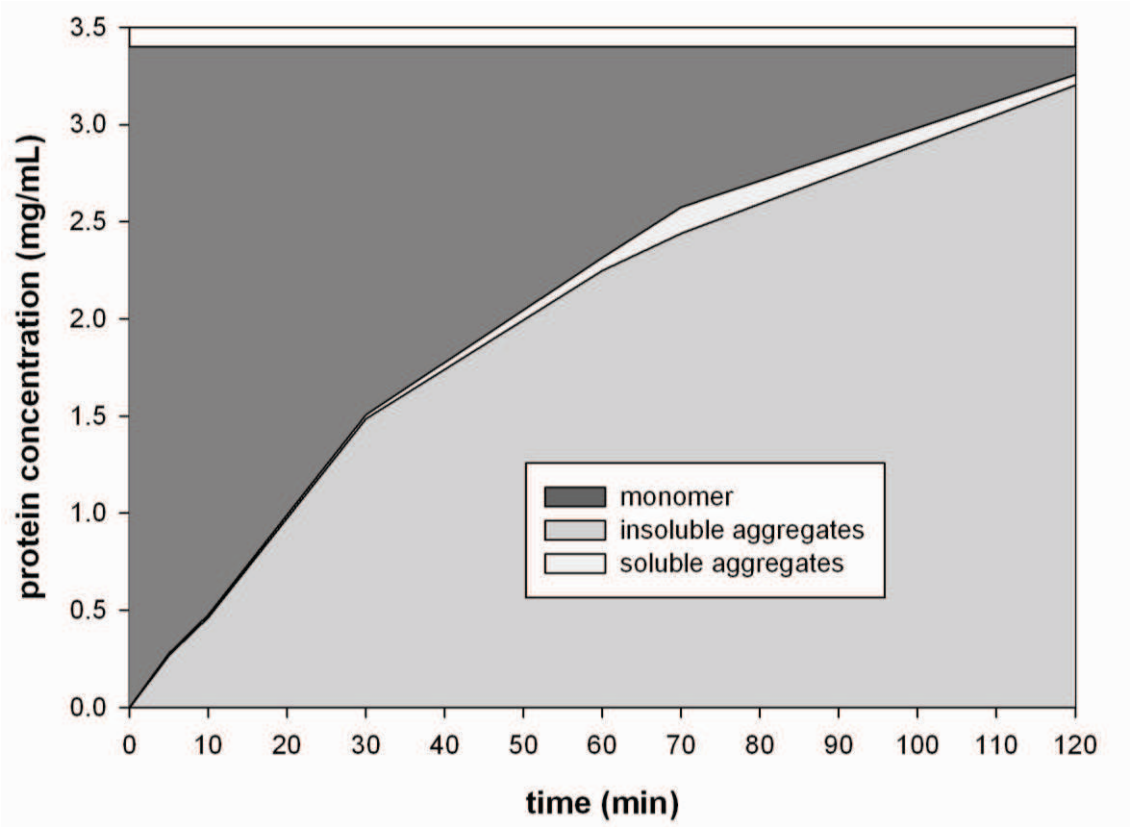


**Figure S5: Quantitative distribution of hGH monomer, soluble associates and precipitate for the shaking experiment.** The amount of precipitated (insoluble) aggregates was determined using UV measurements (protein loss). For distinguishing between monomeric hGH and soluble aggregates we used SEC-HPLC data. The data indicate that the amount of soluble aggregates formed was negligible.

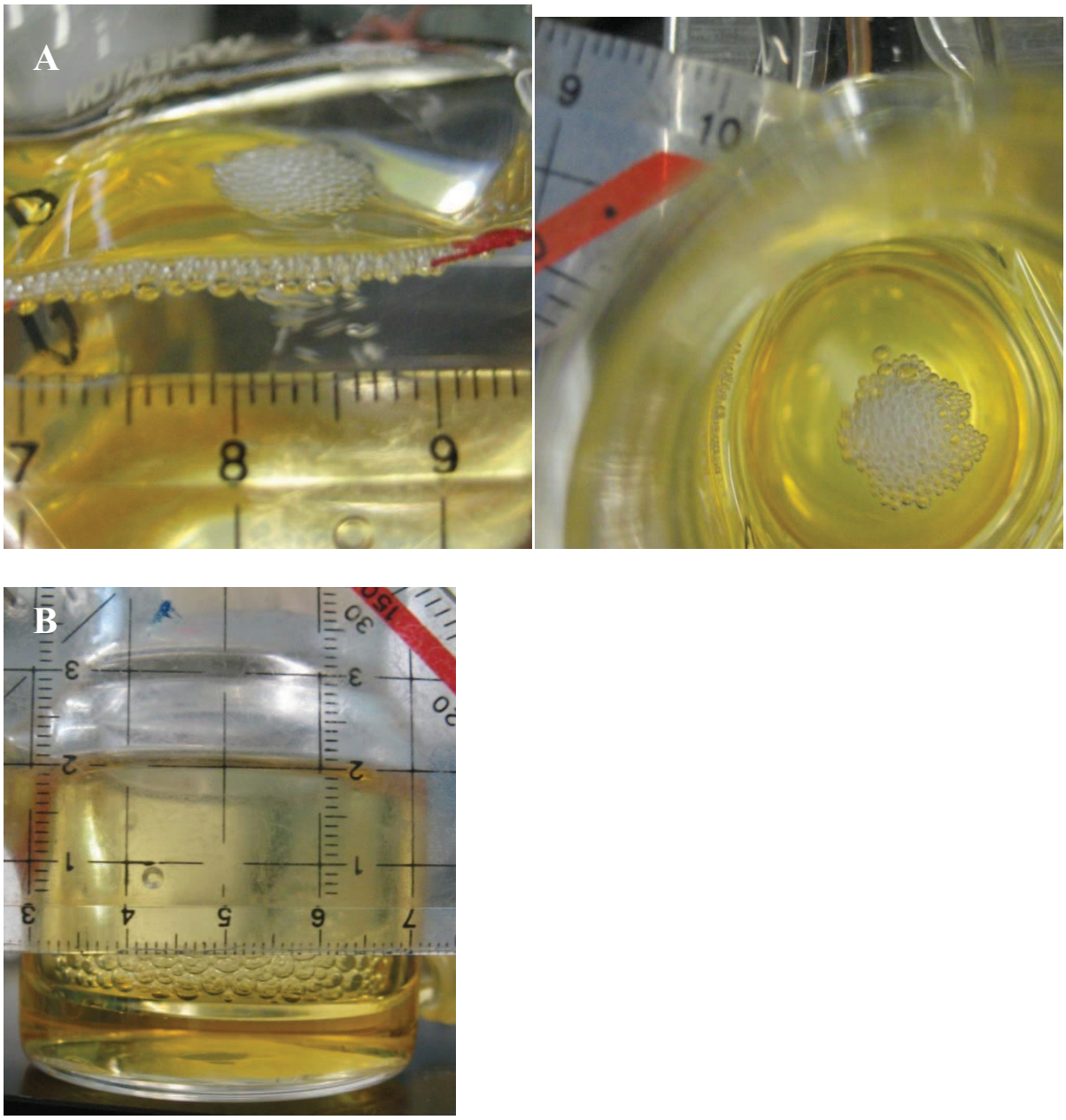


**Figure S6: Size and shape of air bubbles during stirring and shaking**

*Panel A:* From left to right the air bubbles formed during stirring are shown. Air bubble size could influence the size and shape of the aggregates formed, next to other forces [7].

*Panel B:* Size and shape of air bubbles formed during shaking at 300 rpm and 25 °C.

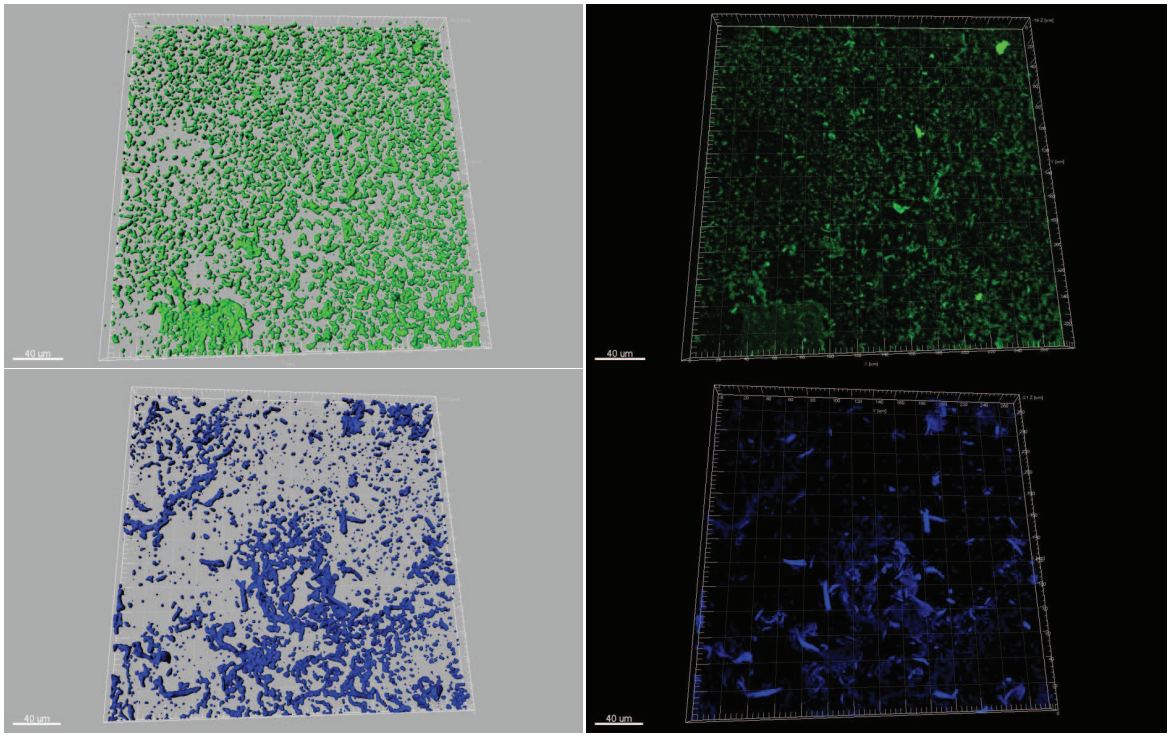


**Figure S7: Comparison of three-dimensional confocal models of aggregate hGH created by Imaris 7.0 (top: FITC; bottom: ANSA)**

*panel A:* Size and shape of aggregates formed by stirring for 96 h (300 rpm, 25 °C). No significant difference for FITC (top) and ANSA (bottom) labeling could be detected.

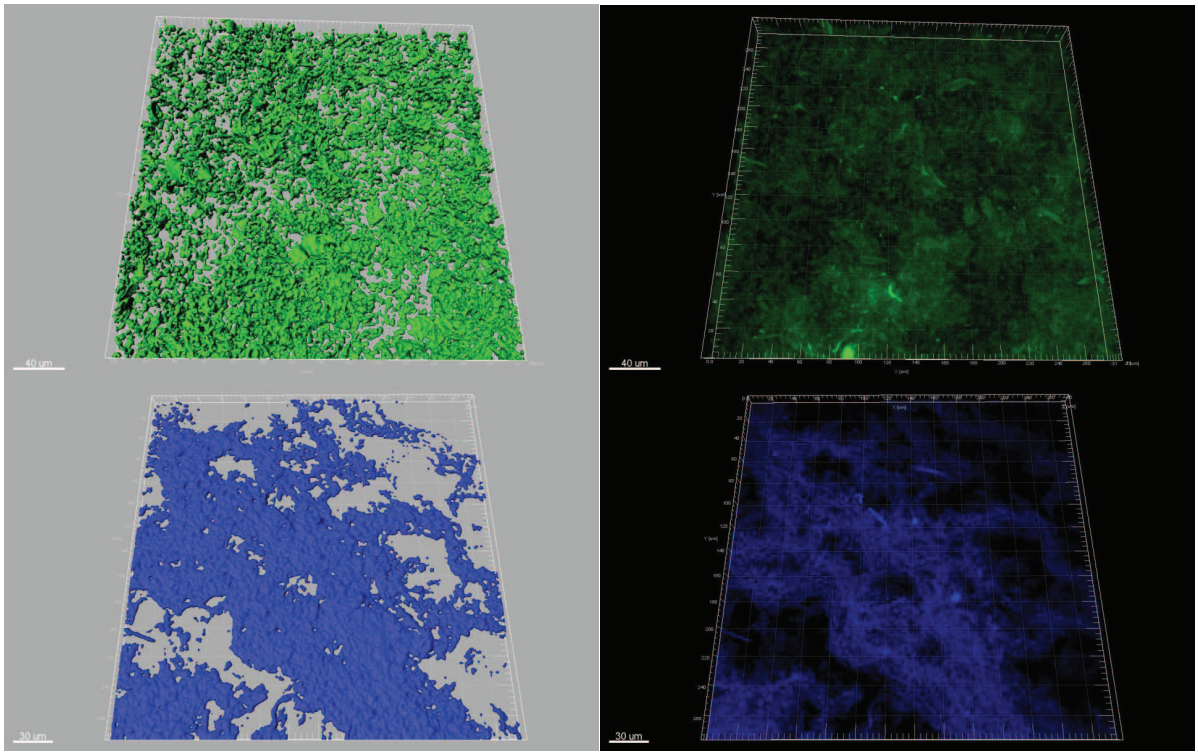


*panel B*: Size and shape of aggregates formed by shaking for 2 h, 300 rpm and 25 °C. ANSA-labeled particles appear more flat than FITC-labeled particles. Otherwise no difference was found between FITC and ANSA-labeled particles.

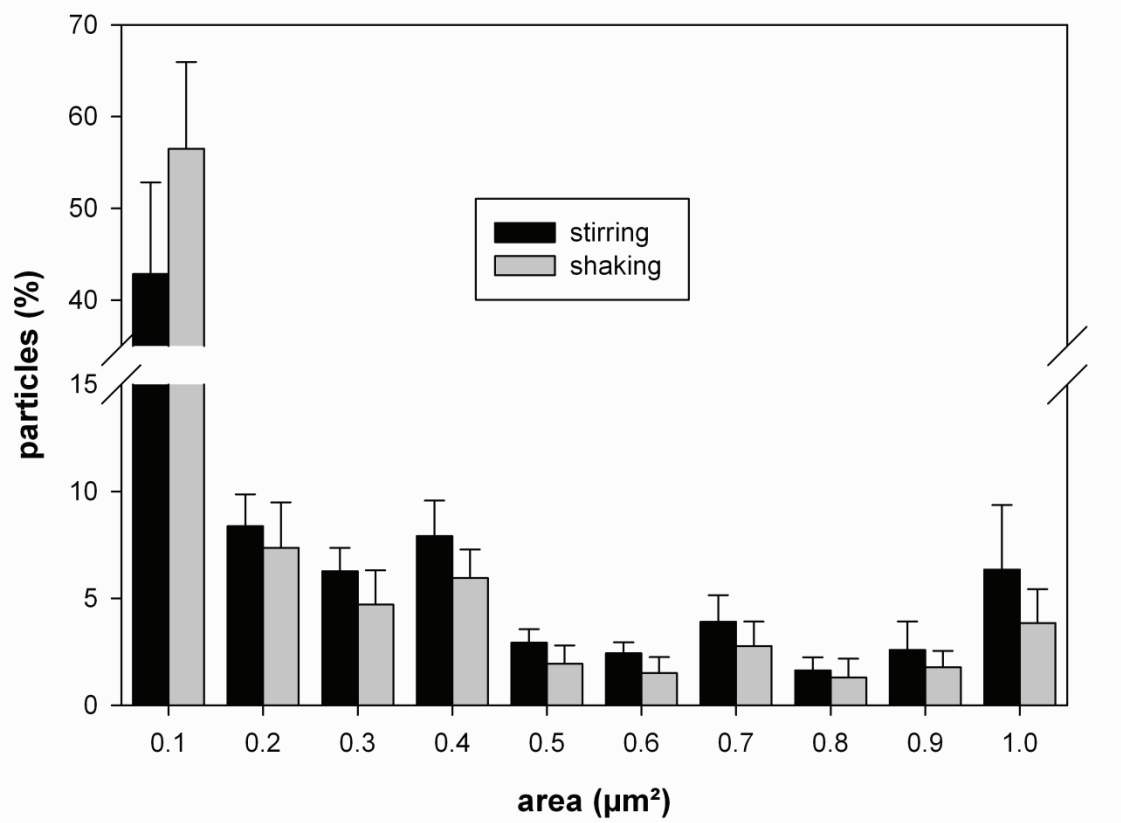


**Figure S8: CLSM analysis with ImageJ software**

Data processing of two-dimensional projections was performed using ImageJ software [7]. The particle area range 0.1 - 1 µm² contained 85 ± 10 % and 88 ± 10 % of all particles analyzed in the sample from stirring and shaking, respectively.

## References


[1] Perez JAS, Porcel EMR, Lopez JLC, Sevilla JMF, Chisti Y. Shear rate in stirred tank and bubble column bioreactors. Chem Eng J 2006;124:1-5.

[2] Buechs J, Maier U, Milbradt C, Zoels B. Power consumption in shaking flasks on rotary shaking machines: I. Power consumption measurement in unbaffled flasks at low liquid viscosity. Biotechnol Bioeng 2000;68:589-593.

[3] Doran PM. Bioprocess Engineering Principles. London: Academic Press Limited; 2000. p 130-163.

[4] Manning MC, Patel K, Borchardt RT. Stability of protein pharmaceuticals. Pharm Res 1989;6:903-918.

[5] Manning MC, Chou DK, Murphy BM, Payne RW, Katayama DS. Stability of protein pharmaceuticals: an update. Pharm Res 2010;27:544-575.

[6] Soos M, Moussa AS, Ehrl L, Sefcik J, Wu H, Morbidelli M. Effect of shear rate on aggregate size and morphology investigated under turbulent conditions in stirred tank. J Colloid Interface Sci 2008;319:577-589.

[7] Abramoff MD, Magelhaes PJ, Ram SJ. Image processing with ImageJ. Biophotonics Int 2004;11:36-42.

## 3 The air-liquid interface: its role in aggregation of hGH, critical parameters and stabilizing strategies

In preparation for Journal of Colloid and Interface Science

# The air-liquid interface: its role in aggregation of hGH, critical parameters and stabilizing strategies

Johanna Wiesbauer[1,2], Ruth Prassl[3], and Bernd Nidetzky[1,2]

[1]*Research Center Pharmaceutical Engineering, Graz, Austria*

[2]*Institute of Biotechnology and Biochemical Engineering, University of Technology Graz, Austria*

[3]*Institute of Biophysics and Nanosystems Research, Austrian Academy of Science, Graz, Austria*

*Corresponding author*: Nidetzky, B. (bernd.nidetzky@tugraz.at).

Institute of Biotechnology and Biochemical Engineering
Graz University of Technology
Petersgasse 12/I, A-8010 Graz, Austria
Fax: (+) 43 316 873 8434
E-mail: bernd.nidetzky@tugraz.at

**ABSTRACT**

In this study a well-defined and comparable set-up was used in order to compare aggregation during stirring and bubble aeration. Despite the fact that the shear rate and the air-liquid interface were comparable, bubble aeration led to a ~40 fold increased protein loss due to insoluble aggregation. Upon analysis of aggregation rates at various protein concentrations (0.67 to 6.7 mg/mL) it was found, opposite to expectation from literature, that protein loss rates were constant for bubble aeration (0.5 mg/h or 8.3 µg/min) and stirring (0.014 mg/h or 0.2 µg/min). We could further show that the strong foam formation in bubble aeration does not influence protein loss significantly. Furthermore we could demonstrate that aggregation rates for aeration and stirring depend on the specific surfaces and show a linear and positive correlation. In order to understand the differences between aggregation rates for aeration and stirring we show that the absolute amount of present interface (dependent on observation time span) is relevant for aeration as well as the surface renewal rates (dynamic air-liquid interface) for both methods. The absolute amount of air-liquid interface is much higher for aeration as new bubbles are frequently formed.

The amphiphilic (hydrophobic-hydrophilic; PPG-PEG) block-copolymer Pluronic F-68 was shown to prevent aggregation at the air-liquid interface due to a protein surfactant interaction. Further experiments with the individual building blocks PPG 2,000 and PEG 2,000 and 8,000 showed that PPG 2,000 stabilized hGH during stirring, shaking and bubble aeration, whereas PEG 2,000 and 8,000 could not suppress aggregation. For PPG 2,000 we suppose a protein surfactant interaction or competition with hGH for the air-liquid interface. This knowledge can be used for the selection or design of stabilizing excipients as well as for design of production processes.

**Keywords:** protein aggregation; adsorption; air-liquid interface; accelerated stress test; foam formation; surfactants.

## 1. Introduction

Apart from medical implication in a number of pathologies [1-4] aggregation influences the production of proteins and the shelf life of biopharmaceuticals and is therefore of concern for biotechnology and pharmaceutical industry [5-14]. However, prediction and control of protein aggregation is challenging [15-20] and literature shows that general prediction of protein long-term stability based on short-term prescreening experiments (elevated temperature, accelerated stress conditions) is difficult to extrapolate [18,20-23]. So a better understanding of prescreening experiments and their critical parameters is desired.

Proteins are amphiphilic, surface active biomolecules which adsorb at several interfaces during production and processing [14,24-30]. On a molecular basis mainly the 3D and tertiary structure is changed upon adsorption. At hydrophobic air-liquid interfaces often at least partial unfolding and (reversible) denaturation occurs due to interactions between the surface and the (buried) hydrophobic protein core [13,14,31]. Additionally the extent of interfacial denaturation is further dependent on factors like the decrease in surface free energy, forces at the interface, available surface area for adsorption, hydrophobicity and surface properties of the protein, number of disulfide bonds as well as the surface pressure against the molecule has to expand in order to unfold and the intrinsic protein stability [14,24,31-37]. After desorption of the structurally perturbed protein from the interface aggregation can take place in the bulk solution [14,38].

Thinking of air-liquid interfaces probably air bubbles in liquid solutions come first to our mind. Bubble aeration was commonly used to study air-liquid interfaces during fermentation and processing e.g. filling processes [34,39,40]. However not all proteins seem to be equally sensitive to air-liquid interfaces like shown in several comparisons [34,41]. During bubble aeration the effect of foam formation and surface tension on protein aggregation is discussed, suggesting antifoam additives and surfactants for stabilization at the interface [34].

Foam formation during commercial production (fermentation, mixing, ultrafiltration) can lead to protein damage and therefore aggregation [42]. Proteins as surface active molecules adsorb at the air-liquid interface, decrease the surface tension and stabilize the foam. Additionally they might undergo unfolding and surface denaturation at different time scales, influencing foaming propensity [24,33,34,42]. A recent study showed that apart from antifoam reagents optimum ionic strengths and pH can reduce the damage to the protein during foaming [42].

In general surfactants are popular excipients as they can be used at very low concentrations, prevent or inhibit adsorption of the protein at surfaces as well as aggregation during several process conditions e.g. refolding or freeze-thawing through interaction with the protein and/or protection against the interface [43-47]. Nevertheless, it has been shown that nonionic surfactants like Tween (Polysorbates) stabilized proteins during agitation but during storage it accelerated aggregation [48] or chemical modification possibly by contaminants such as peroxides [47,49-51]. As there is no universal recipe against aggregation so far due to complex aggregation mechanisms [52], these information are of importance for formulation development.

In general aggregation is protein concentration dependent [7,8]. For the involvement of air-liquid interfaces an inverse relationship between protein concentration and aggregation was reported (decreased protein concentration, increased aggregation) [42,48]. Normally, the transport of the protein to the interface should be diffusion controlled at least through the boundary layer and therefore dependent on the bulk protein concentration [36,53]. However, structural rearrangements are more likely if the available surface area is not limited by newly arriving proteins [53]. So for agitation studies the ratio of interface-to-protein, which is inverse to the protein concentration, seems to be critical and control aggregation. During quiescent shelf-life studies a correlation between protein concentration and aggregation is explained assuming an increased collisional frequency due to higher protein concentrations [48].

In our previous work we showed that human growth hormone (hGH), a 22 kDa globular therapeutic protein [54-56] only tends to aggregate in the presence of a dynamically renewed air-liquid interface due to stirring and shaking in accelerated stress prescreening experiments. These experiments should represent conditions leading to instabilities like unfolding, denaturation or aggregation during processing steps in a comparable experimental design within days [8,34,35,38,57-61]. Here we investigate the aggregation behavior of hGH during bubble aeration and stirring. Further the influences of protein concentration and specific air-liquid surface ($m^2/m^3 = m^{-1}$) on aggregation where studied and gave interesting results, which allowed us deeper insights into interfacial phenomena. In general nonionic surfactants (Tween 20, 80 and Pluronic F-68) were shown to have a stabilizing effect on hGH during aggregation at or above their critical micelle concentration (cmc) values, as they compete for surfaces or interact with the protein for the air-liquid interface. However it was also found that the conformational stability (thermodynamic) was decreased [43,62]. In literature the interaction of hGH and Tween 20 and 80 [45,46] was investigated and stated to be of a hydrophobic nature with little perturbation of the secondary structure. Further an interaction stoichiometry of 9-10 and 8-9 was found for hGH and Tween 20 and 80, respectively [44]. In this study we tried to gain better understanding of the stabilizing effect comparing Pluronic F-68 and its hydrophobic (polypropylenglycole – PPG) and hydrophilic (polyethylenglycole – PEG) building blocks.

## 2. Experimental section

### *2.1 Materials*

A recombinant preparation of hGH produced in *E. coli*, termed rhGH, was kindly supplied by Sandoz GmbH (Kundl, Austria). Unless noted otherwise, all chemicals were bought from Carl Roth (Karlsruhe, Germany). Fluorescein 5(6)-isothiocyanate (FITC) and Pluronic F-68 were from Sigma Aldrich (Vienna, Austria), 8-anilino-1-naphthalenesulfonic acid ammonium salt (ANSA) was from Merck KGaA (Darmstadt, Germany) and Polypropylenglycole 2,000 (PPG), Polyethylenglycole 2,000 and 8,000 from Fluka (Buchs, Switzerland). SlowFade® Gold Antifade Reagent was from Molecular Probes (Eugene, OR, USA).

### *2.2 Protein preparation*

Solutions of 10.4 ± 0.6 mg/mL hGH were obtained in 10 mM sodium phosphate buffer pH 7.0. The protein was stored at – 20°C until further use. Prior to use, the bulk solution was filtered using 0.22 μm PVDF filters from Millipore (Carrigtwohill, Ireland). Unless noted otherwise the protein concentration was adjusted to 3.4 ± 0.3 mg/mL. The concentration was measured by absorbance at 280 nm, assuming a molar extinction coefficient of 17,670 $M^{-1}$ $cm^{-1}$ (ExPASy ProtParam [63,64]) and a molecular mass of 22,125 Da.

### *2.3 Accelerated Stress Methods – Experimental set-up*

#### *2.3.1 Bubble aeration*

Bubble aeration was carried out with compressed air if not noted otherwise. Therefore we used a Stasto Automation pressure regulator (model R-M14-08-R; Innsbruck, Austria) followed by a flow gauge in order to adjust constant air flow rate of 3 L/h. The air flow was piped into the protein solution with an autoclavable plastic tube LAB/FDA/USP grade VI with 4 mm inner diameter (Fig. S1). The liquid filling level was 14 mm. An evaporation of

about 10 % over 7 h was observed after using a pre-humidified air supply, but not further considered for calculations. We used hGH at 6.7 (300 µM), 3.4 (150 µM), 1 (45 µM) and 0.67 (30 µM) mg/mL with a flow rate of 3 L/h to study the influence of the protein concentration on aggregation.

In experiments at 3.4 mg/mL hGH where compressed air was replaced with $N_2$, all other conditions and set-ups were kept like described above. In several experiments Antifoam polypropylene glycol 2,000 (PPG) was diluted (1:100) and 120 µL of this suspension were added into 12 mL hGH ($0.1 \times 10^{-3}$ % (v/v)) in a protein to PPG ratio of 3:1 prior to bubble aeration. Over time aliquots of 600 µl were taken, cooled and centrifuged at 13,200 rpm for 10 min. Afterwards the samples were used for analysis. Further dilutions of the aggregates samples 1:10, 1:5, 1:2 and undiluted were kept at 4°C over one week to show the reversibility/irreversibility of the aggregation by UV measurements.

*2.3.2 Stirring*

A double walled borosilicate 3.3 glass miniature bioreactors with a diameter of 32 mm (804 $mm^2$) was used at 25°C with a magnetic stirring bar at 300 rpm [65]. Furthermore a set of experiments was carried out using the same concentration range (6.7 to 0.67 mg/mL) of hGH as during aeration.

*2.3.3 Specific surface and procedural characterization*

The air-liquid interface as well as the Reynolds number and the shear rate for stirring were determined as previously described [65-67]. The calculated interface and the liquid volume were used to calculate the specific surface areas. Variation of the specific surface was achieved by usage of different fill levels (12, 16, 24, 32, 60 and 55 mL – with reduced interface set-up; see Table S2).

Bubble size determination was carried out using a stroboscope and a digital camera. The images were analyzed using ImageJ Software. The surface at the top liquid level was calculated using the diameter (32 mm) of the glassreactor (top area see Table 1 control) [68]. A more detailed description is given in the Supporting Information (Table S1). Due to the strong foam formation the fill level could not be varied for bubble aeration. So the aeration rates were changed (1.5, 2, 3, 4 and 5 L/h; see Table S3).

*2.3.4 Combined stress from aeration and stirring*

Insoluble aggregates from combined experiments of aeration and stirring were analyzed using confocal laser scanning microscopy (CLSM). Therefore, 3.4 ± 0.3 mg/mL hGH was first aerated for 7 h and afterwards stirred for 24 h. Over time (2 h, 15 h and 24 h) samples were taken and prepared for CLSM analysis.

*2.3.5 Stabilization by usage of surfactants (Pluronic F-68, PPG 2,000, PEG 2,000 and 8,000)*

3.4 ± 0.3 mg/mL hGH (150 µM) were supplemented with 2 mg/mL Pluronic F-68 (240 µM, below cmc) [69] in a molar protein to surfactant ratio of 1:1.6 prior to bubble aeration and stirring, respectively (24 h). These samples were further used for small angle X-ray scattering (SAXS) measurements. Additionally PPG 2,000, PEG 2,000 and PEG 8,000 were used in the same molar ratio during stirring, shaking and bubble aeration.

*2.3.6 Surface tension, viscosity and density determination*

Density was determined using a DSA 5000 M density and sound velocity meter from Anton Paar (Graz, Austria). For viscosity an Anton Paar MCR 300 (Graz, Austria) rotational viscosimeter with a double-gap cylinder (DG26.7) was used for dynamic viscosity. All measurements were carried out in triplicate.

Surface tension was determined using an Easydrop FM40MK2 equippment from Krüss (Hamburg, Germany) with 3 measurements each.

*2.4 Analytical methods*

*2.4.1 Turbidimetric analysis*

For turbidity measurements wavelength scans were carried out at 25°C using a Beckmann DU 800 spectrophotometer and the spectra were analyzed at 400 nm [43,70,71]. The instrument was calibrated against formazin reference suspensions [72].

*2.4.2 SEC-HPLC*

Analyses were carried out like previously described [65] using a Merck-Hitachi LaChrome LC system equipped with a L-7250 autosampler and a L-7400 UV detector. All samples were centrifuged prior to analysis at 13,200 rpm for 10 min.

*2.4.3 Fluorescence measurements*

Measurements were done on a software-driven Hitachi F-4500 fluorescence spectrophotometer (Tokyo, Japan). Measurements were carried out within 24 hours after sampling. Intrinsic tryptophan fluorescence was recorded at 25°C, using an excitation wavelength of 295 nm. Emission spectra were obtained in the range 300 – 500 nm. Slit widths of 5 nm were used. The centrifuged samples were diluted to a concentration of 0.5 mg/mL. The native protein shows maximum emission at 333 to 335 nm, while for unfolded hGH, this value is at around 350 nm [56,73].

*2.4.4 Confocal laser scanning microscopy (CLSM)*

Visualization of the precipitated hGH by CLSM with FITC and ANSA was performed as described [65]. CLSM images were acquired with a Leica TCS SPE confocal system (Leica Microsystems, Mannheim, Germany) equipped with solid state and UV lasers. Three-

dimensional confocal models were created with the software IMARIS 7.0 (Bitplane, Zurich, Switzerland).

*2.4.5 Far-UV Circular Dichroism (CD) measurements*

hGH samples with Pluronic F-68 were stressed over 24 h (stirring, aeration, shaking) and prepared by diluting the protein samples to 0.5 mg/ml with sodium phosphate buffer pH 7.0 for CD measurements. Measurements were carried out like previously described [71], however a 0.2 mm quartz cuvette was used at 25°C and Spectra were recorded between 190 and 260 nm. The spectra were processed using CD tool software [74] and the secondary structure contents were estimated using the CDSSTR program (set 4) on the online server DICHROWEB [75].

*2.4.6 SAXS measurements*

SAXS curves were measured with a SWAXS camera system (System 3, Hecus X-ray Systems, Graz, Austria) mounted on a sealed X-ray tube generator from Seifert (Ahrensburg, Germany) at 20°C as reported recently [71]. The exposure time was 1 h. SAXS patterns were recorded in a q-range between 0.19 $nm^{-1}$ and 3.0 $nm^{-1}$, where $q = 4p \sin(q/l)$ is the scattering vector, 2q the scattering angle and l = 0.154 nm the wavelength of the X-ray beam. The data were buffer background corrected, normalized to intensity and corrected for slit collimation geometry. The processed data were subsequently analyzed with the program package ATSAS 2.3. Indirect Fourier transformation was performed with the programs PRIMUS [76] and GNOM [77] and the theoretical scattering curve for hGH in aqueous solution was derived from the crystal structure (PDB-code: 3HHR) using the program CRYSOL [78].

## 3. Results and discussion

### *3.1 Bubble aeration and stirring*

All experiments were carried out in the miniature glass bioreactors (Methods, Fig. S1). Compared to our control sample (25°C, 0 rpm), which led to no observable aggregation, bubble aeration resulted in turbid samples where soluble hGH undergoes phase transitions to insoluble aggregates. Following protein loss over time (UV measurements) we found that the formation of insoluble aggregates was 40-fold faster for bubble aeration than during stirring (Fig. 1). According to our characterization summarized in Table 1 (see also Table S1 and Fig. S2), these differences cannot be simply explained by shear rates and static air-liquid interfaces. So a detailed analysis of bubble aeration and the formed aggregates was carried out to identify the trigger for aggregation.

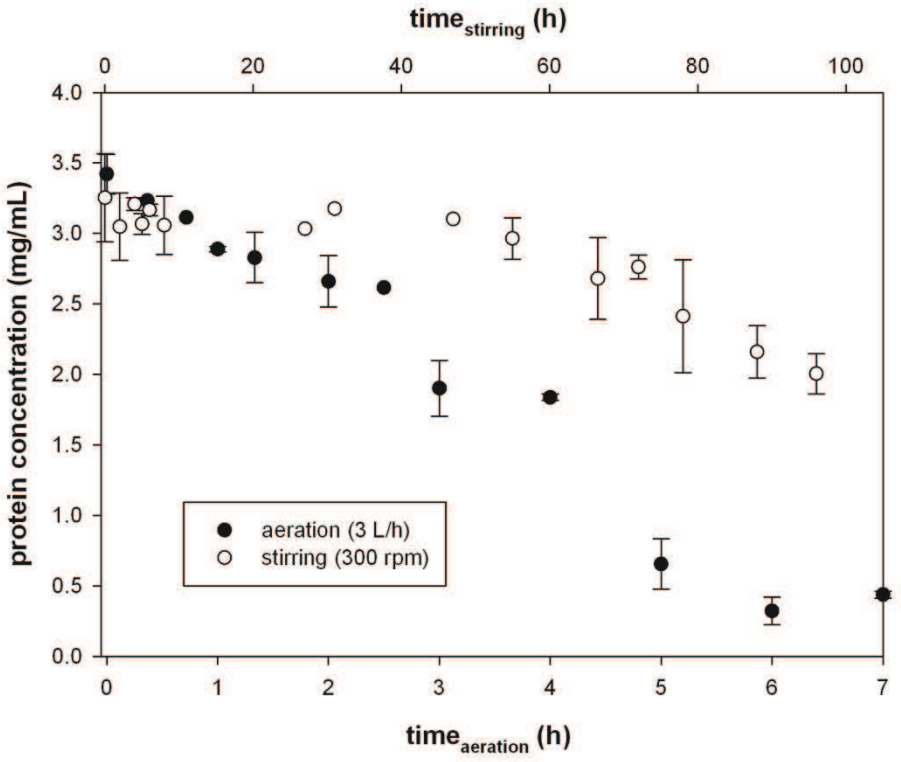


**Fig. 1: Time course protein concentration in the supernatant during aggregation**
Comparison of the protein loss and phase transition to insoluble aggregates for stirring (open cirlces) and bubble aeration (black circles) for hGH. The protein concentration was determined in the centrifuged supernatant.

Analysis of the aerated samples (supernatant plus precipitate) using PAGE showed that also bubble aeration results in non-covalent insoluble high molecular weight aggregates, which vanish after treatment with SDS in the absence of reducing agents like recently reported for stirring and shaking [65] (data not shown). As previously found for other stress methods no stable and soluble associates were detected (PAGE; SEC-HPLC data not shown). Aggregation was found to be irreversible upon dilution and temperature change (4°C) monitored over one week (UV protein determination).

Additionally, centrifuged samples (supernatant) analyzed with intrinsic and ANSA fluorescence measurements as well as PAGE and SEC-HPLC analysis showed no significant structural perturbations or increased amounts of soluble aggregates. These results are similar to previous results for shaking and stirring [65].

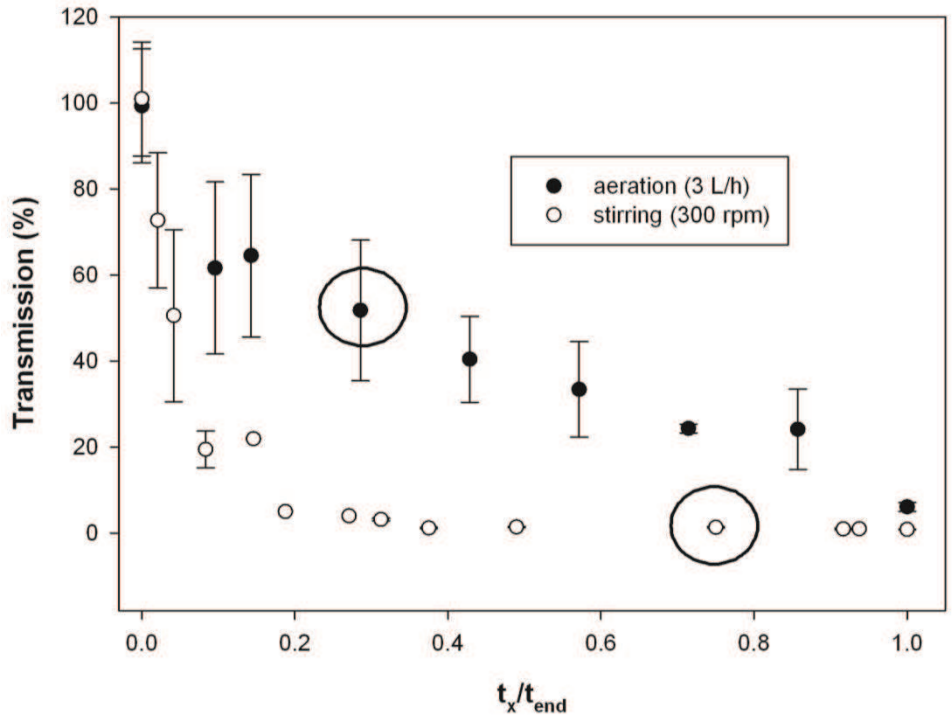


**Fig. 2: Turbidity (transmission) during accelerated stress conditions for hGH normalized to the overall aggregation time.**

Time points for equal aggregation level are marked (open circle) for stirring and bubble aeration.

Interesting results were found measuring the turbidity of the samples. Although turbidity measurements cannot give results regarding size, shape and number of particles formed [70], a clear difference to stirred samples could be detected. Whereas stirring led to a dramatic increase in turbidity early on, bubble aeration shows only slight increasing turbidity even at the same amount of protein loss (Fig. 2, open black circle). In Fig. 2 the results are shown as changes in transmission. Measurements were carried out using wavelength scans (250 to 660 nm) and additionally after centrifugation the samples became clear and so we exclude other effects or artifacts. Based on these findings and visual inspection we state the formation of larger particles during bubble aeration compared to stirring.

For CLSM analysis of bubble aeration labeling of the protein was done with FITC and ANSA as previously described [65]. Several pictures were acquired for ImageJ particle analysis in an area of 275 x 275 µm, using different dilutions of the labeled protein suspension. Although we used dried samples and the effective hydrodynamic radius is underestimated, we can clearly detect differences regarding size and shape of the particles (Fig. S3). In a qualitative comparison of stirring and aeration we found that extremely large particles are formed during bubble aeration. This effect was already observed during turbidity/transmission measurements. There are several possible explanations for the size and shape of the aerated aggregates. First of all strong foam formation is observed and so these large aggregates could be related to that and the large size of the air bubbles. Furthermore the aerated solution is less turbulent (Table 1) as a stirred solution and therefore these large complexes could be stable, whereas they are possibly destroyed during stirring. This will be further discussed later when aeration and stirring are combined. Altogether the use of FITC and ANSA labeled samples gave consistent results, and again mainly aggregates showing high affinity to hydrophobic dyes are found. The shape and size indicate amorphous aggregates [79]. We conclude that (partial) unfolding (ANSA binding) is an essential step in the aggregation of hGH induced by accelerated stress conditions.

**Table 1: Accelerated stress conditions used to examine aggregation of hGH.**

| Stress type | Volume ($\times 10^{-6}$ m³) | Air-liquid interface ($\times 10^{-6}$ m²) | *Re* number[a] | Shear rate[a] ($s^{-1}$) | hGH aggregation |
|---|---|---|---|---|---|
| Control | 11.4 | 800 | 0 | 0 | None |
| Stirring (300 rpm) | 11.4 | 1,090 ± 40 [b] | 4,800 | 40-100 [a] | Precipitation, turbidity formation |
| Aeration (3 L/h) | 11.4 | 960 ± 10 [c]<br>156 ± 9 [d]<br>46,000 ± 3,000[e] | 720 | 100 | Precipitation, turbidity formation |

[a] The Supporting Information shows determination of *Re* numbers and shear rates [65,66] for the different conditions used (Table S1 and S2).

[b] The surface area was calculated assuming a paraboloid of revolution; see the Supporting Information under Table S1.

[c] Static "average" air-liquid interface: bubble surface area x frequency x life time + top liquid level surface

[d] Static "average" air-liquid interface: only bubble area x frequency x life time

[e] absolute (dynamic) air-liquid surface for 1 min: bubble area x frequency ($min^{-1}$) x observation time span (min) = 42 ± 3 fold increased compared to stirring.

As bubble aeration went along with massive foam formation we investigated this effect in more detail. As proteins are amphiphilic polymers they decrease the surface tension and can stabilize foams against coalescence very effectively [33,42]. In literature [34] strong foam formation was previously reported as cause for aggregation, as most aggregates were found within. So the usage of antifoam reagents was suggested for prevention of aggregation. In our study we used the polymer PPG 2,000 to suppress the foam formation but our results showed that aggregation was not prevented if no foam is formed. PPG 2,000 reduces the surface tension more (44.4 ± 0.3 mN/m) than buffer (71.2 mN/m) and the protein solution (56.5

± 0.4 mN/m) alone (Table S1). Therefore we assume that the proteins and PPG 2,000 compete for adsorption at the air-liquid interface and influence foam formation. Whereas during foam formation the air bubbles do not burst on the surface (Fig. S4) they do in the presence of anti-foam. As the time course for both experiments is similar within experimental errors and even the aggregates look comparable (Fig. S5) we conclude that foam formation is not a critical parameter during aggregation. Further the bursting of the bubbles does not seem to influence aggregation of hGH as previously shown for pepsin, bovine serum albumin and human immunoglobulin G as the released energy is dissipated at a larger length scale compared to a protein molecule [40]. Bubble aeration experiments using $N_2$ instead of compressed air were performed to check if the nature of the gas is of importance. Regarding aggregation propensity we could not detect a significant difference (Fig. 3)

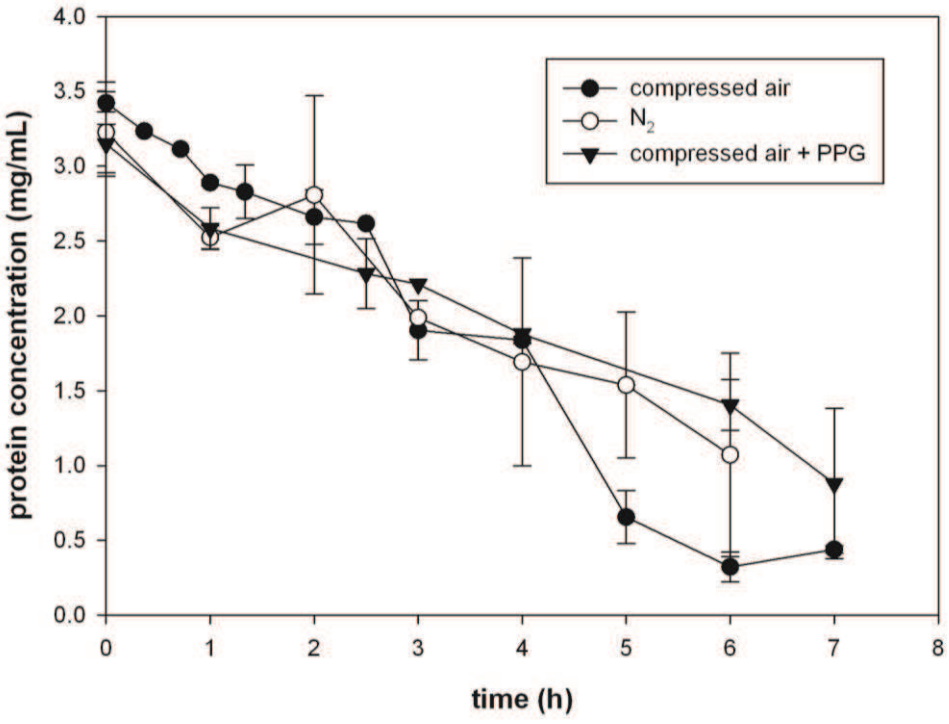


**Fig. 3: Influences on bubble aeration.**

Bubble aeration was performed with compressed air and the influence of foam formation was studied using PPG 2,000. The comparison of aeration with compressed air and nitrogen gave no significant difference.

.

*3.2 Combined stress from aeration and stirring*

By monitoring the shape and size changes of aggregates formed during aeration if stirred for 24 h, we found that stirring prevents the formation of large and complex structures (Fig. S6). A similar behavior was also found for polystyrene latex particles in literature [80]. From this we conclude that the difference in the size and shape of the aggregates does not necessarily imply a different aggregation mechanism.

*3.3 Static and dynamic air-liquid interfaces*

New insights into the processes at the air-liquid interface were gained, when the concentration of hGH was varied from 6.7 (300 μM) to 0.67 mg/mL (30 μM) (Table S1 and Fig. 4). As discussed in the introduction we would expect a dependency of the aggregation rate on the protein concentration [36,48,53]. In order to compare the data more easily we used the relative protein concentration and relative protein loss due to aggregation. So we observed that with higher protein concentration less aggregation was detected. Having a look on the absolute amount of protein lost per hour, however we found that for all four conditions approximately 0.014 ± 0.002 mg/h (0.20 ± 0.03 μg/min) hGH precipitated during stirring independent of the initial protein concentration. For bubble aeration a rate of 0.50 ± 0.03 mg/h (8.3 μg/min ± 0.5 μg/min) was determined (~ 40-fold increase). As the denaturability of the protein should not be changed our results indicate a scenario where reversible associates are formed which protect hGH at higher protein concentrations. The formation of reversible associates was recently investigated in NMR measurements for hGH [81]. So independent of the protein concentration only a certain amount (proteins in outer spheres), probably also limited by the available effective surface, can unfold and aggregate, although with increased protein concentration we would expect more partners for aggregation. This is contrary to reported results for pegylated megakaryocyte growth and development factor (PEG-MGDF), granulocyte colony-stimulating factor (PEG-GCSF) and osteoprotegerin protein fused with the sequence from the

Fc portion from an immunoglobulin OPG-Fc [48]. The authors state an inverse relationship of protein concentration and aggregation at air-liquid interfaces.

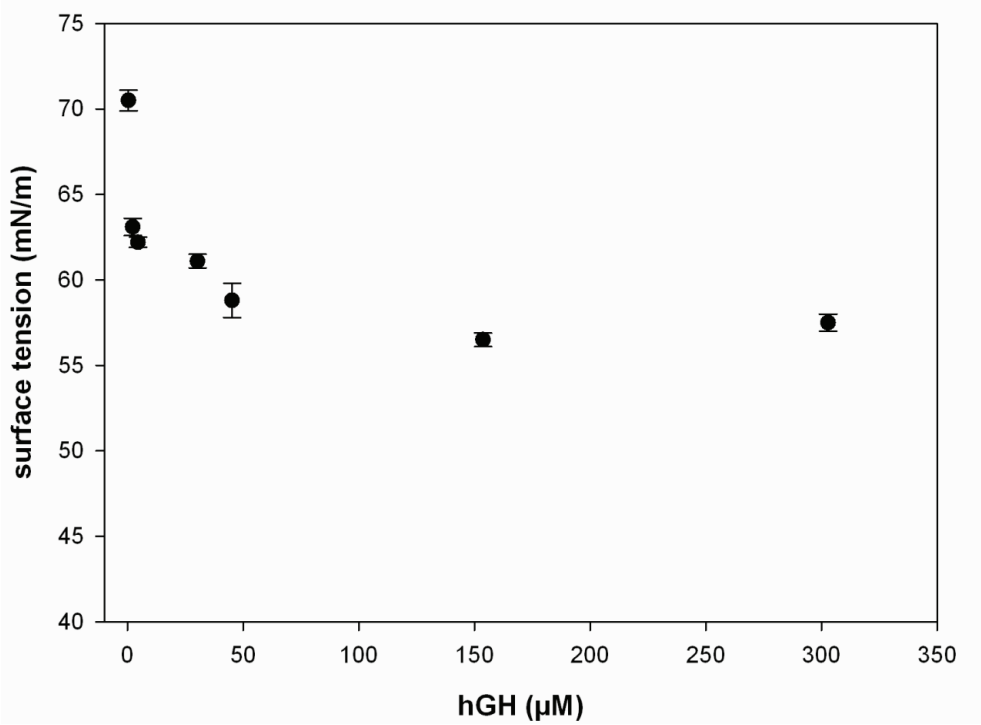


**Fig. 4: hGH concentration versus surface tension.**
In our experiments hGH solutions with constant surface tension were used (> 30µM).

The ~40-fold increased aggregation rate during aeration is generally difficult to understand, if we compare the available (static) air liquid interfaces. According to Table 1 a permanent static "average" air-liquid interface of 1,090 x $10^{-6}$ m² is present during stirring. For aeration a similar static air-liquid interface was calculated for the bubble aeration (bubble area x frequency x average lifetime) and the top liquid surface (960 ± 10 x $10^{-6}$ m²). However, if we use the absolute available surface area by taking the area of one bubble times the formation frequency for e.g. a 1 min time span (Table 1), the difference in available surface is about ~40-fold like the detected aggregation rate ratio. Further this would mean that the air-liquid surface is either not additionally renewed during stirring and bubble rising or with an equal rate. Further calculations carried out for 1 h of bubble aeration (bubble aera x frequency $h^{-1}$ x h) indicate that the air-liquid surface during stirring has to be renewed ~70-fold per hour (1.2

$min^{-1}$) to maintain this 40-fold detected difference in the aggregation rates. Here we have to note, that higher surface renewal rates during stirring could be compensated through surface renewal of the rising bubble. Additionally, the air-liquid interface on top (liquid level = 800 x $10^{-6}$ $m^2$) was neglected during bubble aeration because the air bubble surface seems to be the dominant interface due to its high formation frequency (see control, Table 1 and Fig. S1). Further we lack aggregation in our unstressed control experiment (25°C 0 rpm, liquid level = 800 x $10^{-6}$ $m^2$). Due to the rather low Reynolds number we assume that diffusion and convection to the top air-liquid interface is rather slow compared to the interaction with the bubbles. We also assume that the different curvatures of the surfaces (stirring and bubble aeration) do not have an influence on a microscopic level. Therefore we designed further experiments where the specific surface was varied for stirring and bubble aeration, which are discussed later.

*3.4 Influence of the specific surface*

As a constant amount of protein precipitates during stirring and bubble aeration respectively, the air-liquid interface was further investigated (Table S2 and S3). During our control experiments with a flat air-liquid interface no protein aggregation was observed over 10 days. Transport to the interface might happen only by diffusion and from a hydrodynamic radius of ~ 3 nm and the Stokes-Einstein equation a diffusion coefficient at 25°C of $10^{-10}$ $m^2/s$ was assumed. This might explain why we do not detect aggregation at the air-liquid interface over 10 days. During stirring, shaking or bubble aeration the transport to and fro the interface is accelerated by convection and mixing which increases the amount of absorbable protein. A variation in the specific surface ($m^2/m^3 = m^{-1}$) led to a change in the aggregation rate. The overall trend indicated that with decreased specific surface aggregation decreased (Fig. 5). For stirring (after an initial lag phase of about ~ 20 h) we determined a rate of 0.0026 ± 0.0008 µg/(min x $m^{-1}$). For aeration we used the findings presented in 3.3 and calculated a dynamic

air-liquid interface for the time span of 1 min. So a rate of 0.0046 ± 0.0005 µg/(min x $m^{-1}$) is obtained (~2-fold increased compared to stirring).

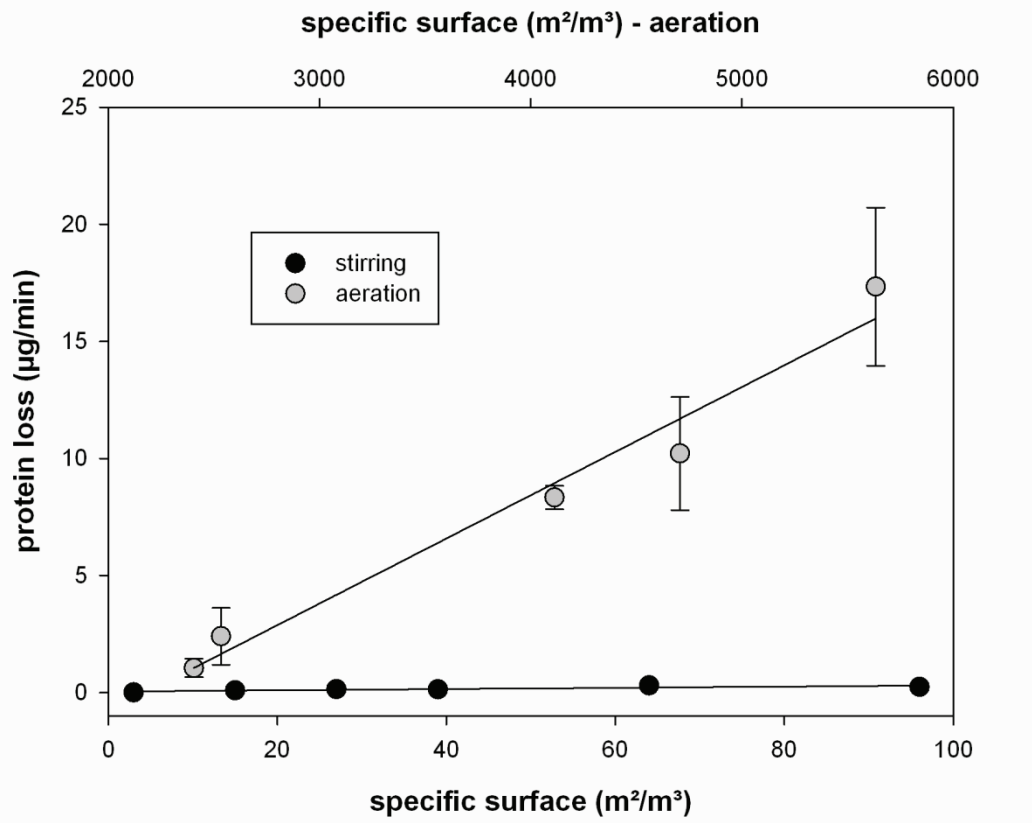


**Fig. 5: Dependency of aggregation rates on the specific surface for stirring and bubble aeration.** For bubble aeration the specific surface was calculated by the bubble surface x formation frequency for an observation time span of 1 min (Talbe 1 and Table S3). Values for stirring were derived from the static specific surface (Table 1 and Table S2).

As this is only twice the number we obtained during protein concentration variations, this could be explained by the fact that about twice as many bubbles per second are formed if the aeration rate is increasing from 1.5 to 5 L/h. With the aeration rate also the shear rate is increased (Table S3) but as the differences are little and as shear does not seem to be a predominant force in aggregation, this fact was neglected. Further we assume an increase in mixing during aeration rate variations whereas the surface generation during stirring is probably slowed down with increasing distance (volume) from the stirrer. For stirring the overall air-

liquid interface is not changed drastically even if the volume is increased. In general we could show that the air-liquid interface is a critical parameter for aggregation in accelerated stress conditions like stirring and aeration. As a static average air-liquid interface does not explain our findings, dynamics at the interface and surface renewal cannot be neglected. A linear and positive correlation between aggregation rates and specific surface ($m^2/m^3$) can be further used for stabilization strategies like design of production vessels or storage vials. We assume that stirring and bubble aeration can be compared regarding aggregation and the critical parameters. This can be further used for generalized stabilization strategies. As the air-liquid interface is of a hydrophobic nature [35] and our aggregates bind a hydrophobic fluorescence dye we further investigated possible excipients (amphiphilic, hydrophilic, hydrophobic) for stabilization.

*3.5 Stabilization by usage of surfactants (Pluronic F-68, PPG 2,000, PEG 2,000, PEG 8,000)*

In our study we could show that hGH is stabilized by the surfactant Pluronic F-68 used at concentrations below its cmc [69] for at least 24 h independent whether shaking, stirring or bubble aeration were applied. During this time period no significant protein loss or turbidity was detected (data not shown). However, SAXS measurements showed only a slight change in scattering curves (Fig. 6) and the pair-distribution function shows a more elongated sample (Fig. 7) indicating some interaction between hGH and Pluronic F-68. Therefore we assume an interaction between hGH and Pluronic F-68 and so only buffer was subtracted in the following measurements. Furthermore analysis of the protein structure in the presence of Pluronic F-68 supports a theory where hGH is preserved in its native structure. In a Kratky plot (Fig. S7) no unfolding not even partially is detected [82]. Results from SAXS measurements are summarized in Table S4.

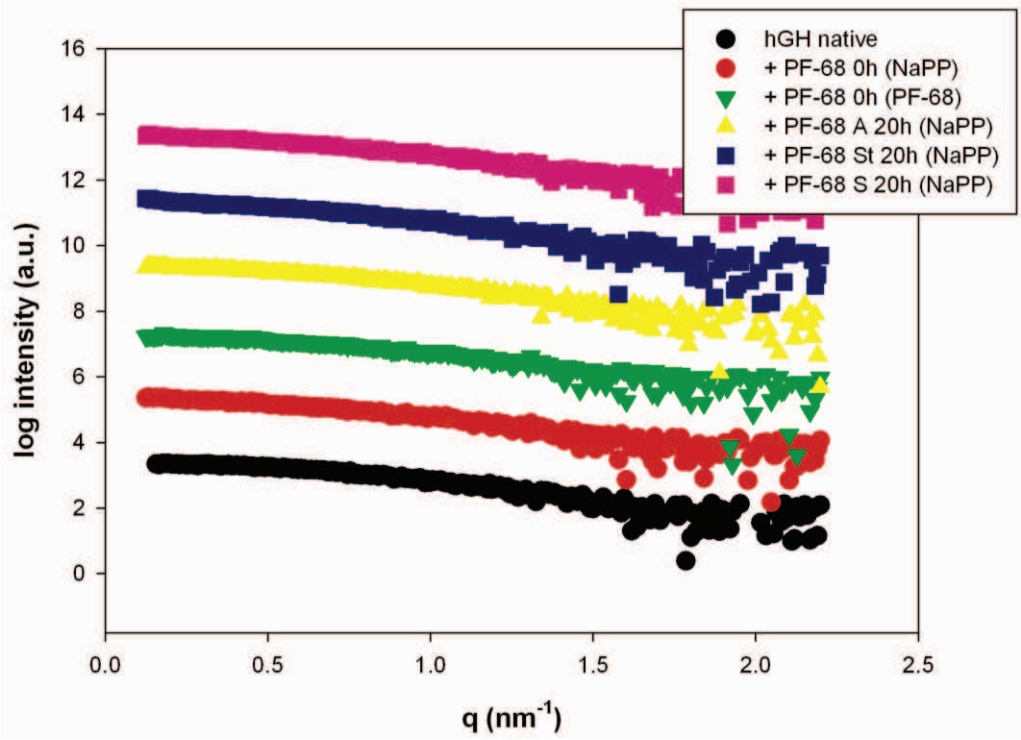


**Fig. 6: Scattering curves (log I vs. q) for hGH and hGH + Pluronic F-68 (PF-68).** The curves were shifted by the value of 2 from measurement to measurement for better visualization. (PF-68) Pluronic F-68 in 10 mM NaPP pH 7.0 and (NaPP) 10 mM NaPP buffer pH 7.0 subtracted as background; (A) aeration 3 L/h; (St) stirring 300 rpm; (S) shaking 300 rpm.

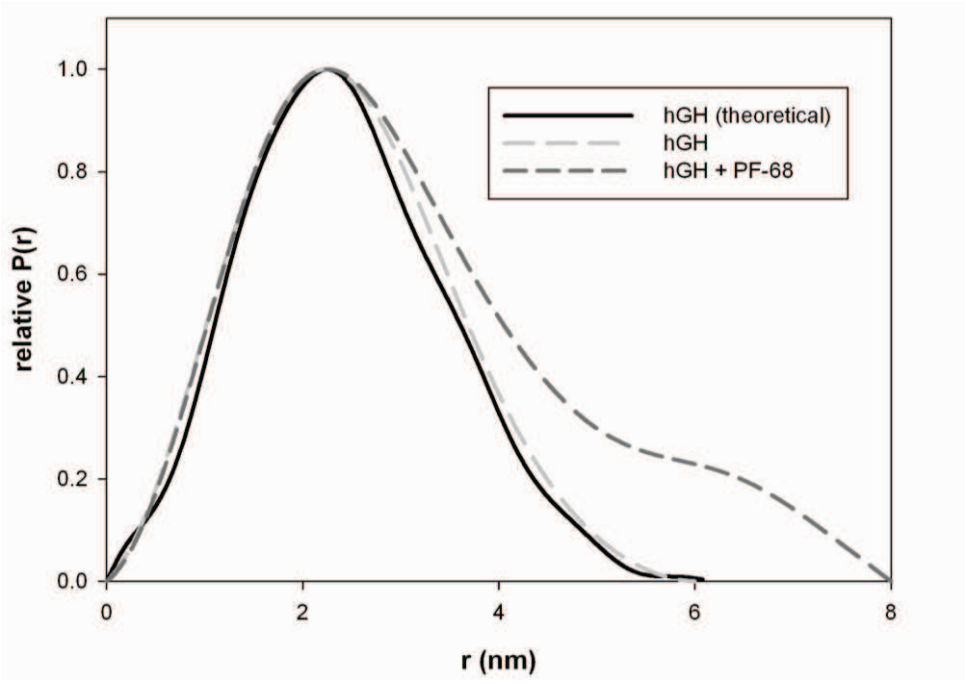


**Fig. 7: Pair-distribution functions for hGH and hGH + Pluronic F-68.** A theoretical pair-distribution function (crystal structure) is compared with hGH in solution and in the presence of Pluronic F-68 (PF-68).

CD measurements show that the secondary structure is unchanged (Table 2 and Fig. S8). This is interesting as reports in literature show that Pluronic F-68 can also stabilize unfolded proteins in solution [45,83], which is not the case in our experiments.

**Table 2: Secondary structure of hGH in the presence of polymers (CDSSTR analysis, Set 4).**

| Sample | α-helix | β-sheet | turns | unordered |
|---|---|---|---|---|
| hGH | 0.70 | 0.02 | 0.08 | 0.19 |
| + Pluronic F-68 | 0.71 | 0.02 | 0.12 | 0.16 |
| + PPG 2,000 | 0.70 | 0.03 | 0.06 | 0.20 |
| + PEG 8,000 | 0.72 | 0.03 | 0.06 | 0.18 |
| + PEG 2,000 | 0.75 | 0.02 | 0.05 | 0.18 |

Pluronic F-68 reduced the surface tension less than PPG 2,000 (Table 3), however prevented aggregation in a close to 1:1 protein to surfactant ratio compared to reported higher values for Tween 20 and 80 [44,46]. Comparing Pluronic F-68 and Tween variants the first reveals a higher hydrophile-lipophile balance (HLB) number (Table S5) and should be therefore more hydrophilic. A close look at the structures reveals that Pluronics consists of two hydrophilic polyoxyethlylene (PEO, PEG) and one central, hydrophobic polyoxyproyplene (PO, PPG) segments, whereas Tween 20 and 80 mainly consist of PEOs and one hydrophobic tail (Figure S9). So hGH could be rescued by the large hydrophobic segment of Pluronic F-68 interacting with the hydrophobic air-liquid interface. This is further supported by our results showing that hGH is also stabilized by about equimolar PPG 2,000 (240 μM) as summarized in Table 3.

**Table 3: Surface tension, foam formation and aggregation of hGH in the presence of different polymers (~ equimolar).**

| Sample | σ (mN/m) | Foam formation | Aggregation | Relative aggregation rate[a] |
|---|---|---|---|---|
| hGH | 56.5 ± 0.4 | Yes | Yes | 1 |
| + Pluronic F-68 | 49.6 ± 0.2 | No | No | 0 |
| + PPG 2,000[b] | 44.4 ± 0.3 | No | Yes | 1 |
| + PPG 2,000 | 39.2 ± 0.1 | No | No | 0 |
| + PEG 8,000 | 60.0 ± 0.8 | Yes | Yes | 0.25[c]<br>1[d] |
| + PEG 2,000 | 59.2 ± 0.5 | Yes | Yes | 1 |

[a] relative to rates for hGH without additives (stirring 0.014 mg/h; aeration 0.3 mg/h)

[b] 0.1 x $10^{-3}$ % (v/v) PPG 2,000 a protein to polymer ratio of 3:1.

[c] Comparison hGH pH 7.0 and hGH + PEG 8,000 stirring, shaking

[d] Comparison hGH pH 7.0 and hGH + PEG 8,000 aeration

PEG 2,000 and PEG 8,000 do not prevent foaming (bubble aeration) and aggregation (shaking, stirring, bubble aeration) of hGH. Similar effects were seen upon heat denaturation in the presence of Pluronic F-68 and PEG 8,000 [83]. However, PEG 8,000 reduced aggregation rates during stirring and shaking about 4-fold. For bubble aeration it was found that although the solution remains rather clear all the protein is lost into foam denaturation in the same rate as for hGH alone. For PEG it was shown in several studies that this cosolute stabilizes the proteins via preferential exclusion from the protein surface [83-86] or by stated binding to the protein by hydrophobic and hydrophilic interactions [87-89]. However, PEG 2,000 and 8,000 were not able to stabilize hGH against aggregation at the concentrations we used. Decreased

aggregation of hGH during stirring and shaking (not aeration) in the presence of PEG 8,000 could be related to stabilizing preferential exclusion effects [85,86]. More likely PEG 8,000 could influence the dynamics at the air-liquid interface and the adsorption at the interface (surface tension increased) as only stirring and shaking are affected, as during aeration constantly a new interface is created. Contrary to PEG Pluronic F-68 obtains also hydrophobic segments. These are believed to interact with solvent exposed hydrophobic side chains of structurally perturbed proteins and release the protein in its native and fully hydrated conformation [83]. For PPG 2,000 a similar mechanism as for Pluronic F-68 might be possible as well as surface tension values (Table 3) might also indicate competition for available surface between hGH and PPG 2,000 at the interface. This is further supported by the drastic decrease of the surface tension in the presence of PPG 2,000. In general all tested stress conditions gave comparable results for critical parameters and detectable stabilizing effects and are therefore comparable.

## 4. Conclusion

In our defined experimental test-system we could show that in spite of application of similar overall stress parameters (shear rate, air-liquid interface) differences in the aggregation rates of stirring and bubble aeration were found (~ 40-fold). Our results can be explained if we consider a dynamically renewed (increased) interface for bubble aeration instead of a strictly static one. A positive and linear correlation between the aggregation rate and specific surface ($m^2/m^3 = m^{-1}$) was found for both stress conditions and also the different rates can be explained (static and dynamic air-liquid interface areas). As differences in the aggregation rates can be correlated to the air-liquid interface itself in our set-up, we assume similar events initiating aggregation independent of the stress method. Therefore also general stabilization strategies for our different stress conditions should be possible like reducing the specific surface of the production vessels and storage vials.

As a second general stabilization strategy we investigated aggregation of hGH in the presence of about equimolar concentrations of the amphiphilic surfactant Pluronic F-68 and its individual building blocks PPG 2,000 (hydrophobic) and PEG 2,000 and 8,000 (hydrophilic). Stabilizing cosolutes (Pluronic F-68 and PPG 2,000) at the air-liquid interface decreased the surface tension and exposed hydrophobic segments in order to 1) interact preferentially with the hydrophobic air-liquid interface or 2) hydrophobic protein intermediates states. Again our accelerated stress conditions deliver comparable conclusions for stabilization strategies and do not intrinsically affect the results.

**Acknowledgements**

This project was supported by FFG, Land Steiermark and SFG. Thanks go to Sandoz GmbH, Austria for kindly supplying the protein used in this study. Dr. Massimiliano Cardinale (Institute of Environmental Biotechnology, Graz University of Technology) is thanked for help with the CLSM measurements. The help of Christoph Neubauer and Michael Piller (RCPE GmbH) with the surface tension, density and viscosity measurements is greatly acknowledged. Further the authors would like to thank Prof. Matthäus Siebenhofer, Prof. Günter Brenn and Prof. Andreas Pfennig for helpful discussion and input. Mag. Andras Böszörmenyi, Prof. Walter Keller and Mag. Kerstin Fauland are thanked for their help with the CD measurements.

## References


[1] V. Bellotti, P. Mangione, M. Stoppini, Cell. Mol. Life Sci. 55 (1999) 977.
[2] C.M. Dobson, Trends Biochem. Sci. 24 (1999) 329.
[3] M.E. Huff, W.E. Balch, J.W. Kelly, Curr. Opin. Struct. Biol. 13 (2003) 674.
[4] A. Pastore, P. Temussi, J. Phys. Condens. Matter. 24 (2012)
[5] E.Y. Chi, S. Krishnan, T.W. Randolph, J.F. Carpenter, Pharm. Res. 20 (2003) 1325.
[6] W. Wang, S. Nema, D. Teagarden, Int. J. Pharm. 390 (2010) 89.
[7] H.C. Mahler, W. Friess, U. Grauschopf, S. Kiese, J. Pharm. Sci. 98 (2009) 2909.
[8] W. Wang, Int. J. Pharm. 185 (1999) 129.
[9] J.L. Cleland, M.F. Powell, S.J. Shire, Crit. Rev. Ther. Drug Carrier Syst. 10 (1993) 307.
[10] M.E.M. Cromwell, E. Hilario, F. Jacobson, Pharm. Res. 8 (2006) E572.
[11] A. Mitraki, J. King, Nat. Biotechnol. 7 (1989) 690.
[12] C.H. Schein, Nat. Biotechnol. 8 (1990) 308.
[13] M.C. Manning, K. Patel, R.T. Borchardt, Pharm. Res. 6 (1989) 903.
[14] M.C. Manning, D.K. Chou, B.M. Murphy, R.W. Payne, D.S. Katayama, Pharm. Res. 27 (2010) 544.
[15] M. Vendruscolo, C.M. Dobson, J. Mol. Biol. 350 (2005) 379.
[16] C.M. Dobson, F. Chiti, M. Vendruscolo, J. Mol. Biol. 380 (2008) 425.
[17] W.F. Weiss, T.M. Young, C.J. Roberts, J. Pharm. Sci. 98 (2009) 1246.
[18] C.J. Roberts, T.K. Das, E. Sahin, Int. J. Pharm. 418 (2011) 318.
[19] N. Chennamsetty, V. Voynov, V. Kayser, B. Helk, B.L. Trout, Proc. Natl. Acad. Sci. U. S. A. 106 (2009) 11937.
[20] A.V. Filikov, R.J. Hayes, P. Luo, D.M. Stark, C. Chan, A. Kundu, B.I. Dahiyat, Protein Sci. 11 (2002) 1452.
[21] A.C. King, M. Woods, W. Liu, Z. Lu, D. Gill, M.R.H. Krebs, Protein Sci. 20 (2011) 1546.
[22] R.K. Brummitt, D.P. Nesta, C.J. Roberts, J. Pharm. Sci. 100 (2011) 4234.
[23] B.A. Kerwin, M.C. Heller, S.H. Levin, T.W. Randolph, J. Pharm. Sci. 87 (1998) 1062.
[24] G. Yampolskaya, D. Platikanov, Adv. Colloid Interfac. 128-130 (2006) 159.
[25] F. Felsovalyi, P. Mangiagalli, C. Bureau, S.K. Kumar, S. Banta, Langmuir 27 (2011) 11873.
[26] M.C.L Maste, E.H.W. Pap, A. van Hoek, W. Norde, A.J.W.G. Visser, J. Colloid. Interface Sci. 180 (1996) 632.
[27] T. Zoungrana, G.H. Findenegg, W. Norde, J. Colloid Interface Sci. 190 (1997) 437.
[28] S. Colombie, A. Gaunand, B. Lindet, Enzyme Microbial Technol. 28 (2001) 820.
[29] K. Nakanishi, T. Sakiyama, K. Imamura, J. Biosci. Bioeng. 91 (2001) 233.
[30] A. Sadana, Chem. Rev. 92 (1992) 1799.
[31] T.L. Donaldson, E.F. Boonstra, J.M. Hammond, J. Colloid Interface Sci. 74 (1980) 441.
[32] P. Walstra, in: E. Dickinson, R. Miller (Eds.), Food colloids: fundamentals of formulation, Royal Society of Chemistry, Cambridge, 2001, p. 245.
[33] P.J. Wilde, Curr. Opin. Colloid Interface Sci. 5 (2000) 176.
[34] Y.F. Maa, C.C. Hsu, Biotechnol. Bioeng. 54 (1997) 503.
[35] C.R. Thomas, D. Geer, Biotechnol. Lett. 33 (2011) 443.
[36] J.D. Andrade, V. Hlady, A.P. Wei, Pure Appl. Chem. 64 (1992) 1777.
[37] A.A. Townsend, S. Nakai, J. Food Sci. 48 (1983) 588.
[38] H.C. Mahler, R. Müller, W. Friess, A. Delille, S. Matheus, Eur. J. Pharm. Biopharm. 59 (2005) 407.

[39] J.S. Harrison, A. Gill, M. Hoare, Biotechnol. Bioeng. 59 (1998) 517.
[40] J.R. Clarkson, Z.F. Cui, R.C. Darton, J. Colloid Interface Sci. 215 (1999) 323.
[41] J.R. Clarkson, Z.F. Cui, R.C. Darton, J. Colloid Interface Sci. 215 (1999) 333.
[42] J.R. Clarkson, Z.F. Cui, R.C. Darton, Biochem. Eng. J. 4 (2000) 107.
[43] M. Katakam, A.K. Banga, Pharm. Dev. Technol. 2 (1997) 143.
[44] D.K. Chou, R. Krishnamurthy, T.W. Randolph, J.F. Carpenter, M.C. Manning, J. Pharm. Sci. 94 (2005) 1368.
[45] N.B. Bam, J.L. Cleland, T.W. Randolph, Biotechnol. Prog. 12 (1996) 801.
[46] N.B. Bam, J.L. Cleland, J. Yang, M.C. Manning, J.F. Carpenter, R.F. Kelley, T.W. Randolph, J. Pharm. Sci. 87 (1998) 1554.
[47] W. Wang, Y.J. Wang, D.Q. Wang, Int. J. Pharm. 347 (2008) 31.
[48] M.J. Treuheit, A.A. Kosky, D.N. Brems, Pharm. Res. 19 (2002) 511.
[49] E. Ha, W. Wang, Y.J. Wang, J. Pharm. Sci. 91 (2002) 2252.
[50] B.A. Kerwin, J. Pharm. Sci. 97 (2008) 2924.
[51] E.T. Maggio, J. Excipients and Food Chem. 3 (20123) 45.
[52] J.S. Philo, T. Arakawa, Curr. Pharm. Biotechnol. 10 (2009) 348.
[53] W. Norde, Adv. Colloid Interface Sci. 25 (1986) 267.
[54] M. Cholewinski, B. Lückel, H. Horn, Pharm. Acta Helv. 71 (1996) 405.
[55] J. L. Cleland, A. Mac, B. Boyd, J. Yang, E.T. Duenas, D. Yeung, D. Brooks, C. Hsu, H. Chu, V. Mukku, A. J. Jones, Pharm. Res. 14 (1997) 420.
[56] R. Pearlman, J.Y. Wang, Stability and Characterization of Protein and Peptide Drugs, Plenum Press, New York, 1993.
[57] J.S. Bee, J.L. Stevenson, B. Mehta, J. Svitel, J. Pollastrini, R. Platz, E. Freund, J.F. Carpenter, T. W. Randolph, Biotechnol. Bioeng. 103 (2009) 936.
[58] Y.F. Maa, C.C. Hsu, Biotechnol. Bioeng. 51 (1996) 458.
[59] S. Kiese, A. Pappenberger, W. Friess, H.C. Mahler, J. Pharm. Sci. 97 (2008) 4347.
[60] N. Rathore, R.S. Rajan, Biotechnol. Prog. 24 (2008) 504.
[61] S. Simon, H.J. Krause, C. Weber, W. Peukert, Biotechnol. Bioeng. 108 (2011) 2914
[62] M. Katakam, L.N. Bell, A.K. Banga, J. Pharm. Sci. 84 (1995) 713.
[63] M.R. Wilkins, E. Gasteiger, A. Bairoch, J.C. Sanchez, K.L. Williams, R.D. Appel, D.F. Hochstrasser, Methods Mol. Biol. 1999;112:531-552.
[64] E. Gasteiger, C. Hoogland, A. Gattiker, S. Duvaud, M.R. Wilkins, R.D. Appel, A. Bairoch, in: J.M. Walker (Eds.), The Proteomics Protocols Handbook, Humana Press Inc, New York, 2005, p. 571.
[65] J. Wiesbauer, M. Cardinale, B. Nidetzky, Process Biochem. submitted.
[66] J.A.S. Perez, E.M.R. Porcel, J.L.C. Lopez, J.M.F. Sevilla, Y. Chisti, Chem. Eng. J. 124 (2006) 1.
[67] P.M. Doran, Bioprocess Engineering Principles, Academic Press Limited, London, 2000.
[68] Abramoff MD, Magelhaes PJ, Ram SJ. Image processing with ImageJ. Biophotonics Int. 2004;11:36-42.
[69] A.V. Kabanov, E.V. Batrakova, V.Y. Alakhov, J. Control. Release 82 (2002) 189.
[70] B.M. Eckhardt, J.Q. Oeswein, D.A. Yeung, T.D. Milby, T.A. Bewley, PDA J. Pharm. Sci. Technol. 48 (1994) 64.
[71] E. Ablinger, S. Wegscheider, W. Keller, R. Prassl, A. Zimmer, Int. J. Pharm. 427 (2012) 209.
[72] Ph. Eur. 2.2.1. Clarity and degree of opalescense of liquids, 6th edition. European Directorate for the Quality of Medicine (EDQM) 2008
[73] J.T. Vivian, P.R. Callis, Biophys. J. 80 (2001) 2093.
[74] J.G. Lees, B.R. Smith, F. Wien, A.J. Miles, B.A. Wallace, Anal. Biochem. 332 (2004) 285.

[75] L. Whitmore, B.A. Wallace, Nucleic Acids Res. 32 (2004) W668.
[76] V.P. Konarev, V.V. Volkov, A.V. Sokolova, M.H.J. Koch, D.I. Svergun, J. Appl. Crystallogr. 36 (2003) 1277.
[77] D.I. Svergun, J. Appl. Crystallogr. 25 (1992) 495.
[78] D.I. Svergun, C. Barberato, M.H.J. Koch, J. Appl. Crystallogr. 28 (1995) 768.
[79] S.D. Stranks, H. Ecroyd, S.Van Sluyter, E.J. Waters, J.A. Carver, L. von Smekal, Phys. Rev. E 80 (2009) 1.
[80] M. Soos, A.S. Moussa, L. Ehrl, J. Sefcik, H. Wu, M. Morbidelli, J. Colloid Interface Sci. 319 (2008) 577.
[81] M.R. Jensen, S.M. Kristensen, C. Keeler, H.E.M. Christensen, M.E. Hodsdon, J.J. Led, Proteins 73 (2008) 161.
[82] C.D. Putnam, M. Hammel, G.L. Hura, J.A. Tainer, Q. Rev. Biophys. 40 (2007) 191.
[83] D. Mustafi, C.M. Smith, M.W. Makinen, R.C. Lee, Biochim. Biophys. Acta 1780 (2008) 7.
[84] R.L. Crisman, T.W. Randolph, Biotechnol. Bioeng. 107 (2010) 663.
[85] T. Arakawa, S.N. Timasheff, Biochemistry 24 (1985) 6756.
[86] R. Bhat, S.N. Timasheff, Protein Sci. 1 (1992) 1133.
[87] J.L. Cleland, S.E. Builder, J.R. Swartz, M. Winkler, J.Y. Chang, D.I. Wang, Nat. Biotechnol. 10 (1992) 1013.
[88] J.L. Cleland, C. Hedgepeth, D.I. Wang, J. Biol. Chem. 267 (1992) 13327.
[89] S. Rawat, C.R. Suri, D.K. Sahoo, Biochem. Biophys. Res. Commun. 392 (2010) 561.

## 3.1 Supporting Information

# Supporting Information

**The air-liquid interface: its role in aggregation of hGH, critical parameters and stabilizing strategies**

Johanna Wiesbauer[1,2], Ruth Prassl[3], and Bernd Nidetzky[1,2]

[1]*Research Center Pharmaceutical Engineering, Graz, Austria*

[2]*Institute of Biotechnology and Biochemical Engineering, University of Technology Graz, Austria*

[3]*Institute of Biophysics and Nanosystems Research, Austrian Academy of Science, Graz, Austria*

Institute of Biotechnology and Biochemical Engineering
Graz University of Technology
Petersgasse 12/I, A-8010 Graz, Austria
Fax: (+) 43 316 873 8434
E-mail: bernd.nidetzky@tugraz.at

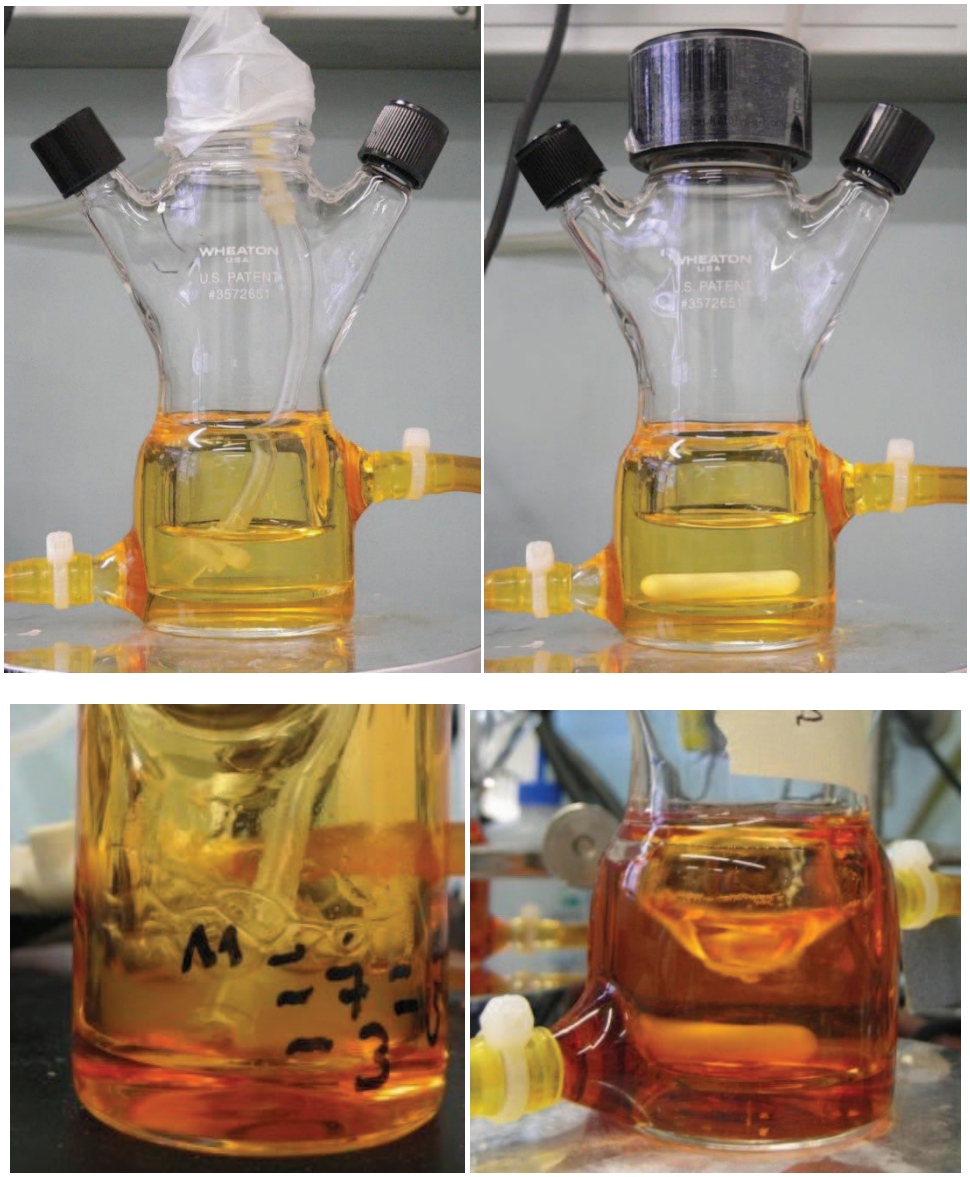


**Figure S1: Geometry of the double-walled glass reactors.** From left to right: Set-up for bubble aeration and for stirring. Bottom row: Set-up during the accelerated stress conditions bubble aeration and stirring.

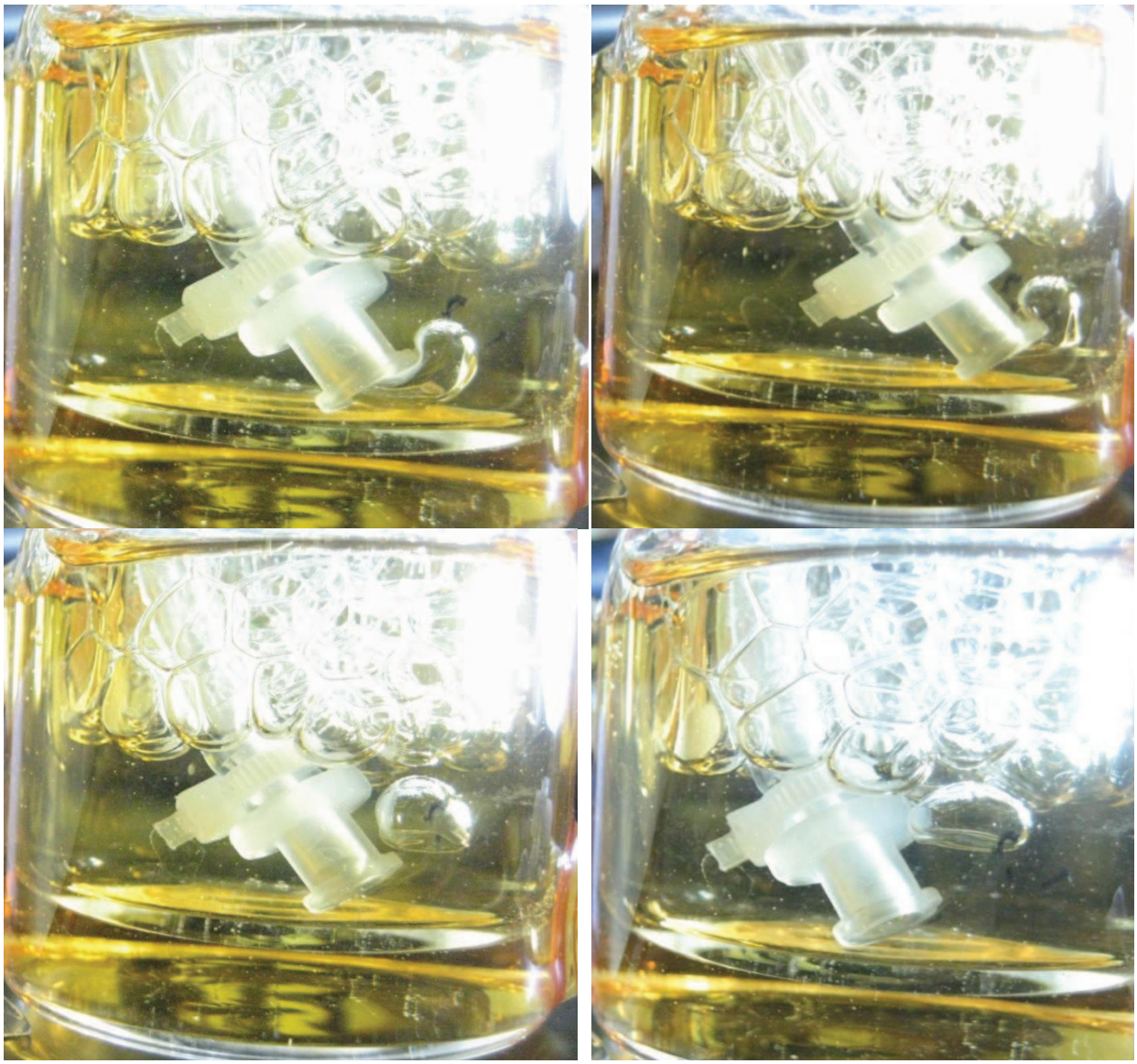

**Figure S2: Bubble formation and rising during aeration.** These pictures were used for the calculation of the bubble surface [1].

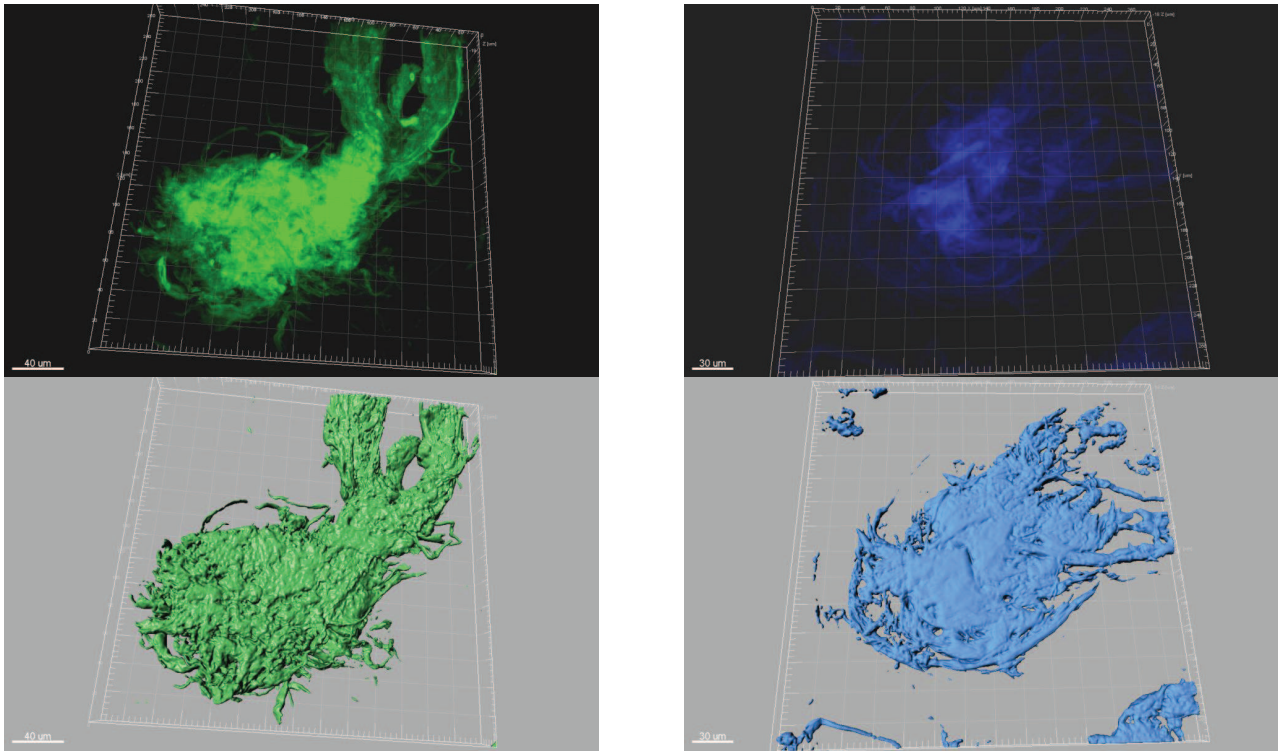


**Figure S3: Characterization of the surface properties of aerated hGH aggregates (Imaris 7.0 - left: FITC - green; right: ANSA - blue)**

Image of the size and shape of aggregates formed by bubble aeration for 7 h (3 L/h, 25 °C). No significant difference in binding to the surface could be detected for both dyes. Therefore we conclude that the surface exposes hydrophobic domains of hGH, probably due to unfolding.

**Figure S4: The role of foam formation in aggregation during bubble aeration.**
(top): from left to right: foam formation during aeration.
(bottom): bubble aeration in the presence of PPG 2,000 (left) and Pluronic F-68 (right).
In the picture it can be clearly seen that caviation does not seem to take place if foam is formed. Upon addition of PPG 2,000 (antifoam) and Pluronic F-68 foam formation is suppressed and bursting of the bubbles occurs on the surface. As the aggregation rate is not changed with PPG 2,000, we conclude that these bursts are not the main reason for aggregation. Pluronic F-68 protects the protein against aggregation.

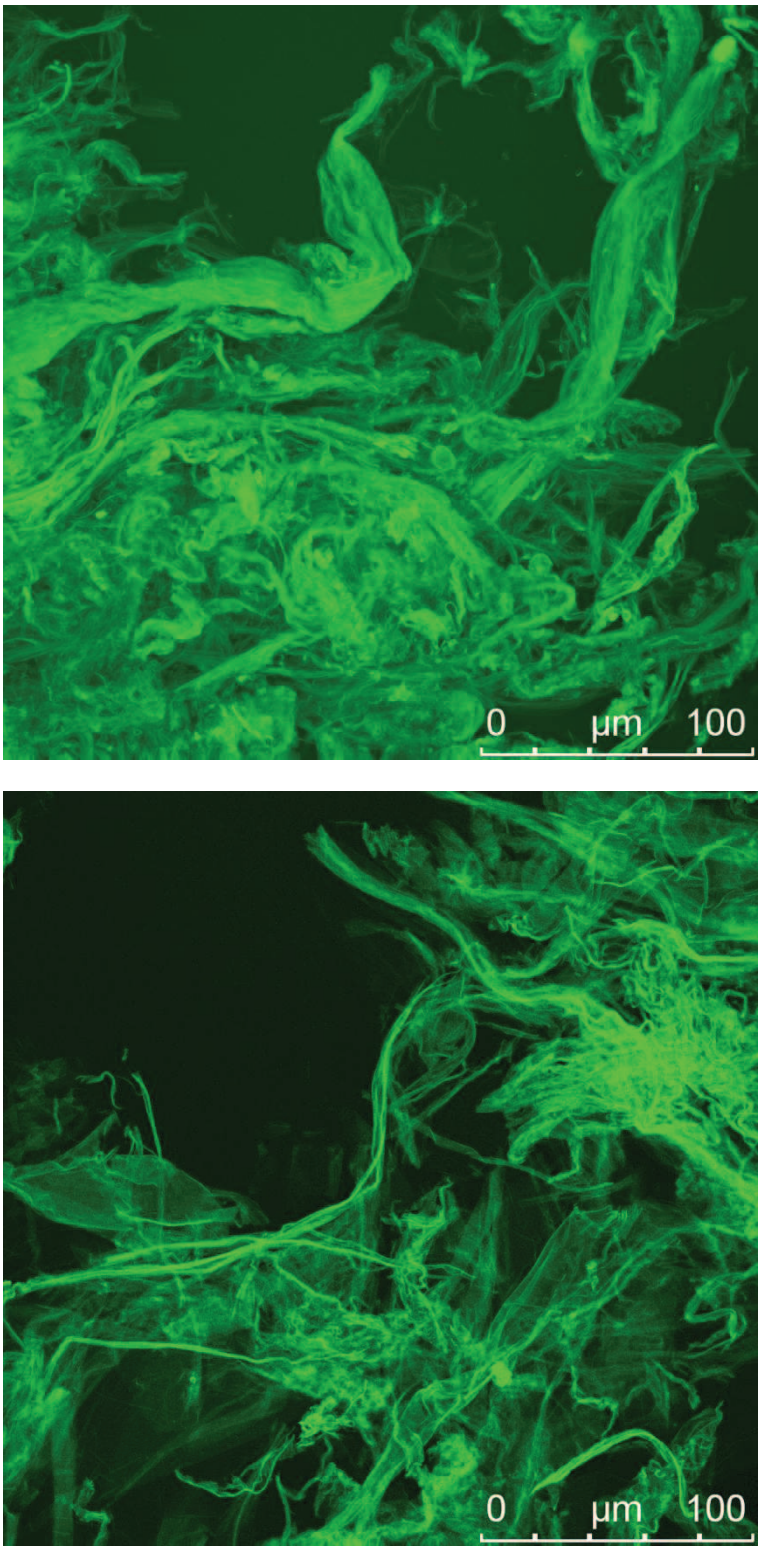


**Figure S5: Size and shape of aggregates formed during bubble aeration.**
(top): Aggregates shape and size upon bubble aeration with compressed air; (bottom): Aggregation in the presence of PPG 2,000 (antifoam) in a protein to PPG ratio of 3 to 1.

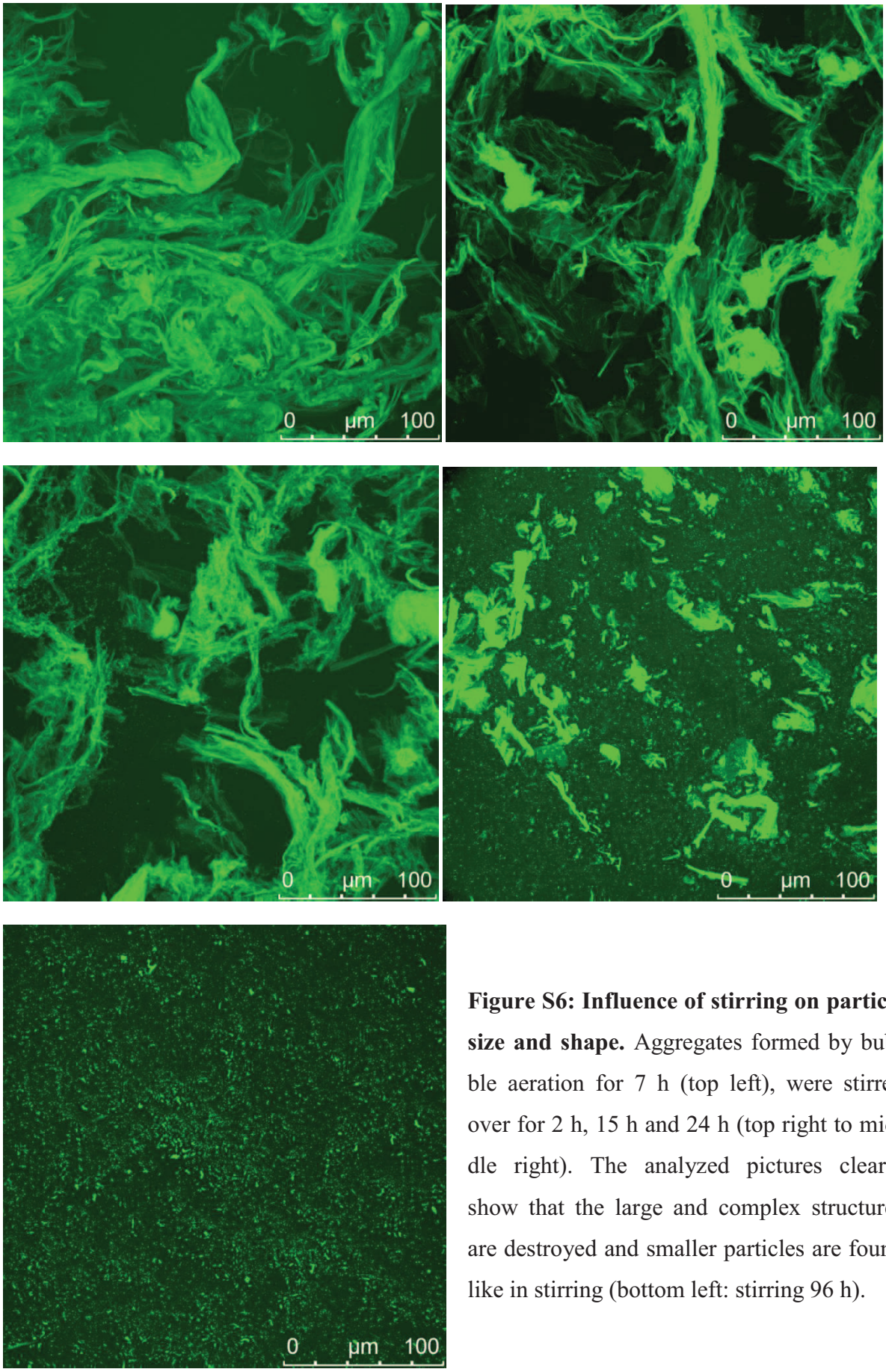


**Figure S6: Influence of stirring on particle size and shape.** Aggregates formed by bubble aeration for 7 h (top left), were stirred over for 2 h, 15 h and 24 h (top right to middle right). The analyzed pictures clearly show that the large and complex structures are destroyed and smaller particles are found like in stirring (bottom left: stirring 96 h).

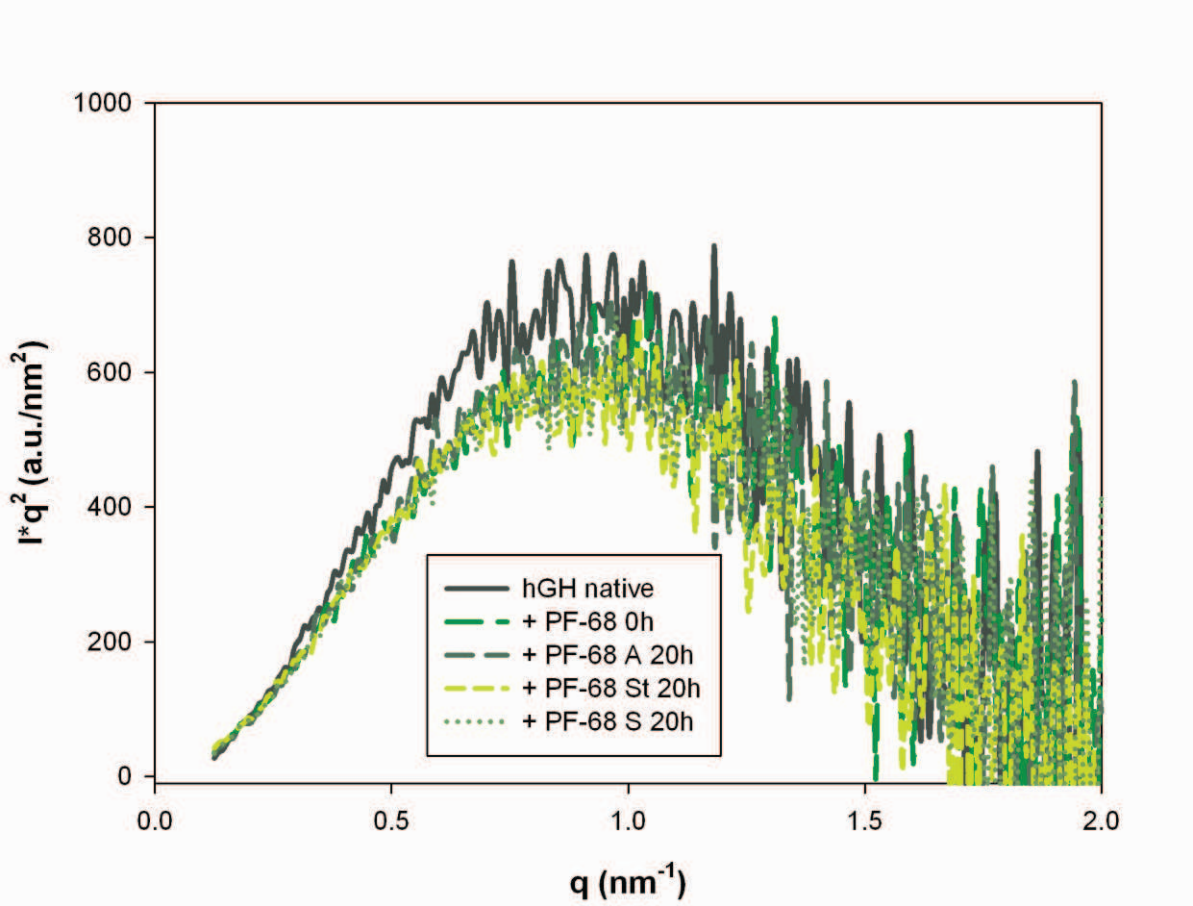


**Figure S7: Scattering curves and Kratky plot for hGH + Pluronic F-68.** Kratky plot for hGH and Pluronic F-68 show that the protein still possesses its native folded structure in the presence of Pluronic F-68 and after 20h stress [5]. (PF-68) Pluronic F-68; (A) aeration 3 L/h; (St) stirring 300 rpm; (S) shaking 300 rpm.

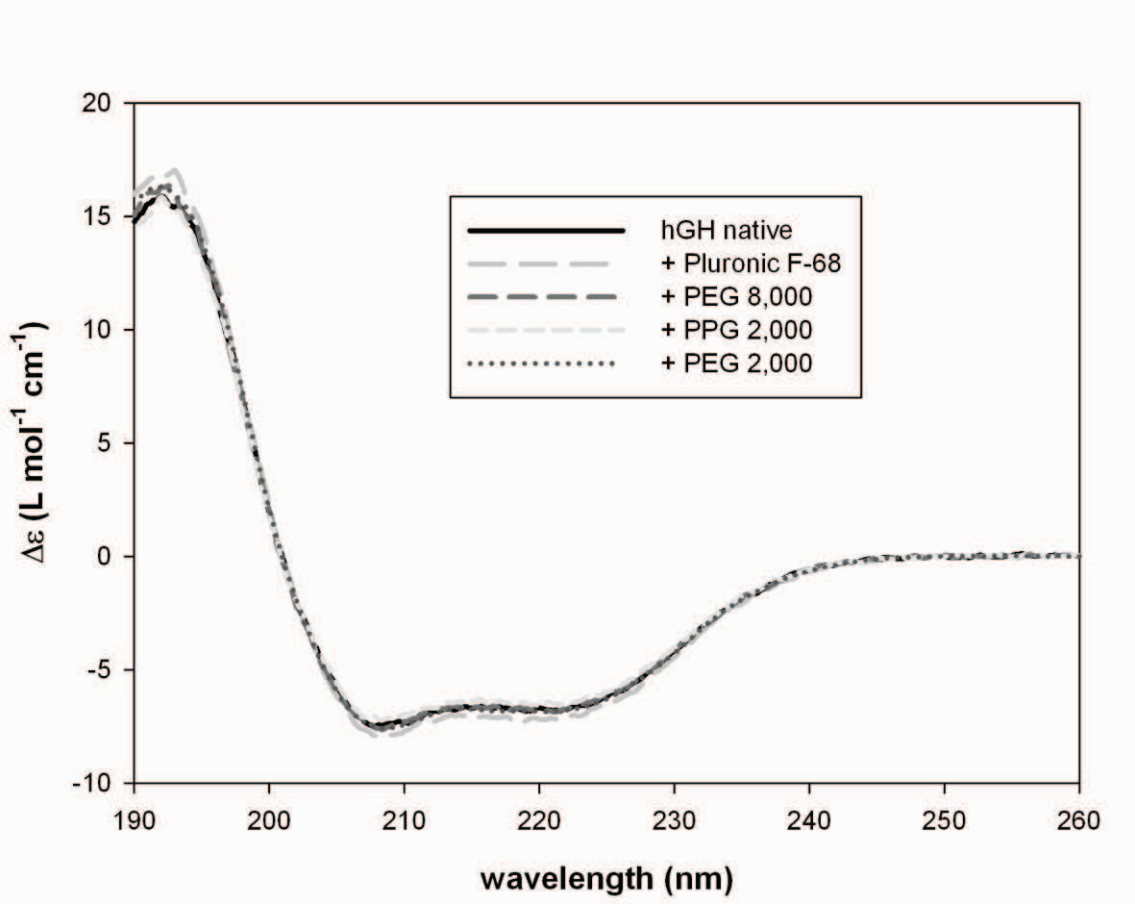


**Figure S8: Circular dichroism (CD) spectra of hGH and in the presence of polymers and surfactants.**

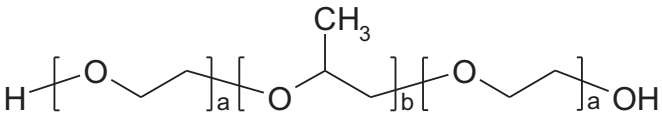


A: Pluronic F-68: PEG-PPG-PEG Blockcopolymer

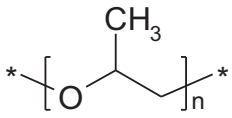


B: PPG – building block

a = 80, b = 27

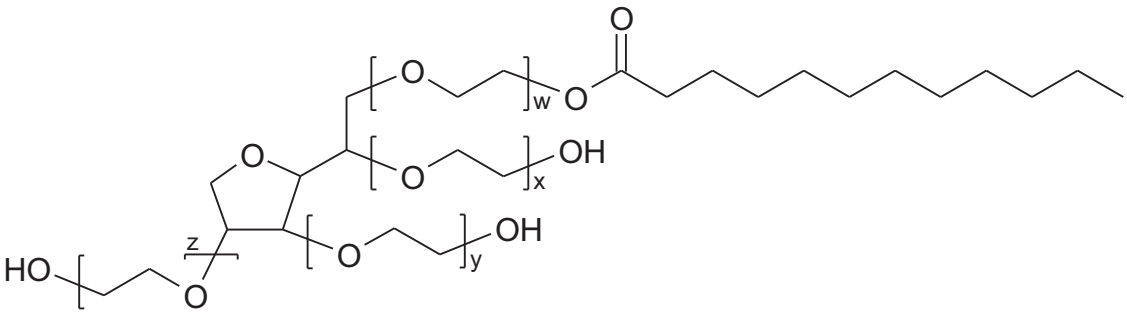


C: Tween 20

w + x +y + z = 20

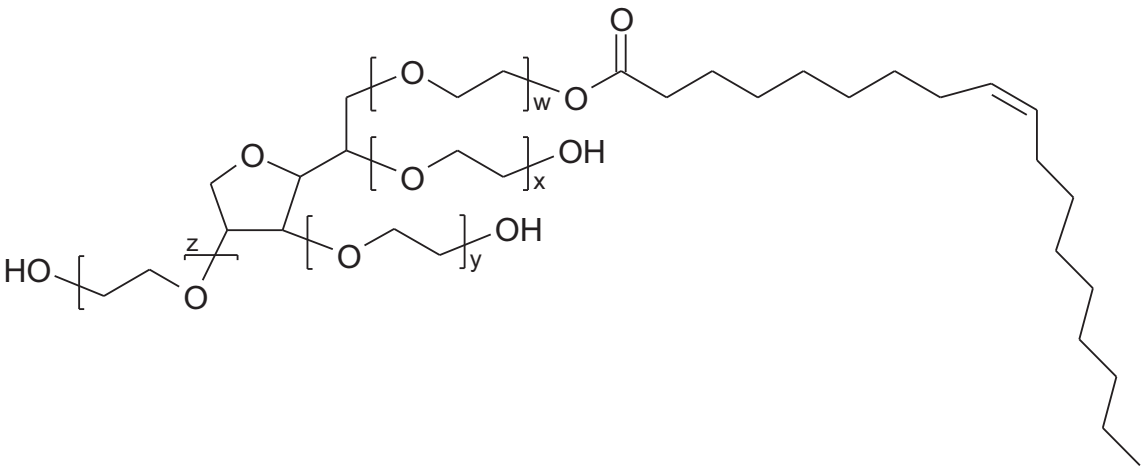


D: Tween 80

w + x +y + z = 20

**Figure S9: Chemical structures of common surfactants and building blocks**

**Table S1: Fluid characterization of the hGH test solutions**

| *Sample* | *Re* | *Mo* (x $10^{-11}$) | *Eo* | σ (mN/m)* | $\gamma$ ($s^{-1}$) |
|---|---|---|---|---|---|
| 6.7 mg/mL hGH | 686 | 5.6 | 1.41 | 57.5 ± 0.5 | 102 |
| 3.4 mg/mL | 720 | 4.8 | 1.46 | 56.5 ± 0.4 | 105 |
| 1.0 mg/mL | 706 | 4.6 | 1.39 | 58.8 ± 1.0 | 104 |
| 3.4 mg/mL + PPG 2,000 | 732 | 9.3 | 1.83 | 44.4 ± 0.3 | 106 |
| 3.4 mg/mL + Pluronic F-68 | 712 | 7.4 | 1.64 | 49.6 ± 0.2 | 104 |

* surface tension of 10 mM NaPP pH 7.0 was 71.2 ± 0.1 mN/m

Density of the hGH solution was 0.996 g/mL, the dynamic viscosity was 0.927 mPa s and surface tension was 56.5 mN/m. All analyses were performed at 25 °C.

Photographs taken of the bubble aeration were processed regarding bubble dimension using ImageJ [1]. The velocities were measured from digital photographic videos. All images and videos were recorded in a parallel plane to the bubble rising direction. According to Eötvös and Morton number a shape regime between wobbling and ellipsoidal regime is prevalent [2]. Although the air bubbles look rather ellipsoidal, over time a wobbling is detected in the photographs (Fig. S2). The characteristic numbers for all bubble aeration experiments are summarized in Table S1.

The shear rate was determined according to literature [3]. The flow index for a Newtonian fluid is 1. Further the consistency index K is equal to the viscosity in our set-up [4]. The superficial gas velocity is defined as the volumetric gas flow rate divided by the cross sectional area of our glass bioreactor (800 x $10^{-6}$ $m^2$). Local shear rates e.g. bursting of the bubbles where not taken into account here. But as shown in Fig. S2 and S4 bursting of the bubbles at the air-liquid interface seems to occur only in the presence of antifoam or surfactants. The decrease in surface tension after adding protein or antifoam or surfactant indicates accumulation at the air-liquid interface.

The air bubbles were slightly elliptically shaped and had a mean diameter of 6.7 mm (characteristic length), corresponding to the projected area of an equivalent sphere. Single bubbles raised from the pipe with an average characteristic flow velocity of 0.10 m/s and for 3 L/h e.g. a frequency of 4.4 $s^{-1}$ without causing a visible wake. These numbers were calculated analyzing videos frame by frame.

The characteristic numbers are equal for all conditions analyzed and we could find no difference in the calculated shear rate either, although the aggregation rates are quite different.

**Table S2: Fill levels and specific surfaces for stirring experiments**

| *Fill level* *(x $10^{-6}$ $m^3$)** | *γ ($s^{-1}$)*** | *Air-liquid interface* *(x $10^{-6}$ $m^2$)**** | *Specific surface* *($m^2/m^3$)* |
|---|---|---|---|
| 12 | 40 – 100 | 1,090 ± 30 | 96 ± 2 |
| 16 | 40 – 100 | 1,020 ± 40 | 66 ± 3 |
| 24 | 40 – 100 | 910 ± 40 | 39 ± 2 |
| 36 | 40 – 100 | 940 ± 40 | 27 ± 1 |
| 60 | 40 – 100 | 865 ± 20 | 15 ± 1 |
| 55 | 40 - 100 | 190 | 3 ± 2 |

* For the specific surface the fill levels were used for calculations. We have to note that 0.6 mL was subtracted for sampling at 0 h.

** To the best of our knowledge, Np values for stirrer bars are not available in literature. We assumed the power number of the magnetic stirring bar to be between the most common stirrer types (paddle impeller = 2; marine propeller = 0.35) [3,4].

*** The air-liquid interface was calculated assuming a paraboloid of revolution. Therefore the height was measured.

**Table S3: Summary of the characterization of different aeration rates**

| *Aeration rate (L/h)* | *$\gamma$ ($s^{-1}$)* | *Air-liquid interface (x $10^{-6}$ $m^2$)** | *Specific surface (bubble)* ($m^2/m^3$)* |
|---|---|---|---|
| 1.5 | 74 | 27,400 ± 300 | 2,410 ± 30 |
| 2 | 86 | 28,900 ± 900 | 2,530 ± 80 |
| 3 | 105 | 47,000 ± 2,000 | 4,100 ± 100 |
| 4 | 121 | 54,000 ± 2,000 | 4,700 ± 200 |
| 5 | 135 | 64,000 ± 2,000 | 5,600 ± 200 |

* 800 x $10^{-6}$ $m^2$ (surface bioreactor) + surface of the air bubbles (average value over time)

** only surface of the bubbles (average value over time)

For the determination of the air-liquid interface and the specific surface the dimensions of the aeration bubble and its frequency were derived from digital photographs and videos. From the dimensions of the air bubble a mean characteristic diameter was derived to calculate the volume and the surface of an assumed sphere. The volume times the frequency should approximately correlate with the set aeration rate, otherwise a correction factor was determined. Based on these assumptions a surface per bubble of 1.4 ± 0.1 x $10^{-4}$ $m^2$ was determined and multiplied with the frequency ($min^{-1}$) for a defined observation time span of 1 min. The surface was divided by the liquid volume (11.4 x $10^{-6}$ $m^3$) to give values for the specific surface. As the differences in the shear rates are little and as shear does not seem to be a predominant force in aggregation, this fact was neglected.

**Table S4: Comparison of radius of gyration ($R_g$) and $D_{max}$ of hGH and in the presence of Pluronic F-68.**

| *Sample* | *$R_g$ (nm)* | *$D_{max}$ (nm)* |
|---|---|---|
| hGH-crystal structure | 1.85 | 6.0 |
| hGH | 1.9 | 6.0 |
| hGH + PF-68[a] | 1.9 | 8.0 |

[a] PF-68 = Pluronic F-68; The buffer scattering curve of 10 mM NaPP pH 7.0 was subtracted from hGH + Pluronic F-68 as background.

**Table S5: HLB values and MW of different surfactants and building blocks**

| *Excipient* | *HLB** | *σ (mN/m)* | *MW (g/mol)* |
|---|---|---|---|
| PEG-PPG-PEG, Pluronic F-68 | 29** | | 8,400 |
| PPG 2,000 | | 38.4 ± 0.3 | 2,000 |
| Tween 20 (PEG subunits) | 16.7* | | 1,228 |
| Tween 80 | 15* | | 1,310 |
| PEG 8,000 | | 60.9 ± 0.2 | 8,000* |
| PEG 2,000 | | 61.6 ± 0.8 | 1,900 – 2,200* |

* derived from Sigma-Aldrich Homepage

** according to literature [6]

The hydrophile-lipophile balance (HLB) numbers are calculated for nonionic surfactants and are between 0-20. HLB numbers >10 have an affinity for water (hydrophilic) and number <10 have an affinity of oil (lipophilic).

## References:


[1] M.D. Abramoff, P.J. Magelhaes, S.J. Ram SJ, Biophotonics Int. 11 (2004) 36.
[2] R. Clift, J.R. Grace, M.E. Weber, Bubbles, Drops and Particles, Academic Press, New York, 1978.
[3] J.A.S. Perez, E.M.R. Porcel, J.L.C. Lopez, J.M.F. Sevilla, Y. Chisti, Chem. Eng. J. 124 (2006) 1.
[4] P.M. Doran, Bioprocess Engineering Principles, Academic Press Limited, London, 2000.
[5] C.D. Putnam, M. Hammel, G.L. Hura, J.A. Tainer, Q. Rev. Biophys. 40 (2007) 191.
[6] A.V. Kabanov, E.V. Batrakova, V.Y. Alakhov, J. Control. Release. 82 (2002) 189.

## 4 Re-solubilization and refolding of nonnative aggregates of the human growth hormone using chaotropic agents: evidence for native-like aggregation in solution

In preparation for PLoS ONE

# Re-solubilization and refolding of nonnative aggregates of the human growth hormone using chaotropic agents: evidence for native-like aggregation in solution

Johanna Wiesbauer[1,2], Andras Boeszoermenyi[3] , Monika Oberer[3] and Bernd Nidetzky[1,2]

[1]*Research Center Pharmaceutical Engineering, Graz, Austria*

[2]*Institute of Biotechnology and Biochemical Engineering, University of Technology Graz, Austria*

[3]*Institute of Molecular Biosciences, University of Graz, Graz, Austria*

*Corresponding author*: Nidetzky, B. (bernd.nidetzky@tugraz.at).

**ABSTRACT**

The unglycosylated form of the human growth hormone (Somatotropin; hGH) was previously shown to become strongly destabilized upon contact with air-liquid interfaces present during agitation and aeration. The consequent nonnative aggregation proceeded through phase transition into an amorphous precipitate, but did not accumulate soluble protein aggregates. We show here that chaotropic agents (urea, guanidine hydrochloride) at concentrations far below denaturation midpoint promote gradual resolubilization of the hGH precipitate by a processive "disaggregation" process, in which besides the native monomer soluble hGH aggregates are now released in large amount (up to 80% of total solubilized protein). Spectroscopic protein characterization using far-UV circular dichroism and fluorescence of the single tryptophan residue (Trp-86) in hGH reveals a pronounced native-like appearance of the resolubilized protein at different levels of structure, clearly indicating that the overall disaggregation has comprised protein refolding events. The soluble hGH aggregates resist dissociation into monomers upon dialysis to buffer lacking chaotropic agent. To form the hGH monomer exclusively, the precipitate needs to be completely unfolded in 6 M guanidine hydrochloride prior to renaturation. The results emphasize that both native-like and nonnative types of aggregation impact on hGH stability; and that native hGH could be recovered from insoluble aggregate formed in agitated/aerated unit operations of the protein production process.

**Keywords**: Native-like and nonnative aggregation; somatotropin; air-liquid interface; protein denaturation; refolding; folding intermediates.

## Introduction

Protein stability and shelf life is in general limited due to chemical or physical instabilities like deamidation, oxidation, aggregation and precipitation [1-5]. With the progress in recombinant DNA technology more and more therapeutic proteins are available for production in large amounts. However, aggregation is now also encountered due to folding and misfolding (inclusion body formation) during production and processing [3,4,6-14]. Formation of visible particles or (soluble) aggregates influences the shelf life of biopharmaceuticals [15], as administration of protein aggregates can lead to reduced bioactivity and enhance immune reactions [3,16]. This affects the quality of formulations regarding requirements for biopharmaceuticals and so improved control of the degree of aggregation is required [17]. Since so far no universal cure against aggregation is known a deeper insight into its numerous mechanisms would be desired in order to undertake counter measures [18]. For analysis and understanding of protein aggregation several definitions are of great importance: Protein association is often described as a reversible process, where two or more native protein molecules associate and often lead to reversible precipitation [3]. Aggregation is considered to be mainly irreversible if no drastic changes in the solvent environment are performed. The interacting proteins can be partially unfolded or even denatured [3,18]. Denaturation is often referred to as the alteration of the global protein fold (3D structure) leading to a loss of tertiary and/or secondary structure [1,2,17]. In this work we refer to nonnative aggregation if initially native proteins (folded) form aggregates containing nonnative protein structure [6].

The single chain protein human growth hormone (hGH, Somatropin, UniProt P01241) consists of 191 amino acids (22.1 kDa) and exposes a 4-helical cytokine fold. Its physiological role involves the regulation of many metabolic and physiological processes like the stimulation of cell growth. Therefore, hGH is mainly used to treat growth hormone deficiency and dwarfism [19-21]. The abundance of studies on hGH make it an ideal model protein to investigate protein instabilities [19,21-34]. Structural data are available and most chemical instabil-

ities (deamidation and oxidation) are described in detail [19,24,25,32,35-37]. As the protein is naturally non-glycosylated it can be expressed in *E.coli* into inclusion bodies and refolded [31,38-41]. For refolding of hGH from inclusion bodies besides chaotropic reagents also an oxido-shuffling system or mixed disulfides are necessary due to nonnative intramolecular disulfide shuffling [38-41]. In human pituitary glands Lewis and coworkers further report about 15% of a "dimeric 45 kDa hGH variant" which seems to be a mixture of several forms of noncovalent and covalent (disulfide and non-disulfide) dimers [25].

In previous studies it was shown that hGH forms noncovalent aggregates if accelerated stress conditions are applied [28,30]. Those aggregates are irreversible under solution conditions [42]. However, "reversible" refolding was achieved at high pressure [30] and combined with moderate amounts of urea and guanidine hydrochloride (GdnHCl) for aggregates produced by agitation [31,41]. The range of GdnHCl was chosen well below the concentration known to unfold or form molten globules [31,41]. From pH 5 to 8 and below a concentration of 8M urea seems to have only little effect on the tertiary structure of hGH [20]. Although urea and guanidine hydrochloride (GdnHCl) are both chaotropic reagents (disorder water structure; hydrophobic molecules are more easily solvated) which stabilize the unfolded state of a protein and show a chemically similar structure they denature proteins differently [43]. First of all GdnHCl is charged whereas urea is not. Further GdnHCl tends to react via stacking interactions (with itself or planar groups) and lacks H-bonding [43]. Studies on helical peptides showed that GdnHCl can be 4-fold more effective than urea when planar amino acids are mainly contributing to helical stability. This could explain the higher tolerance of hGH towards urea than towards GdnHCl. For urea a combination of direct interactions with the protein (polar residues and the peptide backbone) and indirect interactions (water structure, solvation of hydrophobic groups) were detected [43,44].

As pH 7.0 is far from the proteins isoelectric point of pH 5.3 [3,20] and the solubility is around 10 mg/mL and higher [20] we exclude that these aggregates were formed due to

salting out effects or isoelectric precipitation. For the latter it was shown that precipitation can be reversible upon pH change and aggregates retain the native conformation for several proteins. However, hGH and also other proteins showed an increase in nonnative (beta-sheet) structure upon several kinds of aggregation (inclusion bodies, stress induced, heating) [12,30,31,33,41,45]. In the presence of excipients or Zn hGH seems to be able to form reversible insoluble [30,46] and soluble aggregates [46] without a significant change in secondary structures. A FTIR study on the structural similar proteins porcine GH (pGH UniProt P01248; 68% sequence similarity to hGH ) [47] and mink GH (mGH UniProt P19795; 67% sequence similarity to hGH using ClustalW) [48] showed that these proteins retain a native structure upon refolding or after reconstitution from freezing and lyophilization [49].

In order to understand the formation of hGH aggregates we may have to look on the opposite event: protein (re)folding. No significant conformational changes are reported from pH 2 to 11 [34,47,50]. In general protein folding can occur by a common two-state model were only the native (N) and the unfolded (U) states are populated. By equilibrium denaturation studies it was shown that hGH shows a similar folding pathway compared to that of other nonhuman growth hormones. Those refold with equilibrium intermediate states [51,52] which tend to self-associate and further lead to precipitation upon refolding [26,51,53-55]. Additionally experiments at pH 7 to 8 showed that unfolding was irreversible (DSC) [34] and concentration (intermediate level) dependent (DSC and GdnHCl unfolding) [34,51]. As aggregation was reduced if the polarity of the solution was changed (alcohol/water mixtures) [34] or in the presence of surfactants [56] it seems that self association is caused by hydrophobic interactions. The monomeric intermediates found at acidic pH expose structural similarities to the "molten globule state" [51,56], whereas its stability is higher than expected for this state [57]. For hGH it was found that at acidic pH (acidic pH or neutral pH low protein concentration < 0.5 mg/mL) a partially folded intermediate is present [53] with a Gibbs energy close ($\Delta\Delta G_{unf}$ 3 kcal/mol) to that of the native state [58]. This small energy barrier can be overcome and this

intermediate can be populated dependent on the solvent conditions like ligands, pH and temperature.

In this study we used insoluble hGH aggregates of different size, shape and aggregate level formed by three different stress conditions (shaking, aeration and stirring) and investigated their refolding behavior. It was possible to refold all tested insoluble aggregates at least into soluble aggregates (3M GdnHCl and 6M urea) or also into monomer (6M GdnHCl). This was independent of how the initial insoluble aggregates were formed. As up to 80% soluble aggregates could be detected, a detailed structural characterization was possible.

## MATERIALS AND METHODS

### Materials

A recombinant preparation of hGH produced in *E. coli*, termed rhGH, was kindly supplied by Sandoz GmbH (Kundl, Austria). The protein was produced and delivered in 10 mM sodium phosphate buffer, pH 7.0. Prior to use, the bulk solution was filtered using 0.22 µm PVDF filters from Millipore (Carrigtwohill, Ireland). Guanidine hydrochloride (GdnHCl, ≥ 99.5 %) and urea (≥ 99.5 %, p.a.) as well as ZelluTrans regenerated cellulose dialysis membranes (MWCO 8,000 – 10,000) were bought from Carl Roth (Karlsruhe, Germany). Unless noted otherwise, all chemicals were bought from Carl Roth (Karlsruhe, Germany). 8-anilino-1-naphthalenesulfonic acid ammonium salt (ANSA) was from Merck KGaA (Darmstadt, Germany).

### Sample preparation reversible aggregation/refolding

The hGH aggregates were formed by shaking, stirring and bubble aeration in 10 mM NaPP buffer pH 7.0 as previously described [42,59]. For refolding they were incubated in dilutions of urea (stock solution 8M in 10 mM NaPP pH 7.0) and guanidine hydrochlorid (GdnHCl 8M in 50 mM NaPP pH 7.0) from 1 to 6M with a final protein concentration of 0.5 mg/mL in eppendorf tubes. The aggregates were pipetted into the prepared chaotropic reagent dilutions of urea and GdnHCl. Fluorescence measurements over 1h showed that dissolution/refolding occurred within a few minutes for 6M urea and 6M GdnHCl. So incubation was carried out for minimum 1 h at room temperature. Samples were only centrifuged for 10 min at 13,200 prior to SEC-HPLC analysis and protein measurements in the supernatant.

In order to investigate the structure of the regained monomer, aggregates were incubated in 6M urea or 3M and 6M GdnHCl pH 7.0 respectively (3 mL total volume), and dialyzed against 10 mM NaPP pH 7.0 over two days at 8°C in a dialysis membrane with 3 buffer

changes. The dialyzed samples were always centrifuged prior to analysis for 10 min at 13,200 rpm.

All experiments were repeated at least three times on different days and samples were prepared fresh each time. All measurements were carried out within 48 h after sample preparation (urea and GdnHCl incubation or dialysis) in random order.

**Analytical methods**

*Protein concentration determination and turbidimetric analysis*

Protein concentration was determined using UV absorbance at 280 nm. A molar extinction coefficient of 17,670 $cm^{-1}M^{-1}$ was calculated using the ProtParam tool at the ExPASy webserver [60,61]. A molecular mass of 22,125 Da was assumed. For turbidity measurements wavelength scans were carried out using a Beckmann DU 800 spectrophotometer and the spectra were analyzed at 400 nm [23,62,63]. The instrument was calibrated against formazin reference suspensions [64]. In order to detect artifacts due to turbidity all measurements were carried out as wavelength scans. Furthermore turbid samples were centrifuged at 13,200 rpm for 10 min.

*SEC-HPLC*

A Zorbax GF-250 column (Silica, 4 μm, 250 × 9.4 mm) was obtained from Agilent (Waghaeusel-Wiesental, Germany). Analyses were carried out using a Merck-Hitachi LaChrome LC system equipped with a L-7250 autosampler and a L-7400 UV detector. All samples were centrifuged prior to analysis at 13,200 rpm for 10 min. All measurements were carried out using the GF-250 column at 30°C, applying a constant flow rate of 1 mL/min. The mobile phase was 50 mM $NH_4HCO_3$ in the pH range 7.8 - 8.2. Each sample was analyzed for 15 min. Absorbance detection at 214 nm was used.

*Fluorescence measurements*

Measurements were done on a software-driven Hitachi F-4500 fluorescence spectrophotometer (Tokyo, Japan). Measurements were carried out as described within 24 hours after sampling [42]. All samples were diluted to a concentration of 0.5 mg/mL. For turbid samples the concentration was derived from measurements in presence of 6M urea. Samples from 0 to 6M urea or GdnHCl were not centrifuged prior to analysis; dialyzed samples were separated from insoluble aggregates for 10 min at 13,200 rpm. The native protein shows maximum emission at 333 to 335 nm, while for unfolded hGH, this value is at around 350 nm [20,65].

Measurements of solvent-accessible hydrophobic protein surface were performed by adding the fluorescent dye 8-anilino-1-naphthalenesulfonic acid ammonium salt (ANSA). The dye was mixed with protein in a molar ratio of 9:1. Therefore, 60 µL of ANSA solution (1.0 mM) were added to 600 µL of a solution of 0.25 mg/mL hGH (0.011 mM) at 25 °C. Dialyzed samples were centrifuged for 10 min at 13,200 prior to analysis of the supernatant. Excitation was at 388 nm, and emission was recorded between 400 and 650 nm [42]. The emission is shifted from about 490 nm in aqueous environment to smaller wavelengths in unpolar environment. Unstressed but otherwise identical samples were used as controls.

*Far-UV Circular Dichroism (CD) measurements*

Samples of 0.5 mg/mL hGH with sodium phosphate buffer pH 7.0 were used as previously described for CD measurements [59]. Spectra were recorded at 25°C between 190 and 260 nm and between 210 and 260 nm in the presence of urea or GdnHCl using a 0.2 mm quartz cuvette. The background spectra of the respective buffers were recorded and subtracted. For analysis of refolding (urea and GdnHCl) the total sample was analyzed and values at 222 nm were plotted [56,58]. After dialysis all samples were centrifuged prior to analysis for 10 min at 13,200 rpm and only the supernatant was further used. Six spectra were averaged and then

converted to delta epsilon values using a mean residue molecular weight of 115.838 Dalton in the CDtool software [66]. The secondary structure contents were estimated using the CDSSTR program and Set4 on the online server DICHROWEB [67].

## RESULTS AND DISCUSSION

*Effect of chaotropic reagents on native hGH and insoluble aggregates thereof*

We monitored unfolding of native hGH at a concentration of 0.5 mg/mL by urea and GdnHCl using circular dichroism (CD). We found that urea does not unfold our hGH preparation at concentrations up to 7M and that unfolding occurs with a midpoint concentration of 4.5M for GdnHCl (Figure S1). Our results are comparable to literature values [20,51].

After studying the native protein we were interested in the behavior of aggregates of hGH formed under three different stress methods (shaking, aeration, stirring) in the presence of urea and GdnHCl. Results from refolding experiments monitored by UV-Vis wavelength scans (Figure S2) show that hGH aggregates formed during shaking and aeration regain their original clarity and absorbance spectrum at 3M urea and 2M GdnHCl respectively. For stirring these values are around 4M urea and 3M GdnHCl. As these concentrations are below those necessary for unfolding of hGH, we assume that reversible refolding from insoluble aggregates does not involve complete unfolding of hGH. Therefore this might be rather defined as deaggregation or dissolution of insoluble aggregates than refolding.

The UV-Vis scans show the formation of one single and homogeneous protein peak at 280 nm for urea and GdnHCl and so all samples were analyzed for their content of regained monomeric hGH. In Figure 1 the SEC-HPLC spectra in presence of urea and GdnHCl are shown. Here we have to note that until 3M urea and 2M GdnHCl (stirring 4M urea and 3M GdnHCl) also insoluble aggregates were present prior to HPLC sample preparation. The area% values refer only to the supernatant after centrifugation. Further SEC-HPLC data for GdnHCl could only be used up to 3M. At higher concentrations the peaks changed size and shape and results for the monomer content started decreasing again. In Figure 2 we used the total protein concentration (UV and SEC-HPLC) to calculate the absolute amounts of insoluble aggregate, soluble aggregate and monomer for aggregate formation and deaggregation.

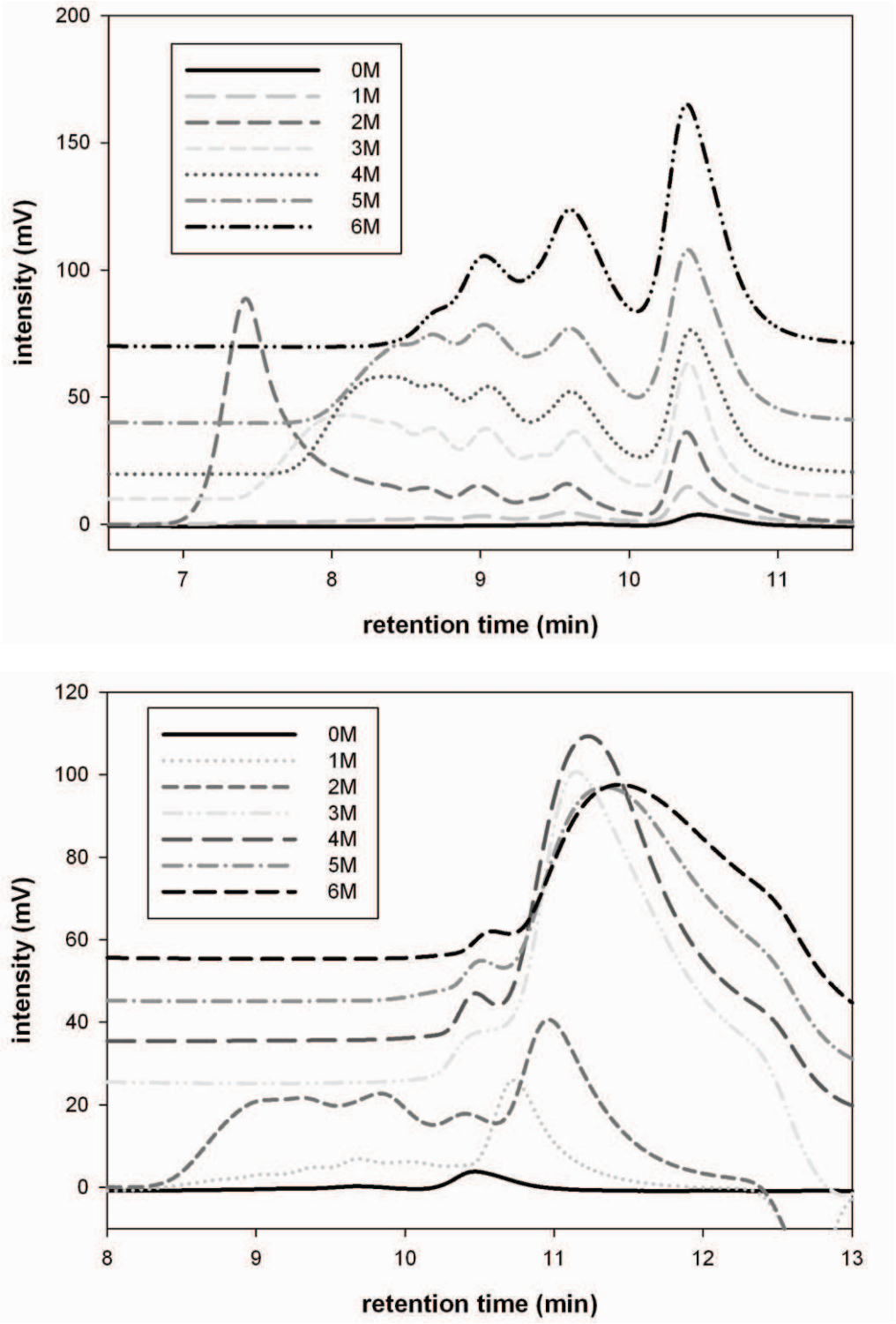


**Figure 1: SEC-HPLC spectra for re-solubilization (urea, GdnHCl) of insoluble aggregates formed by shaking.**

SEC-HPLC spectra for soluble aggregates and monomeric hGH (supernatant) in dependency of the urea (top) and the GdnHCl (bottom) concentration.

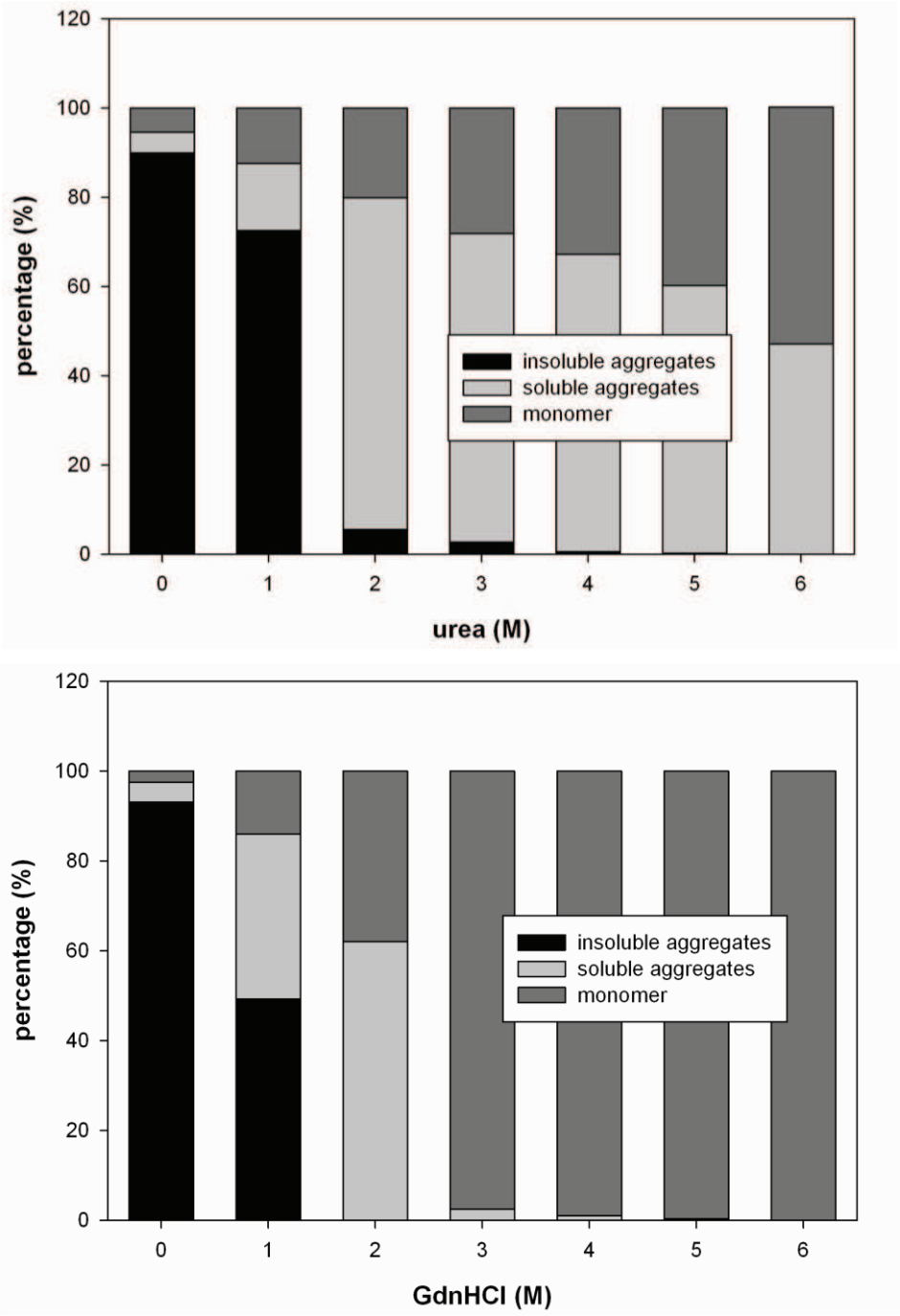


**Figure 2: Overview of insoluble and soluble aggregates formed by shaking as well as monomer hGH during refolding.**

Incubation of hGH samples after 2h of shaking with increasing urea (top) or GdnHCl (bottom) concentrations lead to refolding/deaggregation of the insoluble aggregates into soluble aggregates and monomer.

Results from UV-Vis wavelength scans (increasing clarity) and SEC-HPLC (detection of soluble aggregates) show that the insoluble aggregates are transformed into soluble aggregates in the presence of urea. Although the insoluble aggregates cannot be monitored using SEC-HPLC our data suggest that refolding or rather deaggregation is accompanied by "breaking down" of the aggregates (Figure 1 and Figure 2). Further the amount of soluble aggregates increases until all insoluble aggregates are dissolved and then decreases again (Figure S3). Interestingly, the SEC-HPLC "refolding" patterns look reproducible and similar within 48 h to 72 h for all aggregates independent of the aggregation initiating stress method but different for urea and GdnHCl, respectively. Only the overall percentage of soluble aggregates differs for the individual (stress method) aggregates.

While we find only little amounts of soluble aggregates (~3-5 % of soluble protein) during our aggregation studies [42], during refolding large amounts of solube aggregates can be detected (Figure 2 and S3). The similar behavior regarding the presence of soluble aggregates could be related to the fact that aggregation takes place at the air-liquid interface in all three investigated stress methods [42,59]. Therefore we assume similar aggregation initializing events like adsorption, (partial) unfolding and desorption. The detected differences in the overall percentage of the soluble aggregates (SEC-HPLC) at 6M urea (shaking 51 %, aeration 28 % and stirring 15 %) (Figure S3) could correlate with the fact that different initial amounts of insoluble aggregates were present. For shaking we found irreversible precipitation with > 95 %, for aeration 88 ± 3 % and for stirring 42 ± 3 % of insoluble aggregates [42, 59]. Differences between the soluble aggregate levels for aeration (6M urea = 28 %) and shaking (6M urea = 51 %), although their content of insoluble aggregates is similar, are not easy to explain. We do not have data about the exact size distribution of the aggregates, however from our previous studies we know that during aeration larger but fewer particles are formed than during shaking [42,59]. As refolding occurs at comparable chaotropic concentrations and also

monomer is regained, we do not think that the insoluble aggregates are simply dissolved into "smaller" and soluble components.

*Spectroscopic investigation of the re-solubilization of hGH preparations*

As soluble aggregates were formed in significant amounts we were interested in their structure compared to the insoluble aggregates and the native protein. Intrinsic fluorescence measurements (Trp86, Figure 3 and Figure S4) show that native hGH and hGH in presence of 6M urea give comparable spectra, whereas the protein unfolds in the presence of 6M GdnHCl. Based on these findings deaggregation in the presence of increasing amounts (1 to 6M) of urea or GdnHCl was monitored using fluorescence (Figure S5) and CD measurements (Figure S6).

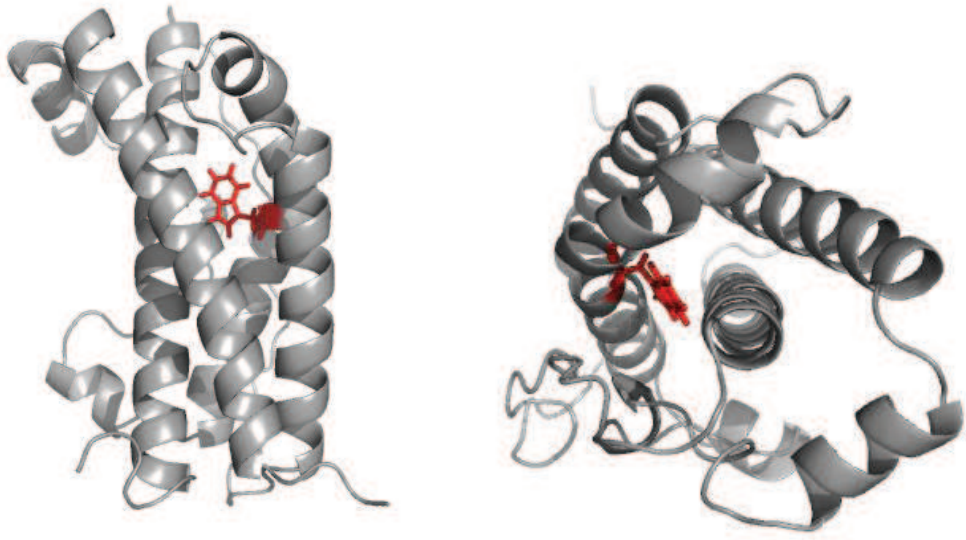

**Figure 3: Structure of hGH (3HHR) and position of Trp86.** The overall 3D structure shows that the Trp86 is buried in the core of the protein. (left) sideview; (right) topview.

From 0 to 4M both chaotropic salts show similar results for intrinsic fluorescence (Figure S5) whereas at > 4M GdnHCl unfolding was detected. Unfolding was not observed in the presence of urea. We also observed during refolding at 295 nm that the fluorescence spectra are slightly broader than that of the native protein (Figure S5). Further also the maximum

emission wavelength is shifted from 333 ± 1 nm towards 335 ± 1 for urea and for GdnHCl from 337 ± 2 nm (0 to 4M) to 350 nm (5 and 6M – due to unfolding Trp86 is solvent exposed). We think this broadening in the spectra is due to the presence of different intermediates which are structurally slightly perturbed around the buried Trp86 residue. Due to strong signals of urea and GdnHCl in CD measurements below 210 nm, refolding could only be monitored from 260 to 210 nm (Figure S6). The signals at 222 nm show that ≥ 3M urea the signals equal to that of the native protein. For GdnHCl this was only observed up to 4M GdnHCl, afterwards the signal decreases due to unfolding. Based on these measurements we think that although soluble aggregates are formed they expose native-like secondary and tertiary structure. The initial insoluble aggregates (0M) were used for CD measurements [68] and compared to the native protein. The spectra indicate a nonnative secondary structure (Figure 4).

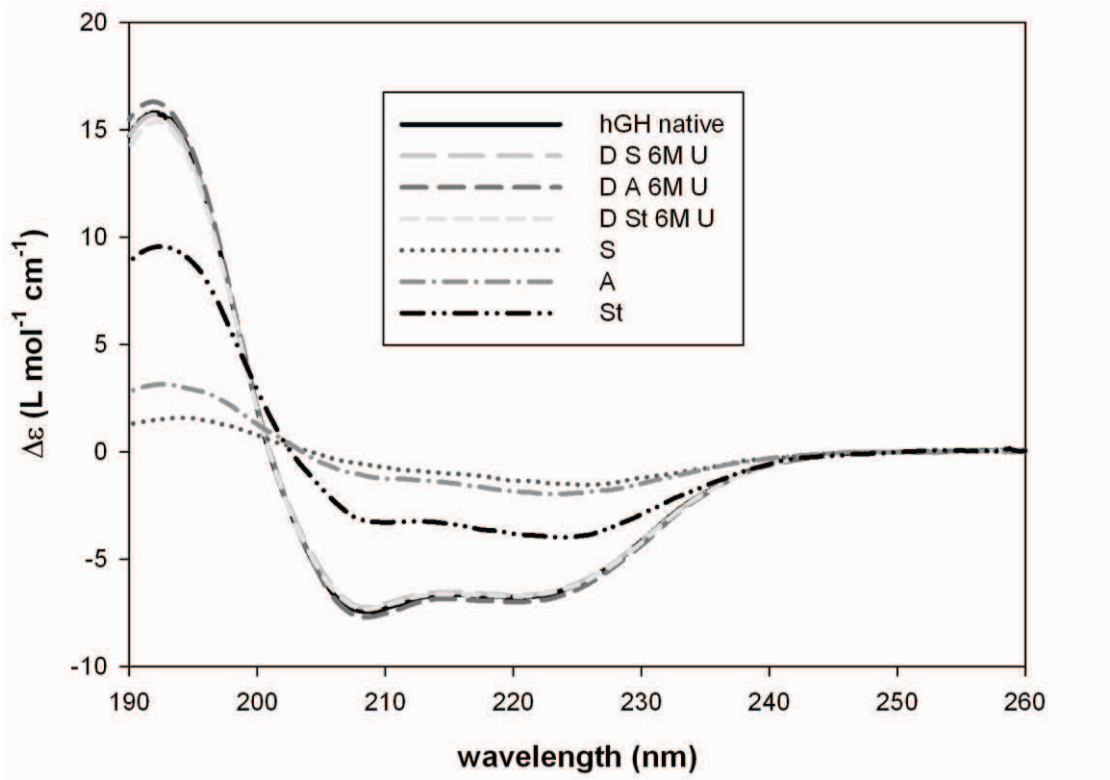


**Figure 4: CD spectra of insoluble aggregates, soluble aggregates and native hGH.** The native hGH and the dialyzed samples (D) show equal secondary structure independent of the presence of up to 50 % soluble aggregates (6M urea). Aggregates samples (S shaking; A aeration; St stirring) show a different structure.

Although CD measurements in the presence of aggregates might lead to artifacts due to scattering [69], a nonnative structure is reported for the aggregates of hGH and structurally similar mainly alpha-helical proteins like granulocyte colony-stimulating factor (G-CSF) and interleukin-2 (IL-2) throughout literature. This nonnative structure (intermolecular beta-sheets) was detected during incubation at elevated temperature [68,70,33], lyophilization [71], in the presence of antimicrobial preservatives [72], water-in-oil emulsions [45], shaking [31,41] or in inclusion bodies [12]. Additionally adsorption studies show that proteins "denature" at interfaces and these adsorbed structures are stabilized by changes in the native secondary and tertiary structure [73-76]. This would mean that addition of urea and GdnHCl below its midpoint concentration for hGH transform originally nonnative aggregates, which also bind a hydrophobic dye [42], into soluble aggregates with a more native-like structure.

*Kinetic stability of soluble aggregates and the effect of the individual chaotropic reagents*

In order to evaluate the efficiency and kinetic stability of the dissolved aggregates, samples incubated with 6M urea and 6M GdnHCl as well as 3M GdnHCl were dialyzed against 10 mM NaPP buffer pH 7.0. All samples showed little precipitation after dialysis. Our results are summarized in Figure 5. Dialyzed samples (D) are compared with samples in the presence of different chaotropic salt concentrations (3M and 6M GdnHCl, 6M urea) for each individual stress method. In general, we found that after dialysis the amount of soluble aggregates is increased compared to before dialysis. Regarding the amount of soluble aggregates we notice (1) a negative correlation with the unfolding efficiency of the chaotropic reagents: 6M urea > 3M GdnHCl > 6M GdnHCl and (2) a positive correlation with initial aggregate levels: shaking > aeration > stirring (Figure 5 and S7). Very low amounts of soluble aggregates (≤ 0.7 area%) were only detected in our experiments using 6M GdnHCl (Figure 5 and Figure S7). Our results suggest that the re-solubilized samples are also kinetically stable to a certain extent if urea and GdnHCl are removed. However, an increase in the amount of soluble aggregates after dialysis suggests that the soluble aggregates lead to further aggregation

upon the decrease of the chaotropic reagent concentration. As only minor amounts of soluble aggregates were detected during aggregation itself [42, 59], the following aggregation might have been shifted into an alternative pathway by re-solubilization and refolding.

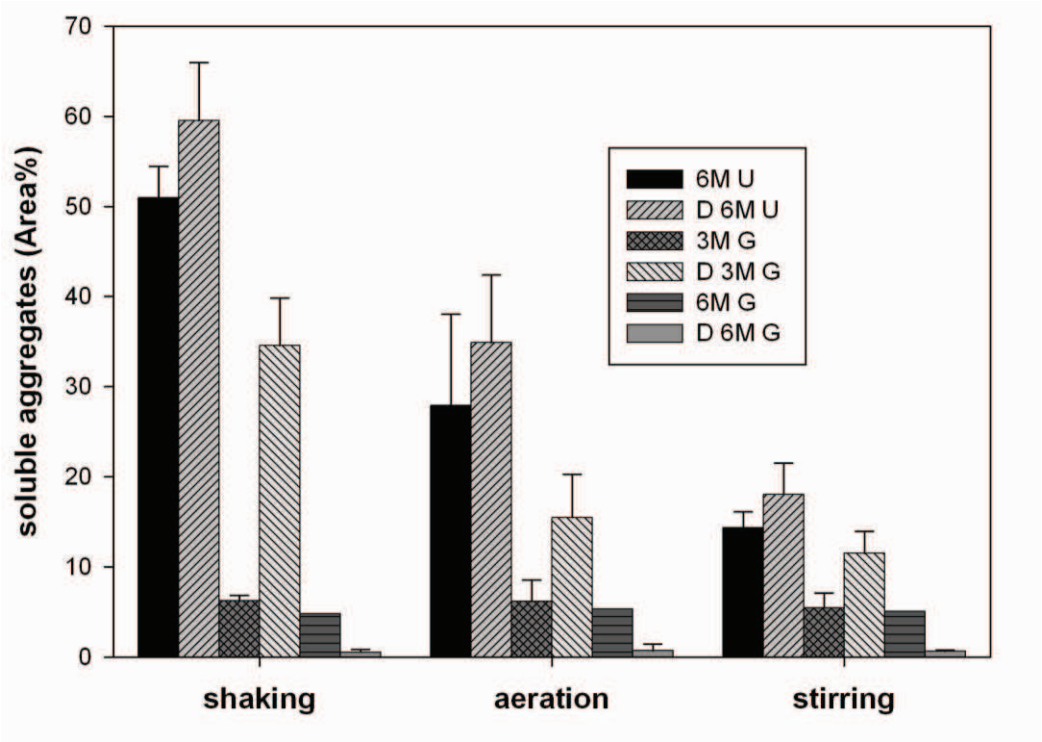


**Figure 5: Comparison of the content of soluble aggregates (supernatant) in the presence of chaotropic salts and after dialysis for shaking, aeration and stirring.**
From left to right: 6M urea, 3M GdnHCl and 6M GdnHCl before and after dialysis. (Shaking) 2 h shaking at 300 rpm; (Aeration) 7 h aeration at 3 L/h; (stirring) 96 h stirring at 300 rpm; (U) urea; (G) GdnHCl; (D) dialysis. We have to note that for 6M and 3M GdnHCl it is hard to define the exact amount of soluble aggregates due to changed SEC spectra.

*Structural characterization of the dialyzed sample preparations*

In the absence of urea and GdnHCl the dialyzed samples could be analyzed from 190 to 260 nm (Figure 4 and Figure S8) and the secondary structure was calculated using the DICHROWEB server (Table 1 and Table S1). Deviations from the theoretical value of hGH (crystal structure PDB 1HGU, 3HHR hGH-receptor complex; DSSP value [77]) are probably due to an additional small helix found in the solution structure by NMR measurements [57].

Comparing our data for refolded and dialyzed samples with the native hGH we found that the secondary structures are within experimental errors (protein concentration) equal (70 % alpha helix and no beta sheets). As some samples (shaking and 6M urea) contain about 50 % soluble aggregates we conclude that these soluble aggregates show no detectable significantly different secondary structure compared to the native protein (Table 1).

**Table 1: Predicted secondary structure of hGH and refolded aggregates**

| Sample | alpha helix | beta-sheet | turns | unordered |
|---|---|---|---|---|
| PDB: 1HGU | 0.45* | 0 | | |
| PDB: 3HHR | 0.64* | 0 | | |
| hGH native | 0.71 ± 0.04 | 0.02 ± 0.01 | 0.07 ± 0.03 | 0.19 ± 0.01 |
| D S 6M urea | 0.70 ± 0.03 | 0.02 ± 0.01 | 0.08 ± 0.03 | 0.19 ± 0.01 |
| D S 3M GdnHCl | 0.71 ± 0.04 | 0.04 ± 0.01 | 0.06 ± 0.02 | 0.20 ± 0.01 |
| D S 6M GdnHCl | 0.73 ± 0.02 | 0.03 ± 0.01 | 0.05 ± 0.01 | 0.18 ± 0.01 |

Values represent mean values n = 3 of independent experiments.

* DSSP value [77]

D dialysis against 10 mM NaPP pH 7.0

S shaking 2h 300 rpm

Fluorescence measurements at 295 nm show emission maxima around 333 ± 1 nm for dialyzed samples previously incubated with 6M urea or 6M GdnHCl and 335 ± 1 nm for 3M GdnHCl. The maximum emission wavelength for hGH is around 333 ± 1 nm. So the micro-environment of the Trp86 residue in the hydrophobic core seems unchanged in the soluble aggregates (Figure 3). Fluorescence measurements using ANSA binding showed that samples

refolded with 6M GdnHCl and dialysis afterwards show spectra comparable to the native protein (data not shown). For samples where soluble aggregates are detected (dissolved by 3M GdnHCl and 6M urea + dialysis) the intensity is increased compared to the native protein but decreased compared to the initial insoluble aggregates (Figure S9). This shows that soluble and insoluble aggregates differ regarding their surface properties and the structural perturbations of the involved proteins. A recent study about weak self-association of hGH suggests that one terminal helix is flexible and might be able to swap, but they could not reliably determine which one. Whether domain swapping can explain the formation of soluble aggregates and increased exposure of hydrophobic patches compared to the native protein has not been investigated so far [21]. Alternatively, DeFelippis and coworkers [58] found equilibrium folding intermediates, which tend to self-associate and show increased surface hydrophobicity and otherwise predominantly native-like structure.

*From insoluble towards soluble aggregates – possible mechanism*

In general we have generated insoluble aggregates with negligible amounts of soluble aggregates (3-5 area% supernatant) by accelerated stress conditions, which show a change in secondary structure (nonnative) compared to the native protein (Figure 4). Further ANSA binding demonstrates the increased exposure of hydrophobic patches and binding pockets (Figure S9). Upon addition of urea and GdnHCl below the midpoint concentration we propose that structurally perturbed monomeric hGH building blocks dissociate from the insoluble aggregate, refold and reduce the unfavorable exposure of hydrophobic surface patches in solution. As shown in literature folding intermediates and monomer both can be populated dependent on the solvent conditions [53]. Therefore we assume that this leads to the regain of monomer and formation of self-associated intermediates in the presence of urea and GdnHCl. This would also explain the more native-like structure of the newly formed soluble aggregates. Further we observe that the levels of soluble aggregates differ significantly for shaking (6M urea = 51 %) and aeration (6M urea = 28 %), although both aggregate samples showed a

similar initial aggregate level (shaking: > 95 %, aeration: 88 ± 3 %). As shaking and aeration show differences regarding size and shape of their aggregates, this might influence the formation of soluble aggregates. In general large (but fewer) particles expose a smaller overall surface than many small particles (same aggregation level). So the re-solubilized protein concentrations might differ locally and influence the formation of soluble aggregates (self-association of intermediates). Reports about hGH intermediates which are able to self-assemble or aggregate [34] cover various hypotheses like the involvement of flexible terminal helices [21], interaction between partially folded intermediates (terminal helices folded) [53] and solvent accessible helices (helix 3, least residue stability) [51,53] or a higher accessibility of the hydrophobic surface of the second and forth helices if partial unfolding of loop regions occurs [57]. Yet, there is common agreement that hydrophobic interactions are the main driving force for aggregation [56], which can be further used for stabilizing strategies.

If hGH aggregates are completely unfolded in the presence of 6M GdnHCl we do not detect these soluble aggregates. Here we suppose that refolding of unfolded proteins takes place, which leads mainly to hGH monomers like described for the native protein [51].

## CONCLUSION

In our work we show that initially insoluble nonnative aggregates formed by exposure to air-liquid interfaces during shaking, aeration and stirring undergo transformation into soluble native-like aggregates (secondary structure and microenvironment of the buried Trp86 residue) in the presence of 6M urea and 3M GdnHCl, respectively. The chosen concentrations of chaotropic reagents are below the midpoint concentration for unfolding. The soluble aggregates show increased binding of the hydrophobic dye ANSA compared to the native protein but reduced binding compared to the insoluble aggregates. We assume that insoluble aggregates are formed by population of native-like folding intermediates, which tend to self-associate. If the aggregates are incubated with 6M GdnHCl dissolution and unfolding takes place. After dialysis monomeric hGH is regained as expected for hGH refolding. This clearly shows that it should be possible to refold and reuse aggregates formed during process conditions. Preparations with 6M urea and 3M GdnHCl showed an increase in soluble aggregates, which further increased after dialysis. For the structure of the intermediates several suggestions exist in literature agreeing on the importance of hydrophobic interactions for self-association and aggregation.

## References


1. Manning MC, Chou DK, Murphy BM, Payne RW, Katayama DS (2010) Stability of protein pharmaceuticals: an update. Pharm Res 27: 544-575.
2. Manning MC, Patel K, Borchardt RT (1989) Stability of protein pharmaceuticals. Pharm Res 6: 903-918.
3. Cleland JL, Powell MF, Shire SJ (1993) The development of stable protein formulations: A close look at protein aggregation, deamidation, and oxidation. Crit Rev Ther Drug Carrier Syst 10: 307–377.
4. Mahler H-C, Friess W, Grauschopf U, Kiese S (2008) Protein aggregation: pathways, induction factors and analysis. J Pharm Sci 98: 2909-2934.
5. Wang W (1999) Instability, stabilization, and formulation of liquid protein pharmaceuticals. Int J Pharm 185: 129–188.
6. Chi EY, Krishnan S, Randolph TW, Carpenter JF (2003) Physical stability of proteins in aqueous solution: mechanism and driving forces in nonnative protein aggregation. Pharm Res 20: 1325–1336.
7. Wang W, Nema S, Teagarden D (2010) Protein aggregation--pathways and influencing factors. Int J Pharm 390: 89-99.
8. Wang W (1999) Instability, stabilization and formulation of liquid protein pharmaceuticals. Int J Pharm 185: 129-188.
9. Cromwell MEM, Hilario E, Jacobson F (2006) Protein aggregation and bioprocessing. AAPS Journal 8: E572-E579.
10. Mitraki A, King J (1989) Protein folding intermediates and inclusion body formation. Nat Biotechnol 7: 690-697.
11. Schein CH (1990) Solubility as a function of protein structure and solvent components. Nat Biotechnol 8: 308-317.
12. Fink AL (1998) Protein aggregation: folding aggregates, inclusion bodies and amyloid. Fold Des 3: R9-R23.
13. Rathore N, Rajan RS (2008) Current perspectives on stability of protein drug products during formulation, fill and finish operations. Biotechnol Prog 24: 504–514.
14. Simon S, Krause HJ, Weber C, Peukert W (2011) Physical degradation of proteins in well-defined fluid flows studied within a four-roll apparatus. Biotechnol Bioeng 108: 2914-2922.
15. Guelseren I, Guezey D, Bruce BD, Weiss J (2007) Structural and functional changes in ultrasonicated bovine serum albumin solutions. Ultrason Sonochem 14: 173-183.
16. Rosenberg A (2006) Effects of protein aggregates: an immunologic perspective. AAPS J 8: E501–E508.
17. Mahler H-C, Mueller R, Friess W, Delille A, Matheus S (2005) Induction and analysis of aggregates in a liquid IgG1-antibody formulation. Eur J Pharm Biopharm 59: 407–417.
18. Philo JS, Arakawa T (2009) Mechanisms of protein aggregation. Curr Pharm Biotechnol 10: 348-351.
19. Cholewinski M, Lückel B, Horn H (1996) Degradation pathways, analytical characterization and formulation strategies of a peptide and a protein. Calcitonine and human growth hormone in comparison. Pharm Acta Helv 71: 405-419.
20. Pearlman R, Wang JY (1993) Stability and characterization of human growth hormone. In: Pearlman R, Wang JY, editors. Stability and Characterization of Protein and Peptide Drugs: Case Histories. New York: Plenum Press. pp. 1-58.
21. Jensen MR, Kristensen SM, Keeler C, Christensen HE, Hodsdon ME, et al. (2008) Weak self-association of human growth hormone investigated by nitrogen-15 NMR relaxation. Proteins 73: 161-172.

22. Katakam M, Bell LN, Banga AK (1995) Effect of surfactants on the physical stability of recombinant human growth hormone. J Pharm Sci 84: 713–716.
23. Katakam M, Banga AK (1997) Use of poloxamer polymers to stabilize recombinant human growth hormone against various processing stresses. Pharm Dev Technol 2: 143-149.
24. Lewis UJ, Cheever EV, Hopkins WC (1970) Kinetic study of the deamidation of growth hormone and prolactin. Biochim Biophys Acta 214: 498-508.
25. Lewis UJ, Peterson SM, Bonewald LF, Seavey BK, VanderLaan WP (1977) An interchain disulfide dimer of human growth hormone. J Biol Chem 252: 3697-3702.
26. Youngman KM, Spencer DB, Brems DN, DeFelippis MR (1995) Kinetic analysis of the folding of human growth hormone. Influence of disulfide bonds. J Biol Chem 270: 19816-19822.
27. Maa Y-F, Hsu CC (1997) Protein denaturation by combined effect of shear and air-liquid interface. Biotechnol Bioeng 54: 503–512.
28. Maa Y-F, Hsu CC (1996) Aggregation of recombinant human growth hormone induced by phenolic compounds. Int J Pharm 140: 155-168.
29. Otzen DE, Knudsen BR, Aachmann F, Larsen KL, Wimmer R (2002) Structural basis for cyclodextrins‘ suppression of human growth hormone aggregation. Protein Sci 11: 1779-1787.
30. Fradkin AH, Carpenter JF, Randolph TW (2009) Immunogenicity of aggregates of recombinant human growth hormone in mouse models. J Pharm Sci 98: 3247-3264.
31. John RJS, Carpenter JF, Balny C, Randolph TW (2001) High pressure refolding of recombinant human growth hormone from insoluble aggregates. Structural transitions, kinetic barriers and energetic. J Biol Chem 276: 46856-46863.
32. Becker GW, Tackitt PM, Bromer WW, Lefeber DS, Riggin RM (1988) Isolation and characterization of a sulfoxide and a desamido derivative of biosynthetic human growth hormone. Biotechnol Appl Biochem 10: 326-337.
33. Pikal MJ, Rigsbee D, Roy ML (2008) Solid state stability of proteins III: calorimetric (DSC) and spectroscopic (FTIR) characterization of thermal denaturation in freeze dried human growth hormone (hGH). J Pharm Sci 97: 5122-5131.
34. Gomez-Orellana I, Variano B, Miura-Fraboni J, Milstein S, Paton DR (1998) Thermodynamic characterization of an intermediate state of human growth hormone. Protein Sci 7: 1352-1358.
35. Chantalat L, Jones ND, Korber F, Navaza J, Pavlovsky AG (1995) The crystal structure of wild-type growth hormone at 2.5 Å resolution. Protein Pept Lett 2: 333-340.
36. de Vos AM, Ultsch MH, Kossiakoff AA (1992) Human growth hormone and extracellular domain of its receptor: crystal structure of the complex. Science 255: 306-312.
37. Ultsch MH, Somers W, Kossiakoff AA, de Vos AM (1994) The crystal structure of affinity-matured human growth hormone at 2 Å resolution. J Mol Biol 236: 286-299.
38. Singh SM, Eshwari ANS, Garg LC, Panda AK (2005) Isolation, solubilization, refolding, and chromatographic purification of human growth hormone from inclusion bodies of Escherichia coli cells: a case study. Methods Mol Biol 308: 163-176.
39. Patra AK, Mukhopadhyay R, Mukhija R, Krishnan A, Garg LC, et al. (2000) Optimization of inclusion body solubilization and renaturation of recombinant human growth hormone from Escherichia coli. Protein Expr Purif 18: 182-192.
40. Crisman RL, Randolph TW (2010) Crystallization of recombinant human growth hormone at elevated pressures: pressure effects on PEG-induced volume exclusion interactions. Biotechnol Bioeng 107: 663-672.
41. John RJS, Carpenter JF, Randolph TW (1999) High pressure fosters protein refolding from aggregates at high concentrations. Proc Natl Acad Sci U S A 96: 13029-13033.

42. Wiesbauer J, Cardinale M, Nidetzky B (2012) Shaking and stirring: comparison of accelerated stress conditions applied to the human growth hormone. Process Biochem (submitted).
43. Lim WK, Roesgen J, Englander SW (2009) Urea, but not guanidinium, destabilizes proteins by forming hydrogen bonds to the peptide group. Proc Natl Acad Sci U S A 106: 2595-2600.
44. Bennion BJ, Daggett V (2003) The molecular basis for the chemical denaturation of proteins by urea. Proc Natl Acad Sci U S A 100: 5142-5147.
45. Jørgensen L, Vermehren C, Bjerregaard S, Froekjaer S (2003) Secondary structure alterations in insulin and growth hormone water-in-oil emulsions. Int J Pharm 254: 7-10.
46. Yang TH, Cleland JL, Lam X, Meyer JD, Jones LS, et al. (2000) Effect of zinc binding and precipitation on structures of recombinant human growth hormone and nerve growth factor. J Pharm Sci 89: 1480-1485.
47. Kauffman EW, Thamann TJ, Havel HA (1989) Ultraviolet resonance Raman and fluorescence studies of acid-induced structural alterations in porcine, bovine and human growth hormone. JACS 111: 5449-5456.
48. Larkin MA, Blackshields G, Brown NP, Chenna R, McGettigan PA, et al. (2007) Clustal W and Clustal X version 2.0. Bioinformatics 23: 2947-2948.
49. Borromeo V, Sereikaite J, Bumelis V-A, Secchi C, Scire A, et al. (2008) Mink growth hormone structural-functional relationships: effects of renaturing and storage conditions. Protein J 27: 170-180.
50. Abildgaard F, Jorgensen AM, Led JJ, Christensen T, Jensen EB, et al. (1992) Characterization of tertiary interactions in a folded protein by NMR methods: studies of pH-induced structural changes in human growth hormone. Biochemistry 31: 8587-8596.
51. DeFelippis MR, Alter LA, Pekar AH, Havel HA, Brems DN (1993). Evidence for a self-associating equilibrium intermediate during folding of human growth hormone. Biochemistry 32: 1555-1562.
52: Cardamone M, Nirdosh KP, Brandon MR (1995) Comparing the refolding and reoxidation of recombinant porcine growth hormone from a urea denatured state and from Escherichia coli inclusion bodies. Biochemistry 34: 5773-5794.
53. Kasimova MR, Milstein SJ, Freire E (1998) The conformational equilibrium of human growth hormone. J Mol Biol 277: 409-418.
54. Havel HA, Kauffman EW, Plaisted SM, Brems DN (1986) Reversible self-association of bovine growth hormone during equilibrium unfolding. Biochemistry 25: 6533-6538.
55. Brems DN, Plaisted SM, Kauffman EW, Havel HA (1986) Characterization of an associated equilibrium folding intermediate of bovine growth hormone. Biochemistry 25: 6539-6543.
56. Bam NB, Cleland JL, Randolph TW (1996) Molten globule intermediate of recombinant human growth hormone: stabilization with surfactants. Biotechnol Prog 12: 801-809.
57. Kasimova MR, Kristensen SM, Howe PWA, Christensen T, Matthiesen F, et al. (2002) NMR studies of the backbone flexibility and structure of human growth hormone: a comparison of high and low pH conformations. J Mol Biol 318: 679-695.
58. DeFelippis MR, Kilcomons MA, Lents MP, Youngman KM, Havel HA (1995) Acid stabilization of human growth hormone equilibrium folding intermediates. Biochim Biophys Acta 1247: 35-45.
59. Wiesbauer J, Prassl R, Nidetzky B (2012) The air-liquid interface: its role in aggregation of hGH, critical parameters and stabilizing strategies. J Colloid Interface Sci (in preparation).
60. Wilkins MR, Gasteiger E, Bairoch A, Sanchez JC, Williams KL, et al. (1999) Protein identification and analysis tools in the ExPASy server. Methods Mol Biol 112: 531-552.

61. Gasteiger E, Hoogland C, Gattiker A, Duvaud S, Wilkins MR, et al. (2005) Protein Identification and Analysis Tools on the ExPASy Server. In: Walker JM, editor. The Proteomics Protocols Handbook. New York: Humana Press Inc. pp. 571-607.
62. Eckhardt BM, Oeswein JQ, Yeung DA, Milby TD, Bewley TA (1994) A turbidimetric method to determine visual appearance of protein solutions. J Pharm Sci Technol 48: 64–70.
63. Ablinger E, Wegscheider S, Keller W, Prassl R, Zimmer A (2012) Effect of protamine on the solubility and deamidation of human growth hormone. Int J Pharm 427: 209-216.
64. Ph. Eur. 2.2.1. (2008) Clarity and degree of opalescense of liquids, 6th edition. European Directorate for the Quality of Medicine (EDQM).
65. Vivian JT, Callis PR (2001) Mechanisms of tryptophan fluorescence shifts in proteins. Biophys J 80: 2093-2109.
66. Lees JG, Smith BR, Wien F, Miles AJ, Wallace BA (2004) CDtool - an integrated software package for circular dichroism spectroscopic data processing, analysis, and archiving. Anal Biochem 332: 285-289.
67. Whitmore L, Wallace BA (2004) DICHROWEB, an online server for protein secondary structure analysis from circular dichroism spectroscopic data. Nucleic Acids Res 32: W668-W673.
68. Natalello A, Ami D, Collini M, D'Alfonso L, Chirico G, et al. (2012) Biophysical characterization of met-G-CSF: effects of different site-specific mono-pegylations on protein stability and aggregation. PLoS ONE 7: 1-9.
69. Kelly SM, Jess TJ, Price NC (2005) How to study proteins by circular dichroism. Biochim Biophys Acta 1751: 119-139.
70. Chi EY, Krishnan S, Kendrick BS, Chang BS, Randolph TW, et al. (2003) Roles of conformational stability and colloidal stability in the aggregation of recombinant human granulocyte colony-stimulating factor. Protein Sci 12: 903-913.
71. Costantino HR, Carrasquillo KG, Cordero RA, Mumenthaler M, Hsu CC, et al. (1998) Effect of excipients on the stability and structure of lyophilized recombinant human growth hormone. J Pharm Sci 87: 1412-1420.
72. Thirumangalathu R, Krishnan S, Brems DN, Randolph TW, Carpenter JF (2006) Effects of pH, temperature, and sucrose on benzyl alcohol-induced aggregation of recombinant human granulocyte colony stimulating factor. J Pharm Sci 95: 1480-1497.
73. Felsovalyi F, Mangiagalli P, Bureau C, Kumar SK, Banta S (2011) Reversibility of the adsorption of lysozyme on silica. Langmuir 27: 11873-11882.
74. Sethuraman A, Vedantham G, Imoto T, Przybycien T, Belfort G (2004) Protein unfolding at interfaces: slow dynamics of alpha-helix to beta-sheet transition. Proteins 56: 669-678.
75. Zhai J, Hoffmann SV, Day L, Lee T-H, Augustin MA, et al. (2012) Conformational changes of α-lactalbumin adsorbed at oil-water interfaces: interplay between protein structure and emulsion stability. Langmuir 28: 2357–2367.
76. Zoungrana T, Findenegg GH, Norde W (1997) Structure, stability and activity of adsorbed enzymes. J Colloid Inferface Sci 190: 437-448.
77. Kabsch W, Sander C (1983) Dictionary of protein secondary structure: pattern recognition of hydrogen-bonded and geometrical features. Biopolymers 22: 2577-2637.

## 4.1 Supporting Information

**Re-solubilization and refolding of nonnative aggregates of the human growth hormone using chaotropic agents: evidence for native-like aggregation in solution**

Johanna Wiesbauer[1,2], Andras Boeszoermenyi[3], Monika Oberer[3] and Bernd Nidetzky[1,2]

[1]*Research Center Pharmaceutical Engineering, Graz, Austria*

[2]*Institute of Biotechnology and Biochemical Engineering, University of Technology Graz, Austria*

[3]*Institute of Molecular Biosciences, University of Graz, Graz, Austria*

*Corresponding author*: Nidetzky, B. (bernd.nidetzky@tugraz.at).

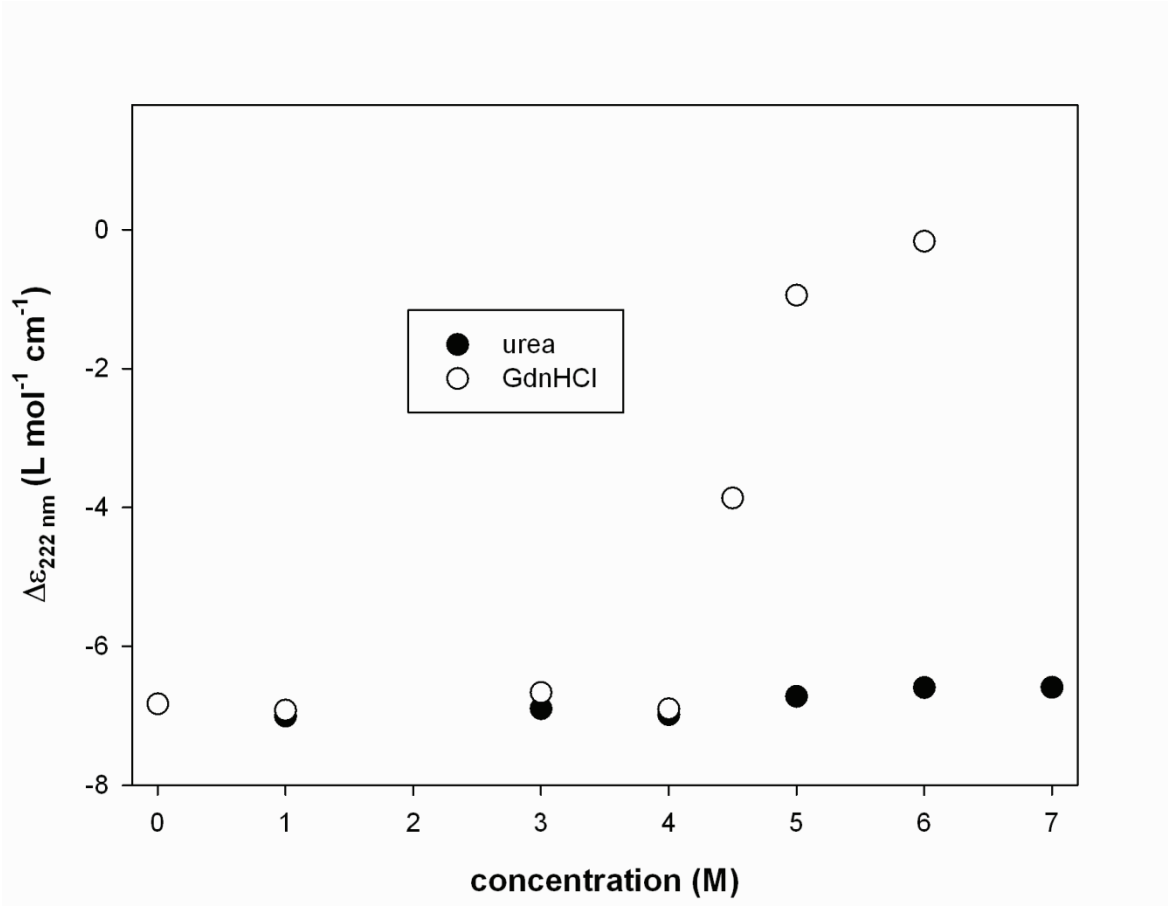


**Figure S1: Effect of guanidine hydrochloride (GdnHCl) and urea on hGH monitored using Circular Dichroism (CD).** Whereas hGH is stable in the presence of up to 7M urea [1] hGH shows unfolding > 4M GdnHCl [2].

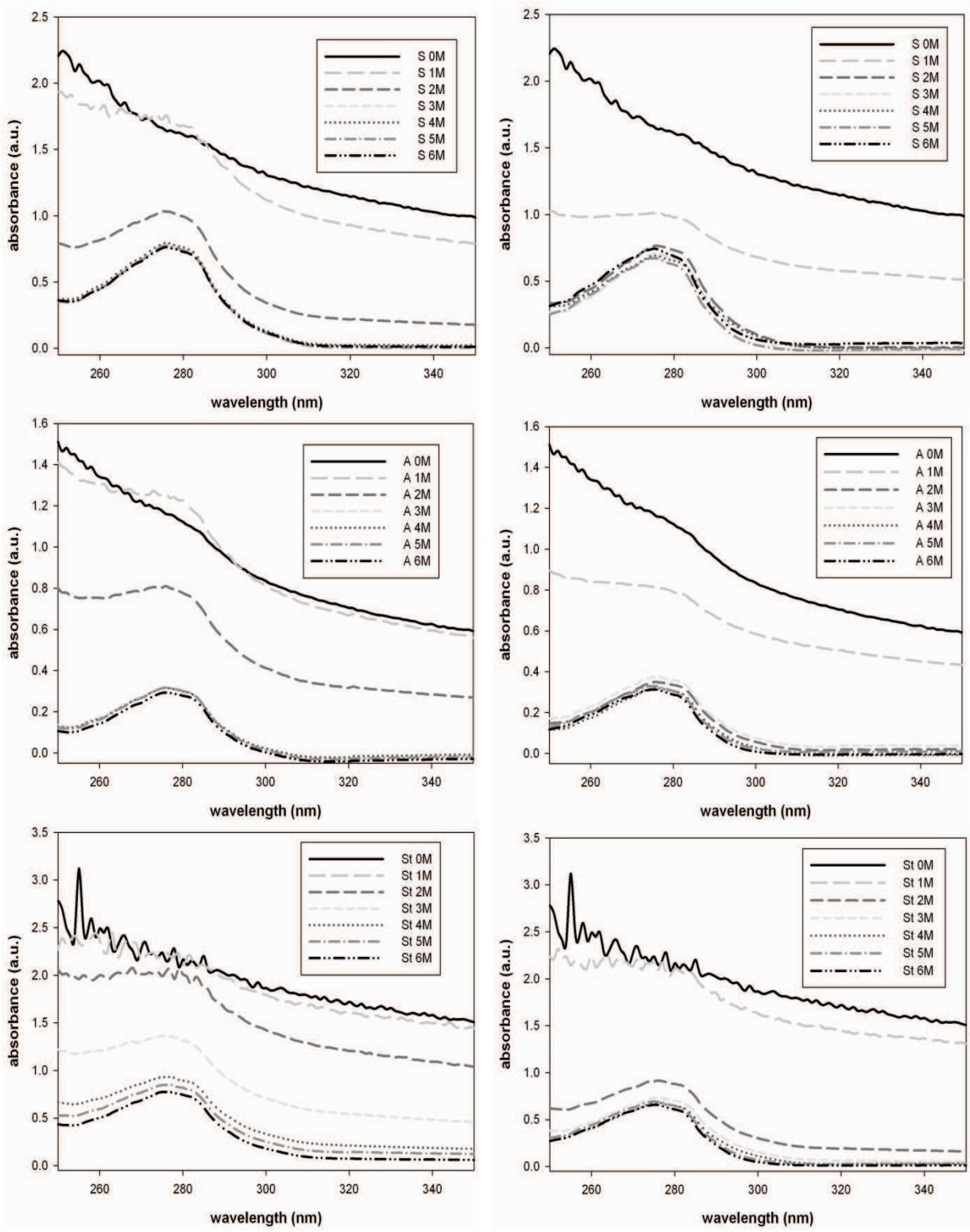


**Figure S2: Turbidity decrease during aggregate refolding for shaking (S), aeration (A) and stirring (St).** (Left from top to bottom): In these figures we show the reversible refolding or re-solubilization of hGH aggregates in the presence of urea. The transition from insoluble aggregates to soluble aggregates takes place around 3M urea. (right top to bottom) The figures on the right show refolding in the presence of GdnHCl at around 2M.

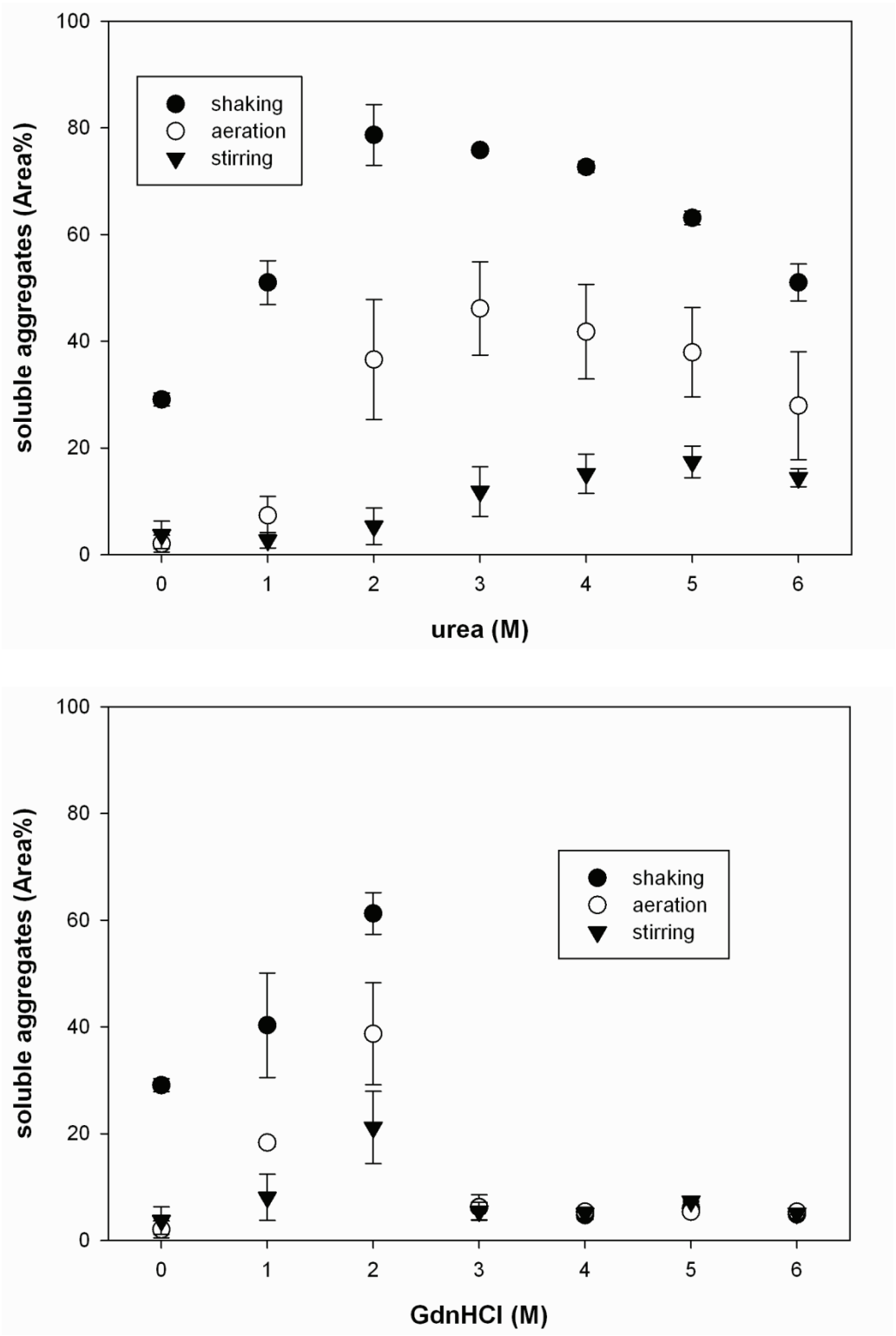


**Figure S3: Refolding/re-solubilization of hGH aggregates by urea and GdnHCl monitored using SEC-HPLC analysis.** The supernatant after centrifugation was used for SEC-HPLC analysis. (top) At ≥ 3M urea all insoluble aggregates are dissolved and only soluble aggregates and monomer remain. (Bottom) Complete dissolution of insoluble aggregates is reached at ≥ 2M GdnHCl. SEC Data above 4M GdnHCl showed strong change in the peak shape of the monomer.

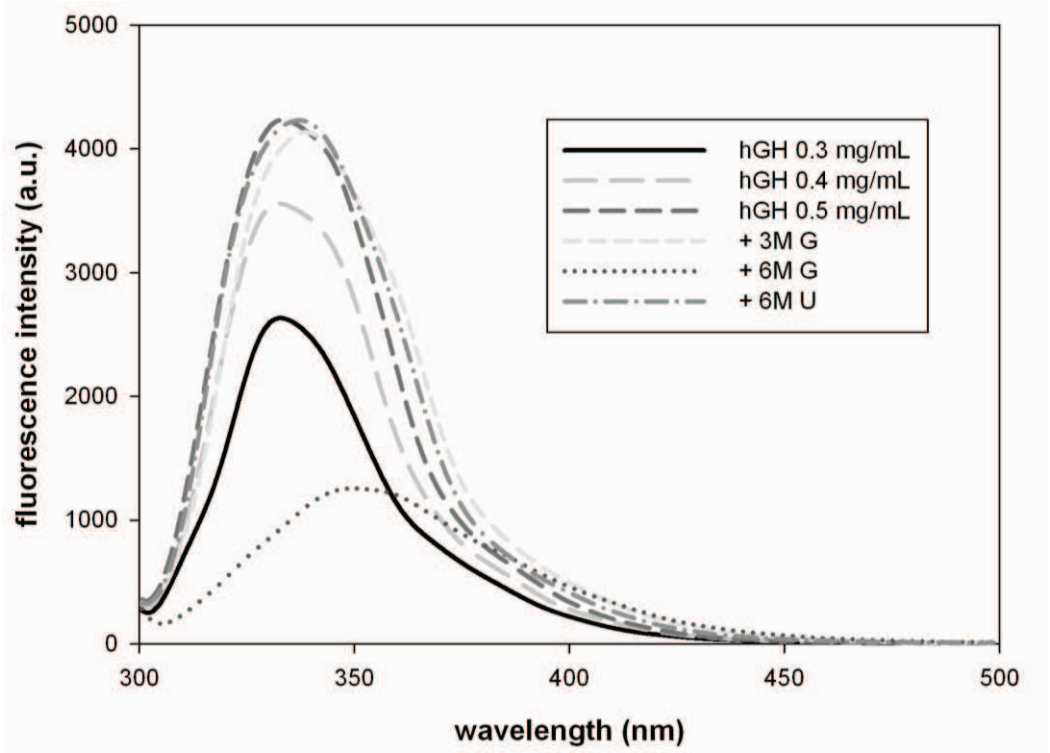


**Figure S4: Fluorescence spectra (Trp, 295 nm) of native hGH after incubation with GdnHCl and urea.** Native hGH (0.5 mg/mL) shows similar spectra as hGH in the presence of 6M urea (U) and 3M GdnHCl (G). In the presence of 6M GdnHCl the protein unfolds and the wavelength maxima is shifted towards 350 nm indicating a solvent-exposed Trp residue.

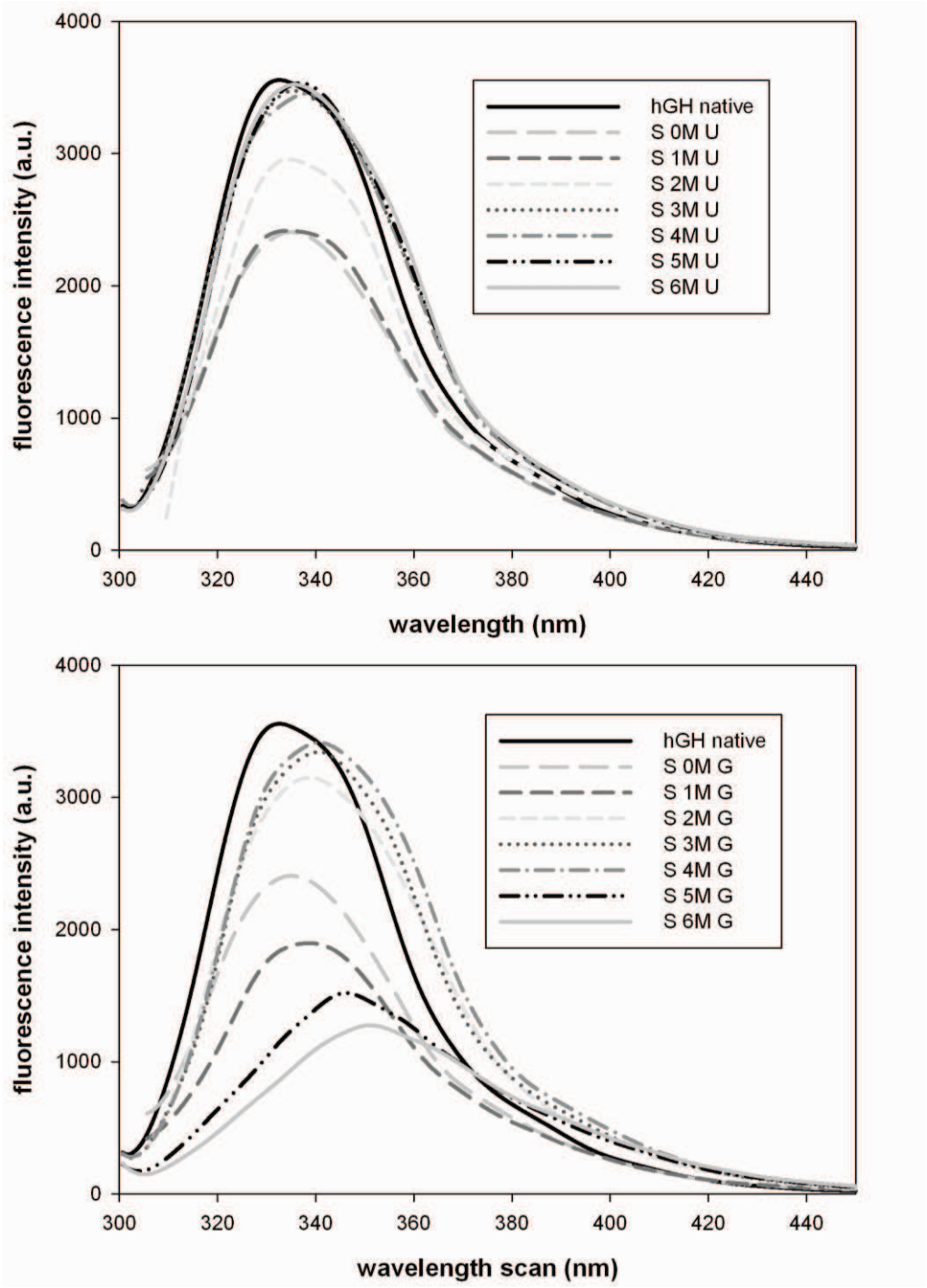


**Figure S5: Fluorescence spectra (Trp, 295 nm) of reversible aggregation of stressed hGH (shaking S) after incubation with 0 to 6M urea (U) and GdnHCl (G).** (top) Re-solubilization of insoluble aggregates in the presence of urea. At 0 and 1M there are still insoluble aggreagates and due to the turbidity and scattered excitation light spectra recording was started at 310 nm. Afterwards the spectra are unchanged up to 6M with an emission maxima aroung 335 ± 1 nm. (bottom) above 4M GdnHCl we can monitor unfolding and shift of the emission wavelength from 335 ± 1 nm to 350 ± 1 nm. In both figures we can see that the spectra during refolding are broader than for the native hGH (emission maxima 333 ± 1 nm).

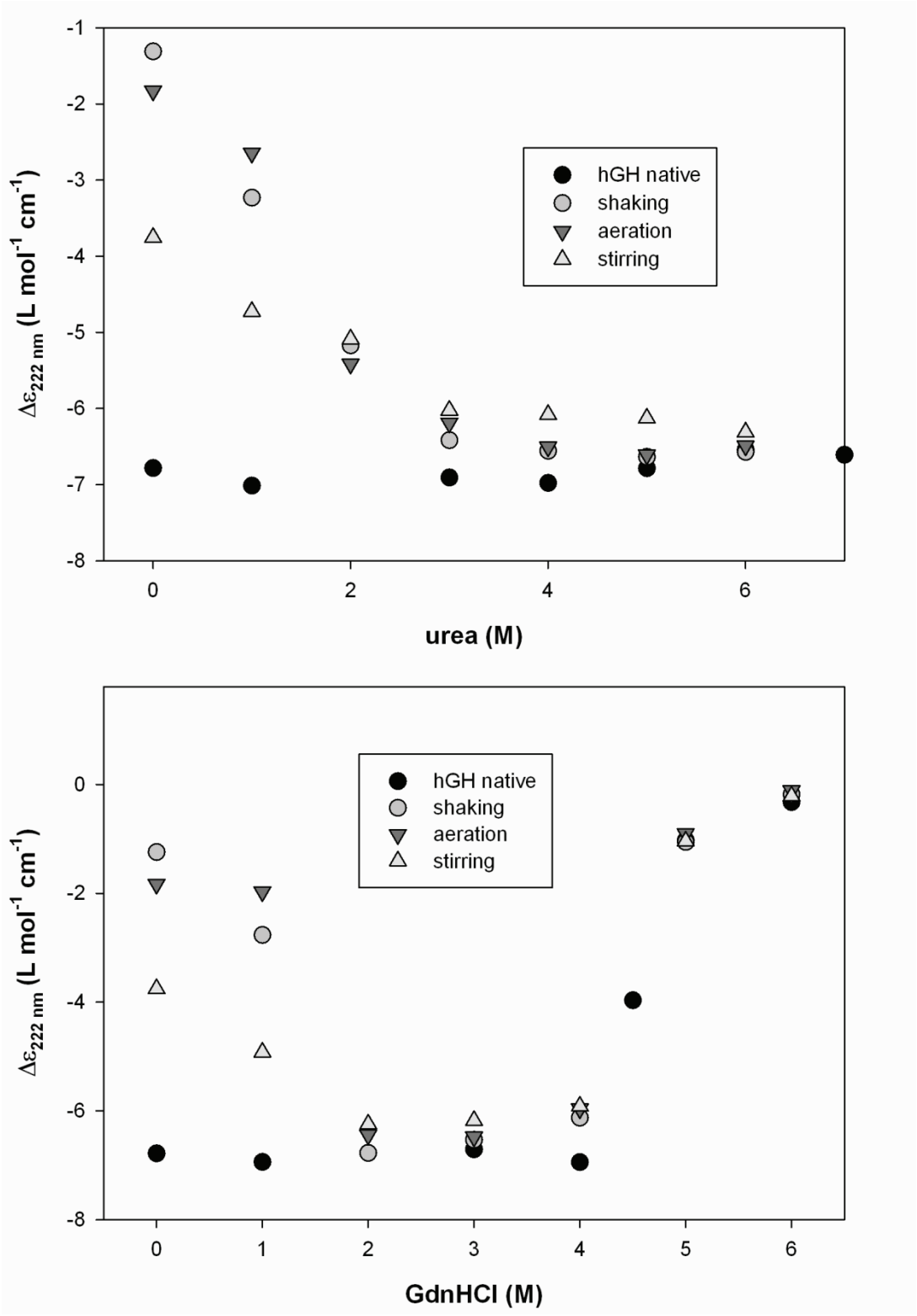


**Figure S6: Delta epsilon values (CD measurements) at 222 nm of hGH aggregates during refolding.** (top) Dissolution of insoluble hGH aggregates with urea in comparison of the native hGH in presence of urea (black dot). (bottom) hGH aggregates incubated with GdnHCl in comparison with the native hGH (black dots). At concentrations above 4M unfolding takes place.

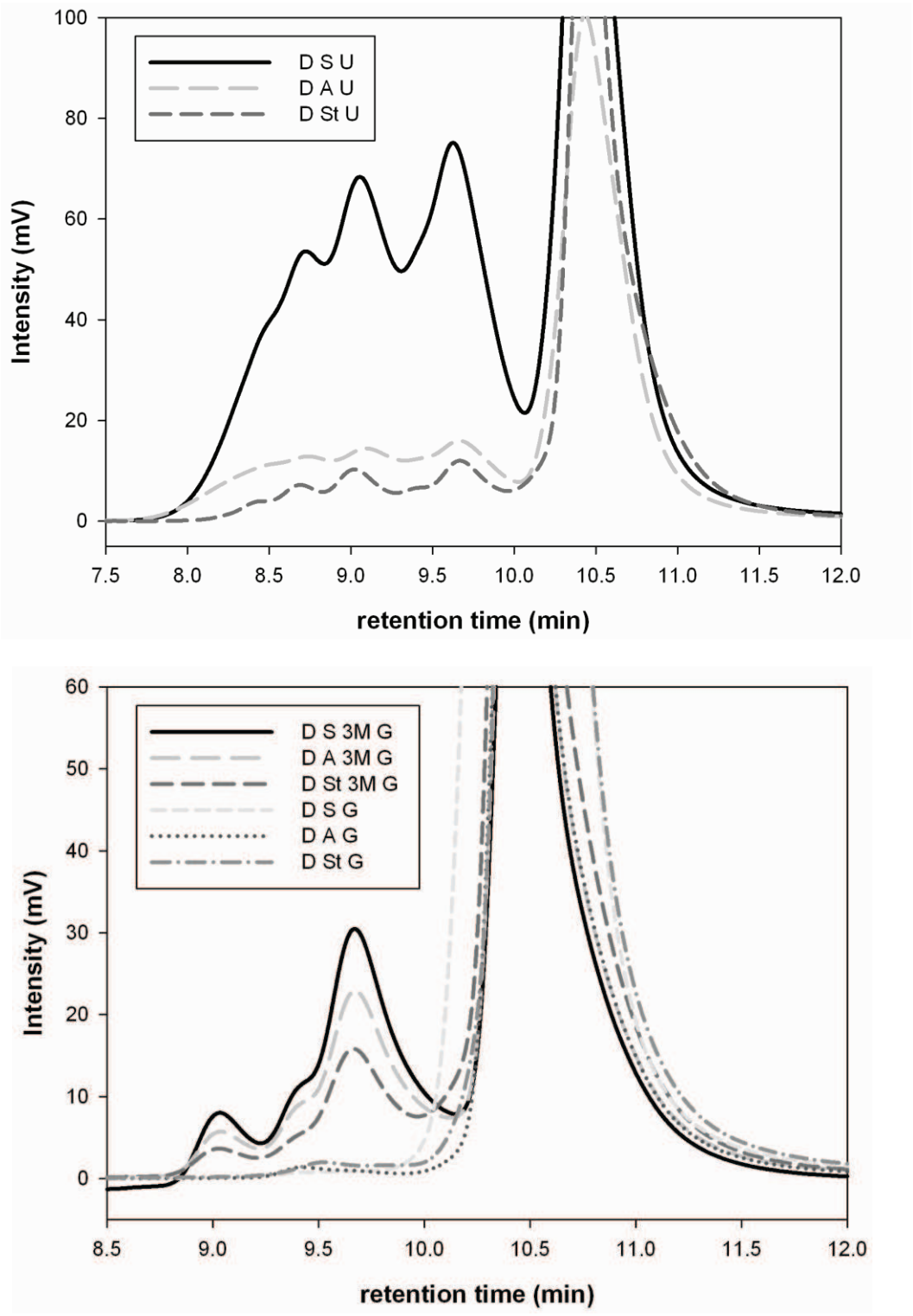


**Figure S7: SEC-HPLC spectra of soluble hGH aggregates after incubation in urea and GdnHCl and dialysis.** The content of soluble aggregates of hGH was detected after dialysis (10 mM NaPP pH 7.0) of re-solubilized aggregates by 6M urea (top) and 3M and 6M GdnHCl (bottom), respectively.

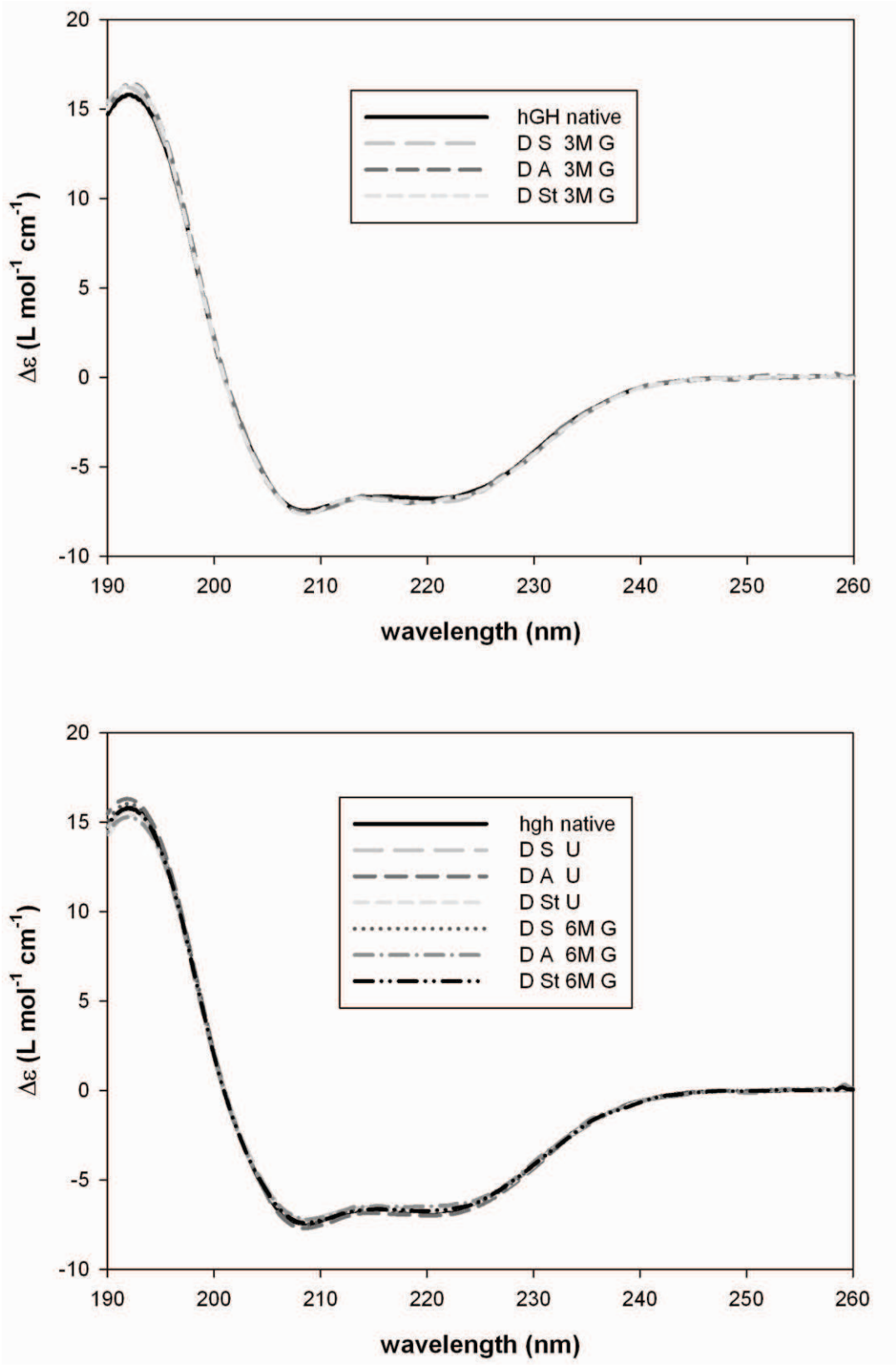


**Figure S8: CD spectra of refolded hGH aggregates after dialysis (D) against 10 mM NaPP buffer pH 7.0.** (S) shaking 2 h 300 rpm; (A) aeration 7 h 3 L/h; (St) stirring 96 h 300 rpm; (G) GdnHCl 3 or 6M; (U) urea 6M.

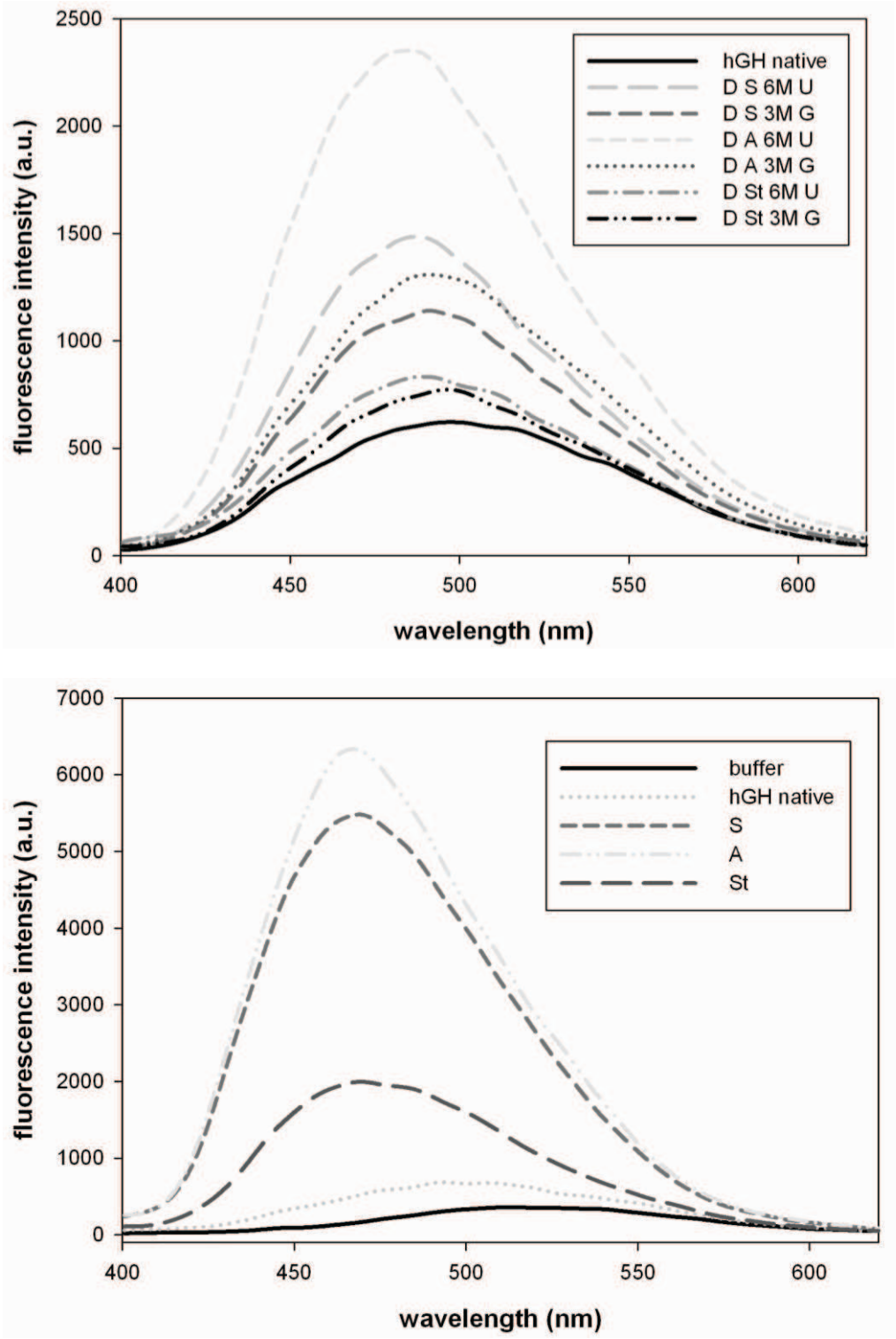


**Figure S9: Comparison of ANSA binding to soluble (top) and insoluble aggregates (bottom) of hGH.** (top) soluble aggregates of hGH show slightly increased fluorescence intensity upon ANSA binding (blue shift) compared to the native protein but decreased compared to the insoluble aggregates (bottom). (S) shaking; (A) aeration; (St) stirring.

**Table S1**

| Sample | alpha helix | beta-sheet | turns | unordered |
|---|---|---|---|---|
| PDB: 1HGU | 0.45* | 0 | | |
| PDB: 3HHR | 0.64* | 0 | | |
| hGH native | 0.71 ± 0.04 | 0.02 ± 0.01 | 0.07 ± 0.03 | 0.19 ± 0.01 |
| D S 6M urea | 0.70 ± 0.03 | 0.02 ± 0.01 | 0.08 ± 0.03 | 0.19 ± 0.01 |
| D A 6M urea | 0.70 ± 0.03 | 0.03 ± 0.02 | 0.08 ± 0.02 | 0.19 ± 0.01 |
| D St 6M urea | 0.70 ± 0.02 | 0.03 ± 0.01 | 0.08 ± 0.03 | 0.19 ± 0.01 |
| D S 3M GdnHCl | 0.71 ± 0.04 | 0.04 ± 0.01 | 0.06 ± 0.02 | 0.20 ± 0.01 |
| D A 3M GdnHCl | 0.69 ± 0.02 | 0.04 ± 0.01 | 0.06 ± 0.01 | 0.19 ± 0.01 |
| D St 3M GdnHCl | 0.70 ± 0.02 | 0.04 ± 0.01 | 0.06 ± 0.01 | 0.19 ± 0.01 |
| D S 6M GdnHCl | 0.73 ± 0.02 | 0.03 ± 0.01 | 0.05 ± 0.01 | 0.18 ± 0.01 |
| D A 6M GdnHCl | 0.69 ± 0.04 | 0.04 ± 0.02 | 0.07 ± 0.02 | 0.20 ± 0.01 |
| D St 6M GdnHCl | 0.72 ± 0.01 | 0.02± 0.01 | 0.06 ± 0.01 | 0.20 ± 0.01 |

Values represent mean values n = 3 of independent experiments.

* DSSP value [3]

D dialysis against 10 mM NaPP pH 7.0

S shaking 2 h 300 rpm

A aeration 7 h 3 L/h

St stirring 96 h 300 rpm

## References


1. Pearlman R, Wang JY (1993) Stability and characterization of human growth hormone. In: Pearlman R, Wang JY, editors. Stability and Characterization of Protein and Peptide Drugs: Case Histories. New York: Plenum Press. pp. 1-58.
2. DeFelippis MR, Alter LA, Pekar AH, Havel HA, Brems DN (1993). Evidence for a self-associating equilibrium intermediate during folding of human growth hormone. Biochemistry 32: 1555-1562.
3. Kabsch W, Sander C (1983) Dictionary of protein secondary structure: pattern recognition of hydrogen-bonded and geometrical features. Biopolymers 22: 2577-2637.

# 5 Nonnative aggregation of recombinant human granulocyte-colony stimulating factor under simulated process stress conditions

# Non-native aggregation of recombinant human granulocyte- colony stimulating factor under simulated process stress conditions

*Ulrich Roessl[1,2], Johanna Wiesbauer[1,2], Stefan Leitgeb[1,2], Ruth Birner-Gruenberger[3] and Bernd Nidetzky[1,2]*

[1] Research Center Pharmaceutical Engineering, Graz, Austria
[2] Institute of Biotechnology and Biochemical Engineering, Graz University of Technology, Graz, Austria
[3] Institute of Pathology and Center for Medical Research, Medical University Graz, Graz, Austria

Effective inhibition of protein aggregation is a major goal in biopharmaceutical production processes optimized for product quality. To examine the characteristics of process-stress-dependent aggregation of human granulocyte colony-stimulating factor (G-CSF), we applied controlled stirring and bubble aeration to a recombinant non-glycosylated preparation of the protein produced in *Escherichia coli*. We characterized the resulting denaturation in a time-resolved manner using probes for G-CSF conformation and size in both solution and the precipitate. G-CSF was precipitated rapidly from solutions that were aerated or stirred; only small amounts of soluble aggregates were found. Exposed hydrophobic surfaces were a characteristic of both soluble and insoluble G-CSF aggregates. Using confocal laser scanning microscopy, the aggregates presented mainly a circular shape. Their size varied according to incubation time and stress applied. The native intramolecular disulfide bonds in the insoluble G-CSF aggregates were largely disrupted as shown by mass spectrometry. New disulfide bonds formed during aggregation. All involved $Cys^{18}$, which is the only free cysteine in G-CSF; one of them had an intermolecular $Cys^{18(A)}$-$Cys^{18(B)}$ crosslink. Stabilization strategies can involve external addition of thiols and extensive reduction of surface exposition during processing.

| | |
|---|---|
| Received | 23 SEP 2011 |
| Revised | 15 FEB 2012 |
| Accepted | 13 MAR 2012 |
| Accepted article online | 15 MAR 2012 |

**Supporting information available online**

**Keywords**: Granulocyte-colony stimulating factor · Process conditions · Protein aggregation · Protein pharmaceuticals

## 1 Introduction

Protein aggregation is a critical issue in the pharmaceutical industry [1, 2]. The International Conference on Harmonisation of Technical Requirements for Registration of Pharmaceuticals for Human Use (ICH) guidance requires protein-based medicines to be stable against any kind of degradation for at least 12 months of storage [3]. These standards serve to minimize patient risk considering that protein aggregates upon parenteral administration have the potential to induce severe immunological reactions up to anaphylactic shock [4]. Protein aggregation represents a major factor determining a protein drug's shelf life [5–8], and its prevention is vital in the development of therapeutic protein formulations. Protein aggregation, therefore, has a strong impact on the design of the protein manufacturing processes and on each unit operation applied [6, 7]. Methods allowing an accurate prediction of protein aggregation at changing conditions during the different steps of the production process and storage would thus be of great value to pharmaceutical producers [9]. An improved understanding of the processes underlying the aggregation of proteins into non-native assem-

**Correspondence**: Prof. Bernd Nidetzky, Institute of Biotechnology and Biochemical Engineering, Graz University of Technology, 8010 Graz, Austria
**E-mail**: bernd.nidetzky@tugraz.at

**Abbreviations**: **ANS**, 8-anilino-1-naphthalenesulfonic acid; **CLSM**, confocal laser scanning microscopy; **rhG-CSF**, recombinant human granulocyte colony-stimulating factor

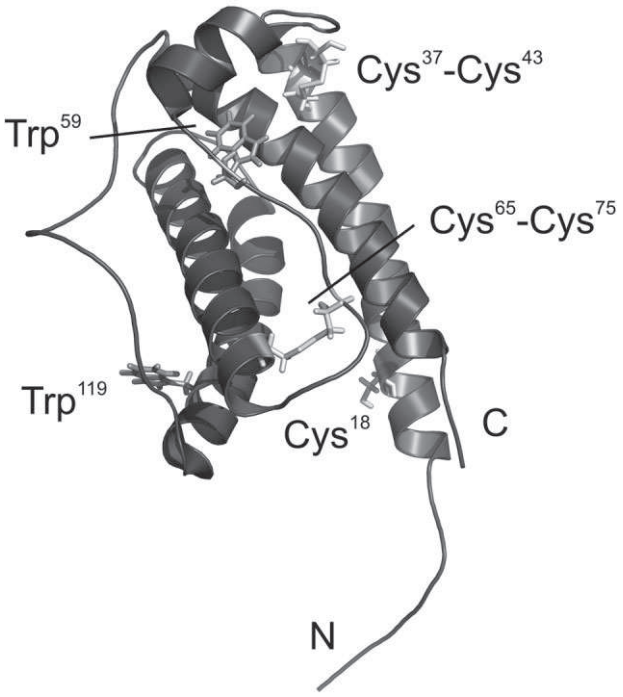


**Figure 1**. NMR structure of hG-CSF [16] with cysteine and tryptophan residues highlighted. The two native disulfide bonds $Cys^{37}$-$Cys^{43}$ and $Cys^{65}$-$Cys^{75}$, as well as the natively free $Cys^{18}$ are indicated. Note the solvent-exposed conformations of the two Trp residues ($Trp^{59}$, $Trp^{119}$).

blies would facilitate the rational design of stabilized high-quality protein preparations [8, 10, 11].

Human granulocyte colony-stimulating factor (hG-CSF) has an important role in hematopoiesis by regulating proliferation and differentiation of neutrophils and neutrophil progenitor cells. hG-CSF exists in two isoforms that result from alternative splicing, whereby the shorter variant lacks residues 66–68 of the full-length form [12]. Therapeutically, hG-CSF is applied in oncology and hematology [13]. The *E. coli*-derived short variant of recombinant (r) hG-CSF used in this study has methionine as the N-terminal amino acid and is not glycosylated at $Thr^{134}$ [14]. Structurally, rhG-CSF shows high similarity to other long-chain cytokines [15], adopting the canonical four-α-helix bundle fold, with long overhand connecting loops. In rhG-CSF, the α-helix bundle exhibits up-up-down-down connectivity, as shown in Fig. 1 [16].

Like other cytokines, such as the human growth hormone [17–19], rhG-CSF is somewhat prone to aggregation irrespective of whether the chosen conditions of incubation favor or perturb the native state of the protein in solution [20, 21]. This has negative consequences on the practical application of rhG-CSF as it implies the requirement for stringent formulation and refrigeration of the protein during storage. Other factors potentially occurring in essentially all unit operations of the manufacturing process can also drive non-native protein aggregation. These involve contact of the target protein with bulk gas and/or solid surfaces, as well as various forms of hydrodynamic force applied to the protein [5, 19, 22–24]. Despite previous advances [25], the relationship between key parameters of the process operation and aggregation of rhG-CSF is not well understood.

It is now generally believed that surface effects at gas-liquid and solid-liquid interfaces represent the principal cause for protein stability issues under physical process stress conditions, including shaking or stirring [24, 26]. However, the interplay of interfacial and shear stresses can produce significantly different stability patterns [19, 24]. We therefore examined the aggregation of rhG-CSF exposed to simulated process stress in the form of stirring and bubble aeration. The protein aggregation triggered under these conditions was analyzed in a time-resolved manner, using different probes for protein conformational stability and aggregate structure. Important characteristics of the aggregation process were elucidated. The applied stress conditions were controlled so that each represented a different composition of surface effects and hydrodynamic force. In the case of bubble aeration, surface effects are much more pronounced compared to those seen with stirring. Hydrodynamic forces, however, can be considered roughly equivalent since substantial shear stresses can also be reached with aeration [24]. The rates of stirring and aeration were therefore adjusted to give comparable average shear rates, as well as comparable and convenient precipitation rates. It should be noted that a complete discrimination of stress factors is very difficult and possibly not representative. Since we consider that any unit operation of a biotechnological process contains hydrodynamic as well as surface effects, we decided to look at different plausible scenarios instead of discrete stress principles.

One molecular feature of rhG-CSF aggregation that has only been partially resolved in prior studies [27] is the participation of the disulfide bond rearrangement in the formation of insoluble protein assemblies. rhG-CSF has five cysteine residues, of which only $Cys^{18}$ is not engaged in a disulfide bond. $Cys^{37}$ and $Cys^{43}$ as well as $Cys^{65}$ and $Cys^{75}$ are linked together in the native structure of rhG-CSF (Fig. 1) as confirmed here by MS. In addition, we showed that breaking of the native disulfide bonds and formation of new ones involving the originally free $Cys^{18}$ are prominent features of rhG-CSF aggregation. The combined data thus identify $Cys^{18}$ as

 

a promising molecular handle for inhibiting disulfide-mediated aggregation of rhG-CSF [28–31].

## 2 Materials and methods

### 2.1 Materials

rhG-CSF was kindly provided by Sandoz (Kundl, Austria). Unless mentioned, all chemicals and reagents used were from Carl Roth GmbH + Co. KG (Karlsruhe, Germany). L-Glutamic acid, 8-anilino-1-naphthalenesulfonic acid ammonium salt (ANS), iodoacetamide, dithiothreitol, ethyl acetate, and toluene were from Sigma-Aldrich. Potassium permanganate and potassium carbonate were from Merck. Mini-PROTEAN TGX 4–20% resolving gels for SDS-PAGE were from Bio-Rad. Novex® sharp unstained protein standard was from Invitrogen. Phast Gel Blue R Coomassie R350 stain was from GE Healthcare.

### 2.2 Protein preparation

Solutions of rhG-CSF were prepared in 10 mM sodium L-glutamate buffer supplemented with 5% sorbitol. A pH of 4.4 was chosen to prevent non-native aggregation in the absence of external stress [20, 32]. The concentration of the protein stock solution was 1.39 ± 0.03 mg/mL. rhG-CSF was stored frozen at –20°C until further use. The protein concentration was measured by absorbance at 280 nm, assuming a molar extinction coefficient of 15 720 $M^{-1}$ $cm^{-1}$ (ExPASy ProtParam [33]) and a molecular mass of 18.8 kDa for rhG-CSF [16]. The isoelectric point of rhG-CSF lies at 6.0 [20].

### 2.3 Experimental set-up

A jacketed miniature reactor fabricated from glass was used. The reactor had an inner diameter of 32 mm and a height of 125 mm. Temperature was controlled at 25°C with a Julabo F25 refrigerated/heating circulator. Stirring was performed with a smooth PTFE-coated magnetic stir bar (30 × 6 mm) using a fixed agitation rate of 400 rpm (see Supporting information, Fig. S1A) for up to 47 h. For stirring, the liquid filling level was 18 mm, corresponding to 15 mL protein solution.

Bubble aeration was carried out by feeding compressed air via a Stasto Automation pressure regulator (model R-M14-08-R; Innsbruck, Austria), followed by a flow gauge adjusting a constant air flow rate of 3 L/h. The air flow was piped into the protein solution (10 mL) through an autoclavable plastic tube LAB/FDA/USP grade VI with 3.2-mm inner diameter. The liquid filling level was 11 mm. Aeration was performed for up to 12 h. A more detailed system description in terms of fluid dynamics and bubble characteristics, a description of the fluid characterization and images of the different set-ups are presented with associated references in the Supporting information. Briefly, the average shear rate of the stirred vessel was calculated to lie between 60 and 248 $s^{-1}$. The average shear rate of our aerated vessel was 91 $s^{-1}$. Local shear rates could be taken into account here. The available air-liquid interface under these conditions was estimated to be 10.3 $cm^2$, corresponding to the conical boundary layer during stirring. Bubble dimensions and velocities were measured from digital photographic images recorded in a plane parallel to the direction of the rising bubbles. The air bubbles were slightly elliptical and had a mean diameter of 4.7 mm, corresponding to the projected area of an equivalent sphere. Single bubbles rose from the pipe with a velocity of 0.14 m/s and a frequency of 4.7 $s^{-1}$ without causing a visible wake. According to the Eötvös number (5.3), Morton number ($1.4 \times 10^{-10}$) and Reynolds number (590) (see the Supporting information), a shape regime between wobbling and ellipsoid may be prevalent. The wobbling regime, however, lies closer at the calculated values, although the shape of the bubbles was rather ellipsoidal in the photographs.

Each experiment was carried out in a minimum of five replicates. The aggregation time course of rhG-CSF was determined by withdrawing samples (1 mL) from the reactor at suitable times. Precipitated protein was carefully removed and collected using centrifugation at 18 400 × $g$ (10 min, 4°C). Both the clear supernatant and the precipitate were used in further analyses. Details on statistical evaluation of analytical data are provided in the Supporting information.

### 2.4 Analytical methods

#### *2.4.1 Fluorescence spectroscopy*

A Hitachi F-4500 fluorescence spectrophotometer equipped with a Julabo F25 refrigerated/heating circulator was used to analyze the supernatant of centrifuged samples at 25 ± 1°C, stressed as described above. Measurements were carried out within 24 h after sampling. Intrinsic protein fluorescence was recorded at 340 nm following excitation at 280 nm or 295 nm. The protein concentration in the sample was 92 μg/mL. For measurement of ANS binding to rhG-CSF, 10 μL ANS solution (1 mM in water) was mixed with 500 μL rhG-CSF solution (92 μg/mL) at room temperature, corresponding to a molar ANS/protein ratio of 4. Exact-

ly 5 min after the mixing, the fluorescence of the solution was measured at 470 nm using excitation at 388 nm. A 5-nm slit width was used in all fluorescence measurements. Unstressed, but otherwise identical samples were used as negative controls.

#### 2.4.2 Size exclusion HPLC

A Merck Hitachi LaChrom liquid chromatography system coupled to a model L-7480 fluorescence detector was used. The rhG-CSF monomer and different non-native oligomeric assemblies of the protein in the supernatant were separated using a TSK-GEL G3000SWXL column that was equipped with a guard column from Tosoh Bioscience. A solution of 50 mM $(NH_4)HCO_3$ in water (pH 7.0) was used as the mobile phase at a flow rate of 0.5 mL/min. The higher pH value compared to the protein stock solution was chosen due to higher reproducibility, sensitivity and column stability. Results were validated using SDS-PAGE in terms of quality and linearity. Column temperature was held at 30°C. Fluorescence was measured at 345 nm following excitation at 280 nm. Calibration of the rhG-CSF monomer peak was performed between 0.8 and 0.1 mg/mL total protein concentration.

#### 2.4.3 Mass spectrometry

Internal sequence information on the rhG-CSF samples was obtained from LC-MS/MS. Protein bands were excised from SDS polyacrylamide gels and then digested with modified trypsin (Promega) according to [34], or with 0.5 μg chymotrypsin (Roche) in 50 mM ammonium bicarbonate and 10 mM $CaCl_2$. The detailed experimental protocol and the methods used for data processing are given in the Supporting information.

#### 2.4.4 Confocal laser scanning microscopy

Precipitated rhG-CSF was suspended at a protein concentration of 1.4 mg/mL, and 10 μL protein suspension was analyzed by confocal laser scanning microscopy (CLSM) after addition of 1 μL 1 mM ANS. CLSM images were obtained with a Leica TCS SPE DM5500 Q microscope at 630-fold magnification. The excitation wavelength was 405 nm, and the emission wavelength range was 450–470 nm. Images were generated by projection of the single z-level images from the particle layer in the preparation. Three to five images were taken from randomly chosen spots of the preparation. The total particle areas and particle counts were all normalized to a total observation area of 1 $mm^2$. Images were carefully checked for the presence of air bubbles. To rigorously rule out artifacts resulting from the presence of air bubbles in the sample, we performed a control experiment in which the sample was centrifuged for 2 min at 8000 × *g* prior to CLSM analysis. The protein pellet was resuspended in buffer and then analyzed. Nine centrifuged and eight non-centrifuged samples were evaluated. Centrifugation, which would be expected to remove most of the air bubbles still present in the sample, did not result in significant reduction of the observed particle number. Contrary to expectation, the centrifuged sample contained a greater number of highly circular particles than unprocessed sample (Supporting information, Fig. S2). In summary, these controls rule out concern about disturbance caused by air bubbles in the CLSM analysis. The program ImageJ [35] was used for image processing and generation of size and shape distributions. A representative image of the particles is shown in the Supporting information, Fig. S3.

## 3 Results and discussion

### 3.1 Stirring and aeration both result in precipitation of rhG-CSF

Solutions of rhG-CSF became cloudy within just a few hours when stirred or aerated using the conditions described in Section 2 (stirring: ~2 h; aeration: ~6 h), and the protein gradually precipitated as an insoluble aggregate that could be removed by centrifugation. Figure 2A depicts the time courses for the decrease in rhG-CSF concentration in supernatants from the stirred and aerated incubations. In both cases, loss of soluble protein to the precipitate was roughly linearly dependent on the incubation time. Considering that formation of turbidity was visually observed earlier under stirring than under aeration, it is interesting that the rate of protein precipitation under stirring stress ($V$ = 22 ± 4 μg/mL/h) was significantly lower than that observed under aeration stress ($V$ = 42 ± 11 μg/mL/h). By way of comparison, incubation of the same rhG-CSF solution at 37°C under otherwise identical conditions in the absence of stirring and aeration did not produce detectable amounts of protein precipitate over a period of 7 days, clearly indicating that the observed aggregation in Fig. 2A was exclusively due to the effects of hydrodynamic and interfacial stresses on the solution stability of the protein.

Nonreducing SDS-PAGE was routinely used to analyze the samples taken from the stress experiments. The results for protein precipitates formed during exhaustive stirring and aeration prior to and after the 7-day incubation at 37°C is shown in the Supporting information, Fig. S4. In contrast to soluble protein, which existed predominantly as

 

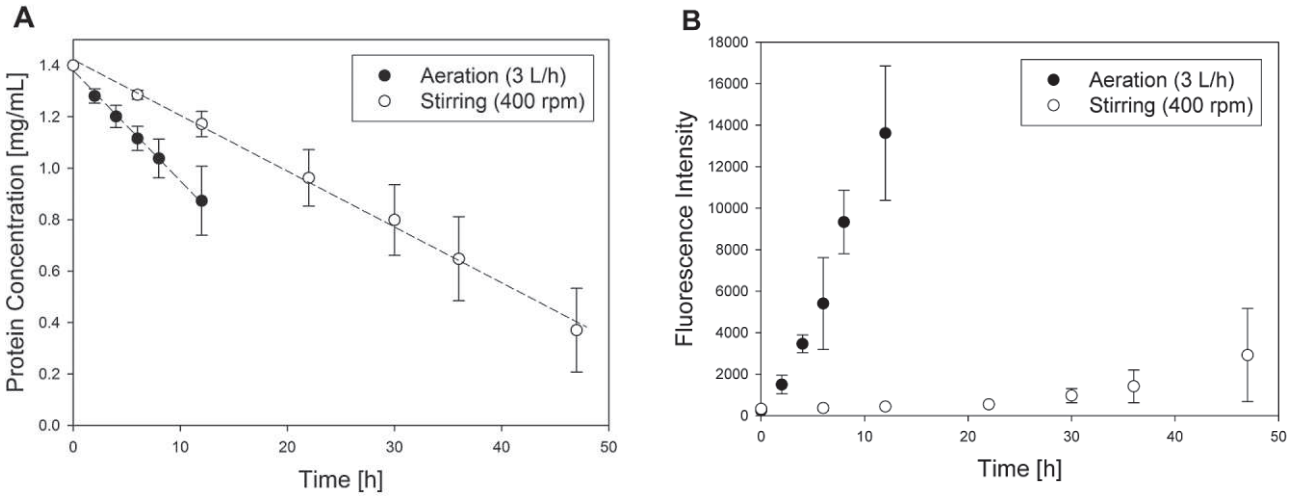


**Figure 2**. (**A**) Dependence of rhG-CSF precipitation on incubation time under stress by aeration ($n$=5) and stirring ($n$=6). Duplicates of rhG-CSF concentration were measured in the supernatant (mean ± SD). (**B**) Dependence of ANS fluorescence (intensity; arbitrary units) of soluble rhG-CSF on incubation time under stress by aeration ($n$=5) and stirring ($n$=6) (mean ± SD).

18.8-kDa monomer, the rhG-CSF precipitates presented additional oligomeric species, which according to their molecular masses could be explained as multiples of the monomer mass. The protein bands present in the precipitate produced by stirring stress were not well focused in the SDS-PAGE (Supporting information, Fig. S4, lane 4), suggesting a high heterogeneity in the protein aggregates formed under these conditions. The use of reducing conditions (10 mM DTT) during sample preparation for SDS-PAGE resulted in the complete disintegration of the aggregated protein species previously seen in the rhG-CSF precipitates. This suggests that non-native aggregation of rhG-CSF exposed to aeration and stirring involved formation of higher oligomeric assemblies linked by disulfide bonds.

### 3.2 Conformational distortion of rhG-CSF during non-native aggregation, analyzed by fluorescence spectroscopy

Intrinsic protein fluorescence and fluorescence resulting from binding of ANS to solvent-exposed hydrophobic regions of the protein were used as reporters of conformational changes in the soluble rhG-CSF that occur in solution during non-native aggregation [36]. Figure 2B depicts the time courses of the ANS fluorescence intensity under stirring and aeration conditions. The corresponding time courses of the intrinsic fluorescence intensity are shown in the Supporting information (Fig. S5). Both analytical methods were capable of capturing the significant conformational distortion in the soluble rhG-CSF that took place as result of the applied hydrodynamic and interfacial stress. Controls in which rhG-CSF was incubated at 37°C in the absence of additional stress did not show changes in either of the fluorescence signals used within limits of the experimental error. It should be noted that the observed increase in intrinsic protein fluorescence intensity ($I_{max}$; Supporting information, Fig. S5) was not accompanied by a shift in the wavelength of maximum fluorescence emission ($\lambda_{max}$), which was constant at about 338 ± 2.5 nm. Considering that the intrinsic fluorescence properties of rhG-CSF are probably determined by the only two tryptophan residues present in the protein ($Trp^{59}$, $Trp^{119}$; Fig. 1), the constant of $\lambda_{max}$ and increasing $I_{max}$ could be explained by the fact that each Trp is already relatively exposed to solvent in the native structure of rhG-CSF [37, 38]. The observed increase of $I_{max}$ upon induction of stress can be explained by loss of quenching effects or conformational flexibility after unfolding. The change in excitation wavelength from the usually used 280 nm to 295 nm did not affect the spectrum of fluorescence emission, but did result in a significant lowering of $I_{max}$ due to the elimination of resonance energy transfer via tyrosine. The increase in ANS and intrinsic protein fluorescence intensities was substantially higher under conditions of aeration as compared to stirring. This suggests that the effect of increased interfacial stress on the distortion of the native conformation of rhG-CSF was by far greater than the corresponding effect of shear with reduced interfacial stress (Fig. 2B). Under aeration conditions, the appearance of hydrophobic protein

surfaces, measured by ANS fluorescence, in the soluble protein corresponded with precipitation of rhG-CSF from solution. Stirring, by contrast, promoted precipitation of rhG-CSF in the apparent absence of exposure of a corresponding amount of hydrophobic protein surface area in the soluble fraction. We show below that aerated samples of rhG-CSF contained a substantial number of soluble aggregates, whereas such aggregates were scarce in the stirred samples. Therefore, it seems plausible that protein unfolding and aggregate formation in solution could mainly be responsible for the observed rise in fluorescence under the conditions of aeration stress. Negative controls, consistence with SEC results and the stability of fluorescence signal refute the possibility that the qualitative nature of the ANS fluorescence data could have been biased by induced unfolding or aggregation of rhG-CSF [39].

### 3.3 Non-native aggregation of rhG-CSF in solution monitored by SEC

High-performance SEC coupled to fluorescence detection was employed to analyze the supernatant of samples taken from the stress experiments. SEC monitored the occurrence of rhG-CSF forms differing from the native protein monomer with regard to their molecular size. Figure 3A displays a superimposition of the fluorescence traces obtained upon analysis of a representative sample from the aerated and the stirred incubation. Within limits of resolution of the analytical method, the starting material comprised only the monomer (≥99%). The results reveal that aeration resulted in a greater number of aggregated protein species and overall amount of soluble aggregates than stirring. We are fully aware of the potential limitation of this analytical method, in that the samples were exposed to bulk conditions slightly different from those used in the stress experiment. Choice of conditions was dictated by optimal analytical performance. However, even though we cannot rigorously rule out secondary effects occurring as result of the analysis, such as partial refolding of rhG-CSF and changes in soluble aggregate content, it is very likely that the comparison of the two samples, with respect to the corresponding results from SDS-PAGE and fluorescence, gives a fully representative picture. Using the peak area for relative concentration determination, we calculated the absolute concentrations of soluble aggregates with respect to the total soluble protein (280 nm measurements) after various periods of incubation (Fig. 3B). Soluble aggregate formation was much more pronounced with aeration as compared to stirring. Of note, protein precipitation occurred to a massive extent under both stress conditions. Therefore, different mechanisms may underlie the aggregation of rhG-CSF induced by aeration and stirring. At the very least, stirring must lead to an increase in growth rate of soluble aggregates compared aeration, so that the observed level of insolubility is reached when applying the stirring stress. This is corroborated by our fluorescence data, which also support different aggregation patterns for the two simulated stress extremes.

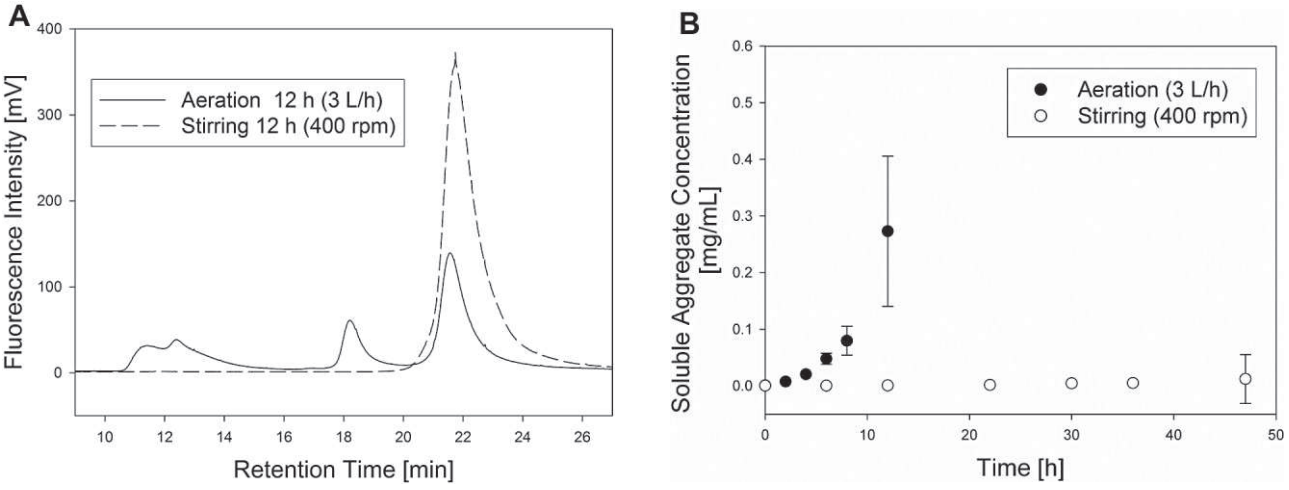


**Figure 3**. (**A**) SEC chromatograms of soluble rhG-CSF in samples from aeration and stirring experiments. The native monomer, aggregated dimer and soluble aggregates can be distinguished. (**B**) Dependence of total number of soluble aggregates in soluble rhG-CSF on incubation time under stress by aeration ($n$=5) and stirring ($n$=6) as determined by SEC. Mean ± SD of duplicate measurements. Peak area was used for quantification.

**Table 1.** Novel disulfide bonds in rhG-CSF subjected to stress by stirring or aeration, as revealed by MS. 'x' indicates that the fragment was detected upon stressing with the respective method.[a)]

| Sequence | Ion score | Mass error [Da] | S-S bridge position | Digestion | Aeration | Stirring |
|---|---|---|---|---|---|---|
| **CLEQVR-CLEQVR** | 52 | 0.0024 | $C^{18}$-$C^{18}$ | Trypsin | x | |
| LLKCL-EQVRKIQGDGAALQEKLCATY | 18 | 0.129 | $C^{18}$-$C^{37}$ | Chymotrypsin | x | |
| **LLKCL-QLAGCL** | 20 | 0.0026 | $C^{18}$-$C^{75}$ | Chymotrypsin | x | x |
| LLKCL-QLAGCLSQL | 20 | 0.0046 | $C^{18}$-$C^{75}$ | Chymotrypsin | x | |

a) Entries in bold represent cross-links with detected fragment ions and MS spectra that are provided in the Supporting information.

### 3.4 Disulfide bridge rearrangement during non-native aggregation

Protein assemblies, identified as distinct bands in the SDS polyacrylamide gels used for electrophoretic characterization of the rhG-CSF precipitate, were excised from the gel, digested with trypsin or chymotrypsin, and subjected to peptide sequencing by LC-MS/MS analysis. Tables containing the sequences of identified peptides in each band, ion scores, mass errors, the number of peptides found per band, sequence coverage and Mascot scores can be found in the Supporting information.

rhG-CSF was located in all analyzed bands. From the sequence coverage of peptides identified in the individual protein bands, we concluded that rhG-CSF had most likely remained intact during non-native aggregation, confirming the opinion obtained from SDS-PAGE done under reducing conditions. Moreover, no significant chemical modification of rhG-CSF aggregates was detected in the protein oligomers on applying error-tolerant Mascot searches of Unimod modifications. However, by tracking the changes in protein disulfide bridges that accompanied the conversion of the native rhG-CSF monomer into the heterogeneous mixture of protein assemblies constituting the precipitate, we obtained relevant insight into the structural distortions underlying the process of non-native aggregation. For this purpose, we alkylated free cysteines in the precipitate prior to nonreducing SDS-PAGE to inhibit disulfide rearrangement during analysis. After in-gel digestion of mono- and oligomeric protein bands and LC-MS/MS, free cysteines were identified by their mass shift through carbamidomethylation in decoy Mascot searches. Peptides cross-linked via disulfide bridges were matched to custom-made databases of linearized disulfide cross-linked peptides of digested rhG-CSF produced by the xComb software. Table 1 shows all novel disulfide bonds. Disulfide cross-linking and detected fragment ions of the two bold entries in Table 1 are shown in the Supporting information, which also gives a detailed interpretation of MS/MS spectra, identifying different disulfide cross-linked peptides. The native pattern of disulfide bonds and the free $Cys^{18}$ was observed in all protein bands, suggesting that breaking or rearrangement of the original disulfide bridges was not a stringent requirement for rhG-CSF to become trapped in the precipitate. However, stress-induced aggregation, especially that triggered by stirring, was clearly associated with partial breaking of the original disulfide bridges because in each samples analyzed, one or more free forms of the natively bound Cys residues were identified (Supporting information, Table S1). Concerning the initial events of the structural distortion in stressed rhG-CSF, the monomer bands observed after aeration and stirring contained a free Cys that must have resulted from disruption of the $Cys^{37}$-$Cys^{43}$ disulfide bridge; free $Cys^{43}$ was detected in the sample from aeration, and $Cys^{37}$ in the sample from stirring. Of the new bonds formed, a $Cys^{18}$-$Cys^{75}$ linkage was predominant in the different aggregate bands (Table 1). However, the high molecular mass aggregate formed under aeration contained an array of disulfides involving $Cys^{18}$. The presence of $Cys^{18}$-$Cys^{18}$ disulfide bridges indicates that aggregation can occur through intermolecular cross-links between rhG-CSF monomers. Interestingly, a greater number of novel free cysteines and fewer novel disulfide bridges were detected in stirred samples compared to the aerated samples. Previous work on bovine G-CSF has provided evidence, based on data from SDS-PAGE, that intermolecular disulfide cross-links are formed during non-native aggregation [27].

### 3.5 Characterization of rhG-CSF precipitates by CLSM

Precipitated rhG-CSF was stained with ANS and visualized using CLSM. Samples taken after various lengths of incubation were analyzed, and results obtained after image processing are displayed in Fig. 4. rhG-CSF formed amorphous precipitates under the stress conditions used. No fibrillar aggregates were observed (for detection and charac-

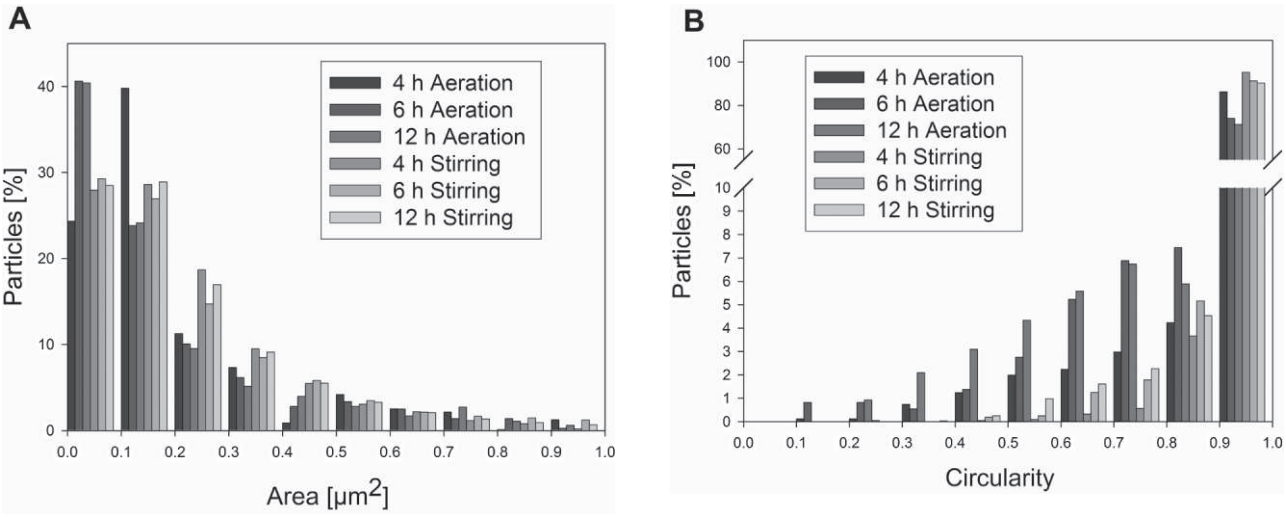


**Figure 4.** (**A**) Area distribution of rhG-CSF aggregate particles under stirring and aeration determined by CLSM. (**B**) Shape distribution of rhG-CSF aggregate particles under stirring and aeration determined by CLSM; 1 = perfect circle, 0 = stick shape.

terization of protein fibrils by CLSM, see [40–42]). The number of particles and their total areas in the sample increased with increasing incubation time, irrespective of the type of stress applied to the rhG-CSF. The total number of aggregate particles per sample varied between 363 and 7539. Due to the high skewness of the particle size distribution towards small particles (Fig. 4A), it would have been inappropriate to compare the samples based on arithmetic means of the particle area; therefore the entire distribution for size and shape had to be considered. In all of the samples analyzed, the vast majority of particles (≥92%) had a size of 1 µm$^2$ or smaller. Despite the increasing particle number, the size distribution did not change dramatically over time, with most of the particles having a size between 0.1 and 0.2 µm$^2$ (Fig. 4A).

Circularity ($C$) was chosen as the shape descriptor for the insoluble protein particles. It is defined by the relationship, $C = 4\pi \times$ *area / perimeter*$^2$, and a $C$ value of 1.0 indicates a perfect circle. Elongated shapes are indicated by substantially lower $C$ values. Figure 4B shows that the majority of the rhG-CSF particles were circular at all times and that this was independent of the type of stress applied. A slight bias towards small and circular particles needs to be accepted for the fraction of vertically pictured, stick-shaped aggregates. However, a clear trend towards the formation of non-circular particles at longer incubation times could be deduced from the data. Additionally, slightly higher numbers of non-circular particles were found in the aerated as compared to stirred samples. Local differences in shear stress from friction or bubble disruption, differences in disulfide shuffling, coalescence, surface area, surface dynamics or energy input are possible explanations for these findings.

### 3.6 Mechanistic considerations of non-native aggregation of rhG-CSF and their implications for stabilization

From the evidence presented here, factors promoting non-native aggregation of rhG-CSF can be categorized broadly according to the severity of their effect: combined hydrodynamic and interfacial stress caused by aeration > predominantly hydrodynamic stress caused by stirring > elevated temperature stress (37 °C). Exposure of rhG-CSF to air-liquid interfaces should thus be reduced to a minimum at all times. Non-ionic surfactants capable of protecting proteins against denaturation at the water-air surface might be useful stabilizers of rhG-CSF [43]. The potential damage to rhG-CSF caused by fluid agitation due to stirring, shaking or pumping should also be considered. Despite the significant differences in soluble aggregate formation, turbidity and protein unfolding observed here under the different stress conditions, we still assume that surface effects were the principal trigger for aggregation in all our experiments. In fact, shear alone has only rarely been shown to cause severe protein damage [24]. It is possible that the coalescence of monomers, dimers and oligomers in solution might be accelerated by stirring as compared to aeration. This fast coalescence of denatured, yet soluble species could partly compensate for lower unfolding rates under stirring than under aeration, so that eventually both stress conditions give similar precipitation rates. However, a more detailed

 

analysis of the kinetic pathways underlying aggregation under the different conditions used was beyond the scope of this study.

The characterization of the different protein forms by MS present in the rhG-CSF precipitate indicated that the disruption of the native $Cys^{37}$-$Cys^{43}$ disulfide bond (Fig. 1) may be one of the early events of denaturation (i.e. a nucleation step). Aggregated monomer containing free $Cys^{43}$ was found under aeration and with free $Cys^{37}$ under stirring. The absence of the stabilization given by the $Cys^{37}$-$Cys^{43}$ disulfide bond is likely to affect the conformation of the large central loop of rhG-CSF (Fig. 1), which is partially fixed in place by $Cys^{65}$-$Cys^{75}$ bond. The additional presence of free $Cys^{65}$ and $Cys^{75}$ in a trimeric aggregate contained in the protein precipitate obtained under stirring would be consistent with a denaturation process that progresses from the $Cys^{37}$-$Cys^{43}$ to the $Cys^{65}$-$Cys^{75}$ disulfide bond.

In addition to the disruption of the native disulfide bridges, the formation of several non-native disulfides bonds was observed in rhG-CSF precipitates. The involvement of the originally free $Cys^{18}$ in all of these new disulfide linkages provides a compelling molecular explanation for observations from previous studies that mutation or PEGylation of $Cys^{18}$ correlates with changes in the conformational stability and aggregation behavior of rhG-CSF [28–31]. Of note, $Cys^{18}$-PEGylated rhG-CSF did not form covalent assemblies during non-native aggregation [31]. Proteins structurally related to rhG-CSF, such as interferon-β and interleukin-2, also undergo non-native oligomerization via thiol/disulfide interchange. This may therefore be considered a common feature of aggregation of long-chain cytokines [44]. While the $Cys^{18}$-$Cys^{18}$ disulfide linkage can only result from intermolecular cross-linking, the origin of the other disulfides, $Cys^{18}$-$Cys^{37}$ and $Cys^{18}$-$Cys^{75}$, is less certain. As can be seen from the structure of rhG-CSF (Fig. 1), the formation of an intramolecular $Cys^{18}$-$Cys^{75}$ disulfide is conceivable for a structurally expanded intermediate of unfolding that has retained the 4-α-helix bundle fold. Unless massive disintegration of this secondary structural core of rhG-CSF occurred, the $Cys^{18}$-$Cys^{37}$ disulfide would rather be formed by an intermolecular reaction. The seemingly high reactivity of $Cys^{18}$ is somewhat surprising considering that, at the pH of 4.4 used here, the thiol side chain should be fully protonated and thus unreactive as a nucleophile. Since disulfide exchange under acidic conditions may involve an electrophilic mechanism, this can proceed in the absence of a thiolate nucleophile [44]. Nevertheless, the increased heat stability of rhG-CSF at pH 4.4 compared to neutral pH [25] could originate from the lower propensity to form covalent aggregates. In any case, the addition of external thiols may help in preventing aberrant disulfide bond formation in rhG-CSF [6].

## 4 Concluding remarks

This work presents a detailed characterization of non-native aggregation of rhG-CSF under stress caused by gas-liquid interfacial contact and exposure to hydrodynamic force. The observation of different types of aggregation behavior related to the varying forms of hydrodynamic and interfacial stress adds significantly to the substantial body of evidence on spontaneous aggregation of the protein in solution. The results suggest that under the pH conditions used in the commercial formulations (pH 4.4), surface and agitation-mediated aggregation could be important factors determining the stability of rhG-CSF. Despite its relative simplicity, we believe that the set-up used here enables the simulation of further combinations of stress factors for future investigations of the relevance of unit operations in terms of protein aggregation.

Although the "accelerated" aggregation experiments of the type described here provide useful information for practical applications, it must be recognized that the transferability of the results to the conditions of real processes is limited. The design of process-stress experiments that would support quantitative extrapolation remains a major challenge in the field.

*Dr. Massimiliano Cardinale (Institute of Environmental Biotechnology, Graz University of Technology) is thanked for supporting measurements with CLSM. Thanks also go to Britta Obrist for technical assistance with MS. This work was supported by the FFG, Land Steiermark, Steirische Wirtschaftsförderung (SFG) and Sandoz GmbH (Kundl, Austria).*

*The authors declare no conflict of interest.*

## 5 References

[1] Chi, E. Y., Krishnan, S., Randolph, T. W., Carpenter, J. F., Physical stability of proteins in aqueous solution: Mechanism and driving forces in nonnative protein aggregation. *Pharm. Res.* 2003, *20*, 1325–1336.

[2] Wang, L., Schubert, D., Sawaya, M. R., Eisenberg, D., Riek, R., Multidimensional structure-activity relationship of a pro-

tein in its aggregated states. *Angew. Chem. Int. Ed. Engl.* 2010, *49*, 3904–3908.
[3] ICH Guideline Q1A(R2). *Stability testing of new drug substances and products*. 2003, 1–18.
[4] Rosenberg, A. S., Effects of protein aggregates: An immunologic perspective. *AAPS J.* 2006, *8*, 501–507.
[5] Mahler, H. C., Friess, W., Grauschopf, U., Kiese, S., Protein aggregation: Pathways, induction factors and analysis. *J. Pharm. Sci.* 2009, *98*, 2909–2934.
[6] Manning, M. C., Patel, K., Borchardt, R. T., Stability of protein pharmaceuticals. *Pharm. Res.* 1989, *6*, 903–918.
[7] Manning, M. C., Chou, D. K., Murphy, B. M., Payne, R. W., Katayama, D. S., Stability of protein pharmaceuticals: An update. *Pharm. Res.* 2010, *27*, 544–575.
[8] Weiss, I. V., William, F., Young, T. M., Roberts, C. J., Principles, approaches and challenges for predicting protein aggregation rates and shelf life. *J. Pharm. Sci.* 2009, *98*, 1246–1277.
[9] Castillo, V., Graña-Montes, R., Sabate, R., Ventura, S., Prediction of the aggregation propensity of proteins from the primary sequence: Aggregation properties of proteomes. *Biotechnol. J.* 2011, *6*, 674–685.
[10] Roberts, C. J., Non-native protein aggregation kinetics. *Biotechnol. Bioeng*. 2007, *98*, 927–938.
[11] Roberts, C. J., Das, T. K., Sahin, E., Predicting solution aggregation rates for therapeutic proteins: Approaches and challenges. *Int. J. Pharm.* 2011, *418*, 318–333.
[12] Nagata, S., Tsuchiya, M., Asano, S., Yamamoto, O. et al., The chromosomal gene structure and two mRNAs for human granulocyte colony-stimulating factor. *EMBO J.* 1986, *5*, 575–581.
[13] Sung, L., Clinical applications of granulocyte-colony stimulating factor. *Front. Biosci.* 2007, *12*, 1988–2002.
[14] Lu, H. S., Boone, T. C., Souza, L. M., Lai, P. H., Disulfide and secondary structures of recombinant human granulocyte colony stimulating factor. *Arch. Biochem. Biophys.* 1989, *268*, 81–92.
[15] Hill, C. P., Osslund, T. D., Eisenberg, D., The structure of granulocyte-colony-stimulating factor and its relationship to other growth factors. *Proc. Natl. Acad. Sci. USA* 1993, *90*, 5167–5171.
[16] Zink, T., Ross, A., Lueers, K., Cieslar, C. et al., Structure and dynamics of the human granulocyte colony-stimulating factor determined by NMR spectroscopy. Loop mobility in a four-helix-bundle protein. *Biochemistry* 1994, *33*, 8453–8463.
[17] Bam, N. B., Cleland, J. L., Yang, J., Manning, M. C. et al., Tween protects recombinant human growth hormone against agitation-induced damage via hydrophobic interactions. *J. Pharm. Sci.* 1998, *87*, 1554–1559.
[18] Cholewinski, M., Lückel, B., Horn, H., Degradation pathways, analytical characterization and formulation strategies of a peptide and a protein. Calcitonine and human growth hormone in comparison. *Pharm. Acta Helv.* 1996, *71*, 405–419.
[19] Maa, Y. F., Hsu, C. C., Protein denaturation by combined effect of shear and air-liquid interface. *Biotechnol. Bioeng.* 1997, *54*, 503–512.
[20] Herman, A., Boone, T., Lu, H., Characterization, formulation and stability of Neupogen® (Filgrastim), a recombinant human granulocyte-colony stimulating factor. *Pharm. Biotechnol.* 2002, *9*, 303–328.
[21] Krishnan, S., Chi, E. Y., Webb, J. N., Chang, B. S. et al., Aggregation of granulocyte colony stimulating factor under physiological conditions: Characterization and thermodynamic inhibition. *Biochemistry* 2002, *41*, 6422–6431.
[22] Clarkson, J. R., Cui, Z. F., Darton, R. C., Effect of solution conditions on protein damage in foam. *Biochem. Eng. J.* 2000, *4*, 107–114.
[23] Di Stasio, E., De Cristofaro, R., The effect of shear stress on protein conformation: Physical forces operating on biochemical systems: The case of von Willebrand factor. *Biophys. Chem.* 2010, *153*, 1–8.
[24] Thomas, C. R., Geer, D., Effects of shear on proteins in solution. *Biotechnol. Lett.* 2010, *33*, 443–456.
[25] Chi, E. Y., Krishnan, S., Kendrick, B. S., Chang, B. S. et al., Roles of conformational stability and colloidal stability in the aggregation of recombinant human granulocyte colony-stimulating factor. *Protein Sci.* 2003, *12*, 903–913.
[26] Kiese, S., Papppenberger, A., Friess, W., Mahler, H. C., Shaken, not stirred: Mechanical stress testing of an IgG1 antibody. *J. Pharm. Sci.* 2008, *97*, 4347–4366.
[27] Bartkowski, R., Kitchel, R., Peckham, N., Margulis, L., Aggregation of recombinant bovine granulocyte colony stimulating factor in solution. *J. Protein Chem.* 2002, *21*, 137–143.
[28] Raso, S. W., Abel, J., Barnes, J. M., Maloney, K. M. et al., Aggregation of granulocyte-colony stimulating factor in vitro involves a conformationally altered monomeric state. *Protein Sci.* 2005, *14*, 2246–2257.
[29] Ishikawa, M., Iijima, H., Satake-Ishikawa, R., Tsumura, H. et al., The substitution of cysteine 17 of recombinant human G-CSF with alanine greatly enhanced its stability. *Cell Struct. Funct.* 1992, *17*, 61–65.
[30] Arakawa, T., Prestrelski, S. J., Narhi, L. O., Boone, T. C., Kenney, W. C., Cysteine 17 of recombinant human granulocyte-colony stimulating factor is partially solvent-exposed. *J. Protein Chem.* 1993, *12*, 525–531.
[31] Veronese, F. M., Mero, A., Caboi, F., Sergi, M. et al., Site-specific pegylation of G-CSF by reversible denaturation. *Bioconjug. Chem.* 2007, *18*, 1824–1830.
[32] Thirumangalathu, R., Krishnan, S., Brems, D. N., Randolph, T. W., Carpenter, J. F., Effects of pH, temperature and sucrose on benzyl alcohol-induced aggregation of recombinant human granulocyte colony stimulating factor. *J. Pharm. Sci.* 2006, *95*, 1480–1497.
[33] Gasteiger, E., Hoogland, C., Gattiker, A., Duvaud, S. et al., Protein identification and analysis tools on the ExPASy server, in: Walker, J.M. (Ed.), *The Proteomics Protocols Handbook,* Humana Press 2005, pp. 571–607.
[34] Shevchenko, A., Wilm, M., Vorm, O., Mann, M., Mass spectrometric sequencing of proteins from silver-stained polyacrylamide gels. *Anal. Chem.* 1996, *68*, 850–858.
[35] Abramoff, M. D., Magelhaes, P. J., Ram, S. J., Image processing with ImageJ. *Biophotonics Int.* 2004, *11*, 36–42.
[36] Hawe, A., Sutter, M., Jiskoot, W., Extrinsic fluorescent dyes as tools for protein characterization. *Pharm. Res*. 2008, *25*, 1487–1499.
[37] Kolvenbach, C. G., Elliott, S., Sachdev, R., Arakawa, T., Narhi, L. O., Characterization of two fluorescent tryptophans in recombinant human granulocyte-colony stimulating factor: Comparison of native sequence protein and tryptophan-deficient mutants. *J. Protein Chem.* 1993, *12*, 229–236.
[38] Vivian, J. T., Callis, P. R., Mechanisms of tryptophan fluorescence shifts in proteins. *Biophys. J.* 2001, *80*, 2093–2109.
[39] Ali, V., Prakash, K., Kulkarni, S., Ahmad, A. et al., 8-Anilino-1-naphthalene sulfonic acid (ANS) induces folding of acid unfolded cytochrome c to molten globule state as a result of

 

electrostatic interactions. *Biochemistry* 1999, *38*, 13635–13642.

[40] Ban, T., Morigaki, K., Yagi, H., Kawasaki, T. et al., Real-time and single fibril observation of the formation of amyloid beta spherulitic structures. *J. Biol. Chem.* 2006, *281*, 33677–33683.

[41] Bateman, D. A., McLaurin, J. A., Chakrabartty, A., Requirement of aggregation propensity of Alzheimer amyloid peptides for neuronal cell surface binding. *BMC Neurosci.* 2007, *8*, 29.

[42] Dickson, T. C., Vickers, J. C., The morphological phenotype of beta-amyloid plaques and associated neuritic changes in Alzheimer's disease. *Neuroscience* 2001, *105*, 99–107.

[43] Wang, W., Protein aggregation and its inhibition in biopharmaceutics. *Int. J. Pharm.* 2005, *289*, 1–30.

[44] Benesch, R. E., Benesch, R., The mechanism of disulfide interchange in acid solution: Role of sulfenium ions. *J. Am. Chem. Soc.* 1958, *80*, 1666–1669.

# 6 List of Publications

***Papers***

- Wiesbauer J, Cardinale M, Nidetzky B: Shaking and stirring: comparison of accelerated stress conditions applied to the human growth hormone. Process Biochem (2012 submitted)

- Roessl U, Wiesbauer J, Leitgeb S, Birner-Gruenberger R, Nidetzky B: Nonnative Aggregation of Recombinant Human Granulocyte-Colony Stimulating Factor (rhG-CSF) under Simulated Process Stress Conditions. Biotechnol J 7 (2012) 8, 1014-1024.

- Bolivar JM, Wiesbauer J, Nidetzky B: Biotransformations in microstructured reactors: more than flowing with the stream? Trends in biotechnology 29 (2011) 7, 333 - 342.

- Wiesbauer J, Bolivar JM, Mueller M, Schiller M, Nidetzky B: Oriented Immobilization of Enzymes Made Fit for Applied Biocatalysis: Non-Covalent Attachment to Anionic Supports using Zbasic2 Module. ChemCatChem 3 (2011) 8, 1299 - 1303.

- Wiesbauer J, Gödl C, Schwarz A, Brecker L, Nidetzky B: Substitution of the catalytic acid-base Glu237 by Gln suppresses hydrolysis during glucosylation of phenolic acceptors by Leuconostoc mesenteroides sucrose phosphorylase. J Mol Catal B 65 (2010) 1-4, 24-29.

***Oral Presentations***

- Wiesbauer J, Meier R, Roberts CJ, Nidetzky B: From accelerated stress conditions and protein-protein interactions towards more stable therapeutic proteins – a case study. - in: 8$^{th}$ Doc Day, NAWI Graz Doctoral School of Molecular Biosciences and Biotechnology, Graz am 13.07. 2012

- Roessl U, Wiesbauer J, Leitgeb S, Birner-Grünberger R, Nidetzky B: Nonnative Aggregation of rhG-CSF under Simulated Process Conditions. - in: 5th International Congress on Pharmaceutical Engineering. am: 30.09.2011

- Nidetzky B, Boniello C, Bolivar JM, Wiesbauer J: Design of carrier-bound immobilised enzymes: oriented binding using a fusion-protein approach, and determination of intraparticle concentration gradients. – in: 8th European Congress of Chemical Engineering and 1st European Congress of Applied Biotechnology. Berlin am: 25.09.2011

- Wiesbauer J, Cardinale M, Prassl R, Nidetzky B: Influence of accelerated stress conditions on aggregation and process stability of human growth hormone. - in: 8th ECCE and 1st ECAB. Berlin am: 25.09.2011

- Wiesbauer J, Rößl U, Leitgeb S, Nidetzky B: Kinetic Pathway Analysis of Aggregation of Therapeutic Proteins. - in: Annual Meeting AIChE 2010. Salt Lake City am: 07.11.2010

- Müller M, Schwarz A, Gödl C, Wiesbauer J, Brecker L, Nidetzky B: Glucosyl transfer catalyzed by sucrose phosphorylase: mechanism and application in synthesis. - in: XXIV International Carbohydrate Symposium. Oslo am: 27.07.2008

***Poster Presentations***

- Roessl U, Wiesbauer J, Leitgeb S, Birner-Grünberger R, Nidetzky B: Aggregation of Recombinant Human Granulocyte-Colony Stimulating Factor under Process Conditions. - in: XV School of Pure and Applied Biophysics. Venedig am: 24.01.2011

- Huettner B, Roessl U, Wiesbauer J, Nidetzky B, Birner-Grünberger R: Identification of disulfide-crosslinks in protein aggregates. - in: 2nd International Congress on Analytical Proteomics (ICAP). Ourense, Spain am: 18.07.2011

- Roessl U, Wiesbauer J, Leitgeb S, Birner-Grünberger R, Nidetzky B: Nonnative Aggregation of rhG-CSF under Simulated Process Conditions. - in: 2011 Colorado Protein Stability Conference. Breckenridge, CO, USA am: 20.07.2011

- Wiesbauer J, Cardinale M, Prassl R, Nidetzky B: Influence and comparison of accelerated stress conditions on human growth hormone. - in: 5th International Congress on Pharmaceutical Engineering (ICPE). Graz am: 29.09.2011

- Wiesbauer J, Cardinale M, Nidetzky B: Influence and comparison of accelerated stress conditions on human growth hormone. - in: 6th DocDay, Doctoral School Molecular Biosciences and Biotechnology. Graz am: 15.07.2011

- Roessl U, Wiesbauer J, Leitgeb S, Birner-Grünberger R, Nidetzky B: Aggregation of Recombinant Human Granulocyte-Colony Stimulating Factor under Process Conditions. - in: Annual Meeting AIChE 2010. Salt Lake City, UT, USA am: 10.11.2010

- Wiesbauer J, Leitgeb S, Nidetzky B: Stirred, not shaken –process-relevant parameters and their effects on stability of human growth hormone. - in: Workshop on Protein Aggregation and Immunogenicity. Breckenridge, CO, USA am: 20.07.2010

- Wiesbauer J, Leitgeb S, Nidetzky B: Human growth hormone – insights into its aggregation behavior using denaturation pathway characterization. - in: 8th Central European Symposium on Pharmaceutical Technology. Graz am: 16.09.2010

- Roessl U, Wiesbauer J, Leitgeb S, Nidetzky B: Kinetic Pathway Analysis of Aggregation of Therapeutic Proteins. - in: 8th Central European Symposium on Pharmaceutical Technology. University Graz am: 16.09.2010

- Wiesbauer J, Müller M, Schwarz A, Brecker L, Nidetzky B: Feasibility of phenolic acceptors in glucosyl transfer reactions catalysed by sucrose phosphorylase. - in: Life Sciences 2008. Graz am: 22.09.2008